UNIVERSITÀ
DEGLI STUDI
DI TRIESTE

UNIVERSITÀ DEGLI STUDI DI TRIESTE

XXXVIII CICLO DEL DOTTORATO DI RICERCA IN

Process and methods for engineering design of the ITER Radial Neutron Camera

Borsa co-finanziata da Università degli Studi di Trieste e Centro di ricerche ENEA

Process and methods for the engineering design of the ITER Radial Neutron Camera: the LAISE tool applied to the Ex-Port RNC

Settore scientifico-disciplinare: **ING-IND15**

DOTTORANDO / A **ENRICO OCCHIUTO**	*Ph.D. student* *Name - Surname*	Enrico Occhiuto
COORDINATORE **PROF. FULVIO BABICH**	*Ph.D. program Coordinator* *Name - Surname*	Fulvio Babich
SUPERVISORE DI TESI **PROF. DOMENICO MARZULLO**	*Thesis Supervisor* *Prof Name – Surname*	Domenico Marzullo
CO-SUPERVISORE DI TESI **BASILIO ESPOSITO**	*Thesis Co-supervisor* *Prof Name - Surname*	Basilio Esposito

ANNO ACCADEMICO 2024/2025

Contents

Acronyms

ABS Acrylonitrile Butadiene Styrene

ALARA As Low As Reasonably Achievable

AP Alignment Procedure

AS Alignment System

BAK Baking

B4C Boron Carbide

CAD Computer-Aided Design

CAM Computer-Aided Manufacturing

CCB Change Control Board

CCWS Component Cooling Water System

CM Configuration Model

CMT Cold Measurement

CMT' Transformed Cold Measurement

CRA Cold ReAlignment

CPU Central Processing Unit

DA Domestic Agency

DAQ Data Acquisition

DD Deuterium-Deuterium

DSM Diagnostic Shielding Module

DSMD DSM Datum system

DT Deuterium-Tritium

DW Dead Weight

ECM Engineering Change Management

ECN Engineering Change Notice

ECR Engineering Change Request

EMC Electromagnetic Compatibility

EM Electromagnetic

EPC1 Equatorial Port Cell 1

EPP Equatorial Port Plug

EPP1 Equatorial Port Plug 1

EPPD Equatorial Port Plug Datum system

EP01 Equatorial Port #1

ESP European Standard Pressure

ESPN European Standard Pressure Nuclear

EU Embarked Unit

FC Fission Chamber

FDR Final Design Review

FEM Finite Element

GPU Graphics Processing Unit

HMT Hot Measurement

HMT' Transformed Hot Measurement

HRA Hot ReAlignment

HRNS High Resolution Neutron Spectrometer

HTC High Tech Computer Corporation

IAF Inertial Amplification Factors

IEC International Electrotechnical Commission

IG ITER Grade

INCOSE International Council on Systems Engineering

IO ITER Organization

ISS Interspace Supporting Structure

ISSD ISS Datum system

ISO International Organization for Standardization

ITER International Thermonuclear Experimental Reactor

LAISE Late-Stage Add-In via Systems Engineering

LHS Left Hand Side

LOCA Loss of Coolant Accident

LOS Lines Of Sight

LTM Long Term Maintenance

LV Low Voltage

MBSE Model-Based Systems Engineering

MCNP Monte Carlo N-Particle

MD Major Disruption

NASA National Aeronautics and Space Administration

NF Norme Française

NOC Normal Operation Conditions

NOS Normal Operation State

PALEO Seismic event category

PCA Port Cell Assembly

PCAD Port Cell Assembly Datum system

PCSS Port Cell Supporting Structure

PBS Plant Breakdown Structure

PDR Preliminary Design Review

PHTS Primary Heat Transfer System

PIC Plant Instrumentation and Control

PLM Product Lifecycle Management

PMS Position Monitoring System

PPA Port Plug Assembly

PPAD Port Plug Assembly Datum system

Ra Roughness Average

RAM Random Access Memory

RAMI Reliability, Availability, Maintainability, Inspectability

RB RCC-MRx rule

RCC-MRx Design code for nuclear components

RGRS Radial Gamma Ray Spectrometer

RHS Right Hand Side

RNC Radial Neutron Camera

RT Room Temperature

sCD single Crystal Diamond

SE Systems Engineering

SIC Safety Important Class

SIR Structural Integrity Report

SL Service Level

SLS System Load Specifications

SMART Specific, Measurable, Achievable, Relevant, Time-bound

SMHV Seismic event category

SMS Seismic Margin Study

SSC Structures, Systems, and Components

SS Stainless Steel

SysML Systems Modeling Language

SVS Secondary Vacuum System

SWX Shieldwerk

TGCS Tokamak Global Coordinate System

TMP Temporary Mechanical Load

TSS Temperature Stabilization System

UF Usage Fraction

UI User Interface

UML Unified Modeling Language

V&V Verification and Validation

VDE Vertical Displacement Event

VR Virtual Reality

VV Vacuum Vessel

WDS Water Distribution System

List of Figures

List of Tables

Abstract

Complex engineering projects, characterized by extended lifecycles and intricate interdependencies among systems, are frequently susceptible to the emergence of unforeseen design challenges during advanced development stages. While traditional Systems Engineering (SE) and Engineering Change Management (ECM) processes provide a robust foundation, they often lack the targeted agility required to integrate major corrective subsystems late in the project lifecycle, potentially leading to significant cost overruns and schedule delays.

This dissertation addresses this limitation through the development and application of the Late-Stage Add-In via Systems Engineering (LAISE) framework. LAISE is a structured, seven-phase workflow designed to systematically manage the integration of corrective subsystems. Its foundational principles include the formalization of performance deviations into traceable requirement gaps, the establishment of explicit Interface Control Contracts, and the implementation of a targeted Verification & Validation strategy to minimize the scope of retesting.

The efficacy of the LAISE method is demonstrated through an in-depth case study involving the ITER Radial Neutron Camera (RNC), a diagnostic system for fusion power control. A comprehensive tolerance chain analysis revealed a substantial risk of mechanical misalignment between the Ex-Port RNC and its optical interfaces, which threatened the diagnostic's core measurement function. Guided by the LAISE framework, this research led to the design, integration, and validation of a bespoke Alignment System (AS). The case study documents the complete technical progression—from problem identification and AS design to validation via functional mock-up testing and Virtual Reality simulation—showcasing LAISE's role in ensuring configuration control, interface management, and full traceability within the ITER ENOVIA PLM system. The framework successfully guided the Ex-Port RNC subsystem from a Preliminary Design Review (PDR) to a Final Design Review (FDR) level of maturity.

The research concludes that the LAISE framework provides a validated, disciplined approach for enhancing project resilience against late-stage engineering changes.

It contributes a specialized procedural framework to the body of SE knowledge, demonstrating that complex late-stage integrations can be executed with rigor, thereby mitigating the disruptive impacts of unforeseen design modifications in high-stakes engineering environments.

Abstract

I progetti di ingegneria complessa, caratterizzati da cicli di vita estesi e intricate interdipendenze tra sistemi, sono frequentemente soggetti all'emergere di sfide progettuali impreviste durante le fasi avanzate di sviluppo. Sebbene i tradizionali processi di Systems Engineering (SE) e di Engineering Change Management (ECM) forniscano una solida base, spesso mancano dell'agilità mirata richiesta per integrare importanti sottosistemi correttivi in fase avanzata del ciclo di vita del progetto, con il potenziale di causare significativi sforamenti di costo e ritardi di programma.

Questa tesi affronta questa limitazione attraverso lo sviluppo e l'applicazione del framework Late-Stage Add-In via Systems Engineering (LAISE). LAISE è un flusso di lavoro strutturato in sette fasi, progettato per gestire sistematicamente l'integrazione di sottosistemi correttivi. I suoi principi fondamentali includono la formalizzazione delle deviazioni prestazionali in gap di requisiti tracciabili, l'istituzione di espliciti Interface Control Contract e l'implementazione di una strategia mirata di Verifica e Validazione (V&V) per minimizzare l'ambito delle attività di retesting.

L'efficacia del metodo LAISE è dimostrata attraverso uno studio di caso approfondito che coinvolge la Radial Neutron Camera (RNC) di ITER, un sistema diagnostico per il controllo della potenza di fusione. Un'analisi completa della catena di tolleranze ha rivelato un rischio sostanziale di disallineamento meccanico tra la RNC Ex-Port e le sue interfacce ottiche, che minacciava la funzione di misura centrale del diagnostico. Guidata dal framework LAISE, questa ricerca ha portato alla progettazione, integrazione e validazione di un Sistema di Allineamento (AS) su misura. Lo studio di caso documenta la completa progressione tecnica—dall'identificazione del problema e progettazione dell'AS alla validazione tramite test su mock-up funzionale e simulazione in Realtà Virtuale—dimostrando il ruolo di LAISE nel garantire il controllo di configurazione, la gestione delle interfacce e la piena tracciabilità all'interno del sistema PLM ITER ENOVIA. Il framework ha guidato con successo il sottosistema RNC Ex-Port da un livello di maturità di Preliminary Design Review (PDR) a uno di Final Design Review (FDR).

La ricerca conclude che il framework LAISE fornisce un approccio validato e

disciplinato per aumentare la resilienza del progetto contro modifiche ingegneristiche in fase avanzata. Contribuisce con un quadro procedurale specializzato al corpus di conoscenze della Systems Engineering, dimostrando che integrazioni complesse in fase avanzata possono essere eseguite con rigore, mitigando così gli impatti dirompenti di modifiche progettuali impreviste in ambienti ingegneristici ad alto rischio.

Chapter 1

Introduction

1.1 Objectives and Contribution

The primary objective of this research is to contribute to the broader implementation of Systems Engineering principles within the context of the ITER Radial Neutron Camera project (RNC).

1.2 Objectives and Contribution

The International Thermonuclear Experimental Reactor (ITER) stands as one of the most ambitious and complex scientific undertakings of our time. This multi-decade, international mega-project aims to demonstrate the feasibility of fusion energy, a pursuit that pushes the boundaries of engineering, physics, and large-scale project management. One of the ITER diagnostic systems is the Radial Neutron Camera (RNC), designed for controlling the fusion reaction by providing real-time measurements of neutron emission. This research is embedded within the challenge of designing and developing such a system, where immense complexity meets uncompromising precision.

The core objective of this dissertation is to address a recurrent and costly problem in large-scale engineering: the integration of essential corrective subsystems late in

the project lifecycle, when design maturity is high and the cost of change is severe. To this end, this work proposes, develops, and validates a novel methodological framework termed Late-Stage Add-In via Systems Engineering (LAISE). LAISE provides a structured, disciplined pathway to manage these critical interventions, ensuring they are executed with rigor, traceability, and minimal disruption to the established project baselines. This theoretical contribution is substantiated and demonstrated through its comprehensive application to a concrete and critical issue within the ITER RNC.

The author conducted the detailed tolerance chain analysis which quantified a critical design risk: potential mechanical misalignments between the Ex-Port RNC and the Diagnostic Shielding Module optical paths, a deviation that would undermine the diagnostic's measurement integrity by causing vignetting and erroneous line-of-sight positioning.

Driven by these findings, the author led the subsequent systematic investigation, design, and integration of a dedicated Alignment System (AS). This work involved conceiving a mechanical solution capable of adjusting the position of the entire 17-tonne Ex-Port structure along three translational degrees of freedom. To physically validate the alignment procedure, tooling, and measurement concepts, the author then designed, procured, and tested a functional, full-scale AS mock-up. This hardware validation proved the system's capability to achieve millimetric precision in compensating for the identified tolerance stack-ups.

Throughout this design evolution, the author was responsible for the CAD management and configuration control within the ITER ENOVIA PLM environment. This involved the creation, modification, and promotion of all relevant 3D models and 2D drawings for the Ex-Port RNC and the AS, ensuring strict version control, interface management, and traceability of every component and requirement within the ITER digital thread.

In parallel, to validate the maintainability of the detector cassettes, the author developed and deployed a Virtual Reality simulation. This immersive tool incorporated ergonomic guidelines from ITER standards to analyze and optimize human intervention for tasks such as detector replacement within the radioactive Port In-

terspace environment.

This research documents the complete design maturation of the RNC, structured around a clear progression. The In-Port subsystem is presented as a finalized design, having successfully passed its Final Design Review (FDR). For the Ex-Port subsystem, the thesis details its evolution from the Preliminary Design Review (PDR) stage. This baseline design then underwent a series validation activities: the VR simulation for maintenance V&V, a comprehensive structural assessment, and the application of the LAISE tool to manage the integration of the Alignment System, validated by the physical mock-up. The outputs and design modifications resulting from this structured process directly fed into the successful Ex-Port Final Design Review (FDR).

1.3 The ITER Project

ITER, meaning "the way" in Latin, is more than an experiment; it is a global partnership of nations including China, the European Union, India, Japan, Korea, Russia, and the United States. Its goal is unequivocal: to prove that nuclear fusion—the process that powers the stars—can be harnessed on Earth as a viable, large-scale, and carbon-free source of energy. Located in Cadarache, France, ITER seeks to achieve a ten-fold return on energy ($Q \geq 10$), producing 500 MW of fusion power from 50 MW of input heating power, and to sustain a burning plasma where the fusion reactions become the primary source of plasma heating.

The complexity of ITER is defining a new paradigm for engineering projects. It is a "system of systems" comprising approximately ten million individual components, each requiring precise specification, manufacturing, and integration. These components are sourced from hundreds of companies across the three dozen participating countries, necessitating unprecedented levels of international coordination and standardization. The machine itself operates under extreme conditions: intense neutron irradiation, extreme thermal loads, powerful magnetic fields, and ultra-high vacuum, all of which dictate exotic materials and novel engineering solutions.

Perhaps most challenging is the project's extended and irreversible timeline. With

construction spanning over a decade and operations planned for twenty years, ITER cannot afford design errors. This lifecycle demands a robust Systems Engineering (SE) approach to navigate the web of requirements, interfaces, and changes. It is within this context of complexity, long lifetime, and high stakes that the need for advanced SE tools like LAISE becomes beneficial for success.

1.4 The Radial Neutron Camera

The Radial Neutron Camera is a diagnostic for ITER, tasked with a mission critical to both machine operation and scientific discovery. Its purpose is to measure the spatial distribution and intensity of the neutrons born from the fusion reactions. By measuring the uncollided 14 MeV (from deuterium-tritium reactions) and 2.5 MeV (from deuterium-deuterium reactions) neutrons, the RNC provides data for evaluating fusion performance, controlling plasma stability, and ensuring compliance with safety licensing limits.

To capture a complete picture of the plasma, the RNC employs a two-part architecture that functions in unison. The In-Port RNC is embedded within the Port Plug, very close to the plasma. Its six Lines of Sight (LOS) are aimed at the plasma edge. The Ex-Port RNC, located further out in the diagnostic interspace, utilizes sixteen LOS to view the plasma core. This dual-system design is complementary: the In-Port system provides high-resolution data on the edge region, where gradients are steep and physics complex, while the Ex-Port system covers the broader core where the majority of fusion power is generated. The measurements from these two collimated fan-shaped arrays are computationally combined to reconstruct the full two-dimensional neutron emissivity profile across the plasma cross-section. This comprehensive profile is needed to derive parameters such as the fusion power density, the fuel mixture ratio, and the ion temperature.

The structure of this thesis reflects the distinct design maturity of the two RNC subsystems, offering a comparative study in engineering development. The In-Port RNC is presented as a system that has navigated the full design cycle, having reached the Final Design Review (FDR) stage. Its description serves as an exemplar of

applied Systems Engineering, showcasing a stable design where requirements have been validated, interfaces are frozen, and manufacturing readiness is achieved.

In contrast, the Ex-Port RNC description captures a dynamic journey of problem-solving and refinement. It begins at the Preliminary Design Review (PDR) stage, where the basic architecture and interfaces are established but detailed analyses reveal latent risks. The core of this thesis then documents the transition from PDR to FDR, a journey driven by the identification of a critical misalignment risk and solved through the application of the LAISE methodology. This process included the comprehensive tolerance analysis, the consequent design and integration of the Alignment System, the validation of maintenance operations via VR simulation, and the structural assessments. Therefore, this work not only describes the final Ex-Port RNC design but provides a detailed case study of the disciplined engineering process required to get there, highlighting how a late-stage, major design change was managed and resolved.

1.5 Thesis Structure

This dissertation is organized to guide the reader from principles, through methodological development, and into practical application. Chapter 2 establishes the background, reviewing core Systems Engineering concepts, requirements management, and the challenges of Engineering Change Management in complex projects. Chapter 3 introduces the novel LAISE framework, detailing its motivation, core characteristics, and its structured seven-phase workflow.

Chapter 4 forms the substantial application core of the thesis. It first provides an overview of SE within the ITER project and the specific design requirements of the RNC. It then presents the matured design of the In-Port RNC. The subsequent focus is on the Ex-Port RNC: beginning with its PDR design, it details the tolerance analysis that revealed the alignment crisis, and then walks through the complete LAISE-guided process of designing, integrating, and validating the corrective Alignment System, culminating in the Ex-Port RNC's FDR-ready design. Finally, Chapter 5 synthesizes the conclusions of this research, reflecting on the demonstrated efficacy

of the LAISE method and its implications for managing complexity in future engineering endeavors.

The use of documents and technical reports and their contents within this work has been approved by ITER Organization, Fusion For Energy and RNC Consortium.

Chapter 2

Background

2.1 Systems Engineering

2.1.1 Definitions and Core Principles of SE

Systems Engineering (SE) is a multidisciplinary, iterative methodology focused on the successful design, creation, and management of intricate systems across their entire lifespan, from conception through development, deployment, operation, maintenance, and eventual decommissioning [1]. It establishes a systematic, disciplined framework for translating stakeholder requirements into a functional system [2]. According to the INCOSE Systems Engineering Handbook, Systems Engineering is defined as "*an interdisciplinary approach and means to realize successfully an innovative system, with a life cycle perspective, considering business reality, needs, and constraints of customers and stakeholders*". At NASA, "*systems engineering*" is defined as "*a methodical, multi-disciplinary approach for the design, realization, technical management, operations, and retirement of a system*" [3]. Furthermore, the handbook elaborates on this by defining a "*system*" as "*the combination of elements that function together to produce the capability required to meet a need*" [3]. These elements encompass "*all hardware, software, equipment, facilities, personnel, processes, and procedures needed for this purpose*" [3]. The handbook also highlights that Systems Engineering is "*a way of looking at the 'big picture' when making techni-*

cal decisions," aimed at "achieving stakeholder functional, physical, and operational performance requirements in the intended use environment over the planned life of the system within cost, schedule, and other constraints" [3]. It is also described as "*a methodology that supports the containment of the life cycle cost of a system*" [3]. The fundamental tenets of SE emphasize a holistic perspective, ensuring that all system elements—including functionality, interfaces, performance, cost, and schedule—are considered from inception to retirement [4]. This integrated approach is vital for managing complexity, mitigating risks, and guaranteeing that the final system accurately fulfills its intended purpose and operates as anticipated [5]. The primary goal of SE is to transform an operational need into a defined system configuration and to manage that configuration throughout its entire life [4]. The effective implementation of a rigorous Systems Engineering program is critical for project success, particularly in managing stakeholder needs and requirements throughout the system's lifecycle [4]. For large-scale, complex initiatives like ITER, a comprehensive systems engineering framework is essential for coordinating diverse activities and maintaining project coherence [1]. This systematic approach encompasses both technical processes and management processes, ensuring that all aspects of the system's development and operation are planned and controlled [1]. The discipline of Systems Engineering is characterized by its emphasis on a robust lifecycle perspective, ensuring that all technical and management activities are integrated and considered throughout the entire system's existence. This holistic view aims to balance competing requirements and constraints, optimize system performance, and minimize risks associated with complexity and uncertainty. By adhering to these principles, SE aims to deliver systems that are not only technically sound but also meet the evolving needs of stakeholders and adapt to changing environments.

2.1.2 Key SE Processes and Methodologies

The application of Systems Engineering involves a series of interconnected processes and the adoption of various methodologies designed to manage the complexity inherent in large-scale projects. These processes are often visualized through lifecycle

models, with the "V-model" being a traditional, widely recognized representation. However, modern SE incorporates more iterative and flexible approaches to adapt to dynamic project environments. Key SE processes and methodologies include:

1. Requirements Engineering: This foundational phase involves systematically identifying, documenting, and managing the needs and constraints of the system. It encompasses:

    - Requirements Elicitation: Gathering information from stakeholders through various techniques to understand what the system must do. For ITER, Project Requirements are decomposed into system requirements and further into sub-system and component requirements as the design matures [1]. The "Systems Requirement Definition" is a top-down process aimed at identifying the Project Requirements to be fulfilled by a specific Plant Breakdown Structure element [1]. This process is based on the system requirements definition process as defined in ISO 15288 [1].
    - Requirements Analysis: Refining and categorizing requirements to ensure they are clear, unambiguous, verifiable, and consistent. For ITER, these requirements are applied to successive levels of the PBS and repeated at the same level for each Configuration Item and project phase to trace the evolution of designs and project maturity [1].
    - Requirements Specification: Documenting requirements in a formal and traceable manner, often linking them to higher-level needs and lower-level design elements. This ensures traceability from initial needs to final system components.
    - Requirements Validation: Confirming that the specified requirements accurately reflect the true needs of the stakeholders and are achievable.

2. Architectural Design: This process defines the high-level structure and organization of the system, breaking it down into major subsystems and components. It focuses on:

- System Decomposition: Dividing the complex system into manageable parts, defining their boundaries and responsibilities. The ITER Plant Breakdown Structure is detailed at various levels, from system to subsystem and assembly/loop, ensuring each element can be uniquely identified, designed, and manufactured [1]. This decomposition helps in managing complexity by allowing engineers to focus on smaller, more defined units.
- Interface Definition: Specifying how different components and subsystems interact with each other and with external systems. Clear interface definitions are crucial for ensuring seamless integration and interoperability between different parts of the system.
- Trade-off Analysis: Evaluating alternative architectures against defined criteria to select the optimal solution. This involves assessing various design options based on factors such as performance, cost, reliability, and manufacturability to ensure the most suitable architecture is chosen.

3. Detailed Design: This phase elaborates on the architectural design, detailing the internal workings of each subsystem and component. It involves:

    - Component Specification: Defining the specific characteristics, parameters, and behaviors of individual parts, including their physical dimensions, material properties, performance metrics, and operational limits.
    - Material Selection and Manufacturing Considerations: Incorporating practical aspects related to production and assembly early in the design process is crucial. This proactive approach helps avoid costly redesigns later by ensuring that chosen materials are feasible to procure and work with, and that manufacturing processes align with available technologies and capabilities. Early consideration also facilitates the optimization of the system for cost-effectiveness and timely production, directly impacting project feasibility and success.

- CAD-centric approaches play a fundamental role here, translating abstract designs into precise digital models [6].

4. Implementation/Realization: This involves the actual creation or acquisition of system components based on the detailed design specifications.

5. Integration: As individual components are realized, they are progressively assembled and connected to form larger subsystems, and eventually the complete system. This phase manages the interfaces between components to ensure they work together seamlessly.

6. Verification: This process confirms that the system has been built correctly, according to its specified requirements and design. It answers the question: "Are we building the system right?" This involves testing and analysis throughout the development lifecycle, from unit testing to subsystem and system-level verification [4]. For ITER, requirements are verified to ensure the system is built the right way [1].

7. Validation: This critical process ensures that the right system has been built — meaning it meets the actual needs and expectations of its stakeholders and users in its intended operational environment. It answers the question, "Are we building the right system?" Validation typically occurs later in the lifecycle, often involving operational testing and user acceptance [4]. For ITER, requirements are validated to ensure the right system is built [1]. This validation process extends throughout the design phases, from conceptual to manufacturing design, with verification matrices initiated early to track compliance [1]. Furthermore, the comprehensive use of digital mock-ups facilitates this validation by enabling virtual prototyping and simulation of complex systems like the ITER Remote Handling system, thereby reducing the need for costly physical prototypes [7].

2.1.3 Evolution of SE in Complex Projects

The field of Systems Engineering has undergone significant evolution, driven by the increasing scale and complexity of modern projects. Initially focused on hardware development, SE has broadened its scope to encompass software, human-system interaction, and intricate organizational dynamics [5]. This expansion is a direct response to the need to manage vast interdependencies and cross-disciplinary integration. Contemporary SE actively incorporates agile methodologies to address rapidly changing requirements and shrinking development times, particularly for dynamic and interdisciplinary products like mechatronic systems [5, 8]. Research in engineering design methods continuously synthesizes and refines these approaches, aiming for improved problem-solving capabilities and fostering innovation across the discipline [9]. SE also recognizes the inherent ambiguities and uncertainties in design, necessitating adaptable strategies for managing often conflicting requirements and emerging knowledge [10, 11]. Furthermore, the role of SE paradigms in both education and practice is continually adapting to incorporate principles of sustainable development, reflecting a broader societal responsibility [12].

2.2 Tools and methodologies of SE

Systems Engineering relies on a diverse set of tools and methodologies to effectively manage the complexity of large-scale projects, facilitating collaboration, data management, and decision-making across the lifecycle. These tools can broadly be categorized by their primary function within the SE process.

The V-Model

A classic sequential lifecycle model that illustrates the relationship between development phases and corresponding testing activities [1]. The left side of the "V" represents decomposition and definition (requirements, high-level design, detailed design), while the right side represents integration and verification (unit testing, integration testing, system testing, acceptance testing) [4]. The traditional V-model

is a 2-dimensional representation of a multi-dimensional concept, as shown in Figure 2.1. In a complex system of systems such as the ITER machine, there are multiple V-models in development at different levels of maturity, each connected through defined interfaces [1].

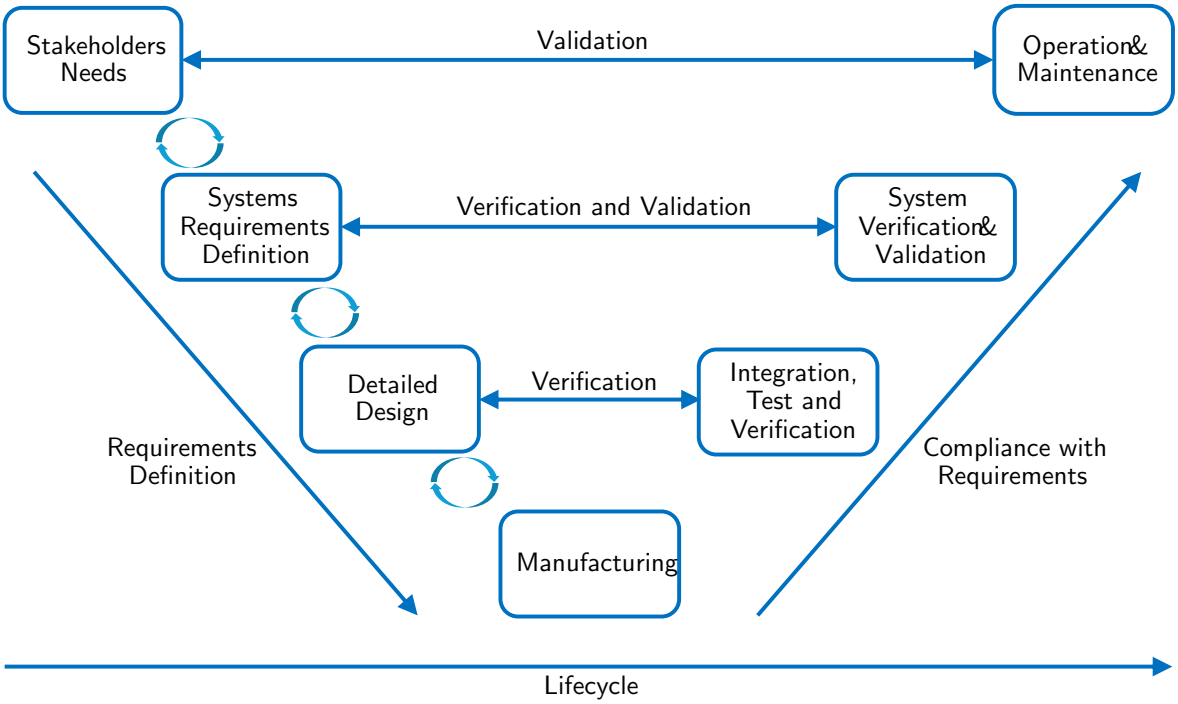

Figure 2.1: An example of V-model ([13]).

A full description of the V-model will be discussed in the Section 4.1.1, where the application of the SE approach to the ITER project and the RNC system is described.

Iterative and Recursive Processes

For complex systems like ITER, processes are both iterative and recursive. Iterative means that the same processes are repeated on the same systems, and recursive means that the same processes are repeated at successive levels of a system [1]. This allows for continuous refinement and adaptation. This iterative approach enables early

identification and mitigation of risks, while recursion facilitates managing complexity by applying consistent engineering principles across different hierarchical levels of the system [1].

Model-Based Systems Engineering

This approach emphasizes the use of models as the primary means of information exchange and collaboration throughout the system lifecycle, rather than relying solely on document-centric approaches. MBSE enables more precise communication, automated analysis, and better traceability. The concept of managing complex product dimensional quality through a "Closed Loop PMI Driven Dimensional Quality Lifecycle Management Approach for Smart Manufacturing System" [14] strongly implies a model-driven, integrated approach to managing system data and properties. Similarly, the development and use of Digital Twins are intrinsically linked to MBSE principles, as they rely on robust system models. MBSE tools enable the creation and management of system models using standardized modeling languages like SysML and UML [15]. These tools support the visualization, analysis, and simulation of system architectures, behaviors, and interfaces. MBSE tools facilitate early validation of design concepts, improve communication among multidisciplinary teams, and provide a single source of truth for system information, thereby reducing errors and rework [15].

Requirements Management Tools

Requirements management tools are central to ensuring that stakeholder needs are captured, tracked, and fulfilled. These tools support the elicitation, analysis, specification, verification, and validation of requirements, providing traceability throughout the system lifecycle. Key features include version control, change management, baseline control, and reporting capabilities. Effective requirements management ensures a common understanding among all stakeholders and forms the basis for design, development, and testing activities [16].

Configuration Management Tools

Configuration management tools are essential for maintaining the consistency and integrity of a system throughout its lifecycle. They manage changes to baselines, track versions of software, hardware, and documentation, and control access to configuration items. In the context of large engineering projects, CM ensures that all project artifacts are identifiable, controlled, and that changes are managed systematically, supporting traceability and accountability. [17, 18]

Product Lifecycle Management Systems

PLM systems provide a comprehensive framework for managing product data and processes across its entire lifecycle, from ideation to end-of-life [19]. These integrated platforms encompass various SE tools, including CAD/CAM, requirements management, configuration management, and project management functionalities. PLM systems centralize data, automate workflows, and facilitate collaboration among geographically dispersed teams, serving as the backbone for managing complex product development processes. They are crucial for maintaining a "digital thread" that connects all aspects of a product's definition and evolution [20].

Simulation and Analysis Tools

Simulation and analysis tools are vital for predicting system performance, identifying potential issues, and optimizing designs before physical prototyping. These include finite element analysis software for structural and thermal analysis, computational fluid dynamics tools for fluid flow simulations, and specialized simulation environments for various engineering disciplines. These tools enable engineers to perform "what-if" scenarios, validate design assumptions, and refine system parameters, significantly reducing development time and costs.

2.3 Requirements Management

Requirements management is a cornerstone of effective Systems Engineering, ensuring that the development efforts are aligned with stakeholder needs and project objectives [21] [16]. It is a continuous process that spans the entire system lifecycle, from initial concept to deployment and beyond [22] [3]. This iterative process is fundamental for maintaining project alignment and adapting to the dynamic nature of complex systems.

2.3.1 Principles of Effective Requirements Management

Effective requirements management is guided by several key principles:

- Completeness: Requirements should capture all necessary functions, performance criteria, interfaces, and constraints of the system.
- Consistency: Requirements must not contradict each other [22]. Inconsistencies can lead to design flaws and rework.
- Clarity and Unambiguity: Each requirement should be stated precisely, with no room for misinterpretation [22]. Vague language can result in systems that do not meet user expectations.
- Verifiability: Requirements must be testable or measurable [3]. If a requirement cannot be verified, it is difficult to determine whether the system successfully meets it.
- Traceability: Requirements should be traceable forward to design, implementation, and test cases, and backward to originating stakeholder needs [23]. This enables impact analysis for changes and facilitates validation.
- Prioritization: Requirements should be prioritized to guide design decisions, especially when faced with resource constraints or trade-offs [24].

- Manageability: The set of requirements must be manageable, organized in a structured manner that supports maintenance and evolution.

Another efficient way to identify the core characteristics of the requirements is summed-up by the SMART acronym. The SMART criteria provide a framework for creating well-defined and effective requirements or objectives, ensuring they are clear, actionable, and trackable [25]. This acronym stands for Specific, Measurable, Achievable, Relevant, and Time-bound [25] (Figure 2.2).

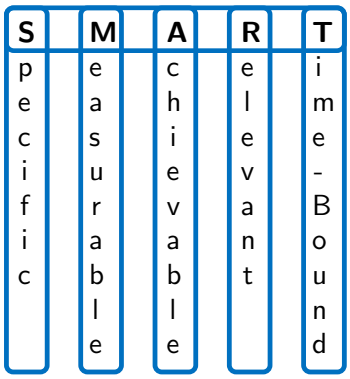

Figure 2.2: The SMART criteria.

- **Specific**: A requirement should clearly and precisely define what needs to be accomplished, leaving no room for ambiguity or misinterpretation. It should answer questions like "What exactly needs to be done?", "Who is involved?", and "Why is this important?" [25]. This aligns with the principle of "Clarity and Unambiguity" in effective requirements management, ensuring that vague language does not lead to systems that fail to meet user expectations. Ambiguity in requirements can significantly hinder large-scale projects and lead to poor project selection decisions [26].

- **Measurable**: It must be possible to quantify or evaluate whether a requirement has been met. This involves establishing clear metrics or indicators of progress and success [25]. A requirement's verifiability is paramount; if it cannot be measured, it's difficult to confirm if the system successfully fulfills it.

This aspect helps define the criteria for acceptable performance, such as how much, how often, how fast, or how accurate the outcome should be [27].

- **Achievable**: The requirement should be realistic and attainable given the available resources, constraints, and timeframes. While challenging, it should not be impossible to achieve [25].
- **Relevant**: The requirement needs to align with the overall project goals and organizational objectives. It should contribute meaningfully to the project's success and be worthwhile pursuing [25]. For researchers, having a SMART focus is essential to achieve desired results [28].
- **Time-bound**: A clear deadline or timeframe must be associated with the requirement, establishing a sense of urgency and providing a target for completion. This helps in planning and tracking progress [25].

By ensuring requirements adhere to the SMART principles, teams can improve communication, facilitate accurate design and development, and enable robust verification and validation processes, ultimately contributing to project success [28]. The application of SMART goals can also be adapted to various fields, including science diplomacy, to set clear, achievable, and measurable objectives [29].

2.3.2 Requirements Traceability and its Importance

Requirements traceability, the ability to link requirements to other related artifacts, is paramount in complex projects [30]. It provides:

- Impact Analysis: When a requirement changes, traceability allows for quick identification of all affected components, tests, and documentation, enabling accurate assessment of the change's impact [23]. This prevents unforeseen ripple effects and aids in maintaining system integrity.
- Verification and Validation: It ensures that every requirement is tested and validated, and that no extraneous functionality is built [3]. Traceability also

serves as a critical mechanism for maintaining bidirectional links between stakeholder expectations, system requirements, design documents, and test procedures throughout the product lifecycle.

- Coverage Analysis: Traceability matrices can demonstrate that all parts of the system are covered by requirements and vice versa. Furthermore, robust traceability supports regulatory compliance by providing an auditable record of the system's development against specified requirements.

- Compliance: It helps demonstrate compliance with regulatory standards and contractual obligations [31]. This bidirectional linkage is essential for effective change management, as modifications to requirements often necessitate corresponding adjustments in design, implementation, and testing to maintain data consistency across the development lifecycle [32].

- Improved Communication: A clear traceability framework enhances understanding among stakeholders about how specific needs are being addressed in the system [30].The strong impact of traceability completeness on the defect rate suggests that traceability is of great practical value for any kind of project, even if it is not mandated by a standard or regulation [33].

2.3.3 Challenges in Requirements Management

Despite its critical importance, requirements management in large-scale projects faces significant challenges:

- Evolving Requirements: Stakeholder needs can change throughout a long project lifecycle, necessitating robust change management processes [34]. This evolution often arises from new market insights, technological advancements, or a deeper understanding of user needs as the project progresses.

- Complexity and Volume: Managing thousands or even millions of interconnected requirements manually is impractical and error-prone [35]. The sheer

scale and interdependencies between requirements in large systems demand specialized tools and methodologies for effective oversight.

- Stakeholder Communication: Bridging the gap between diverse stakeholder perspectives and technical specifications can be difficult. Ensuring that all stakeholders, from end-users to technical teams, have a shared understanding of the requirements is a significant challenge.

- Tool Integration: Ensuring seamless integration between requirements management tools and other SE tools is often complex. The diversity of tools used in systems engineering and the need for data interoperability create significant integration hurdles.

- Scope Creep: Uncontrolled addition of new requirements can lead to project delays and budget overruns. Without a stringent process for evaluating and approving new requirements, projects can deviate significantly from their original objectives.

- Ambiguity and Incompleteness: Poorly written or incomplete requirements are a persistent challenge, leading to misunderstandings and design flaws.Addressing these challenges requires a disciplined approach, the appropriate application of requirements management tools, and continuous communication among all project participants. Furthermore, the integration of model-based systems engineering methodologies can significantly mitigate these challenges by providing a holistic framework for requirements definition, analysis, and verification [32].

2.4 Engineering Change Management

Engineering Change Management (ECM) is a systematic process for managing modifications to a product's design, documentation, and processes throughout its lifecycle [36, 37]. In complex engineering projects, changes are inevitable due to evolving requirements, design flaws, manufacturing issues, technological advancements,

or lessons learned [38, 39]. Effective ECM ensures that these changes are controlled, documented, and implemented efficiently, minimizing negative impacts on cost, schedule, and quality [40]. Engineering changes can make a significant impact on various process chains, both internal and external to the company, leading to considerable error costs and time shifts, with 30 to 50 percent of development costs often attributed to technical changes [39].

2.4.1 Engineering Change Process

A typical engineering change process follows a structured workflow, often involving several key steps [32, 37], as shown in fig. 2.3.

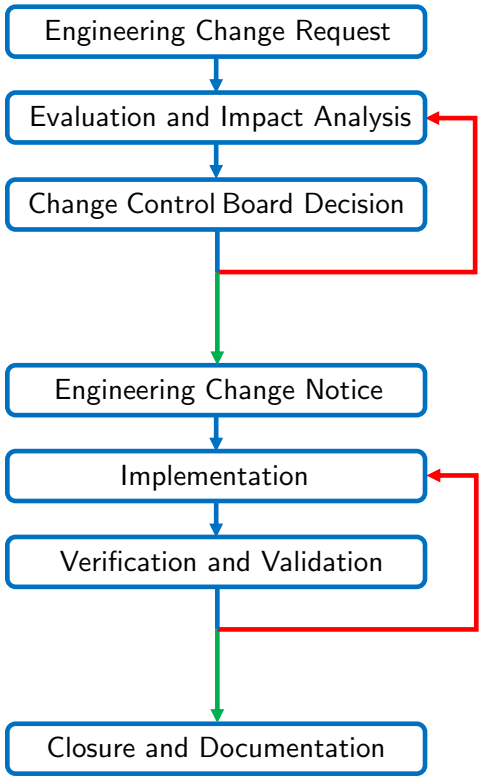

Figure 2.3: Example of Engineering Change Process.

The steps are:

1. **Engineering Change Request:** The process begins with the identification of a need for a change, documented in a formal request [32]. This request outlines the proposed modification, the reasons for it, and its perceived benefits [32].

2. **Evaluation and Impact Analysis:** The proposed change undergoes a thorough evaluation by relevant stakeholders (e.g., engineering, manufacturing, quality, procurement) [38]. This includes assessing its technical feasibility, potential impact on other components and systems, cost implications, schedule adjustments, and risks [32, 41]. Tools such as MBSE models [32] and PLM systems [42] are invaluable in performing accurate impact analyses.

3. **Change Control Board Decision:** Based on the evaluation, the change is either approved, rejected, or sent back for further refinement [3]. In large organizations, a Change Control Board comprising representatives from various departments makes this decision, ensuring all perspectives are considered [3].

4. **Engineering Change Notice:** Once approved, an official Engineering Change Order or Engineering Change Notice is issued [43]. This document formally authorizes the change and specifies all necessary modifications to design, documentation, manufacturing processes, and affected parts. It includes detailed instructions and identifies all affected items and their new revisions.

5. **Implementation:** The authorized change is then implemented across all relevant areas, including updating CAD models, drawings, manufacturing instructions, and software code [44]. This step requires careful coordination to ensure all affected departments apply the change consistently.

6. **Verification and Validation:** After implementation, the modified system or component undergoes verification and validation to confirm that the change has been correctly applied and that the system still meets its intended requirements without introducing new issues [32].

7. **Closure and Documentation:** The change process concludes with formal closure, where all documentation is updated, baselines are re-established, and lessons learned are captured for future reference [32].

2.4.2 Challenges in Engineering Change Management

Managing engineering changes in complex projects presents several challenges:

- Late-Stage Changes: Changes introduced late in the project lifecycle are typically more expensive and disruptive due to the extensive rework and re-testing required [32]. Engineering changes are generally getting more elaborate and expensive the later they occur within the development process, since more parts of the system are already defined [32]. This increased cost and disruption stems from the need to modify already established design elements, components, and potentially even manufacturing processes, as well as re-validate integrated systems.

- Communication and Coordination: Ensuring consistent communication and coordination among numerous stakeholders, particularly in globally distributed projects, is difficult [45]. Miscommunication of design change can generate significant cost and delay [43], leading to errors, duplicated efforts, and missed deadlines.

- Maintaining Baselines: Accurately tracking and controlling multiple baselines and versions of design artifacts is complex, necessitating robust configuration management practices [20]. Failure to maintain clear and accurate baselines can result in the wrong versions of designs or documentation being used, causing significant rework and project delays.

- Impact Assessment Accuracy: Inaccurate or incomplete impact assessments can lead to unforeseen problems downstream, increasing costs and delays [38]. A thorough understanding of all potential ripple effects across systems, subsystems, and processes is crucial for effective change management.

- Resistance to Change: Human factors, including resistance to change from project teams, can impede efficient implementation. Overcoming this requires strong leadership, clear communication of benefits, and involving teams in the change process.

Effective ECM is critical for maintaining product quality, controlling costs, and ensuring project schedule adherence in dynamic development environments [46]. It provides the structured approach necessary to adapt to new information and overcome unforeseen technical hurdles.

2.5 Summary

This chapter has established the foundational understanding of Systems Engineering, detailing its core principles, essential processes (Requirements Engineering, Architectural Design, Detailed Design, Implementation, Integration, Verification, and Validation), and various key methodologies. It highlighted the evolution of SE in complex projects and its indispensable role in mega-projects like ITER. Furthermore, the chapter explored the critical tools that underpin SE practices, including dedicated software for requirements management, MBSE, configuration management, comprehensive PLM systems, and various simulation and project management tools. A detailed discussion on Requirements Management emphasized the principles, importance of traceability, and common challenges. Finally, the chapter delved into Engineering Change Management, outlining its structured process and the inherent difficulties in managing design modifications in complex environments. This comprehensive background sets the stage for introducing a novel methodology, LAISE, designed to specifically address the challenges of late-stage integration in such projects.

Chapter 3

Methodology

This chapter presents the novel SE tool, named LAISE - Late-Stage Add-In via Systems Engineering. The LAISE tool is a purpose-driven framework designed to enable the seamless integration of new corrective subsystems at an advanced stage of a complex engineering project. The chapter presents the novelty of the LAISE tool, its core characteristics and the schematic workflow.

3.1 Motivations

In complex, large-scale engineering projects, despite rigorous Systems Engineering practices, the emergence of unforeseen design challenges or performance deviations at advanced stages of development is not uncommon [41]. These issues can arise from new scientific understanding, unexpected interactions between subsystems, limitations exposed during detailed analysis (e.g., tolerance stack-up violations, thermal performance issues), or changes in external conditions. When such a deviation indicates that an original system requirement cannot be met with the existing design, a corrective subsystem or significant modification becomes necessary. Systems integration itself is a major challenge, with technical, project, organizational, or environmental problems often arising from improper integration [47]. This requires a flexible and adaptive process to make constituent parts of systems work together [48].

Integrating a new, corrective subsystem late in the project lifecycle presents substantial challenges [49]. Traditional change management processes, while robust, may struggle with the increased complexity and potential for cascading impacts on mature designs, tightly integrated interfaces, and already optimized schedules and budgets [41]. Rework, extensive re-validation, and potential delays can be prohibitive. There is a clear need for a specialized methodology that can efficiently and systematically manage these "late-stage add-ins" by leveraging core SE principles and modern digital engineering tools, thereby minimizing disruption and ensuring the successful delivery of project objectives.

3.2 Late-Stage Add-In via Systems Engineering

To address this specific critical gap, this thesis proposes the original design method that has been called LAISE. The Late-Stage Add-In via Systems Engineering method is a newly-developed, purpose-driven framework designed to enable the seamless integration of new corrective subsystems at an advanced stage of a complex engineering project. It is specifically triggered when tolerance analyses, performance testing, or verification activities reveal that an original requirement cannot be met with the existing design, necessitating a significant design intervention. The LAISE method formalizes this intervention within a structured Systems Engineering context, leveraging a PLM-centric environment and MBSE capabilities to ensure control, traceability, and minimized impact.

3.2.1 Core Characteristics of LAISE

The LAISE method is characterized by several key features that enable its effectiveness in managing late-stage integrations:

- **Purpose-driven:** Its explicit goal is to facilitate the integration of a new corrective subsystem at an advanced stage of a complex engineering project. This focus differentiates it from general engineering change processes by targeting

a specific type of intervention—one necessitated by an identified requirement gap.

- **Requirement Gap Formalization:** A critical characteristic of LAISE is its approach to defining the problem. Any identified deviation or inability to meet an original requirement is formally treated as a requirement gap. This gap is then translated into a new, derived, or modified requirement. This rigorous formalization ensures consistency with established Systems Engineering practice and prevents ad-hoc, poorly documented fixes, maintaining the integrity of the requirements baseline.

- **Interface Contracting:** Recognizing the critical importance of boundaries in late-stage integrations, LAISE mandates the establishment of an explicit Interface Control Contract. This contract precisely defines the geometric, dimensional, thermal, and functional boundaries between the existing system and the new late-stage subsystem. This formal agreement minimizes ambiguities and prevents interface mismatches, a common source of errors and delays.

- **PLM-centric:** The method is fundamentally built upon a robust Product Lifecycle Management environment, specifically leveraging a "Digital Thread" approach (e.g., using ENOVIA). All associated requirements, parts, interfaces, manufacturing processes, and verification activities related to the new subsystem and its interactions with the existing system are meticulously linked within this single PLM environment [19]. This provides global visibility, ensures stringent change governance, and maintains comprehensive configuration control across all affected project artifacts [20]. The ability to integrate and manage information from various sources across the product lifecycle is crucial for complex construction projects [50].

- **MBSE Impact Analysis:** LAISE integrates Model-Based Systems Engineering principles to perform rigorous impact analysis. Using SysML or equivalent system models, engineers can map how the new subsystem affects existing requirements, functions, interfaces, and Verification & Validation activities [15].

MBSE offers significant potential for enhancing systems engineering activities by providing a formal and consistent representation of the system [15]. This allows for the generation of an impact matrix and enables the exploration of *what-if* scenarios for different design alternatives before committing to a solution, optimizing decision-making [51].

- **Tolerance & Interface Budgeting:** For mechanical systems in high-precision environments (like ITER-like diagnostics), LAISE emphasizes the introduction of dimensional/geometric stack-up analysis. This enables the allocation of alignment error budgets across interacting components. This detailed analysis is crucial for ensuring manufacturability, assemblability, and performance within tight tolerances.

- **Targeted V&V:** To minimize cost and schedule impact, LAISE focuses Verification and Validation efforts specifically on the *impacted requirements and interfaces*. This "test debt pay-down" approach avoids the need for full retesting of the entire system, significantly reducing the burden of late-stage changes while still ensuring the functional integrity of the modified system.

- **Governed Change Implementation:** The method operates within a formally governed Engineering Change process. It follows a standard workflow (ECR $\rightarrow$ evaluation $\rightarrow$ CCB decision $\rightarrow$ ECN), ensuring that all changes are systematically reviewed, approved, and documented. This structured approach facilitates knowledge capture and embeds lessons learned for future reuse in similar contexts [32].

3.2.2 LAISE Operational Workflow

The LAISE method follows a seven-phase operational workflow, designed to guide the integration of late-stage corrective subsystems systematically (Figure 3.1).

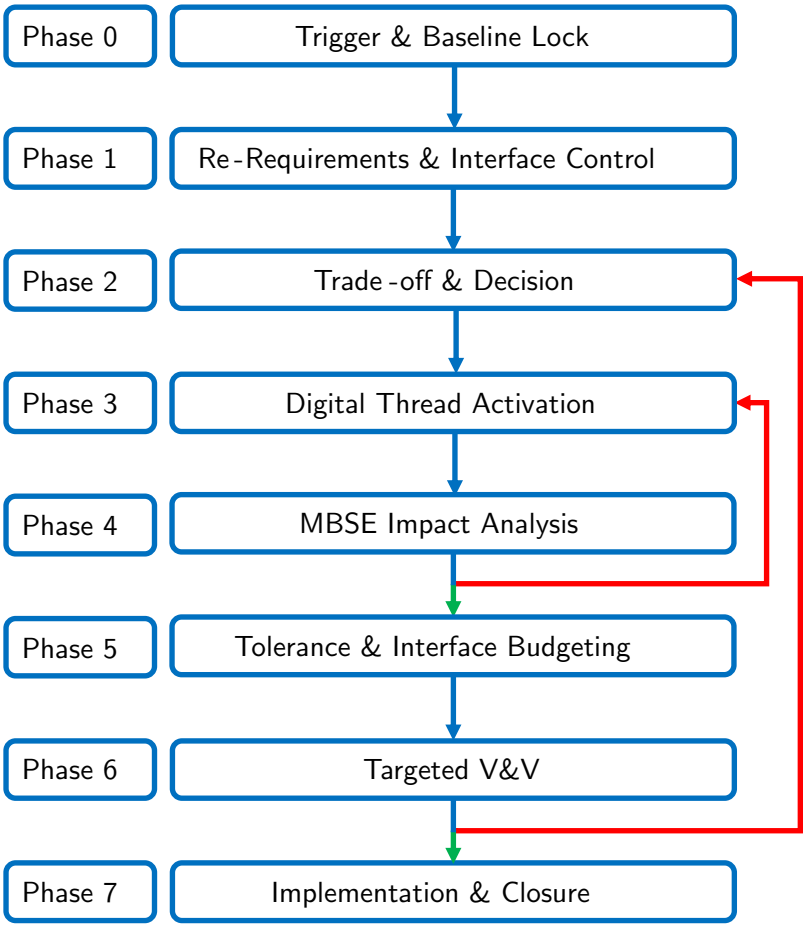

Figure 3.1: The LAISE workflow.

The phases are:

- **Phase 0 — Trigger & Baseline Lock:**
  - Trigger: The workflow is initiated when a significant requirement deviation is identified, typically through a tolerance violation, performance gap, or other verification failure.
  - Baseline Lock: The current system baseline is formally frozen within the PLM environment to create a stable reference point for the change.

  - ECR Raised: An Engineering Change Request is officially raised to initiate the change process [37, 43].

- **Phase 1 — Re-Requirements & Interface Control:**
  - Requirement Update: The existing requirement set is updated to reflect the identified gap, leading to the definition of new, derived, or modified requirements that the corrective subsystem must satisfy [3].
  - Interface Control Established: A formal Interface Control is created, precisely defining the technical and operational boundaries between the existing system and the proposed late-stage subsystem [3].
- **Phase 2 — Digital Thread Activation:**
  - PLM Linkage: All new and modified requirements are linked to corresponding design elements, assemblies, manufacturing processes, and test procedures within the PLM system (e.g., ENOVIA) [19, 52].
  - Configuration Management Update: The configuration management system is updated to reflect the planned changes, ensuring traceability and version control for all affected artifacts [52, 53].
- **Phase 3 — MBSE Impact Analysis:**
  - Model Update: System models are updated to represent the system both with and without the proposed new subsystem, allowing for comparative analysis [15, 32].
  - Impact Matrix Generation: An "impact matrix" is generated, systematically mapping the relationships and impacts across requirements, parts, interfaces, and test procedures [41, 51].
- **Phase 4 — Tolerance & Interface Budgeting:**
  - Dimensional/Geometric Stack-up: A detailed dimensional and geometric stack-up analysis is performed to ensure physical compatibility and performance within specified tolerances.

  - Error Budget Allocation: Error budgets are formally allocated across the interacting components, and sensitivity analyses are executed to understand the system's robustness to manufacturing and assembly variations.

- **Phase 5 — Trade-off & Decision:**
  - Alternative Comparison: Different alternative solutions for the corrective subsystem are rigorously compared based on technical performance, cost, risk, schedule implications, and safety considerations [3].
  - CCB Decision: The Change Control Board reviews the analysis and trade-offs, makes a formal decision, and authorizes the preferred solution [3].
  - Baseline Update: The system baseline is updated to incorporate the approved design for the corrective subsystem.

- **Phase 6 — Targeted V&V:**
  - Test Plan Generation: A specific test plan is generated, focusing only on the requirements and interfaces directly affected by the new subsystem [3]. This avoids unnecessary full-system retesting.
  - Documentation: Acceptance criteria for the new subsystem are thoroughly documented within the PLM system [3]. Technical reports are consequently produced to keep trace of the completed work.

- **Phase 7 — Implementation & Closure:**
  - Subsystem Integration: The corrective subsystem is physically integrated into the existing system.
  - ECN Issuance and Baseline Update: An Engineering Change Notice is issued to formally document the completed change, and the system baseline is updated to reflect the final as-built configuration [43].
  - Lessons Learned: Key lessons learned throughout the LAISE process are meticulously recorded to inform and improve future similar interventions [32].

This structured workflow ensures that late-stage integrations are managed with the same rigor as initial design phases, providing transparency, control, and efficiency in complex project environments.

Chapter 4

Application of the LAISE tool to the ITER RNC

The implementation of the LAISE methodology within the context of the ITER RNC serves as a critical case study to validate its efficacy in managing complex, late-stage engineering changes within high-precision, large-scale scientific projects [54].

Prior to presenting the case study on the integration of the Alignment System with the RNC, this section will outline the application of the Systems Engineering approach to the ITER project. Subsequently, it will detail the RNC's design requirements and elucidate how these requirements influenced its final design. Finally, the critical issue concerning the misalignment of the lines of sight will be addressed, followed by the application of the LAISE tool in order to integrate the Alignment System.

4.1 Overview on the ITER project

This section presents the ITER project with a focus on the Systems Engineering principles application, highlighting the necessity of SE theory for dealing with complex systems such as ITER.

The International Thermonuclear Experimental Reactor - ITER, whose name

means “the way” in Latin, is a globally collaborative and highly ambitious scientific endeavor currently under construction in St Paul-lez-Durance, southern France [55]. It involves a broad partnership including the European Union (along with Switzerland), China, India, Japan, the Russian Federation, South Korea, and the United States [55]. The fundamental objective of the ITER project is to demonstrate the scientific and technological feasibility of fusion as a viable energy source for the future [56], [55], [57]. Given its immense scale, comprising approximately 10 million parts and thousands of intricate interfaces, coupled with a projected timeline of over ten years for construction and commissioning followed by two decades of operation, ITER represents an unprecedented challenge in nuclear fusion research [52], [56]. This complexity necessitates a robust system engineering approach to ensure design consistency, effective project management, and seamless collaboration among international contributors [52].

4.1.1 Application of Systems Engineering to the ITER project

The ITER project exemplifies the critical role of Systems Engineering in managing highly complex engineering initiatives. ITER is characterized by its immense scale, comprising approximately 10 million parts and thousands of intricate interfaces that require identification and control [52]. Given the project’s extended duration—with construction and commissioning anticipated over ten years, followed by two decades of operation—the application of a robust SE framework is essential to navigate its technical and managerial complexities [52].

Systems Engineering on the ITER project is defined as an interdisciplinary approach aimed at integrating all engineering disciplines and specialized groups into a cohesive effort to achieve project objectives [52]. This systematic methodology focuses on managing essential requirements, conducting integrated system analysis, and establishing a structured development process that spans the entire system lifecycle [52]. This lifecycle encompasses the initial concept phase, through design, delivery, fabrication, installation, operation, maintenance, and ultimately, decommissioning [1, 52].

A core aspect of SE in ITER is the management of stakeholder needs and requirements throughout the project's lifecycle, which is crucial for ensuring its success [1]. This involves the decomposition of Project Requirements into detailed system, subsystem, and component requirements as the design matures [1]. Furthermore, SE processes ensure that requirements are not only verified—confirming that "the system is built right"—but also validated, ensuring that "the right system is built" to meet its intended purpose [1] (Figure 4.1).

ITER V-model

The ITER project largely follows the "V-model" as its standard lifecycle process, although in a complex system-of-systems such as ITER, the traditional V-model expands into multiple, interconnected V-models at varying levels of maturity [1].

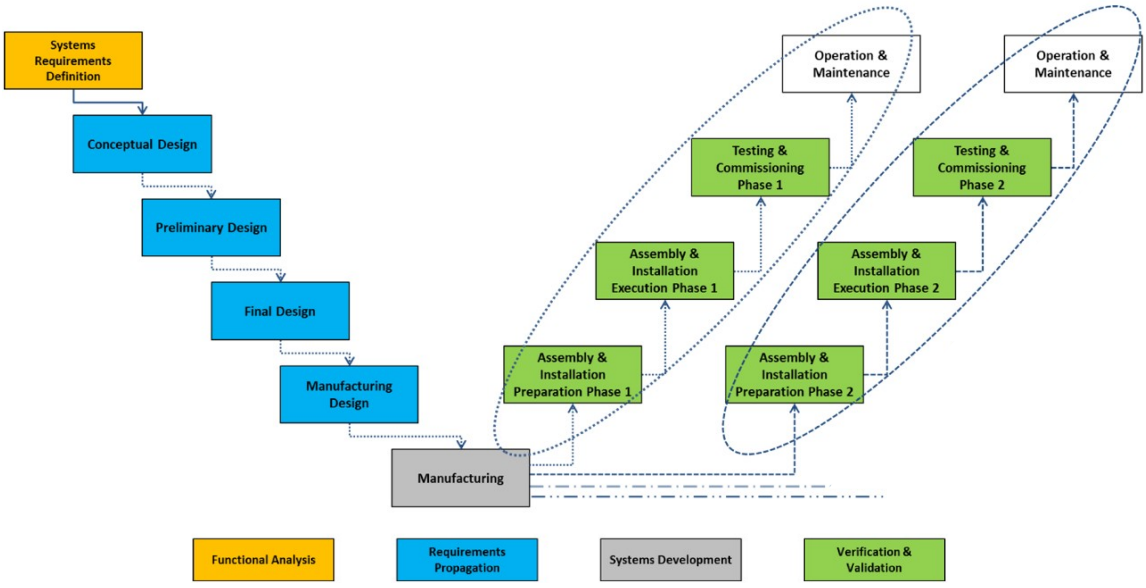

Figure 4.1: V-model for ITER Project ([1]).

These models are linked through defined interfaces between systems and subsystems, reflecting the multi-dimensional nature of the project. Many technical and

management processes within ITER run concurrently, facilitating parallel actions such as simultaneous design and preparatory work for system construction [1]. This concurrent approach is vital for managing the project's complexity and its evolving configuration, which will undergo changes, design improvements, and modifications throughout its operational lifetime [52].

Configuration Management is tightly integrated with SE in ITER, serving to ensure that accurate information, consistent with the physical and operational characteristics of the project, is readily available. This capability is paramount for cost-effective construction, maintaining the plant's configuration, and supporting future upgrades [52]. The need for proper procedures and tools for this interdisciplinary approach was recognized early in the project, drawing from experiences in similarly large scientific and industrial endeavors [52]. The overarching scope of SE in ITER is to define the project's requirements, establish its physical architecture, and continuously assess the performance of the current design [52].

ITER lifecycle model

The ITER project's Systems Engineering approach encompasses a comprehensive lifecycle model, systematically guiding the project through distinct phases from initial concept to long-term operation [1]. This lifecycle is punctuated by formal review gates (Figure 4.2) that serve as critical decision points, ensuring the system's development aligns with requirements and objectives [1].

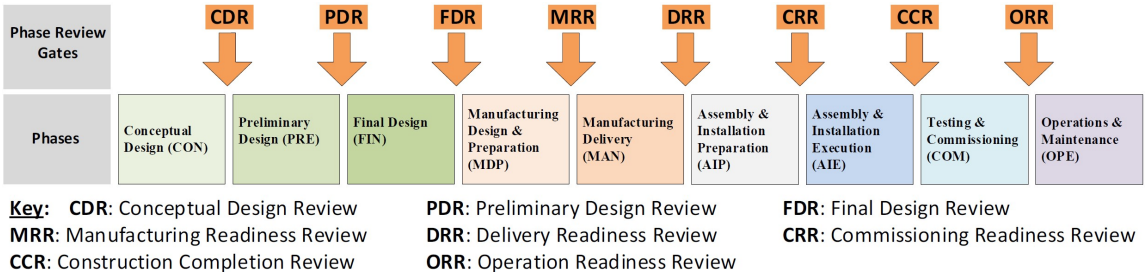

Figure 4.2: ITER Phase Review Gates and Phases ([1]).

The primary systems engineering technical phases (Figure 4.2) identified for ITER

include:

- **Conceptual Design:** During this initial design phase, various design solutions are considered, and the resulting configuration is documented and placed under change control [1]. Functional requirements form the basis for development, and requirements verification can begin here [1].
- **Preliminary Design:** As the design matures through this phase, requirements continue to be broken down into more defined specifications [1]. The Preliminary Design Review marks a significant review gate at the end of this phase, where the design is evaluated against its requirements to ensure correctness and adherence to project needs [1]. A successful PDR establishes baselines and solidifies the design [1].
- **Final Design:** This phase further refines the design, with requirements continually propagating down and being verified [1]. The Final Design Review is the review gate for this phase [1]. For complex systems, multiple FDRs may occur for lower-level systems before the complete final system is achieved [1]. While the Conceptual Design Review is listed as a phase review gate and an acronym for Conceptual Design Review [1], the provided sources do not detail its specific function as a formal review gate.
- **Manufacturing Design & Preparation & Manufacturing Delivery:** Following the design phases, the project transitions into manufacturing. During the Manufacturing Delivery phase, the system is actively being produced, with requirements continuing to be managed and verified [1].
- **Assembly & Installation Preparation & Assembly & Installation Execution:** In these phases, components are assembled and installed. Requirements are continuously verified, and as the system is integrated, requirements are also validated [1].

  Testing & Commissioning: This phase is crucial for the final validation of requirements, confirming that "the right thing" has been built and that the system is ready for operation [1].

- **Operations & Maintenance:** This represents the final phase for the ITER project's full operation, ensuring sustained safe operation [1].

Throughout these phases, design activities are continuous, adapting to evolving requirements and integrating new information. Each phase ends with a review that serves as a decision point to confirm the phase's data and allow progression to the next [1].

ITER and ENOVIA PLM

Product Lifecycle Management Product Lifecycle Management is a strategic business approach that encompasses a consistent set of business solutions designed to support the collaborative creation, management, dissemination, and use of product definition information throughout its entire lifecycle [58–60]. This lifecycle spans from the initial concept and design through manufacturing, service, and ultimately to the product's retirement or end-of-life [60].

Key aspects and functionalities of PLM include:

- Centralized Data Management: PLM systems centralize and organize all product-related data, acting as a single source of truth [58, 61]. This includes requirements, specifications, CAD models, manufacturing instructions, and test procedures.

- Process Integration: It integrates various processes such as requirements definition, system design, simulation, detailed design, manufacturing planning, quality management, and customer support [60]. This integration helps streamline workflows and reduce errors.

- Collaboration: PLM fosters collaboration among diverse teams, suppliers, and stakeholders, often across different geographical locations, by providing secure access to up-to-date product information [58, 62].

- Configuration and Change Management: A critical function of PLM is managing product configurations and controlling engineering changes throughout the

lifecycle. This ensures that accurate information consistent with the physical and operational characteristics of the product is always available [63].

- Knowledge Reuse: PLM facilitates the reuse of design data, processes, and knowledge, which can significantly improve efficiency and reduce development times for new products [58].

PLM is considered a mission-critical enterprise system, essential for companies seeking to optimize product development, enhance efficiency, and react more quickly to changing customer requirements [60, 64].

The Role of Plant Breakdown Structure The Plant Breakdown Structure is a hierarchical decomposition of a complex system into its constituent hardware and software products [3]. It systematically breaks down the entire plant or project into manageable levels, providing a clear and exhaustive dictionary of all components involved [65].

In general, a PBS serves several purposes:

- Component Identification: Each element within the structure can be uniquely identified, designed, and manufactured [1].

- Traceability: It ensures that all relevant requirements, design solutions, and associated documentation can be traced down to the corresponding elements [1].

- Management of Complexity: By breaking down a vast project into smaller, interconnected parts, the PBS allows for better management of complexity and clearer assignment of responsibilities [66].

- Common Understanding: It guarantees a common understanding among all project participants regarding the physical scope of the system [65].

The PBS is distinct from a Functional Breakdown Structure, which focuses on functions and activities, whereas the PBS is product-oriented [56]. In the context of

PLM, a PBS can be compared to a Bill of Materials, detailing the components and their quantities at various stages of the product lifecycle [67].

ENOVIA as a PLM Manager in ITER In the context of ITER, ENOVIA plays a pivotal role as the core Product Lifecycle Management tool [52]. ENOVIA, a virtual product data management software developed by Dassault Systèmes and widely utilized across industries like automotive, aeronautics, and shipbuilding, is central to managing ITER's intricate engineering and configuration [52].

Here's how ENOVIA functions as a PLM manager within ITER:

- Centralized Product Data: Every part of the ITER plant is entered into a central ENOVIA database, receiving a unique identifier [52]. This entry includes various technical and non-technical attributes, such as its location, the specific system or loop it belongs to, and the procurement team responsible [52].

- Digital Mock-ups and Navigation: ENOVIA enables the creation of digital mock-ups and offers powerful filtering and navigation capabilities. For instance, users can generate a digital mock-up of all parts within a specific room or compile a list of all components connected to a particular power supply line [52].

- Configuration Management Integration: The ITER Plant Breakdown Structure is directly aligned with ENOVIA [1]. ENOVIA ensures stringent configuration management by linking drawings, 3D models, and technical data to specific parts or assemblies, thereby preventing information duplication and managing the versioning and lifecycle of all project documents throughout ITER's operational lifespan [52].

- Global Collaboration: ENOVIA provides web interfaces that allow remote users to access and, depending on their defined roles, modify the database. This global accessibility is critical for seamless international collaboration among the numerous contributors to the ITER project [52].

- Traceability: The system supports the traceability of requirements and solutions to individual components, which is important for maintaining design consistency and effective project management in such a complex endeavor [1, 52].

The integration of ENOVIA with the detailed PBS is fundamental for managing the vast interdependencies and cross-disciplinary integration required for ITER, ensuring that all aspects of the system's development and operation are planned, controlled, and continuously updated.

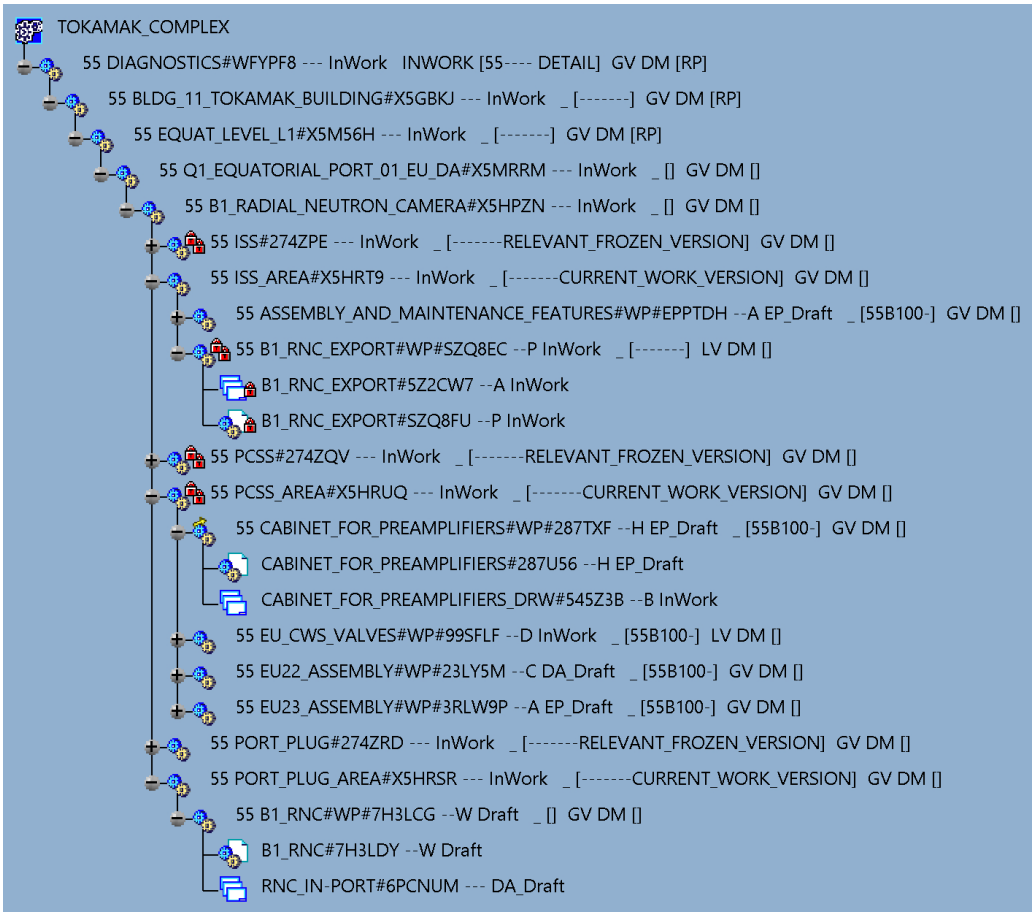

Figure 4.3: ITER ENOVIA PBS organization, focused on the RNC leaves - Ex-Port, Cabinet and In-Port.

A visual example of ITER ENOVIA's PBS is given in Figure 4.3. Figure 4.3 shows the hierarchical structure of the ITER PBS: starting from the TOKAMAK_COMPLEX (that contains all the elements of the ITER machine - from the concrete structure to each single screw), the structure descends through the PBS 55 (the PBS branch dedicated to all the diagnostics), focusing on the TOKAMAK building ($BLDG\_11$), at the level of the EQUATORIAL PORT, considering only the diagnostics designed by the EU DA (Domestic Agency of the EU - Fusion For Energy), and arrives at the RNC branch. Here it is finally divided in three: Interspace Supporting Structure (ISS) where the Ex-Port RNC is located, Port Cell Supporting Structure (PCSS) where the Cabinet for preamplifiers is assembled, and Port Plug where the In-Port RNC is located. The detailed description of these sub-systems is fully reported in the next section.

The ENOVIA leaves elements - the work package "WP" B1_RNC_EXPORT, CABINET_FOR_PREAMPLIFIERS and B1_RNC (In-Port) - contain the CATIA models of the corresponding RNC subsystem. Only the leaf elements contain the 3D and 2D CAD models, that can be opened in another window (CATIA window) to be opportunely modified and saved.

Figure 4.3 shows the RNC model at the FDR design stage. For each subsystem, the version is indicated with a letter (for example the letter "P" for the Ex-Port): the versions correspond to different design phases of the CAD model. When the CAD model is being modified, its status is set as "InWork". When requested, a promotion process is executed on the CAD model. The promotion can be accepted if the model passes three CAD controls: clash analysis (to check whether each component clash with others or not), the quality assessment (related to several CAD quality indicators), and the link-between-the-parts analysis. If the CAD model passes the promotion, it is set as "DA_Draft", that means it passed the controls by the DA. Finally, if it is successful with the IO controls, its status is set to "Draft".

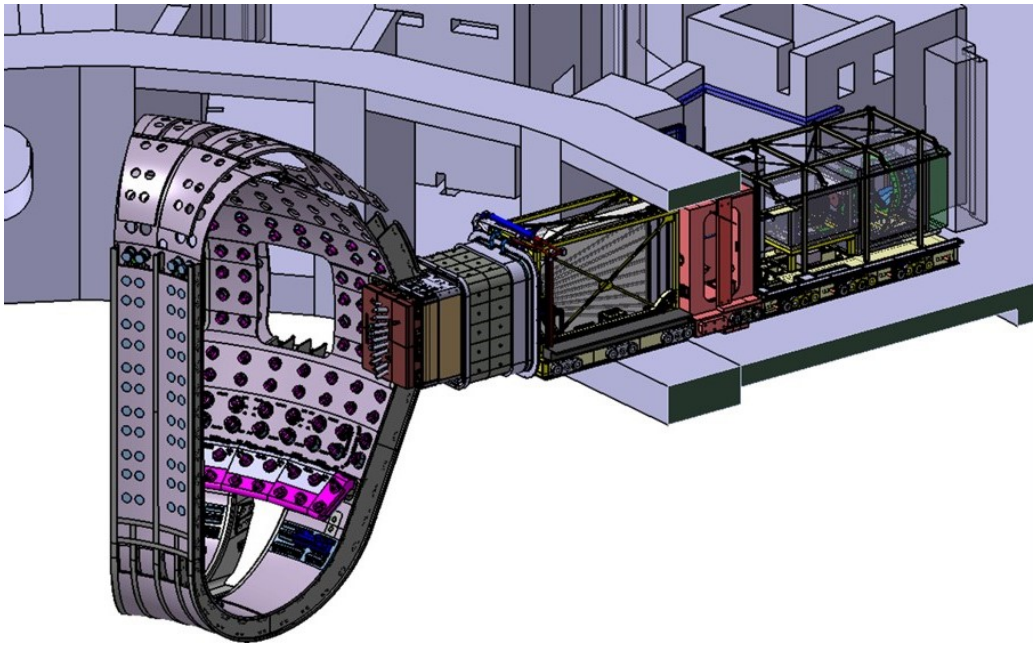

Figure 4.4: ITER Equatorial Port n.1 viewed from the Vacuum Vessel.

4.2 Design of the ITER Radial Neutron Camera

This section presents the Radial Neutron Camera, a neutronic diagnostic of ITER. The section shows the successful application of the Requirements management for a complex project such as the RNC.

The Radial Neutron Camera (RNC) is a diagnostic located in ITER Equatorial Port n.1 and is composed by two collimating structures, In-port RNC system and Ex-port RNC system viewing the plasma radially through vertical slots in the diagnostic shielding module (DSM) of the port plug (Figure 4.4).

The RNC measures the uncollided 14 MeV and 2.5 MeV neutrons from deuterium-tritium (DT) and deuterium-deuterium (DD) fusion reactions through an array of neutron flux detectors located in collimated Lines Of Sight (LOS).

The RNC shall measure neutron and alpha source profiles with 10% accuracy, provide measurement of fuel ratio profile with spatial resolution for a/10 and 0.2 accuracy, and measure fusion power density with a/10 spatial resolution. The system also

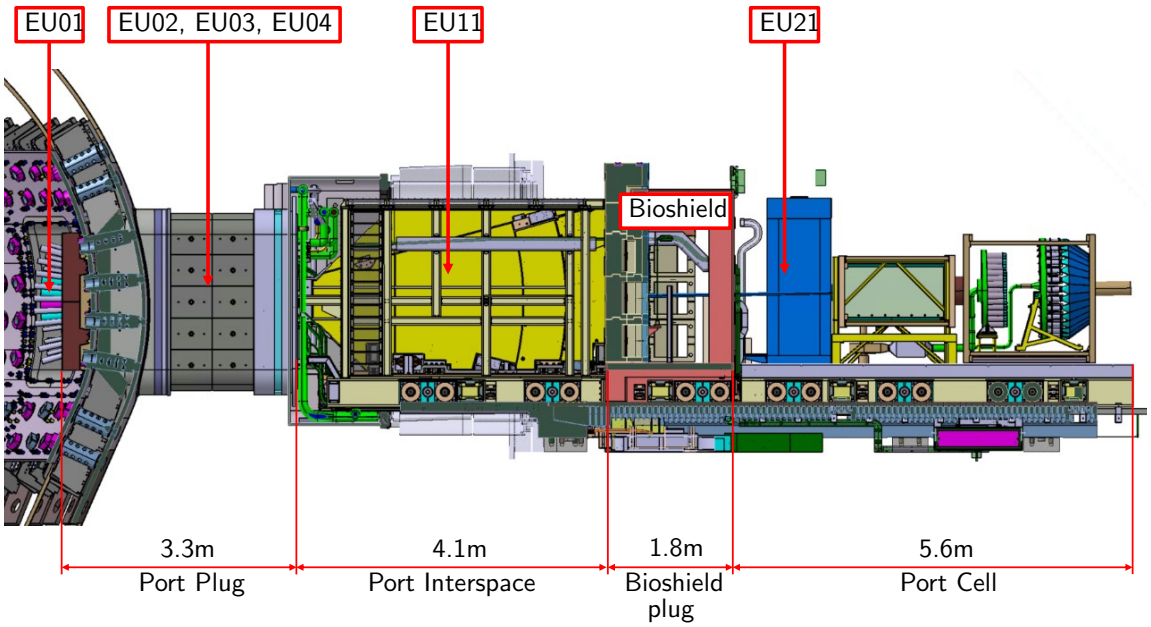

Figure 4.5: Overview of the ITER Equatorial Port n.1 ([68]).

plays safety-relevant roles, providing measurements of fusion power to demonstrate that the fusion power has not exceeded 700 MW and neutron fluence to demonstrate it has not exceeded $0.3 MWa/m^2$, arising from licensing considerations.

A well-defined volume (Configuration Model, CM) has been allocated in the port plug, the port interspace and port cell (Figure 4.5) to accommodate the RNC high level components, defined as Embarked Units (EU). An Embarked Unit is a Part of the Diagnostic that makes sense to be treated separately to organize the integration, either for technical or management reasons at design, manufacturing, installation, testing, or commissioning phases.

Apart from the In-Port and Ex-Port RNC systems, a cabinet (EU21) located in the Port Cell is associated to the diagnostic, containing the front-end electronics (Preamplifiers) for the full RNC.

Requirements management for RNC design

The functional analysis performed on the RNC system resulted in a schematic statement of the RNC mission, which highlights the main goals of the RNC diagnostic (Figure 4.6).

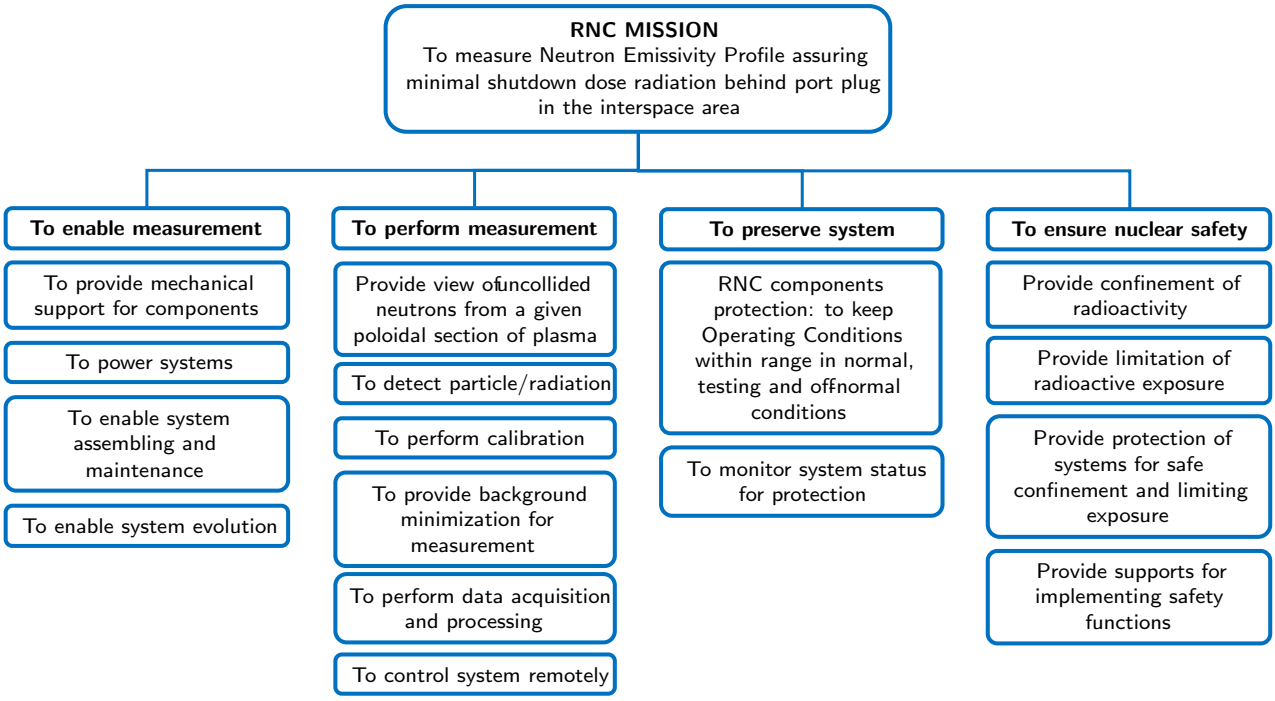

Figure 4.6: RNC mission.

These macro-objectives are then divided into a chain of sub-objectives and characterized as requirements and constraints, as presented in Section 2.3.

This section will present the main technical requirements and constraints for the ITER RNC system, including the identification of interfaces with other ITER systems. For a complex project like ITER, which uses a robust Systems Engineering framework, requirements are not just a simple list but a hierarchical, comprehensive set that encompasses various aspects of the system. The set contains all of the top level functional, design, safety, operational, maintenance and quality requirements

for the RNC System of ITER and its impact on the environment.

The requirements for the RNC system can be systematically categorized as follows:

- **General Scope and Purposes:** Defines the overall function, context, and high-level objectives of the RNC System within the ITER project [69].
- **General Design Requirements:** Covers fundamental design considerations, operational parameters, and roles of the RNC system, including its expected lifespan and operational cycles.
- **System Specific Requirements:** Details particular performance parameters and functional roles of the RNC, such as measurement ranges, resolutions, and its classification in various diagnostic functions.
- **System Composition and Location:** Describes the physical structure of the RNC, including its sub-systems and their precise placement within the ITER facility.
- **Structural Requirements:** Addresses the RNC's ability to withstand various mechanical loads, including seismic events, and mandates adherence to specific design codes and standards for structural integrity.
- **Mechanical Requirements:** Focuses on the physical resilience of RNC components against internal and external forces, ensuring critical functions are maintained and differential movements are accommodated.
- **System Alignment:** Specifies the need for precise positioning and alignment of the RNC's lines of sight to ensure accurate measurements.
- **Material Requirements:** Outlines criteria for material selection, considering factors like decontaminability, resistance to steam exposure, and proper handling/storage.
- **Electrical Requirements:** Sets standards for the electrical equipment, power supplies, and control mechanisms of the RNC.

- **Grounding and Insulation Requirements:** Defines proper electrical grounding and insulation practices to ensure safety and electromagnetic compatibility for the RNC system.
- **Instrumentation and Control Requirements:** Pertains to the RNC's capabilities for calibration, maintenance, and overall operational control, including personnel safety.
- **Vacuum Requirements:** Establishes strict criteria for maintaining vacuum integrity, including design, manufacturing, leak testing, and safety leak rates for vacuum components.
- **Electromagnetic Requirements:** Ensures compliance with electromagnetic compatibility and radiation policies to prevent interference and ensure proper system function.
- **Safety Design Requirements:** Covers all aspects of designing the RNC to meet safety standards, including compliance with regulations, preventing functional loss, and ensuring a safe state during abnormal events.
- **Fire Protection:** Details measures to prevent and mitigate fire hazards, protect personnel, and limit damage or release of hazardous materials.
- **RAMI:** Encompasses requirements for the RNC's overall performance in terms of its reliability, operational availability, ease of maintenance, and inspectability.
- **Maintainability:** Focuses on design features and processes that facilitate the detection, identification, location, and repair of failures, along with requirements for a comprehensive maintenance plan.
- **Manufacturing, Construction, Assembly, Installation:** Specifies requirements for the entire lifecycle of RNC components from fabrication through installation, including quality assurance, welding standards, and segregation of activated components.

The subsequent Table 4.1 provides a detailed breakdown of these requirements, assigning a unique identifier to each for comprehensive traceability throughout the design and verification phases. The requirements listed in Table 4.1 are a reduced number of selected requirements from the complete list of RNC requirements. This selection is realized to simplify the workflow and address it to the LAISE application.

Table 4.1: RNC requirements.

Category	**Requirement ID**	**Requirement Description**
General Design Requirements	[Req.#1]	The RNC in-vessel and in-port plug components shall withstand the loading conditions derived from the pulses during ITER operation to keep the integrity of the vacuum vessel.
	[Req.#2]	The system shall be designed to operate with a pulse period time not exceeding 1800 seconds for burn duration less than 450 seconds.
	[Req.#3]	Diagnostic systems shall be designed to be capable of operating for periods of 11 consecutive days while accommodating three-shift daily plasma operation, followed by 3 days of routine maintenance.
	[Req.#4]	Diagnostic systems shall be designed so that plasma operation can be conducted for periods of up to 16 months continuously in three 8h work-shift daily operating mode to perform the following actions: plasma operations, test, conditioning, routine maintenance.
System Specific Requirements	[Req.#5]	The 55.B1 RNC can be considered as one system.
	[Req.#6]	This Technical PA Requirements Annex contains the technical requirements and constraints for the ITER 55.B1 system, including identification of interfaces with other ITER systems.

Continued on next page

Table 4.1 continued from previous page		
Category	**Requirement ID**	**Requirement Description**
	[Req.#7]	55.B1 – RNC shall provide measurement of fuel ratio profile in the plasma core (r/a<0.85) in the range 0.01 - 10.
	[Req.#8]	55.B1 – RNC shall provide measurement on core Ti profile in the plasma core (r/a<0.85) in the range 0.5 - 40 keV.
	[Req.#9]	55.B1 – RNC shall provide measurement on core Ti with a time resolution of 100 ms.
	[Req.#10]	55.B1 – RNC shall measure fusion power density with 10% accuracy.
	[Req.#11]	55.B1 – RNC shall measure neutron and alpha source profile with 10% accuracy.
	[Req.#12]	55.B1 – RNC shall measure fusion power with an accuracy of 10%.
	[Req.#13]	55.B1 – RNC shall provide measurement of fuel ratio profile with spatial resolution for a/10 and 0.2 accuracy.
	[Req.#14]	55.B1 – RNC shall provide measurement on core Ti profile with a spatial resolution of a/10 and 0.1 accuracy.
	[Req.#15]	55.B1 – RNC shall measure fusion power density with a/10 spatial resolution.
	[Req.#16]	55.B1 – RNC shall provide measurement of fuel ratio profile in real time with a time resolution of 200 ms and a range of 0.01-0.2.
	[Req.#17]	Defined requirements concerning measurements and diagnostics involved in safety-relevant functions concern plasma current, fusion power, tritium, and dust.

Continued on next page

Table 4.1 continued from previous page		
Category	**Requirement ID**	**Requirement Description**
	[Req.#18]	RNC system shall provide a measurement of the fusion power to demonstrate that the fusion power has not exceeded the design value of 700 MW.
	[Req.#19]	RNC system shall provide a measurement of the neutron fluence to demonstrate that the neutron fluence has not exceeded the design value of 0.3 MWa/m^2.
	[Req.#20]	Safety-relevant roles are defined for plasma current, neutron fluence, and fusion power, arising from licensing considerations.
System Composition & Location	[Req.#21]	The RNC shall be composed by two fan-shaped collimating sub-systems. 55.B1 will be located in Equatorial Port Cell 1.
	[Req.#22]	The 55.B1 In-Port RNC shall be located in Drawer #3 of the Port Plug and will have 6 Lines Of Sight, with 3 detector aiming at lower and 3 detector aimong at upper plasma regions.
	[Req.#23]	The 55.B1 Ex-Port RNC shall have 16 LOS and it is composed by two parts: the collimators located in Drawer #2 of the PP, and part in the Port Interspace, which contains the Flight Tubes, Collimation Units, the Detector Modules, and the Shielding Block.
Structural Requirements	[Req.#24]	The RNC in-vessel and in-port plug components shall withstand the loading conditions derived from ITER operation pulses.
		Continued on next page

Table 4.1 continued from previous page		
Category	**Requirement ID**	**Requirement Description**
	[Req.#25]	The DA shall provide the RNC SIR as input for IO-CT to demonstrate that RNC does not jeopardize the functioning of other components that provide a safety function during or after an earthquake.
	[Req.#26]	The DA shall design the System according to Category 1, 2, 3 and 4 Load Cases including combinations of these driving the structural integrity of all SSCs, as defined in the Load Specifications.
	[Req.#27]	Selected codes and standards will be in agreement with those defined in the Codes and Standards for ITER Mechanical Components.
	[Req.#28]	SMS and PALEO-earthquake response spectra are calculated in accordance with the Codes and Standards.
Mechanical Requirements	[Req.#29]	Safety functions of the PIC SSCs shall be guaranteed against internal and external aggressions described in the SLS.
	[Req.#30]	The System shall accommodate differential movements between the port plug closure plate and interspace structure, and maintain alignment during normal operation, as defined in the System Load Specifications.
System Alignment	[Req.#31]	55.B1 shall enable Positioning and alignment for lines of sight.
Material Requirements	[Req.#32]	Interspace, Port Cell, and Gallery components shall be made of materials with easily decontaminable surfaces.
	[Req.#33]	The DA shall transport and store PIC SSCs in clean and dry conditions, protected from normal hazards and abnormal accelerations.
Continued on next page		

Table 4.1 continued from previous page		
Category	**Requirement ID**	**Requirement Description**
	[Req.#34]	When selecting materials for in vessel components, the DA will assess the impact of steam exposure, as defined in the System Load Specifications.
	[Req.#35]	RNC components in the vacuum vessel shall be designed to minimize as much as reasonably achievable the effect of exposure to steam resulting from a water leak.
Electrical Requirements	[Req.#36]	The DA shall ensure that the tests of the RNC system electrical equipment are compliant with the test standards given in the ITER Electrical Design Handbook - Part 4: Electromagnetic Compatibility .
	[Req.#37]	Steady-state power supplies used by 55B1 RNC will provide remote-controlled breakers and switchgear, such that all major non-safety loads may be disconnected by the plant electrical control centre.
	[Req.#38]	55B1 RNC that does not use Class II power supplies can use Class IV power supplies.
Grounding & Insulation Requirements	[Req.#39]	All RNC ex-vessel system metallic elements which are not mechanically and galvanic interconnected, shall be interconnected by means of an accessible protection conductor with a cross-section at least equal to the LV supply cable cross-section.
	[Req.#40]	Ex-vessel electrically conducting SSCs shall have an electrical bonding point at least every four meters compromised between every 1 to 4m maximum, the first bonding being the EMC Zones boundary (including outside tokamak complex).
Continued on next page		

Table 4.1 continued from previous page		
Category	**Requirement ID**	**Requirement Description**
	[Req.#41]	As RNC has multiple earth points in the LCZ (in-vessel), the DA shall demonstrate the system ability to sustain the EM loads.
	[Req.#42]	The electrically conducting SSCs inside vacuum shall be electrically bonded to the Port-Plug or Vessel wall.
Instrumentation & Control Requirements	[Req.#43]	55.B1 shall enable Calibration of single detectors with embedded sources, both In-Port and Ex-Port parts.
	[Req.#44]	55.B1 shall enable Cross calibration with other diagnostic with dedicated plasma discharges.
	[Req.#45]	55.B1 shall enable Maintenance for detectors and possible detector replacement (cassette replacement for In-Port RNC).
	[Req.#46]	55.B1 shall enable Provide occupational and personnel safety.
	[Req.#47]	55.B1 shall enable Measurement of neutron flux and emissivity during normal operation phase.
	[Req.#48]	55.B1 shall enable Measurement of fuel ratio in plasma core during normal operation phase.
	[Req.#49]	55.B1 shall enable Measurement of ion temperature profile during normal operation phase.
Vacuum Requirements	[Req.#50]	Vacuum envelopes (components that form part of the vacuum boundary, including their penetrations) will be designed and manufactured using appropriate standards.
	[Req.#51]	There shall be no trapped volumes in any RNC component in the primary vacuum.

Continued on next page

Table 4.1 continued from previous page		
Category	**Requirement ID**	**Requirement Description**
	[Req.#52]	The DA shall develop the Leak Test Procedure for RNC vacuum components.
	[Req.#53]	The DA shall leak test VQ classified SSCs forming a vacuum barrier, after any pressure testing and before delivery to the ITER site.
	[Req.#54]	Vulnerable SIC-1 SSC forming part of the first confinement barrier shall be double vacuum barrier with a monitored interspace connected to the SVS.
	[Req.#55]	The RNC confinement barrier elements shall have a safety leak rate of less than 0.007 Pa.m^3/s per feedthrough under a pressure differential of 0.1 MPa.
	[Req.#56]	The DA shall design VQC1a SSCs to be accessible for leak localisation.
Electromagnetic Requirements	[Req.#57]	EMC and radiation policy shall apply.
Safety Design Requirements	[Req.#58]	If a pressurized item is included in the design, the DA shall apply the ESP / ESPN directives from the French Decree 99 -1046 dated December 13th 1999 and subsequent Order and amendments which introduce in force in France the Pressure Equipment Directive 97/23/EC and the French Order on Nuclear Pressure Equipment, December 2005.
	[Req.#59]	Abnormal state, malfunctioning, damages or possible aggressions from Non-PIC SSC or other PIC SSCs shall not cause loss of safety function of the PIC SSC.

Continued on next page

Table 4.1 continued from previous page		
Category	**Requirement ID**	**Requirement Description**
	[Req.#60]	If the DA adds new components to the RNC system that are not covered by the category of components in the baseline BoM, it shall classify them as part of the BoM updates foreseen in the PA deliverable production plan.
	[Req.#61]	Valves that are part of a confinement boundary of 55B1 RNC shall operate within required periods after detection of the onset of an abnormal event.
	[Req.#62]	If a system has any active PIC components, it shall be able to be placed into their safe state in case of an evacuation.
	[Req.#63]	Assurance of the reliability performance of credited safety functions shall be provided using recognised analysis techniques.
	[Req.#64]	For radiological hazards, the dose objectives will be respected during normal operation and off-normal events (incidents and accidents).
Fire Protection	[Req.#65]	Prevent fire and fire damage that could lead to the release of radioactive or hazardous material to the environment, limit releases in case of postulated fires, ensure personnel safety, and limit damage to the machine and property.
	[Req.#66]	The DA shall implement fire protection provisions necessary to protect all PIC SSCs, from fire loads identified in the corresponding Sub-System Load Specifications.

Continued on next page

Table 4.1 continued from previous page		
Category	**Requirement ID**	**Requirement Description**
	[Req.#67]	Any system safety-related fibres and electrical cables with rated voltage below 1 kV shall be fire resistant according to the IEC 60331 and NF32070 CR1.
	[Req.#68]	SIC SSCs being part of a fire barrier shall have a fire resistance rating REI-120 (R=mechanical resistance, E=leak tightness to hot gases and flames, I= thermal insulation).
Reliability, Availability, Maintainability, Inspectability	[Req.#69]	The availability of the RNC system shall be at least 99.5 % & 88.3% for the ex-port and in-port system respectively for 2 years availability.
	[Req.#70]	RNC diagnostic shall not have planned Remote Handling Maintenance.
Maintainability	[Req.#71]	The RNC system will be designed to reduce the time to detect, identify, locate and repair failures.
	[Req.#72]	A maintenance plan shall be prepared. Minimum information required within this maintenance plan is the following: Scheduled operations (such as controls, checks, adjustments, calibrations, overhauls, and replacements) that are derived from Safety and Security regulations, and identified as necessary by the supplier in order to ensure the best operation of the system in its intended operational scenario. At least task identification and interval is required.
	[Req.#73]	55.B1 shall enable Maintenance for detectors and possible detector replacement (cassette replacement for In-Port RNC).

Continued on next page

Table 4.1 continued from previous page		
Category	**Requirement ID**	**Requirement Description**
	[Req.#74]	The maintenance plan shall include at least task identification and interval.
Manufacturing, Construction, Assembly, Installation	[Req.#75]	The RNC system (components under DA responsibility) will have an optimized availability by means of RAMI.
	[Req.#76]	The appropriate levels of control and requirements for quality assurance will be defined in the specific diagnostic designs.
	[Req.#77]	Diagnostics systems will be designed, constructed, and operated in accordance with the requirements in the ITER Tritium Handbook.
	[Req.#78]	All onsite welding will undergo leak tests, and non-destructive examination on site, as required by the applicable codes and standards.
	[Req.#79]	The DA will verify the design of non-PIC components, according to a verification plan to be agreed at the PDR.
	[Req.#80]	Each diagnostic system shall segregate activated systems or components (wherever possible).
	[Req.#81]	55.B1 shall enable acceptance testing for detectors and calibration sources as single pieces for Ex-Port RNC, already integrated in EQ#1 for In-Port RNC.
	[Req.#82]	55.B1 shall enable commissioning and integration according to PI, particularly for In-Port RNC.

RNC configuration

After having organized the requirements, the RNC configuration must be selected. Design work activities have been pursued leading to a first optimization excercise of the RNC (both In-Port and Ex-Port). The performance analysis techniques and the

system engineering procedure starts from a set of different RNC options selected in order to scan the space of the architectural elements defining the diagnostic: number of LOS and their distribution in the plasma; collimators geometry (length, diameter) and positioning along the LOS; RNC detector set [70].

The five selected architectural options (Figure 4.7) include layouts in which: the In-Port is removed; the In-Port LOS cross the Ex-Port LOS in order to provide the RNC with a rough tomographic capability; the number of LOS is reduced to a minimum. The analysis highlighted the need of a In-Port RNC with LOS viewing the plasma edge to improve the reconstruction of the emissivity profile and that there is no added value from having the RNC layouts in which In-Port LOS cross Ex-Port LOS.

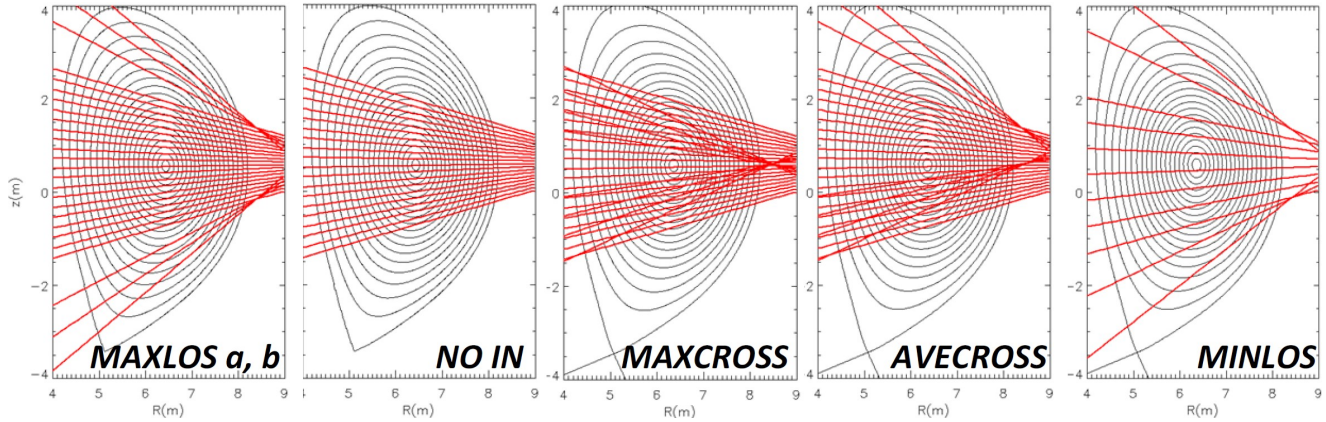

Figure 4.7: RNC layout architectural options considered in the architecture optimization exercise. MAXLOS a and b differ only because of the different diameters used for the collimating units ([70]).

Based on performance analysis and on the scoring of the various architecture trough a cost function the MAXLOSa layout was selected as the most efficient distribution of all RNC LOS across the plasma cross section.

Further analysis pointed out the following issues:

- Need to reduce the diameters of the 3 lower and 3 upper collimators in the Ex-port right hand side plane due to most recent configuration model (CM) constraints.

- Difficulty in alignment of Ex-port collimators with the corresponding port-plug optical paths, whose size was already the maximum allowed by the CM.
- High cost of sCDs employed in all Ex-port LOS.
- Integration/cost issues of scintillators employed in the In-port.
- sCD radiation resistance lower than that required to operate the detector over the whole ITER lifetime (see section 4.2.c).
- Need to integrate two enabled neutron diagnostics (High Resolution Neutron Spectrometer (HRNS) and Radial Gamma Ray Spectrometer (RGRS)) with specific requirements in terms of LOS layout and counts at the detector positions.

These issues are considered in the RNC Baseline Architecture, and their resolutions will be described in the sections related to the RNC subsystems. The geometrical layout (LOS angles, collimator lengths and diameter, etc.) used in the In-Port and Ex-Port RNC is provided in Table 4.2, and shows the MAXLOSa configuration in details.

Table 4.2: RNC LOS geometrical details

LOS #	**Location**	**LOS angle [°]**	**Collimator diameter [mm]**	**Collimator length [mm]**	**r/a**
1	In-port	50.0	32	944	0.85
2	In-port	56.0	32	1294	0.76
3	In-port	62.5	32	1463	0.67
4	Ex-port	73.9	11	2600	0.5
5	Ex-port	75.5	11	3000	0.45
6	Ex-port	77.3	11	3000	0.39
7	Ex-port	78.9	11	3000	0.34
8	shared RNC and RGRS	80.7	11	3000	0.28

Table 4.2 continued from previous page

LOS #	**Location**	**LOS angle [°]**	**Collimator diameter [mm]**	**Collimator length [mm]**	**r/a**
9	Ex-port	82.3	11	3000	0.23
10	Ex-port	84.1	11	3000	0.17
11	exclusive use RGRS	85.7	–	–	0.12
12	Ex-port	87.5	11	3000	0.07
13	exclusive use HRNS	89.1	–	–	0.02
14	Ex-port	90.9	11	3000	0.05
15	exclusive use RGRS	92.5	–	–	0.1
16	Ex-port	94.3	11	3000	0.16
17	exclusive use	95.9	–	–	0.21
18	Ex-port	97.7	11	3000	0.26
19	Ex-port	99.3	11	3000	0.31
20	Ex-port	101.1	11	3000	0.37
21	Ex-port	102.7	11	2300	0.42
22	Ex-port	104.5	11	1800	0.48
23	Ex-port	106.1	8	1400	0.54
24	In-port	117.5	32	1463	0.7
25	In-port	124.0	32	1294	0.8
26	In-port	130.0	32	944	0.88

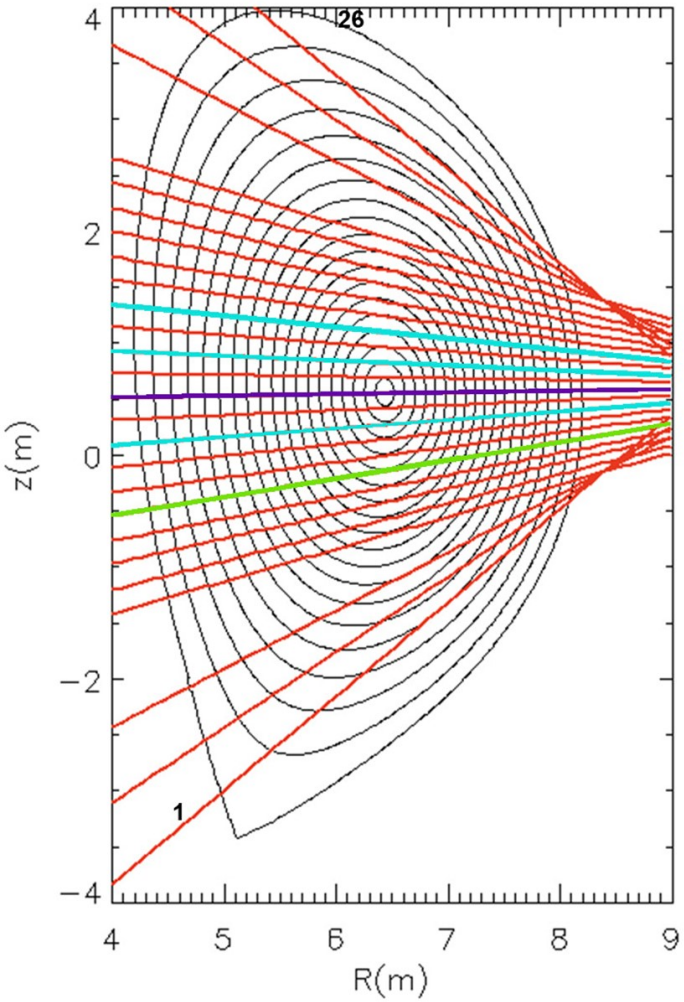

Figure 4.8: RNC MAXLOSa configuration ([70]).

Such a configuration allows the RNC diagnostic to reconstruct the neutron emissivity profile. Neutron emissivity profiles describe the spatial distribution of neutron emission within a fusion plasma and are essential for monitoring fusion power, ion temperature, and fuel composition in devices like ITER. These profiles are reconstructed from line-integrated measurements using inversion algorithms such as Tikhonov regularization and Minimum Fisher Information, which must achieve high accuracy (within 10%) and fast time resolution (10ms) for real-time plasma control.

The RNC performance for the measurement of DT and DD neutron emissivity was analysed using a set of 5 ITER reference plasma scenarios (Figure 4.9).

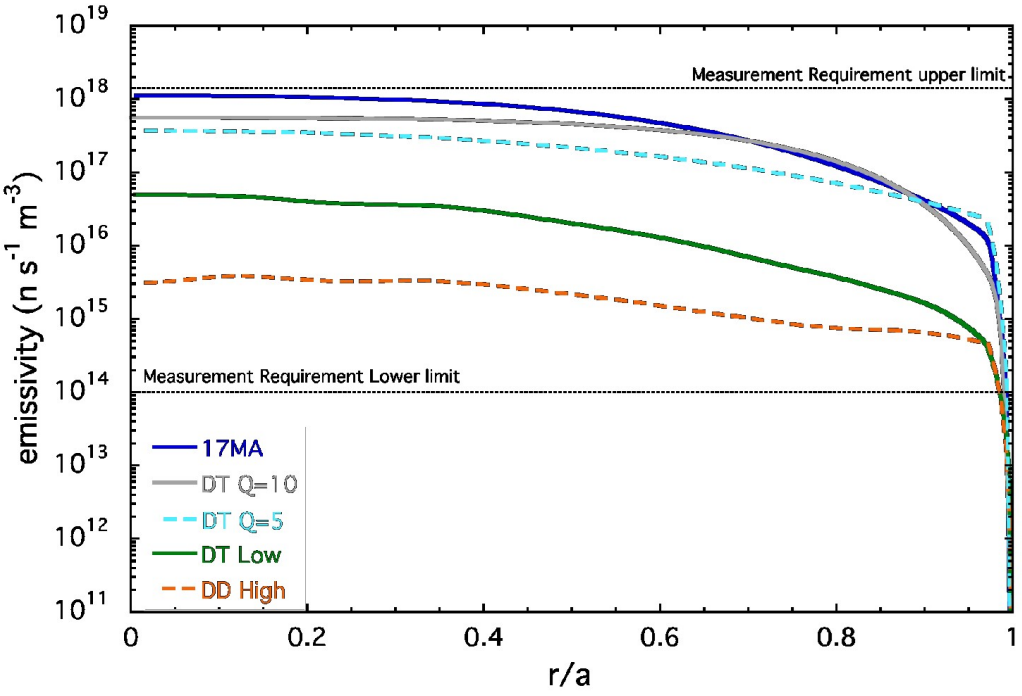

Figure 4.9: Reference neutron emissivity profiles used for performance analysis ([71]).

Figure 4.10 shows the RNC reconstruction results for the DT Q=10 (15 MA) scenario (10 ms time resolution, sCD as In-Port detectors). The example result shows that the reconstruction has a 10% accuracy up to a normalized minor radius (r/a) of 0.8. Similar results are obtained for the other reference neutron emissivity profiles.

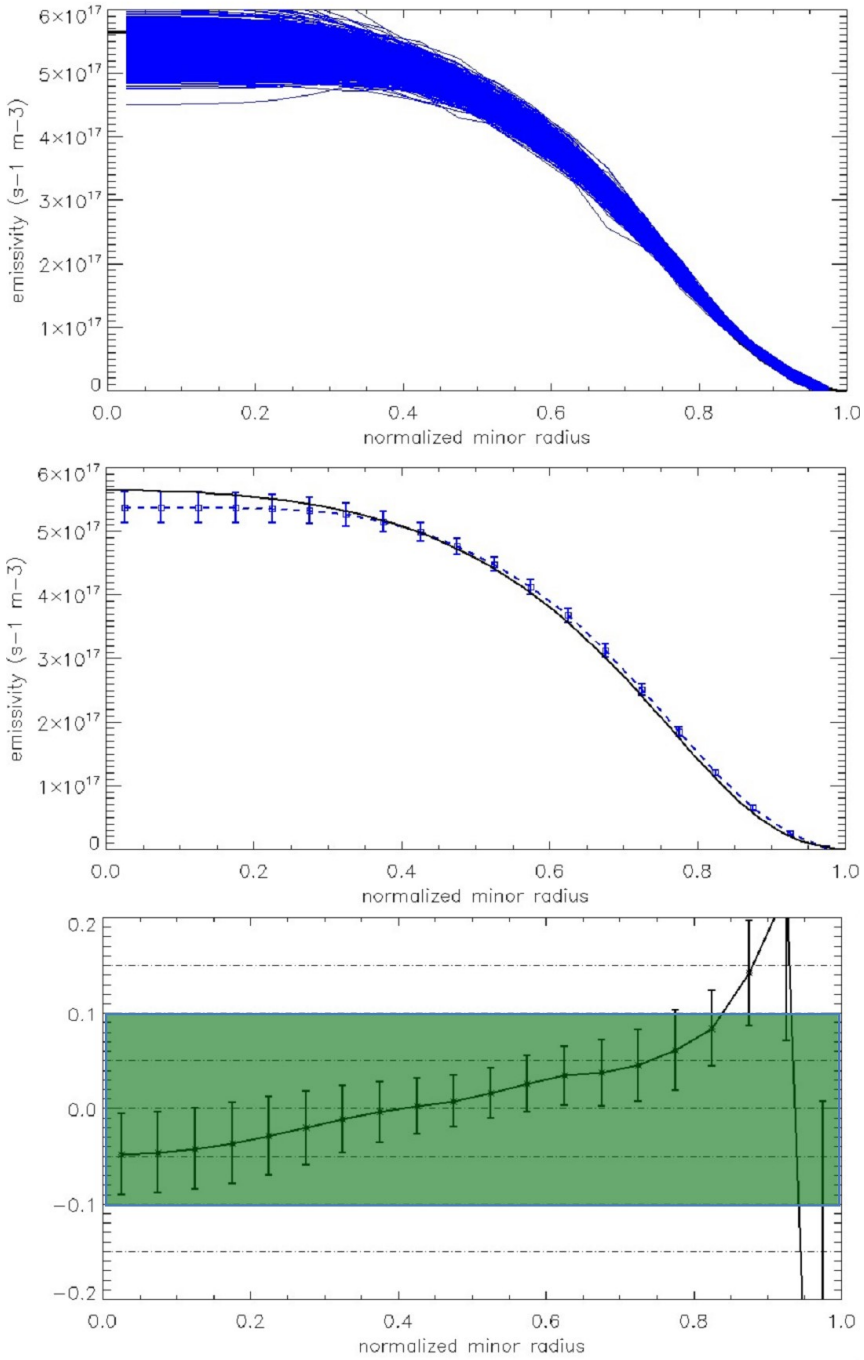

Figure 4.10: Reconstruction results for the DT Q=10 (15 MA) scenario (10ms time resolution, sCD as In-Port detectors). Top: full dataset of 1000 reconstructed emissivity profiles. Center: average reconstructed emissivity profile with 1σ uncertainty Vs. reference profiles (the black line). Bottom: reconstruction accuracy with 1σ uncertainty (light green shaded area delimits 10% accuracy region) ([71]).

4.2.1 In-Port RNC design

This chapter details the design, structural considerations, reliability, maintenance, and manufacturing aspects of the In-Port RNC system, described at the FDR design stage.

In-Port Overview

The In-Port RNC serves as a diagnostic system within ITER's Equatorial Port #1, specifically housed in Diagnostic Shielding Module (DSM) #3 of the Port Plug (Figure 4.11) [71–73][Req.#21][Req.#22].

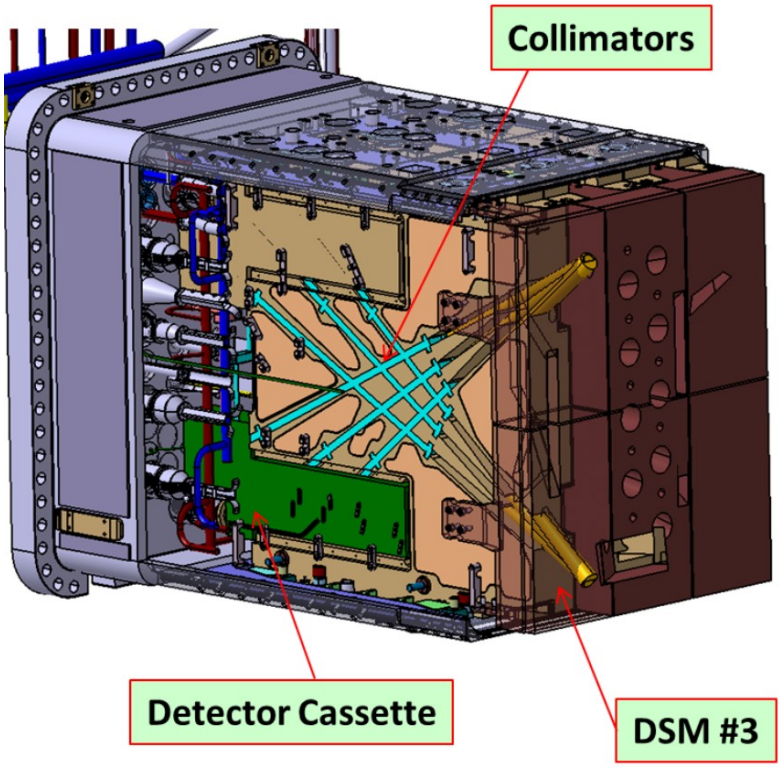

Figure 4.11: Position of EU03 (Detector Cassette) and EU04 (Collimator Tubes) inside ITER DSM #3 ([71]).

Its primary objective is to characterize the edge of the plasma by accurately mea-

suring the profiles of neutron and alpha particle sources [72, 73] [Req.#7] [Req.#8] [Req.#10] [Req.#11] [Req.#12] [Req.#13] [Req.#14] [Req.#15] [Req.#16] [Req.#47] [Req.#48] [Req.#49], thereby contributing to the assessment of fusion power [72, 73][Req.#10][Req.#12][Req.#18]. This is achieved by detecting un-collided 14 MeV and 2.5 MeV neutrons emitted from deuterium-tritium and deuterium-deuterium fusion reactions.

The In-Port RNC is equipped with six Lines Of Sight [71][Req.#22], with its detectors placed within a dedicated Cassette Assembly (Figure 4.12) [72, 73][Req.#22].

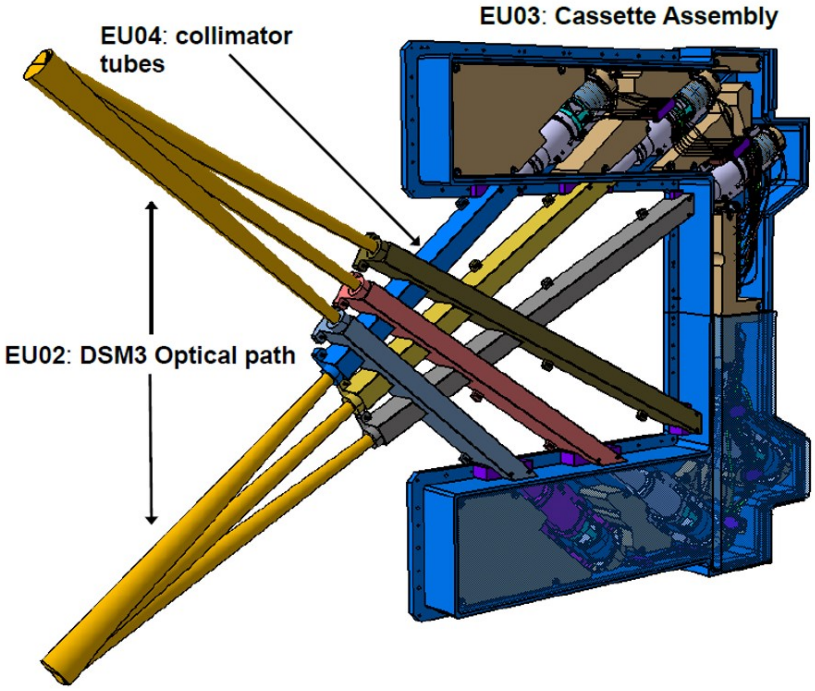

Figure 4.12: Embarked Units of In-port RNC ([71]).

Each line of sight is engineered to allow only uncollided neutrons from a specific plasma region to reach a detector module, which is outfitted with both fission chambers and single-crystal diamond matrix detectors [71, 74]. This diagnostic system, therefore, in combination with the Ex-Port RNC, provides data for understanding plasma behavior and optimizing fusion reactions within the tokamak [71]. The

system is designed to withstand loading conditions from ITER operation pulses [71, 73][Req.#1][Req.#24] and operate for extended periods [71][Req.#2][Req.#3][Req.#4]. The RNC system also has safety-relevant roles, providing measurements of fusion power and neutron fluence [71][Req.#18][Req.#19][Req.#20].

In-Port Subsystems Design Description

The design of the In-Port RNC is characterized by a modular approach, where each interconnected subsystem is engineered to perform specific functions within the challenging ITER environment. This section delves into the mechanical engineering rationale and outcomes for the Detector Module, Collimators, and Cassette Assembly (Figure 4.13).

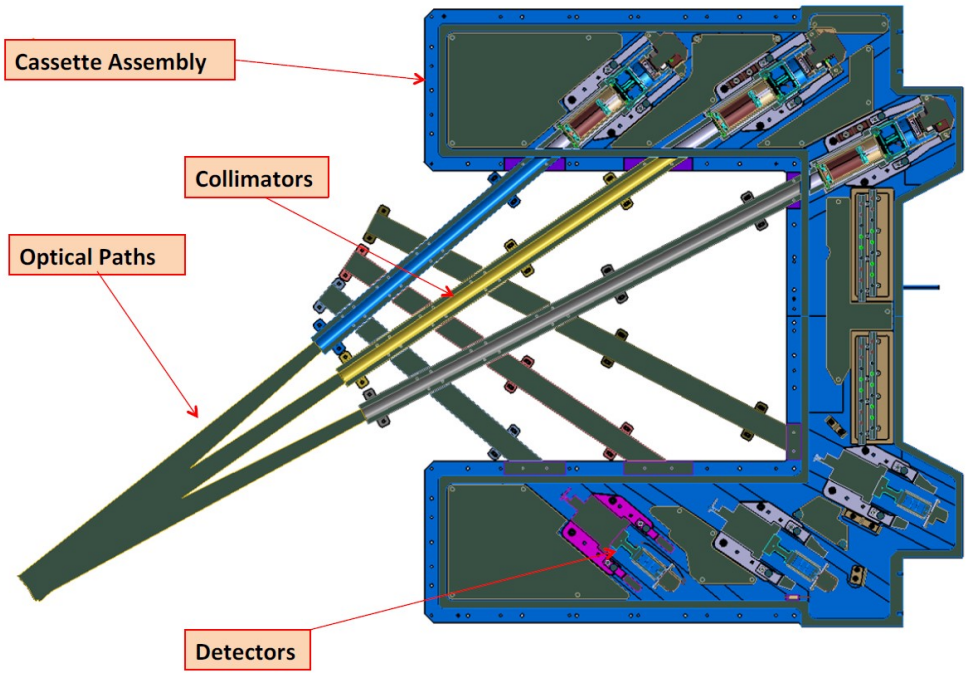

Figure 4.13: Section view of In-Port RNC ([71]).

Detector Module

The accurate measurement of neutron emission profiles is critical for understanding plasma behavior and assessing fusion power [71] [Req.#10] [Req.#11] [Req.#12] [Req.#18]. To achieve this, the Detector Module is designed to house a combination of two distinct types of neutron detectors: 238-U Fission Chambers and single Crystal Diamond Matrix Neutron Detectors [74] (Figure 4.14).

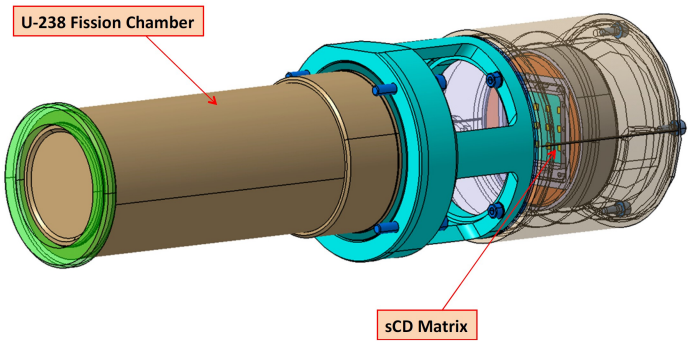

Figure 4.14: In-Port Detector Module ([74]).

This dual-detector approach is justified by the need to measure both 14 MeV and 2.5 MeV neutrons, allowing for precise discrimination of neutron energies and characterization of different fusion products [71, 74].The choice of sCD detectors is further justified by their inherent radiation hardness and thermal stability, which are essential for reliable performance under the extreme conditions within the ITER vacuum vessel, including temperatures up to 240 °C and intense neutron and gamma fluxes [74]. The ability to select an energy threshold in the sCD detector is crucial for mitigating background noise from lower energy neutrons and gamma rays, thereby enhancing the signal-to-noise ratio for precise measurements [74]. The inclusion of an sCD Alpha Calibration Source and thermocouples allows for in-situ calibration [74][Req.#43] and temperature monitoring, ensuring data accuracy and detector health [74]. The system also enables cross-calibration with other diagnostics [71][Req.#44].

The design process has yielded detector modules with specific performance characteristics:

- Detector Configuration: Detector #1 comprises a 238U fission chamber, characterized by a 32 mm diameter sensitive area and a multi-parallel plate configuration containing 145 mg of 238U, specifically designed for 14 MeV neutron detection [71, 74]. Detector #2 utilizes an sCD matrix with approximately 30 pixels, each with a 4 mm x 4 mm sensitive area and a thickness of 50 µm, capable of measuring both 14 MeV and 2.5 MeV neutrons [71, 74].

- Operational Efficacy: The projected operational efficiencies are 5.4×10^{-5} counts/neutron for the 238U fission chamber and 5×10^{-5} counts/neutron for the sCD matrix at 14 MeV [74]. These efficiencies are vital for accurately measuring the wide dynamic range of neutron flux anticipated during various ITER operational phases [74][Req.#47].

- Environmental Robustness: The diamond detectors demonstrate reliable performance up to 240 °C and maintain integrity under intense neutron and gamma fluxes, ensuring sustained diagnostic capability in the harsh ITER environment [74].

Collimators

The collimators are paramount mechanical structures whose primary function is to precisely define the origin of uncollided neutrons within the plasma and ensure that only neutrons from a specific plasma region reach the detector [71]. This is critical to obtaining an accurate spatial profile of neutron emission, free from interference. The design is optimized to minimize the detection of scattered neutrons, whether they originate from the port plug, the detector cassette, or within the collimators themselves [71]. This optimization is achieved through careful selection of shielding materials and precise geometry to reduce in-scattering and backscattering effects that could compromise measurement accuracy [71].The division of the collimators into two parts, separated by the cassette assembly wall, with one section integrated

into the Diagnostic Shielding Module, is justified by the need to enhance shielding capabilities and effectively delineate the specific plasma region under observation [71] (Figure 4.15).

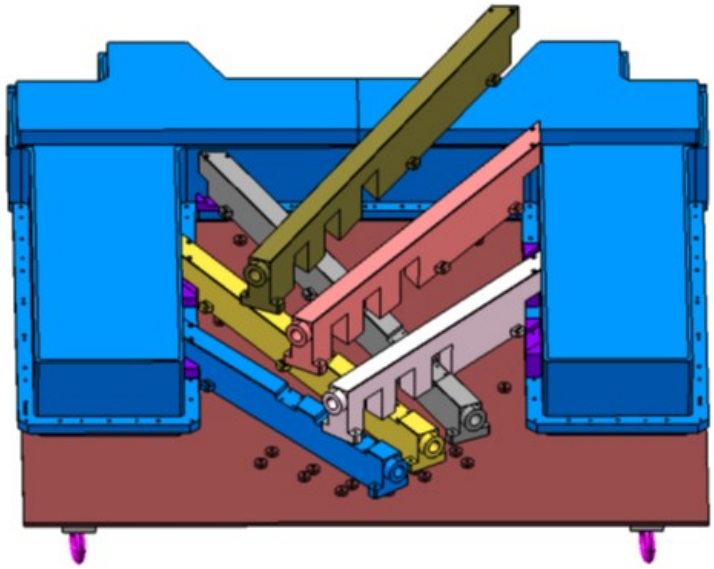

Figure 4.15: In-Port Collimators ([71]).

The design of the collimators has resulted in several key features:

- Neutron Filtering: The collimators effectively ensure that detected neutrons are primarily those that have traveled directly from the plasma core to the detectors [71].
- Material and Configuration: Composed of stainless steel for superior attenuation of fast neutrons, the collimators are divided into two parts, enhancing their shielding capabilities [71].
- Precision Alignment: The critical precision alignment of these collimators is achieved through specialized ribs on the cassette structure with close tolerances, ensuring the toroidal alignment of each detector unit with its corresponding line of sight [71][Req.#31].

Cassette Assembly

The Cassette Assembly is designed as a sealed containment unit, connected to the secondary vacuum system, which is crucial for protecting and ensuring the stable operation of sensitive detector components in the vacuum environment of ITER [73]. It securely houses the Detector Modules, the rear collimator units, Beam Dumps, and essential shielding material [73, 75]. The components are designed to have no trapped volumes in the primary vacuum [69][Req.#51] and be accessible for leak localization [69][Req.#56] (Figure 4.16).

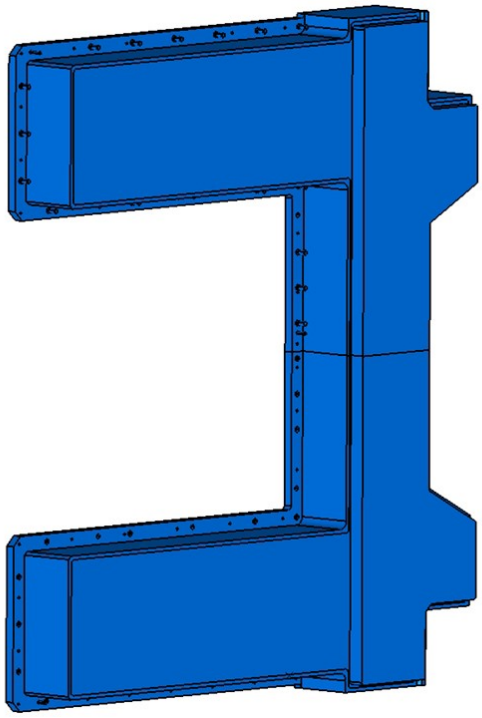

Figure 4.16: In-Port Cassette Overview ([71]).

The selection of AISI316L-IG for the jacket and structural components is justified by its fundamental property of reducing the material activation, sustained by its robust mechanical properties, which are necessary to support the fission chamber and sCD Matrix Neutron Detector, provide secure attachment points, and ensure alignment with the line of sight [71, 74]. In-vessel components' material selection

assesses steam exposure [69][Req.#34][Req.#35]. Ex-vessel components are made of easily decontaminable surfaces [69][Req.#32]. The system must accommodate differential movements [69][Req.#30].

The monolithic design approach of the cassette, involving a very long perimeter weld, presents significant manufacturing challenges. Mitigating the distortion impact of such a weld is paramount to ensure compliance with stringent performance requirements and maintain the precise alignment of internal components [72], as long as being precisely accommodated within the DSM#3 (Figure 4.17).

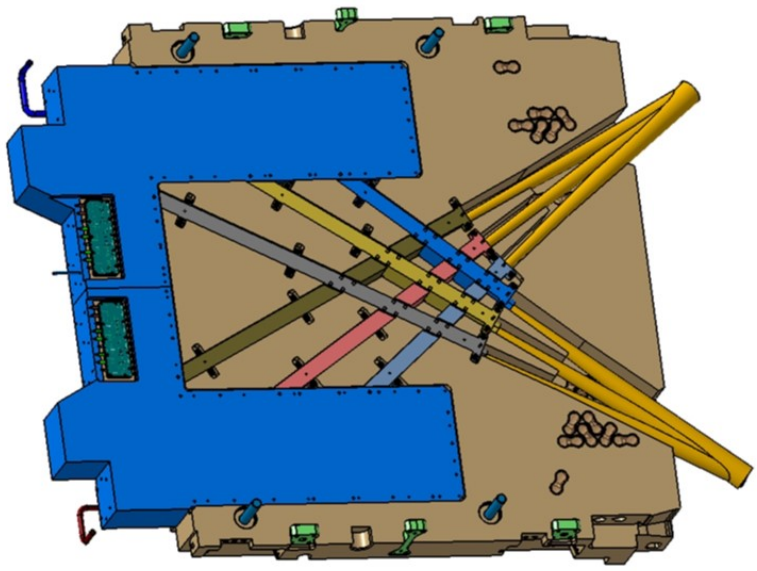

Figure 4.17: In-Port Cassette accommodated inside the DSM #3 ([71]).

The design and manufacturing processes for the Cassette Assembly have yielded a robust and precisely engineered containment unit:

- Structural Integrity and Support: The jacket, constructed from AISI316L-IG, is designed to accommodate and support the fission chamber and sCD Matrix Neutron Detector [74]. It incorporates multiple holes for assembly and alignment (Figure 4.18), including threaded service holes, passing holes for fixation

to the cassette structure, passing holes for positioning pins, and threaded holes for attaching beam dumps [74].

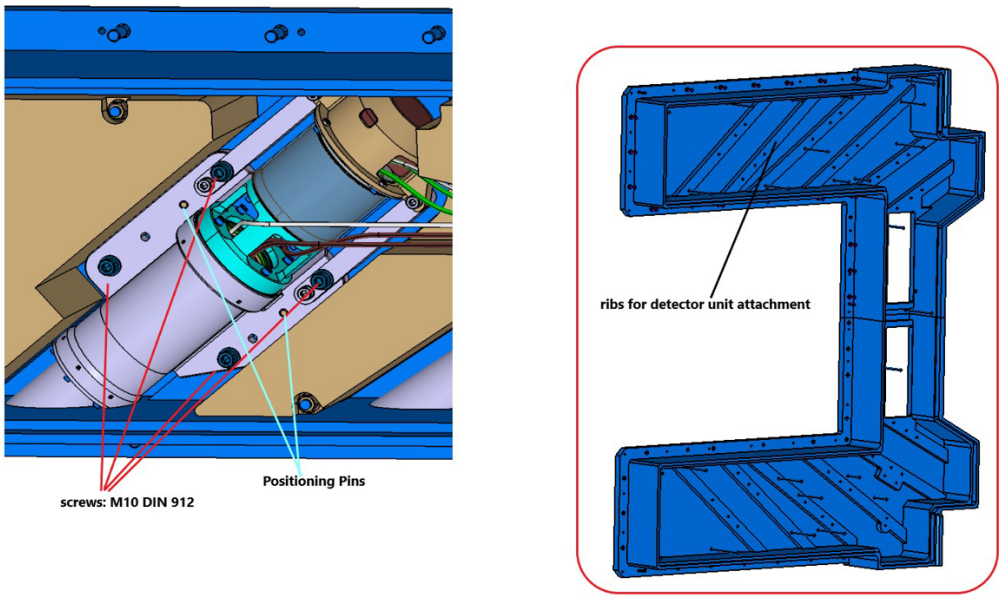

Figure 4.18: In-Port Cassette ribs for detector module fixation ([71]).

- Effective Neutron Shielding: The of Boron Carbide (B_4C) is used as a neutron shielding material due to its low weight, high neutron capture cross-section, high melting point, and negligible activation under irradiation, offering superior shielding efficacy compared to other common materials [71, 72].

- Robust Construction: The cassette structure itself is fabricated from AISI 316L-IG, comprising upper and lower welded components with a 10 mm thickness, further reinforced by ribs for toroidal alignment of detector modules [74]. This all-welded, single-wall construction integrates welded feedthroughs for electrical and vacuum penetrations, enabling robust connectivity and environmental sealing [74]. Vacuum envelopes are designed and manufactured using appropriate standards [69][Req.#50], with a safety leak rate [69][Req.#55] and double vacuum barrier for vulnerable components [69][Req.#54].

- Manufacturing Precision: Precise machining of the cassette body and welding of components, including the B_4C blocks, are critical steps that ensure the structural integrity and precise alignment required [74]. The manufacturing process involves careful assembly of detector modules, installation of fission chambers and diamond detectors with their cable tails, and the integration of threaded cylindrical pins for shielding block positioning (Figure 4.19) [74]. Leak tests are required after pressure testing [69][Req.#53], and a leak test procedure must be developed [69][Req.#52]. All onsite welding will undergo leak tests and non-destructive examination [69][Req.#78].

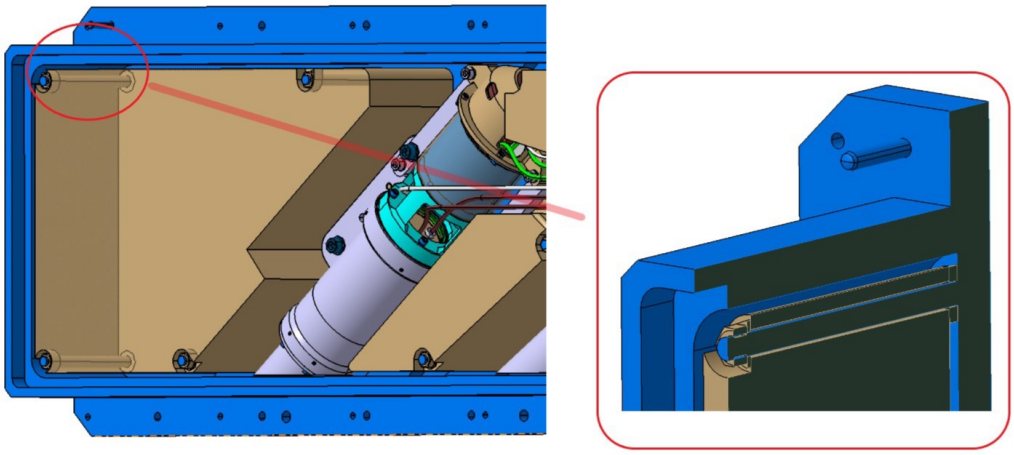

Figure 4.19: In-Port fixation of shielding blocks ([71]).

- Surface Finish Requirements: A maximum surface roughness of Ra 6.3 is mandated for the cassette structure and its integrated feedthroughs, while shielding blocks require a Ra 12.5 maximum and must be produced by sintering to enhance shielding efficacy [74].

- Cable Management: The cassette also contains support structures for cabling and electrical feedthroughs (Figure 4.20), ensuring reliable operation of the detectors within the harsh ITER environment [74]. Electrical equipment tests must comply with standards [69][Req.#36]. The RNC system can sustain EM

loads with multiple earth points [69][Req.#41], and in-vacuum SSCs are bonded to the Port-Plug or Vessel wall [69][Req.#42].

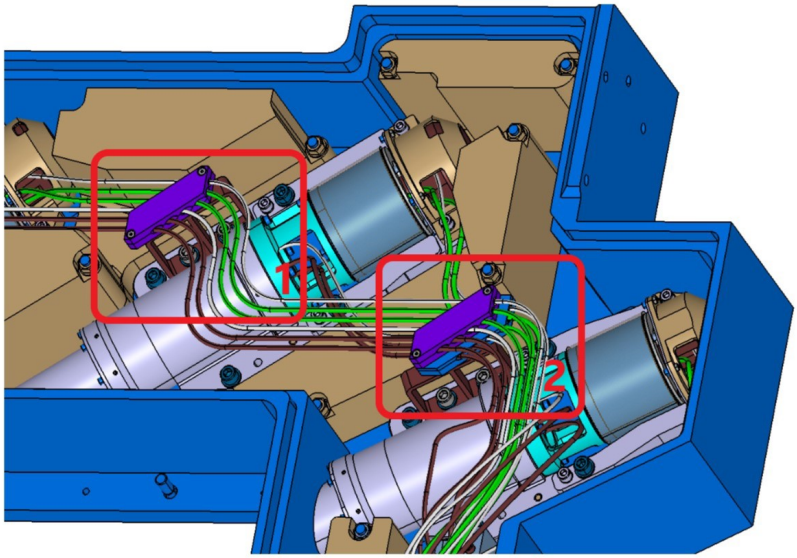

Figure 4.20: Cable supports in the upper part of the In-Port Cassette ([71]).

Structural Assessment

The structural integrity of the In-Port RNC is paramount, necessitating rigorous assessment against a spectrum of anticipated loads [71, 73][Req.#1][Req.#24]. This assessment is guided by detailed System Load Specifications, which encompass structural, electromagnetic, and thermal loads [73][Req.#26][Req.#29]. A comprehensive Structural Integrity Report has been prepared for the in-port RNC port plug components, detailing the analyses conducted to ensure their resilience [72][Req.#25]. This report outlines the structural design criteria, including component classification, potential failure modes, allowable stresses, and specific rules for bolt verification [72]. The structural assessment also addresses the RNC's ability to withstand seismic events without compromising its own safety functions or those of other interconnected ITER components [72][Req.#25].

System Load Combinations The structural analysis of the In-Port RNC components considers a series of individual loads and their combinations. The System Load Specifications document explicitly lists these loads and outlines their categorization [73][Req.#26]. Load combinations for the RNC Port Plug Components are categorized into three main types (I, II, and III), derived from the broader ITER load cases and combinations [73]. These combinations take into account various events such as dead weight, thermal operating, temporary mechanical loads, bolt/pin pre-tension, Major Disruptions, Vertical Displacement Events, and Vacuum Vessel Ice conditions [73]. For example, a load combination might include DW, THO, TMP, and bolt/pin pre-tension for all components, while more complex scenarios combine these with MD or VDE events [73]. Specific single load cases analyzed include dead weight, bolt pre-tension, electromagnetic interface loads, electromagnetic environmental loads due to Eddy Currents, and thermal loads (Baking and/or Normal Operation Conditions - NOC) [72]. Notably, seismic loads, though considered, were found to be negligible compared to other interface loads and were therefore neglected in the final load combination analyses [72].

Standards Used for Verification The structural assessment of the In-Port RNC components, particularly the cassette assembly, is performed in accordance with the RCC-MR 2007 Code [72, 73][Req.#27]. This code, specifically chosen for its applicability to design, manufacturing, and testing of RNC in-port components, dictates the structural criteria and service levels [72, 73]. For all In-Port RNC components within the scope of the SLS, and given that all loading categories correspond to a "Normal" damage limit, a service level "A" has been uniformly applied for all components under any load condition [73]. This ensures a conservative approach to design and verification. The assessed failure modes include P-type damage (negligible creep, Level A, C, and D criteria) and S-type damage (negligible creep, progressive deformation, and fatigue), with buckling not being a considered failure mode due to the absence of compression loads or external pressure on the RNC structure [72]. SMS and PALEO-earthquake response spectra are calculated in accordance with relevant reference documents [72][Req.#28].

Structural Analysis Results A detailed structural analysis was conducted for the main In-Port RNC components located inside the port plug, including the collimators, the cassette assembly, and its internal components [72]. The key findings are summarized as follows:

- Collimators: The current design of the collimators demonstrated the ability to withstand all single loads and load combinations, with one exception: load combination II.RNC.1, which involves thermal baking temperature distribution [72]. Despite this, the M12 bolt layout used in the collimators was verified to withstand all specified loads and load combinations [72].

- Cassette Assembly: The present design of the cassette assembly is capable of withstanding all single loads and load combinations [72]. However, the stresses arising from Major Disruption interface loads were identified as the dominant contributions to the overall stress [72].

- Internal Components: Analysis of the internal components revealed no stresses relevant to their structural integrity, either in single load calculations or in load combinations [72].

- Safety Factors: For single load cases, a summary of maximum Von Mises Stress and corresponding safety factors against yielding (220 MPa at NOC, 144 MPa at baking) and against 3Sm (a measure of primary stress intensity) was provided. For instance, Dead Weight and Bolt Pretension exhibited a safety factor of 4.4, while interface loads from MDII showed a safety factor of 2.8. Thermal loads during NOC and baking conditions yielded safety factors of -3.15 and -1.13 respectively [72].

In conclusion, the structural assessment confirms the general robustness of the In-Port RNC components under most anticipated operating conditions, with specific areas of concern identified in the cassette assembly's bolted connections under certain load combinations [72].

4.2.2 Shielded Cabinet for Preamplifiers

The Shielded Cabinet for Preamplifiers is an essential component of the RNC system, located in the Port Cell approximately 8.5 meters from the detector units [71]. Its primary purpose is to protect sensitive preamplifier electronics from intense radiation, including neutrons and gamma rays, as well as electromagnetic fields, ensuring the reliable operation of the RNC system [71, 75]. The cabinet is a large (250x90x60 cm^3), heavy (7 tons) structure [71], characterized by a multi-layered shielding design.

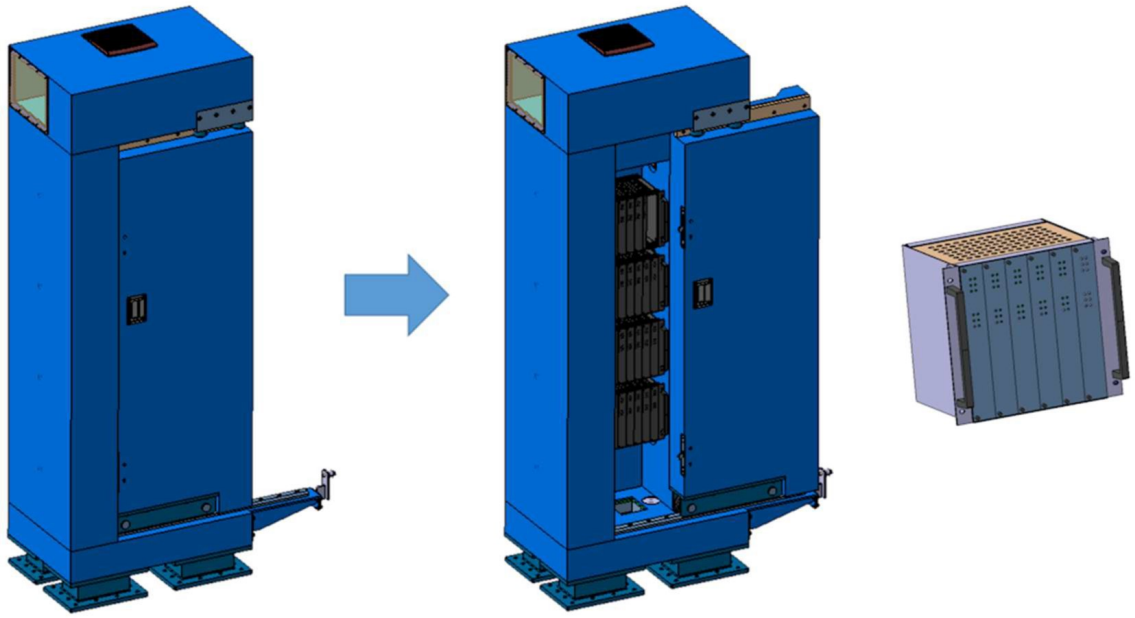

Figure 4.21: Shielded Cabinet for Preamplifiers ([70]).

This design incorporates materials like stainless steel, a neutron thermalization layer, a tungsten carbide layer for gamma absorption, and an iron layer for electromagnetic shielding [71, 76] (Figure 4.21). It houses approximately 100 preamplifiers, including those for the In-Port RNC's sCD and FC detectors, and features an integrated fan for cooling [71, 75].

Design justification

The preamplifiers for RNC detectors need to be located as close as possible to the detectors to minimize signal degradation [71]. However, the radiation levels in the Port Cell, approximately 8.5 meters from the In-Port RNC detector units, exceed the thresholds for non-critical systems containing electronics [71]. The EMC and radiation policy must be applied [69][Req.#57]. This protection ensures the accurate and reliable operation of the RNC system despite the challenging conditions. The use of multichannel preamplifier boards is assumed to minimize volume occupancy and, therefore, maximize the shielding volume [71]. Ensuring the RNC system electrical equipment tests are compliant with standards [69][Req.#36] and that the RNC system can sustain EM loads [69][Req.#41] are key considerations.

Design Results

The design of the Shielded Cabinet for Preamplifiers reflects a multi-layered, robust approach to radiation protection and electromagnetic compatibility:

- Location and Size: The cabinet is situated in the EP01 Port Cell and is bolted onto the Port Cell Supporting Structure [71, 75]. Its volume (250x90x60 cm^3) and weight (7 tons) are at the maximum permissible limits based on constraints from the Port integrator [71].

- Multi-layered Shielding Structure: Protection is obtained through a multi-layered structure (Figure 4.22) based on a specific scheme for shielding [71, 76]:

  - A first layer thermalizes (moderates) fast neutrons by neutron scattering [71, 76].
  - A second layer absorbs the gammas (environmental and produced by capture reactions), such as a Tungsten carbide layer [71, 76].
  - A third layer is for EM shielding, for example, the Metglas [71, 76].

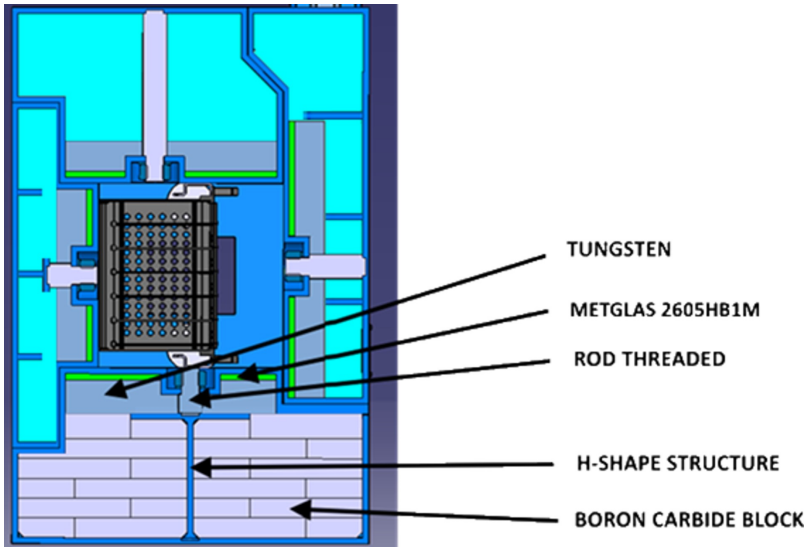

Figure 4.22: Layer structure of the Shielded Cabinet ([70]).

- Construction and Materials: Each of the main 6 parts of the cabinet will be made up of an external stainless steel sheath, holding inside it the different layers of shielding materials [76]. The outer stainless steel sheath and supporting feet can be manufactured by metal plate welding [76]. The internal structures needed to hold the shielding blocks can also be manufactured by plate welding and used to further stiffen the structure [76]. The five parts of the cabinet box (excluding the door) can be joined by welding or bolting [76]. The square tungsten and iron box created by the cabinet's main components around the electronics is visible in sectional views [76]. Ex-vessel metallic elements which are not mechanically and galvanic interconnected shall be interconnected by means of an accessible protection conductor with a cross-section at least equal to the LV supply cable cross-section [69][Req.#39]. Ex-vessel electrically conducting SSCs shall have an electrical bonding point at least every four meters compromised between every 1 to 4 m maximum, the first bonding being the EMC Zones boundary [69][Req.#40].

- Contents: Specifically for the In-Port RNC, it houses 12 sCD preamplifier

boards (two per detector unit) and 6 FC preamplifier boards (one per detector unit) [75]. An integrated fan provides cooling for the front-end electronics [75].

- Electronics Choice: A fast charge preamplifier is chosen for the sCD detector to preserve its energy discrimination capabilities, while a simpler and robust current preamplifier is adopted for the FC, which does not require energy discrimination [71]. Steady-state power supplies used by 55B1 RNC will provide remote-controlled breakers and switchgear [69][Req.#37], and 55B1 RNC that does not use Class II power supplies can use Class IV power supplies [69][Req.#38].

4.3 Ex-Port Radial Neutron Camera

This section provides a comprehensive examination of the Ex-Port RNC system, detailing its design, structural integrity, reliability, maintenance protocols and their validation through VR, and on-site assembly procedures. The focus will be on the mechanical engineering aspects, reflecting the development and specific design choices necessitated by its critical role within the challenging ITER environment. Further information can be found in the paper work [77] by the author of this thesis.

4.3.1 Ex-Port Overview

The Ex-Port RNC is the ex-vessel diagnostic system of the RNC, located in the Port Interspace zone. As already presented, its primary scientific objective is to characterize the core of the plasma, specifically targeting a normalized minor radius (r/a) less than 0.85 [Req.#7][Req.#8]. This is achieved through the precise measurement of un-collided 14 MeV and 2.5 MeV neutrons, which are directly emitted from deuterium-tritium and deuterium-deuterium fusion reactions, respectively [78]. The data acquired by the Ex-Port RNC is fundamental for understanding plasma dynamics, accurately assessing fusion power generation [Req.#10][Req.#12], and optimizing the operational parameters within ITER.

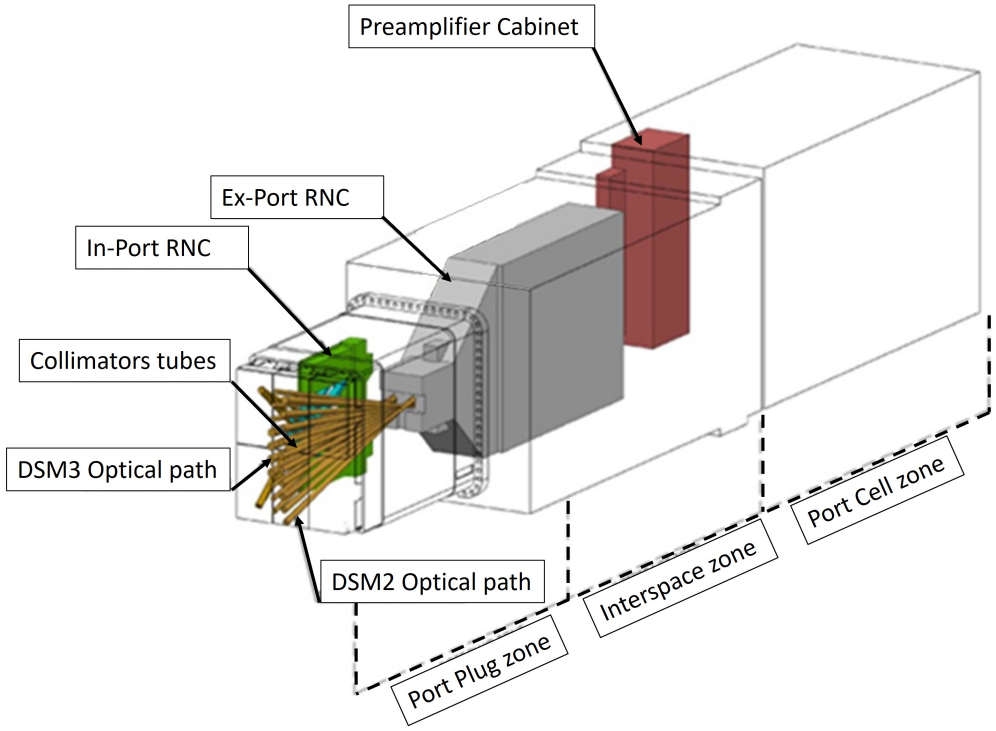

Figure 4.23: RNC overview - EU01 and EU11 inside the Equatorial Port #1 ([77]).

The Ex-Port RNC system is distributed across several key locations within the ITER facility, comprising distinct Embarked Units that interface with various plant systems [68, 70, 79] (Figure 4.23):

- **EU01 DSM2 Optical Path:** Located within Drawer #2 of the Port Plug [Req.#23], this unit defines the specific optical pathways, or Lines Of Sight, that channel neutrons from the plasma to the Ex-Port RNC detectors [68, 70]. The design of these optical paths is a result of optimization to minimize cut-outs within the Diagnostic Shielding Module [70].

- **EU11 IS Equipment:** This major unit is situated in the port interspace of EP01 and is physically mounted onto the Port Cell Supporting Structure [68]. It integrates a multitude of components critical for neutron detection and associated functionalities. These include the Flight Tubes, Collimation Units,

Detector Modules, a robust Shielding Block, Beam Dumps, the Temperature Stabilization System, the Position Monitoring System, and the Alignment System [68, 79][Req.#23].

Located in the Interspace zone of Equatorial Port #1, the Ex-Port RNC interfaces other diagnostics, such as the Radial Gamma Ray Spectrometer and the High-Resolution Neutron Spectrometer [68, 70] (Figure 4.24).

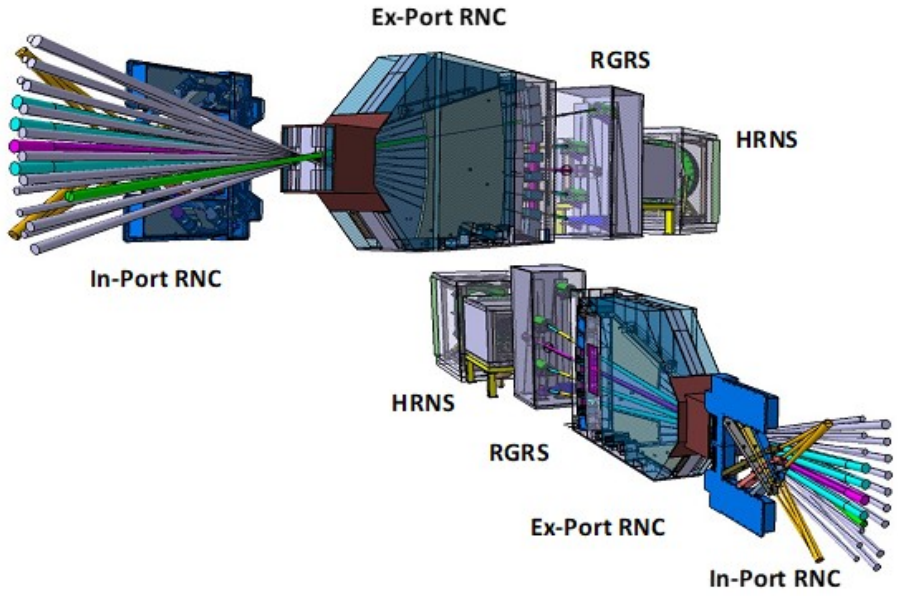

Figure 4.24: In-Port RNC, Ex-Port RNC and the interfacing diagnostics RGRS and HRNS ([80]).

4.3.2 Ex-Port Subsystems Design Description

The design of the Ex-Port RNC subsystems is characterized by a modular approach, where each component is engineered to perform specific functions within ITER's demanding operational environment. The design methodology prioritizes achieving high-precision neutron measurements [Req.#47], while simultaneously ensuring structural integrity, effective thermal management, and robust radiation protection

for all critical elements. The appropriate levels of control and requirements for quality assurance are defined in the specific diagnostic designs [Req.#76].

EPP1 and EPC1 Coordinate Systems

Prior the detailed definition of the Ex-Port RNC subsystems, it is fundamental to define the coordinate systems used. These are the "EPP1 CS", the Equatorial Port Plug 1 Coordinate System and the "EPC1 CS", the Equatorial Port Cell 1 Coordinate System, and the . To identify them, the TGCS (Tokamak Global Coordinate System - the central Coordinate System of ITER) is first rotated of 10° around its z-axis (Figure 4.25).

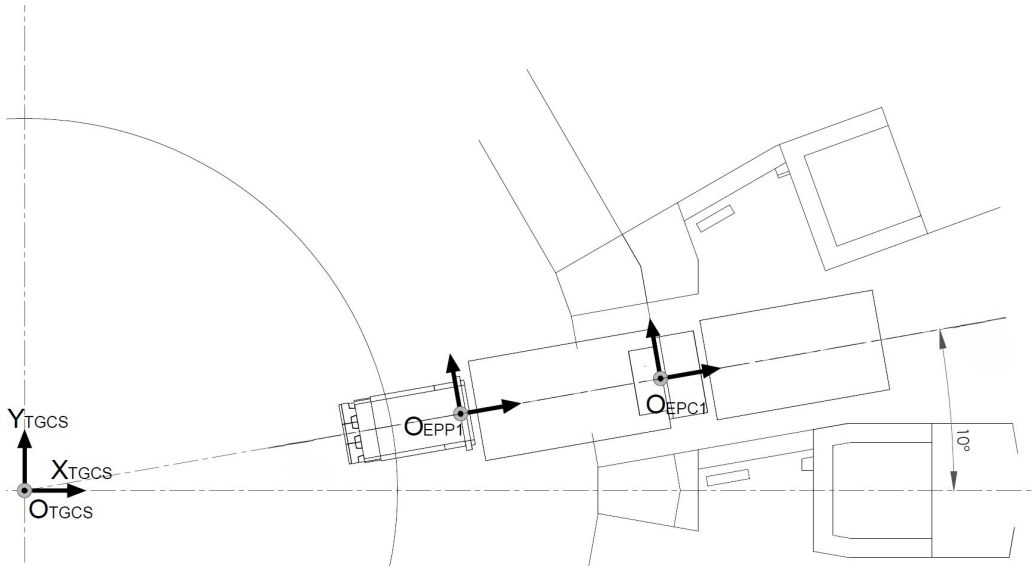

Figure 4.25: Rigid rotation to identify the Equatorial Port #1 ([81]).

Then, two rigid translations are applied, as shown in Figure 4.26.

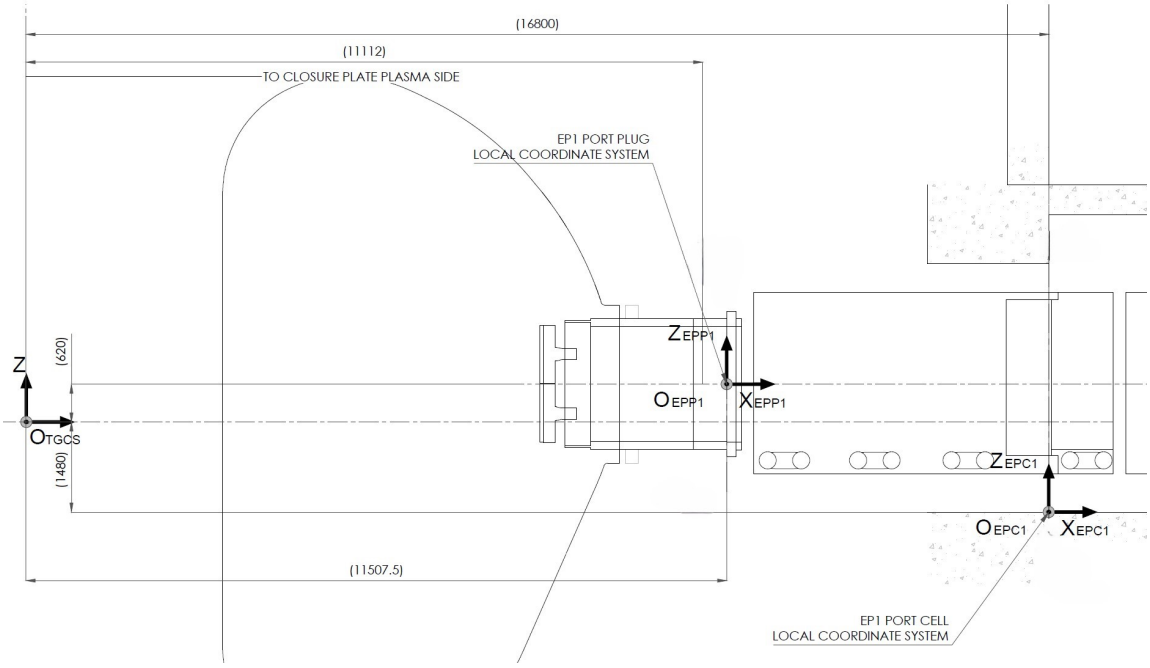

Figure 4.26: Dimension details of EPP1 and EPC1 ([81]).

The coordinates of the origin point, with respect to the TGCS rotated of 10°, of EPP1, EPC1 and EU11 are reported in Table 4.3.

Table 4.3

	$\mathbf{X_{TGCS}}$	$\mathbf{Y_{TGCS}}$	$\mathbf{Z_{TGCS}}$
$\mathbf{O_{EPP1}}$	11507.5	0	620
$\mathbf{O_{EPC1}}$	16800	0	-1480
$\mathbf{O_{EU11}}$	14425	46	-422

EU01 - DSM2 Optical Path Design

EU01, which defines the optical paths for the Ex-Port RNC LOS, is located within the Diagnostic Shielding Module in Port Plug Drawer #2[Req.#23]. The fundamental design rationale for the geometry of these optical paths is to achieve an optimal

balance between maintaining the necessary LOS and minimizing the required cut-outs in the DSM. This design approach aims to preserve the structural integrity and shielding effectiveness of the DSM by avoiding large, singular penetrations. Instead, separate, optimized cut-outs are employed for each LOS where feasible. The material selected for the DSM in EPP 1 by the Port Integrator is stainless steel and water. The RNC in-vessel and in-port plug components shall withstand the loading conditions derived from the pulses during ITER operation to keep the integrity of the vacuum vessel [Req.#1][Req.#24].

EU11 - External Interfaces

The definition of the interfaces with surrounding systems is a critical task with direct consequences on the EU11 design. The definition of the interfaces constitutes a legal document that is crucial for identifying the ownership of the systems - the boundaries of the design contracts between the different designer entities.

EU11 Configuration Model Prior the definition of the interfaces, the design shall be driven by the volume occupation of EU11 inside the Port Interspace zone. EU11 can be modelled within a *Configuration Model - CM*, a box that represents the limits of the EU11 extension in the space. Figure 4.27 shows the EU11 CM located in the EP01, Figure 4.28 shows an isometric view of the EU11 CM and Figure 4.29 shows the dimensions of the EU11 CM.

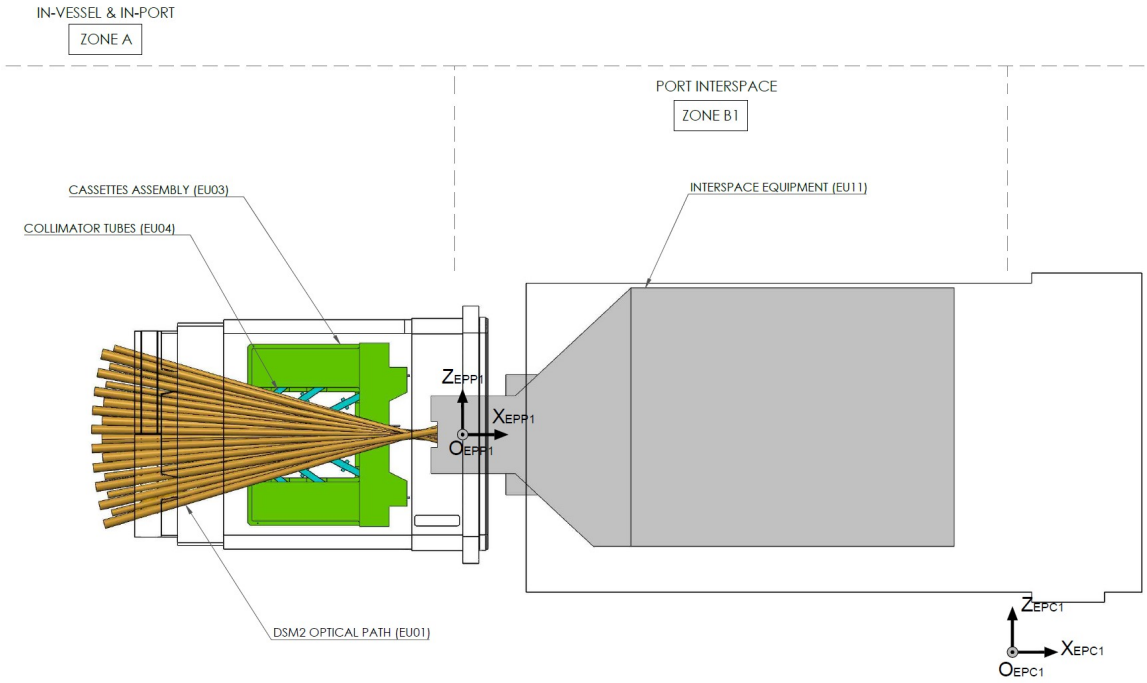

Figure 4.27: Location of the EU11 CM in the Port Interspace ([82]).

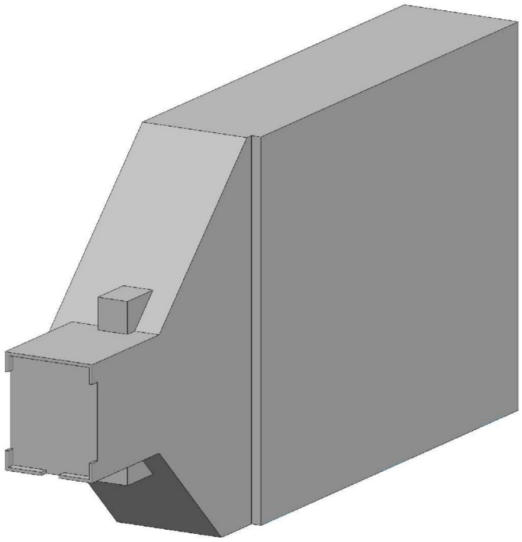

Figure 4.28: Isometric view of the EU11 CM ([82]).

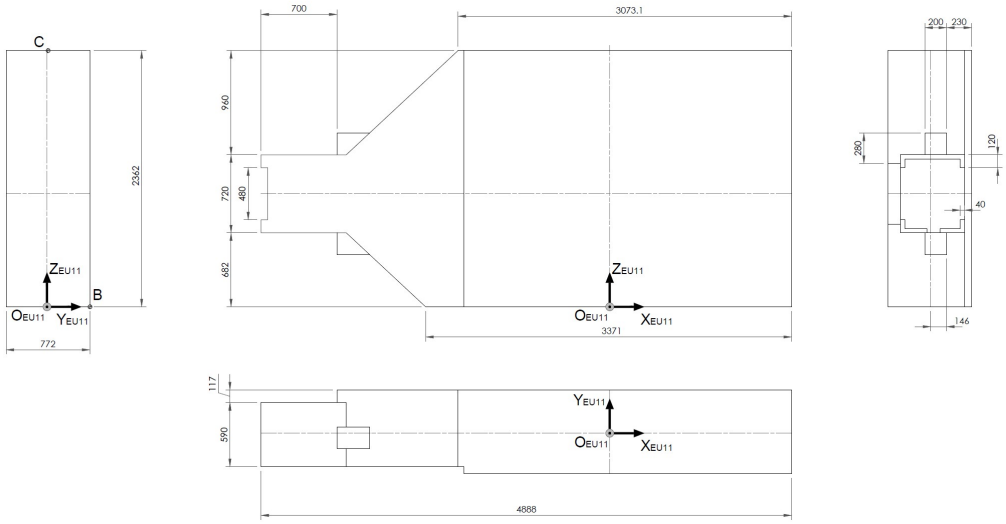

Figure 4.29: Detailed dimensions of the EU11 CM ([82]).

EU11 interface with ISS The interface of the EU11 with the Interspace Supporting Structure is fundamental for the definition of the Ex-Port RNC base and for the definition of the assembly procedures.

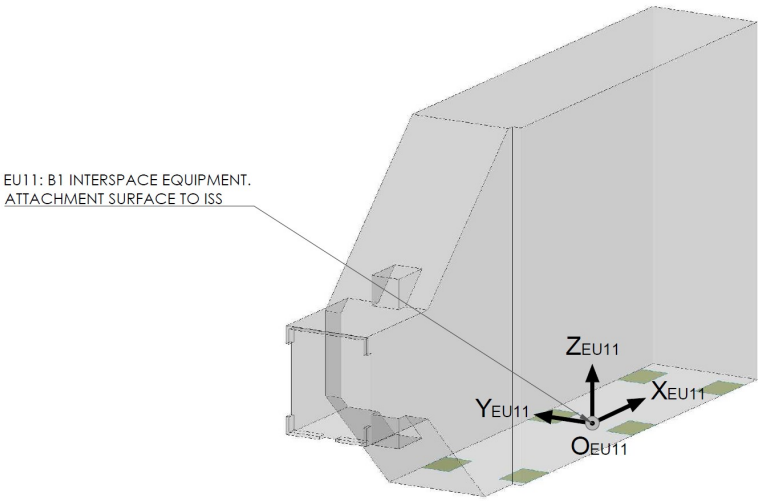

Figure 4.30: Eu11 interface with ISS ([82]).

The interface is realized in the bottom part of EU11 (Figure 4.30) and it formed by 6 matrices of 7 bolted connections, in which the ISS hosts the threaded holes and the EU11 hosts the passing holes. The bolt dimension chosen is M16.

Figure 4.31 shows the detailed dimensions of the interface surface and the position of the holes; Figure 4.32 shows the details of the one of the 6 holes matrices.

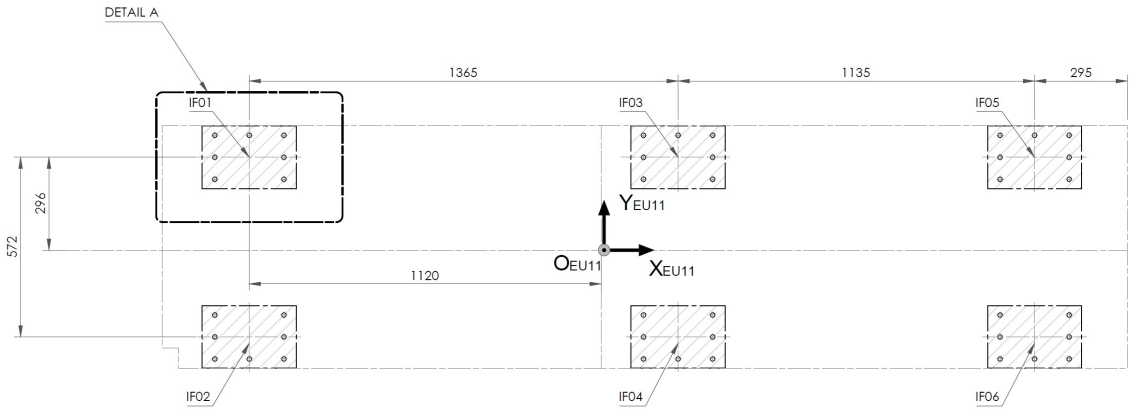

Figure 4.31: Dimensions of the EU11 interface with ISS ([82]).

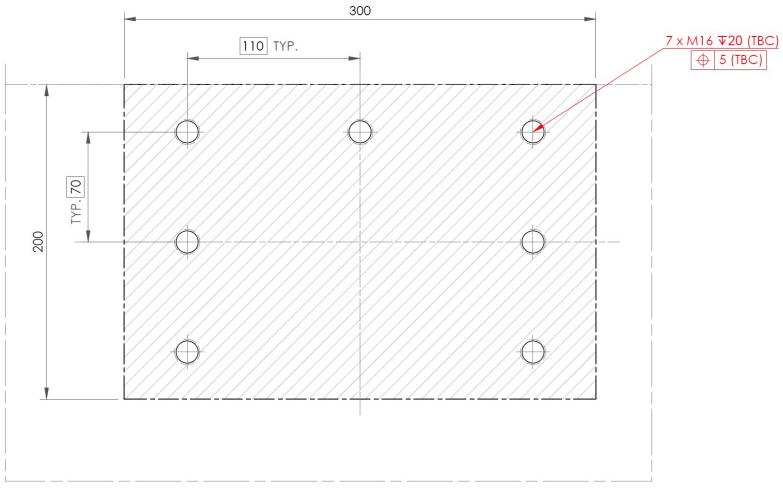

Figure 4.32: Detailed dimensions of the holes matrix ([82]).

EU11 electrical interface The electrical interface of EU11 is based on a defined area through which the cables can pass (Figure 4.33). Figure 4.34 shows the detailed dimensions and positioning of the electrical interface.

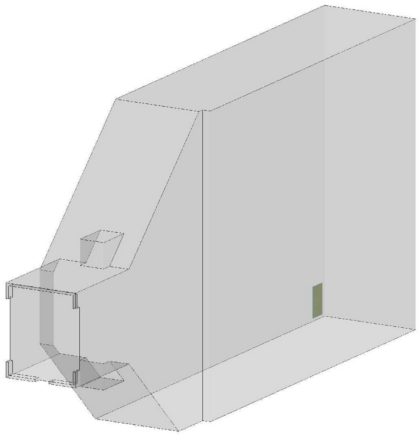

Figure 4.33: Location of the electrical interface in EU11 ([82]).

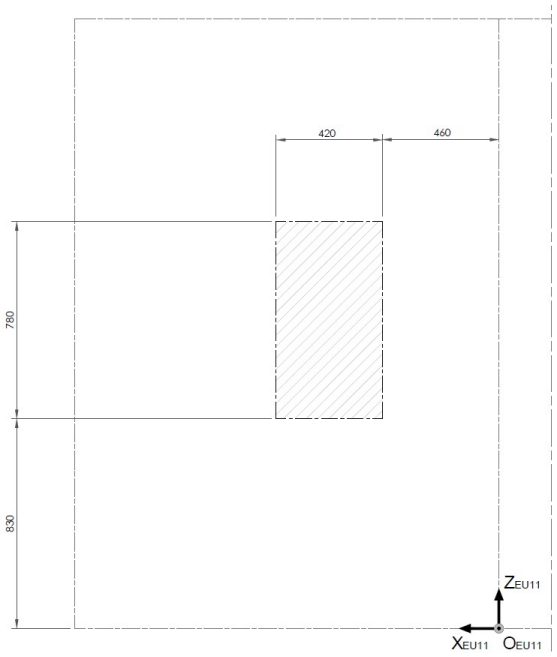

Figure 4.34: Detailed dimensions of the EU11 electrical interface ([82]).

EU11 cooling interface The cooling interface of EU11 is based on two defined areas through which the pipes of the Temperature Stabilization System can pass (Figure 4.35). Figure 4.36 shows the detailed dimensions and positioning of the electrical interface.

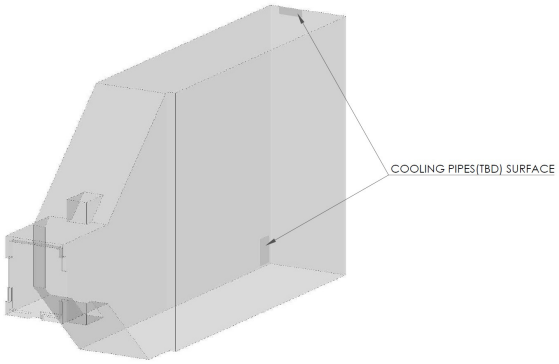

Figure 4.35: Location of the cooling interface in EU11 ([82]).

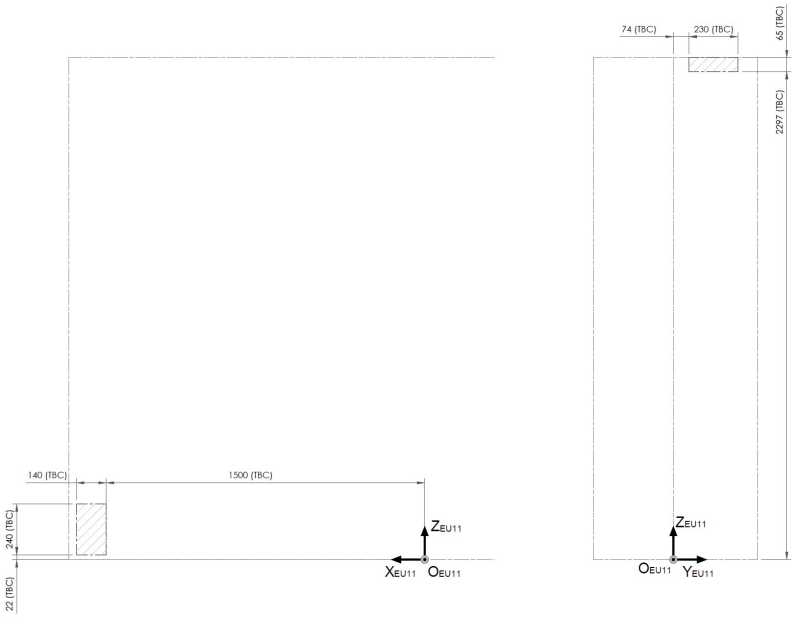

Figure 4.36: Detailed dimensions of the EU11 cooling interfaces ([82]).

EU11 interfaces with Port Plug Closure Plate The Ex-Port RNC is equipped with a Positioning Monitoring System (PMS). Its function, as fully discussed in the next sections, is to measure the relative displacements between the Port Plug Closure plate and the Ex-Port RNC. It is composed by 7 optical fiber-based displacement sensors.

The interfaces of the sensors with the Port Plug Closure plate consist of threaded holes for the attachment of a number of plates needed for the attachment of the sensors wires.

The scheme of the holes is reported in Figure 4.37.

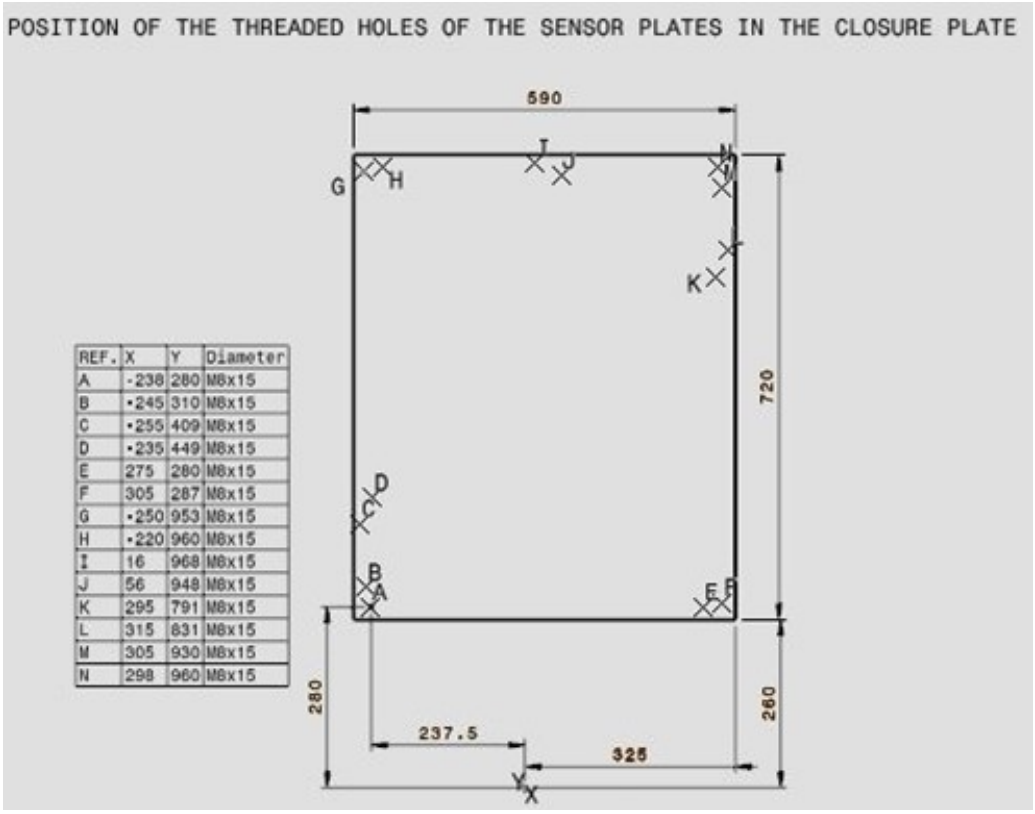

REF.	X	Y	Diameter
A	-238	280	M8x15
B	-245	310	M8x15
C	-255	409	M8x15
D	-235	449	M8x15
E	275	280	M8x15
F	305	287	M8x15
G	-250	953	M8x15
H	-220	960	M8x15
I	16	968	M8x15
J	56	948	M8x15
K	295	791	M8x15
L	315	831	M8x15
M	305	930	M8x15
N	298	960	M8x15

Figure 4.37: Position of interfaces on Port Plug Closure plate ([82]).

EU11 - IS Equipment Mechanical Design

EU11, the largest embarked unit of the Ex-Port RNC, is located in the Port interspace and constitutes the core detection and support system. Its design integrates numerous sub-systems, each featuring specific mechanical designs and material selections tailored for the fusion environment. The total weight of the Ex-Port RNC EU11 is approximately 16200 kg, and the main dimensions are visible in Figure 4.38.

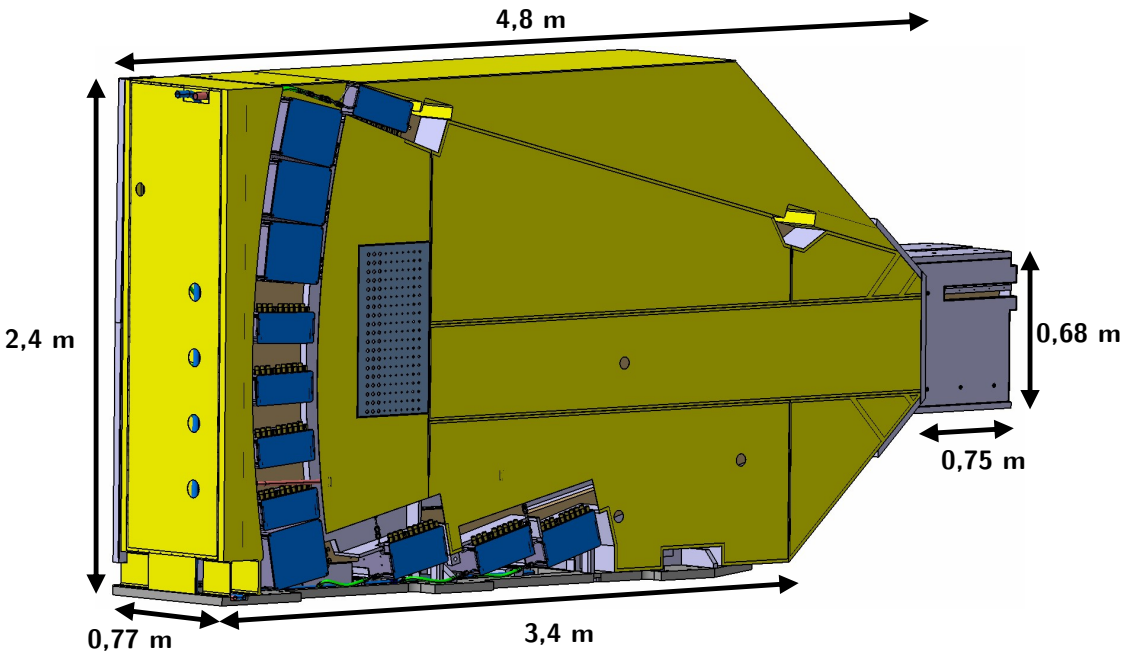

Figure 4.38: Ex-Port RNC EU11 overview ([80]).

The design of the Ex-Port RNC employs two fan-shaped collimating structures (Figure 4.39) that are precisely aligned to view the plasma through dedicated vertical slots within the Diagnostic Shielding Module [78][Req.#21]. This configuration defines 16 interleaved Lines Of Sight [Req.#23] distributed across two radial planes, which intercept the machine axis. This precise arrangement is crucial for minimizing background noise from scattered neutrons and gamma rays at the detector positions, thereby ensuring that primarily uncollided neutrons originating from the plasma are measured.

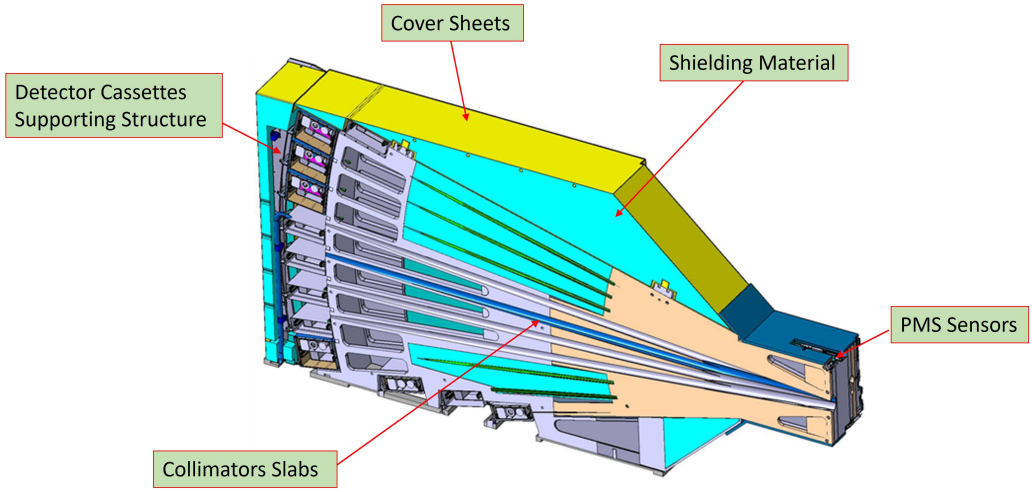

Figure 4.39: Ex-Port RNC EU11 section overview ([80]).

Following the RNC configuration studies (Section 4.2), the LOS are positioned as specified in Table 4.2. This is translated in positioning the Detector Cassettes as shown in following Figure 4.40:

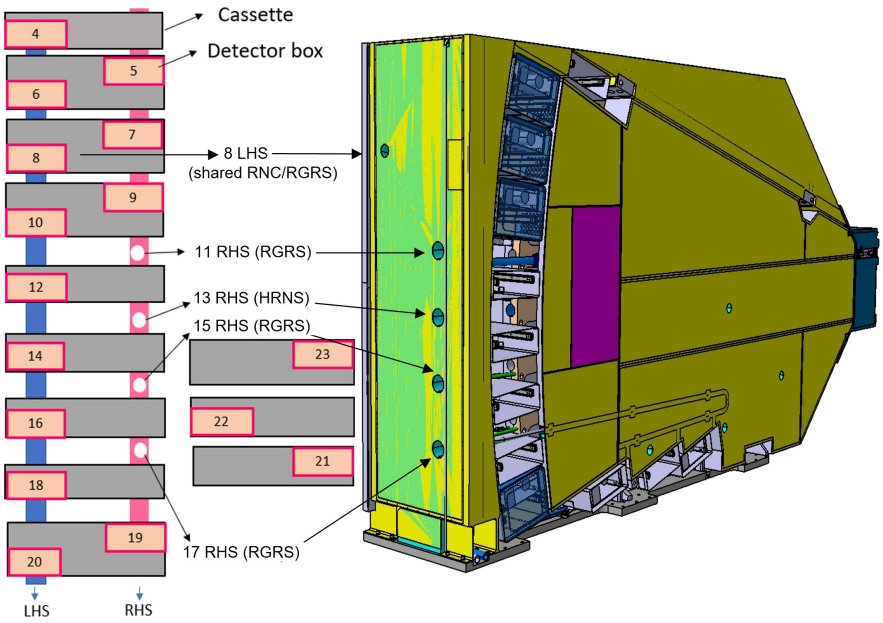

Figure 4.40: LOS arrangement in the Ex-Port RNC ([80]).

An exploded view of the Ex-Port RNC is shown in Figure 4.41 and depicts the main subsystems that will be discussed in the next paragraphs.

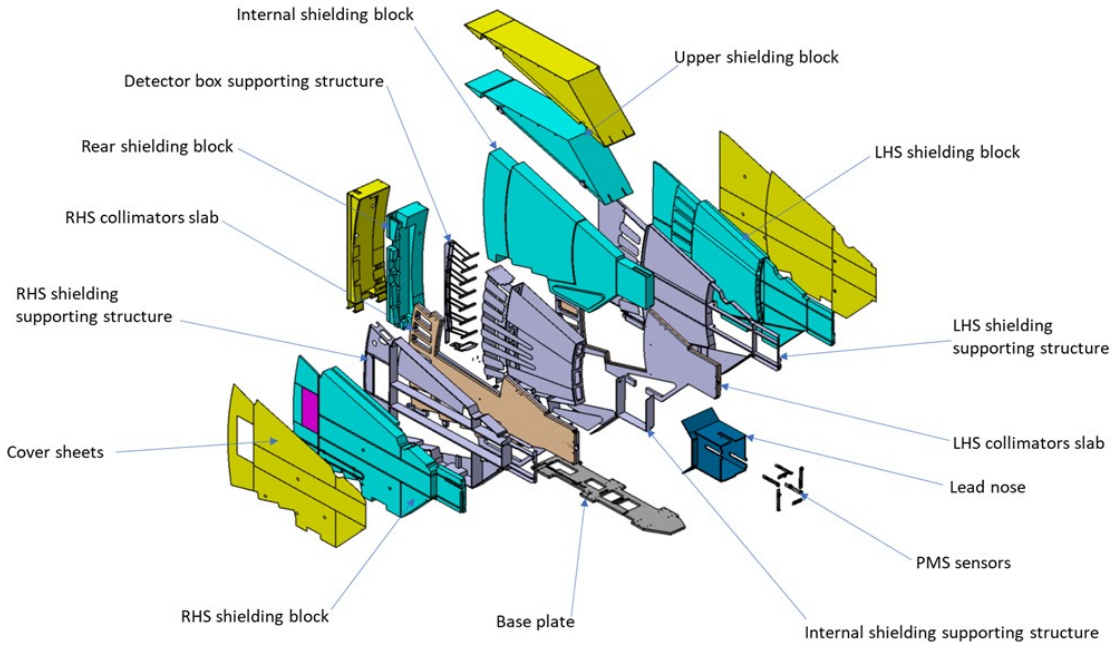

Figure 4.41: Ex-Port RNC exploded view ([80]).

Collimation Units Design The collimation units are precisely manufactured mechanical structures critical for defining the specific neutron Lines Of Sight with high angular accuracy [Req.#31]. All collimators in the Ex-Port RNC are designed with a diameter of 11 mm, with the sole exception of LOS #23, which has a reduced diameter of 8 mm. The optical paths are intentionally designed with larger dimensions than the collimators' fields of view. This design choice aims to accommodate minor misalignments without inducing vignetting (partial or total loss of direct view). This also contributes to maintaining alignment during normal operation [Req.#30]. However, the allowed misalignment depends on the specific LOS.

The manufacturing of collimators is particularly challenging, as achieving the necessary concentricity and tolerances often requires an an assembly of independently manufactured collimators rather than a single monolithic design.

The core of Ex-Port RNC is composed of two couples of SS316L(N)-IG slabs (Figure 4.42) . Each slab is machined on one side to realized half side of the cut-outs for the collimators.

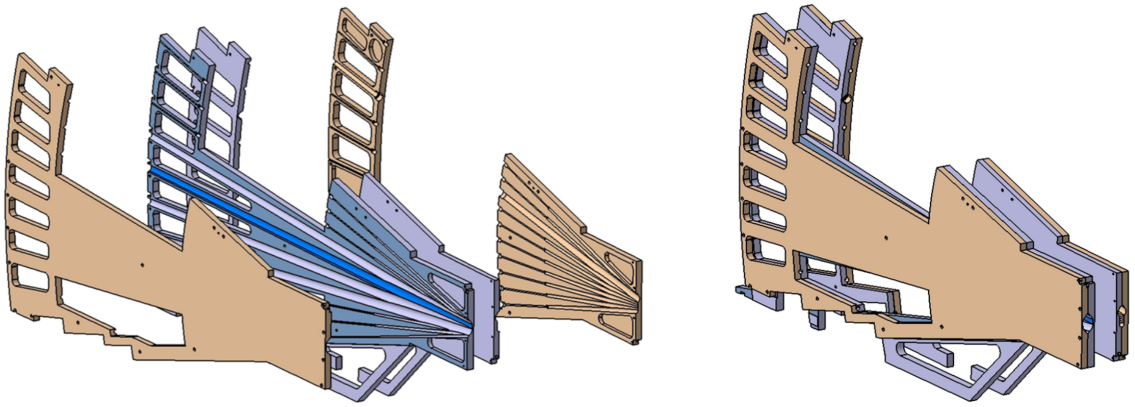

Figure 4.42: Ex-Port RNC collimators slabs ([80]).

The slabs possess thicknesses ranging from 45mm to 55mm, with individual weights spanning from 930kg to 1400kg. Various cut-outs were implemented to reduce the slabs' overall mass. Flight tubes contribute to mass reduction by replacing material in the carved channels of the slabs' cut-out areas. These tubes are inserted into dedicated grooves machined into the two halves of the slabs and subsequently welded. Figure 4.43 illustrates the lengths and diameters of both the collimators and the flight tubes for a generic LOS. Details on dimensions can be read in Table 4.2.

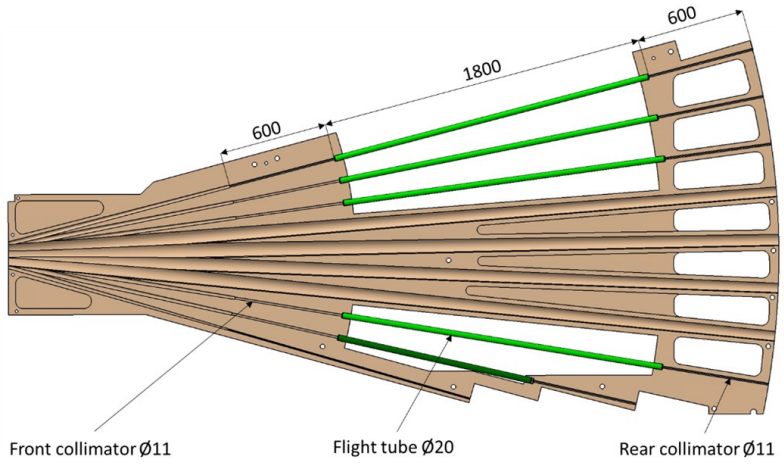

Figure 4.43: Ex-Port RNC collimator slab section with dimensions of collimators and flight tube ([80]).

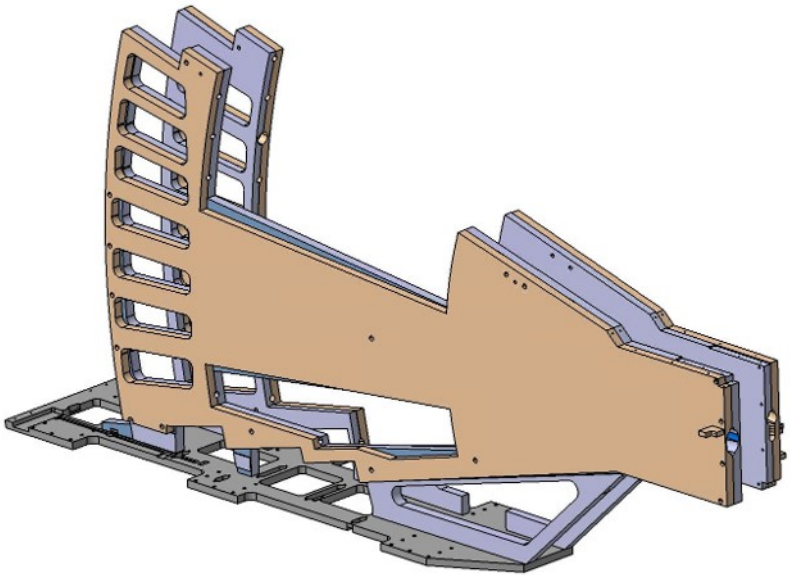

Figure 4.44: Ex-Port RNC collimator slab welded on the Base plate ([80]).

Finally, the collimator slabs are affixed to the Base plate, which serves as the Ex-Port RNC interface component with the ISS. The Base plate, a 40mm thick

SS316L-IG plate weighing 430 kg, is engineered to support the entire mass of the Ex-Port RNC (Figure 4.44).

Shielding Block Design The Shielding Block is a massive, complex structure central to the radiation protection of the Ex-Port RNC components. It is primarily fabricated from stainless steel, incorporating a concrete-like shielding material. The mechanical design of this shielding subsystem is comprehensively detailed.

The main components of the shielding subsystem include:

- Shielding Blocks Supporting Structure: This foundational structure comprises Left-Hand Side and Right-Hand Side shielding block supporting structures, an internal shielding block supporting structure, a robust base plate, and a counterplate. These supporting structures are constructed from Stainless Steel 316L(N)-IG plates, which form the structural skeleton and delineate the volumes for pouring the shielding material. Materials for Ex-vessel components, such as those in the interspace, port cell, and gallery, shall have easily decontaminable surfaces [Req.#32]. Figure 4.45 shows the SS316L(N)-IG plates welded on the collimators slabs.

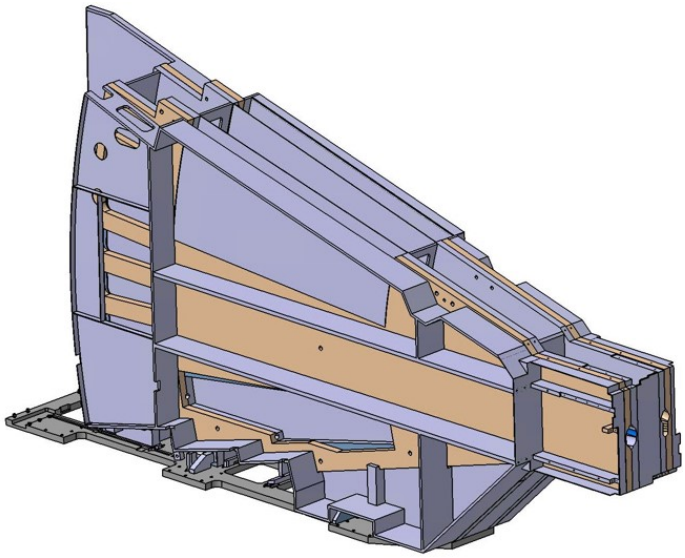

Figure 4.45: Ex-Port RNC SS plates welded on the collimators slabs ([80]).

- Shielding Blocks: These include upper, LHS, RHS, and central shielding blocks, that actively provide to the shielding purposes. The material chosen is Shieldwerx SWX-277Z-5, a concrete-like shielding material fully described in Section 4.3.3. Figure 4.46 shows the shielding blocks once the drying process (described in 4.3.3) is concluded:

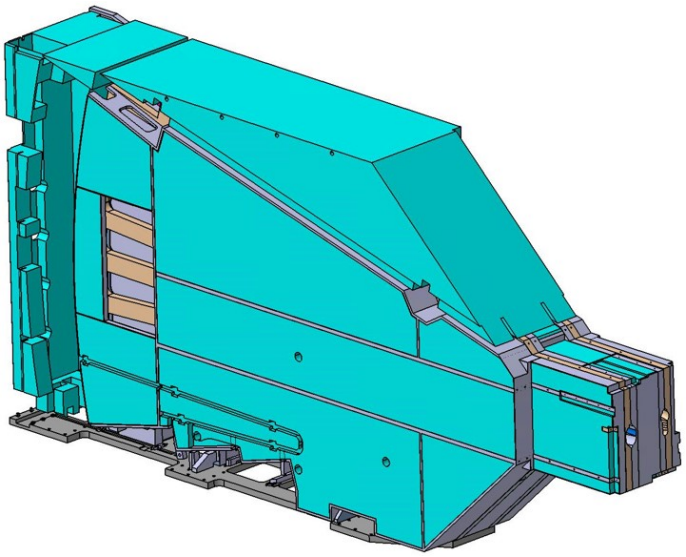

Figure 4.46: Ex-Port RNC shielding blocks on the structure ([80]).

- Cover sheets: to protect the shielding blocks, a number of 1.5mm SS316L(N)-IG cover sheets are used to envelope the entire structure (yellow in Figure 4.47). The cover sheets do not have any structural behavior.

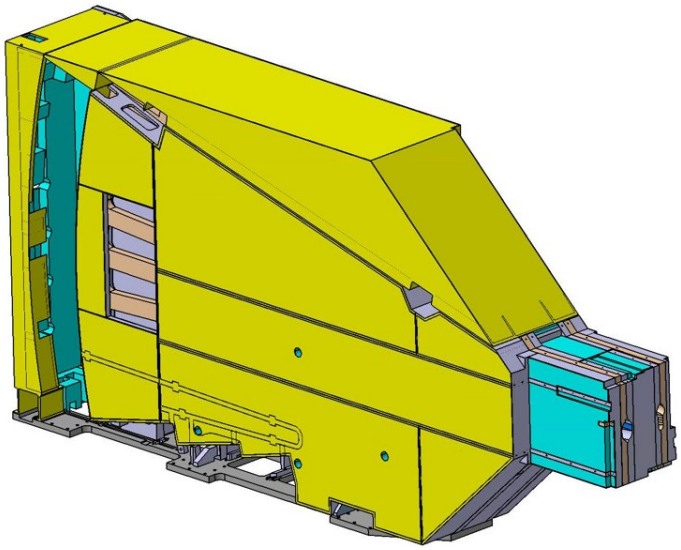

Figure 4.47: Ex-Port RNC cover sheets (in yellow) ([80]).

- Lead Nose: The Ex-Port RNC Nose forms an important part of the shielding. In the front area, there is not the possibility of surrounding Ex-Port RNC nose by Shielding material. Thus, the use of lead plates is proposed (Figure 4.48). Lead plates are 20mm thick, with a total mass of 450kg. They envelope the Ex-port RNC nose, substituting the role of SWX-277Z-5.

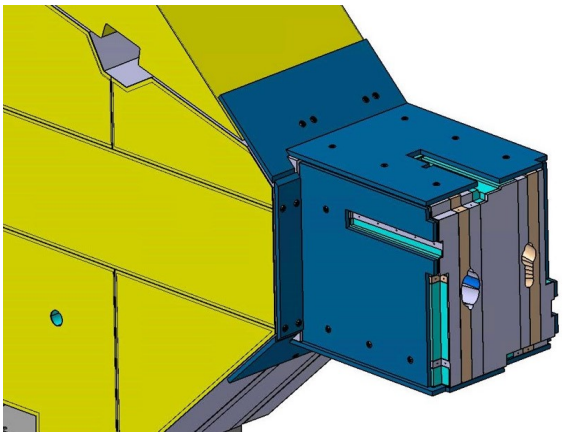

Figure 4.48: Ex-Port RNC lead nose ([80]).

Detector Module Design The detector modules within EU11 are engineered to house a diverse array of advanced neutron detectors, each selected for its ability to provide specific measurement capabilities under varying plasma conditions [Req.#47]. These detectors are enclosed within dedicated detector boxes, which are actively cooled by a specific cooling system to maintain optimal operating temperatures. An embedded calibration source is also integrated within the module design to facilitate accurate in-situ calibration[Req.#43]. Furthermore, 55.B1 shall enable acceptance testing for detectors and calibration sources as single pieces for the Ex-Port RNC [Req.#81].

The selection of detectors for the Ex-Port RNC was the outcome of an extensive trade-off study. This study evaluated critical parameters such as signal-to-noise ratio, inherent radiation hardness, safety considerations, interface compatibility, maintenance feasibility [Req.#45][Req.#73], cost implications, and calibration accuracy[Req.#43]. The resulting RNC Baseline Architecture for Ex-Port incorporates a complementary set of detector types:

- sCD Matrix (Ex-port RNC Detector #1) (Figure 4.49): This detector features a 4-pixel matrix configuration, with each pixel having a thickness of 100 µm. It exhibits an expected efficiency at 14 MeV of 1.6×10^{-3} counts/neutron, based on a 1 MeV deposited energy threshold. An embedded alpha calibration source, composed of a mixed ^{244}Cm/^{239}Pu/^{241}Am radioisotope, with an activity of approximately 6 kBq, is integrated into the sCD matrix[Req.#43]. The design and radiation environment for the Ex-Port RNC sCDs have been analyzed and modeled using MCNP.

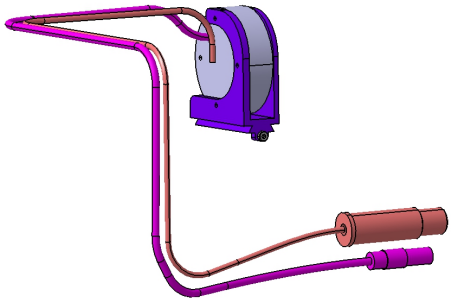

Figure 4.49: sCD Matrix detector ([83]).

- EJ-276G Plastic Scintillator (Ex-port RNC Detector #2) (Figure 4.50): This detector is characterized by a cylindrical geometry with a length of 15 mm and a diameter of 15 mm. Its expected efficiency at 14 MeV is 8×10^{-3} counts/neutron. It includes a temperature monitor (thermocouple) for real-time thermal surveillance and an embedded gamma calibration source [Req.#43]. Experimental tests have confirmed its ability to perform n/γ pulse shape discrimination and its robustness, non-toxicity, and non-flammability, making it a reasonable choice for RNC applications.

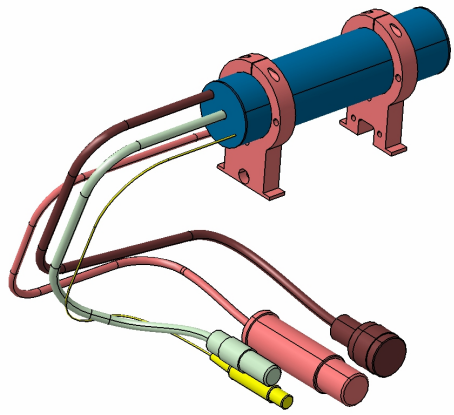

Figure 4.50: Plastic Scintillator detector ([83]).

- Helium-4 Scintillator (Ex-port RNC Detector #3) (Figure 4.51): Operating at a pressure of 80 bar, this detector has a cylindrical form with a length of 30

mm and a diameter of 44 mm. It demonstrates an expected efficiency at 14 MeV of 1.5×10^{-3} counts/neutron and also incorporates a temperature monitor (thermocouple).

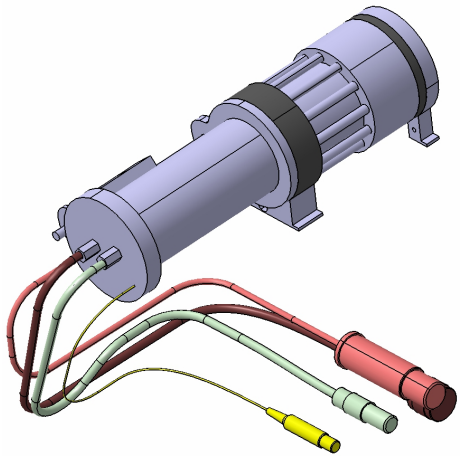

Figure 4.51: 4Helium Scintillator detector ([83]).

- Boron Carbide (B_4C) beam dumps are integrated within the detectors' cassettes. These components are essential for absorbing scattered neutrons and preventing them from reaching other detectors or contributing to undesirable background noise, thereby maintaining the purity of the neutron signal. Diagnostic systems shall segregate activated systems or components wherever possible [Req.#80].

The three detectors and the beam dump are positioned in dedicated machined guides contained inside a cassette. Figure 4.52 shows the detectors aligned along the LOS, marked by the orange arrow that indicates the direction of the neutron beam.

The Detector Module includes a total of 12 detector cassettes, and each one of them is made of steel, in order to achieve a strong protective structure, that is able to optimally protect the sensors located into them. The cassettes are thermally insulated to maintain a constant internal temperature of approximately 35°C for avoiding detector efficiency variations and under 50°C for avoiding the detectors

damage. For this purpose, the excess heat produced by the detectors is removed thanks to a water-cooling system, integrated into the cooling box.

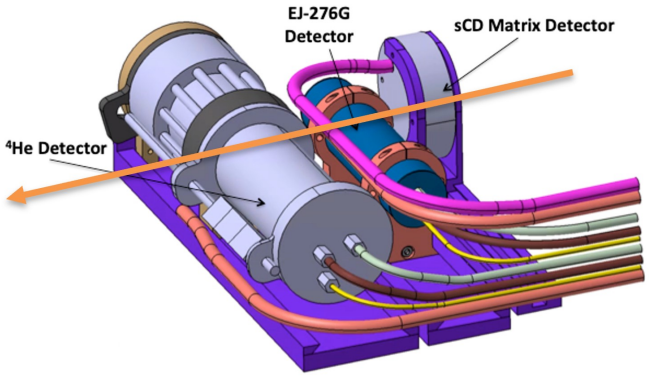

Figure 4.52: Detectors aligned with the LOS, mounted on the machined supports ([83]).

The cassettes are located in front of the collimators of each LOS and 6 of them are right hand side (RHS) and the other 10 are left hand side (LHS) (Figure 4.53).

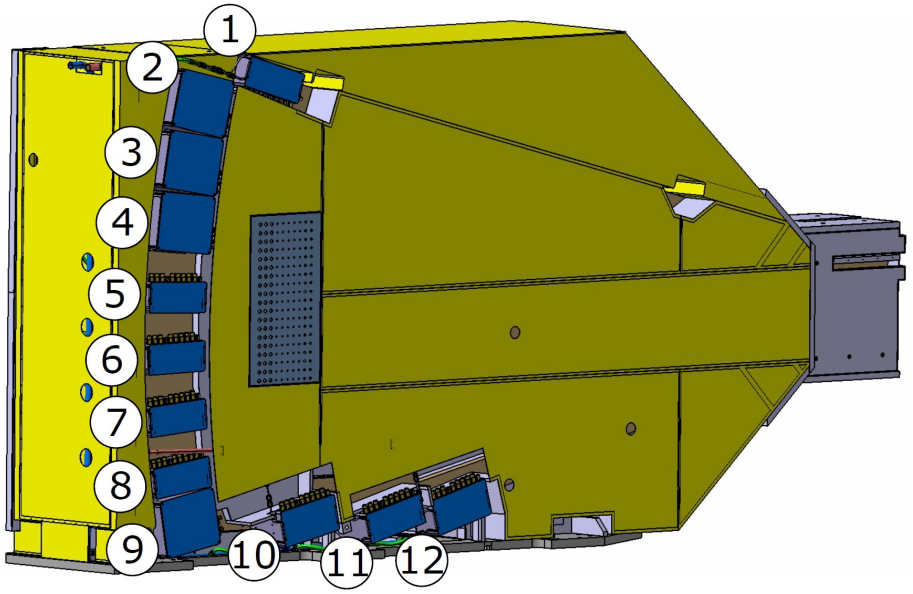

Figure 4.53: Detector cassettes arrangement in the rear zone of Ex-Port RNC ([83]).

Since the LOS are characterized by two fan-shape structures, that are placed side by side (even though not parallel), the RHS LOS plane is closer to the cassettes opening positioned in the RHS, while the LHS LOS is closer to the back of the cassettes. This particular collimators disposition forced the design of the cassettes which are of three types: single RHS, single LHS and double.

Each double cassette (Figure 4.54) cointains two detector boxes, one in the upper front zone of the cassette (for the RHS LOS), and the other in the lower back zone (for the LHS LOS). This structure characterize the cassettes number 2, 3, 4 and 9 (Figure 4.53).

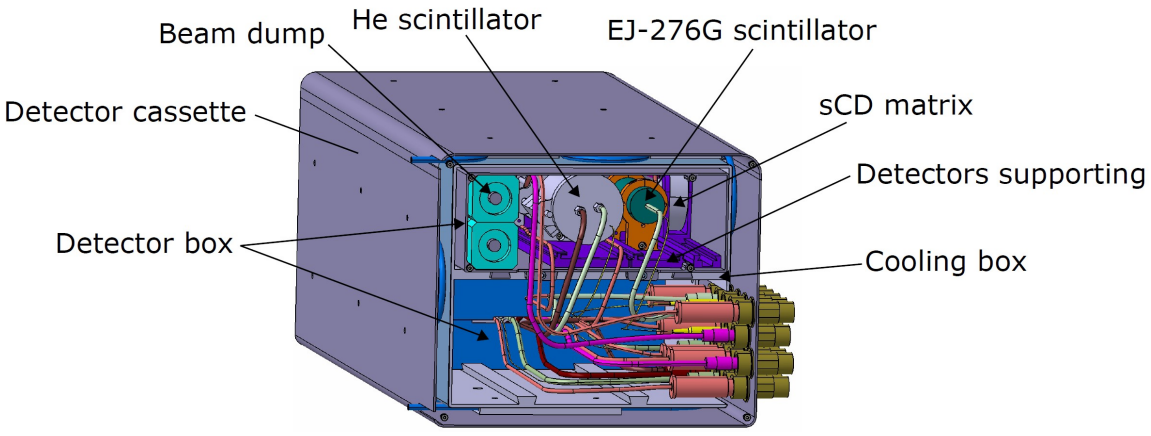

Figure 4.54: Double cassette containing two set of detectors ([83]).

All the other cassettes are single (Figure 4.55): in the cassettes number 10 and 12 the detector box is placed in the front part because they are aligned with RHS LOS, while the other cassettes (1, 5, 7, 8 and 11) are aligned with LHS LOS, and so their detector boxes are placed in the back part of the cassette (Figure 4.53).

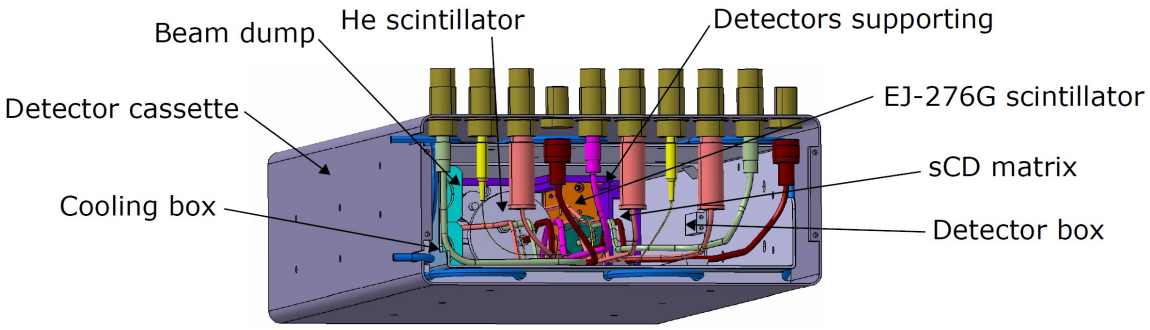

Figure 4.55: Single cassette containing one set of detectors ([83]).

Rear Detector boxes (thus excluding the one on the top and the three on the bottom; number 1, 10, 11 and 12 of Figure 4.53) are mounted on a Detector box supporting structure, a SS361L(N)-IG shelf-like structure (Figure 4.56):

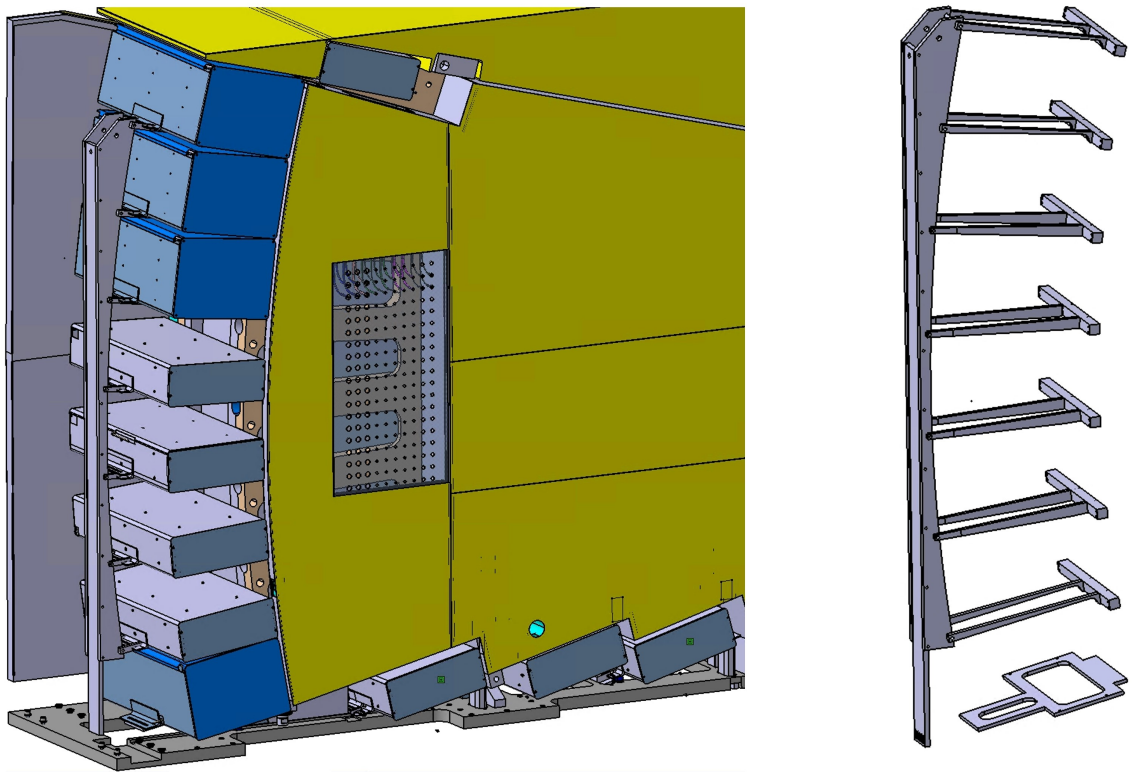

Figure 4.56: Detector box supporting structure ([13]).

The alignment of detectors with the LOS is guaranteed by the manufacturing and installation tolerances of both Detector boxes and Detector boxes supporting structure.

Temperature Stabilization System Design The TSS is engineered to regulate the temperature of the scintillator detectors and their associated Photo Multiplier Tubes (Figure 4.57). A critical design requirement is to ensure that these temperature-sensitive components never exceed 50 °C during ITER operation, which includes port plug baking, draining, and drying phases. The cooling water for the TSS is supplied by the Component Cooling Water System (CCWS-1A), and the operational temperature range for the detectors is 34 °C ± 2 °C, depending on the inlet water temperature.

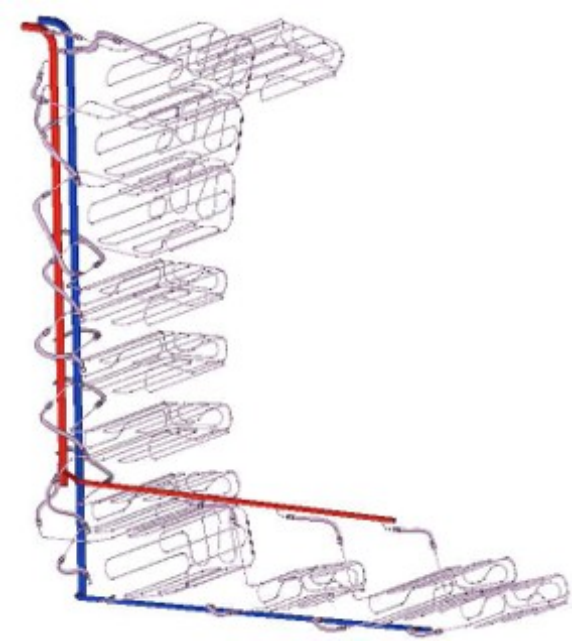

Figure 4.57: Ex-Port RNC Temperature Stabilization System ([80]).

The functional design of the TSS is typically segmented into three primary parts:

- Water Distribution System: This system manages 12 parallel detector cooling channels, which are fed from a central water distribution manifold.

- Water Supply: Responsible for delivering the necessary cooling water to the WDS.

- Drainage: Manages the efficient removal of used cooling water from the system.

The TSS within EU11 is physically composed of tubes, orifices, and main collectors located in the port interspace, while associated pipes, valves, and pressure/temperature sensors are located in the port cell. If a pressurized item is included in the design, the ESP / ESPN directives from the French Decree 99-1046 dated December 13th 1999 and subsequent Order and amendments which introduce in force in France the Pressure Equipment Directive 97/23/EC and the French Order on Nuclear Pressure Equipment, December 2005, shall apply [Req.#58].

Position Monitoring System Design The PMS is an integral subsystem designed for continuous monitoring of the precise alignment of the Ex-Port RNC components [Req.#30][Req.#31]. The PMS operates by monitoring the misalignment between the LOS defined by EU11 and those in DSM2. This monitoring is crucial for detecting and quantifying potential issues such as vignetting (partial or total loss of direct view) or a mismatch between the reference LOS positions used for data inversion and the actual LOS positions.

The PMS sensors function based on a white light signal transmitted along an optical fiber, a design choice that eliminates the need for a separate power supply and minimizes the overall impact on the RNC's complex design. A dedicated software system is utilized to analyze the data from these sensors, enabling the reconstruction of 3D-displacements and providing information for alignment verification.

The PMS is composed by 7 optical-fiber displacement sensors, 2 for each direction (radial, toroidal, and vertical) and 1 for redundancy in radial direction (Figure 4.58). Measured directional displacements are then used as inputs for a correction algorithm that reconstructs the misalignment occurred between Ex-Port RNC and Port Plug closure plate. The entity of misalignment is then associated with a correction factor used to adjust neutron measurements collected by the Ex-Port RNC detectors.

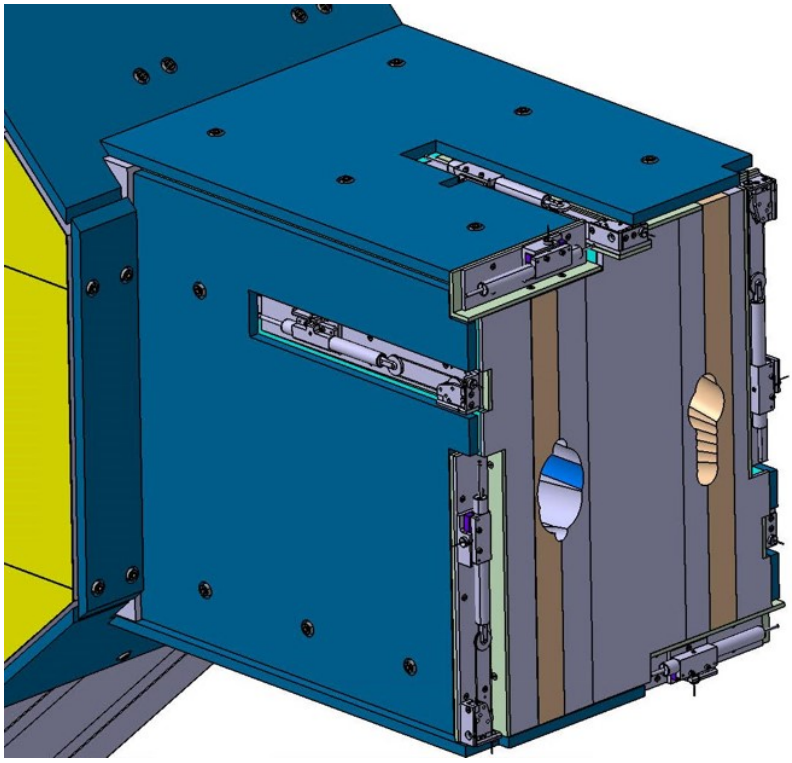

Figure 4.58: Ex-Port RNC Position Monitoring System ([13]).

The 7 sensors are divided into 5 pull-mode sensors and 2 push-mode sensors. The pull-mode sensors embodies a pulley.

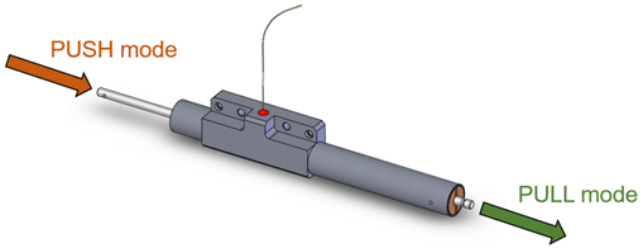

Figure 4.59: Optical-fiber displacement sensor - push/pull modes ([80]).

4.3.3 Ex-Port Manufacturing Assessment

The manufacturing process for the Ex-Port RNC components adheres to stringent quality assurance standards and detailed procedures to ensure the final product meets the demanding specifications for ITER. A preliminary manufacturing and assembly assessment for the Ex-Port RNC has been conducted. The appropriate levels of control and requirements for quality assurance will be defined in the specific diagnostic designs [Req.#76]. All RNC components, including the Shielding, Detector Modules, and Front-End Electronics, undergo verification and validation against established requirements.

Fabrication Techniques

The manufacturing of the Ex-Port RNC foresees an initial logical division of the Ex-Port RNC into Shielding block subsystems (Figure 4.60):

1. Main center block
2. Side block A (RHS)
3. Side block B (LHS)
4. Top block
5. Detectors support structure
6. Rear block
7. Lead nose

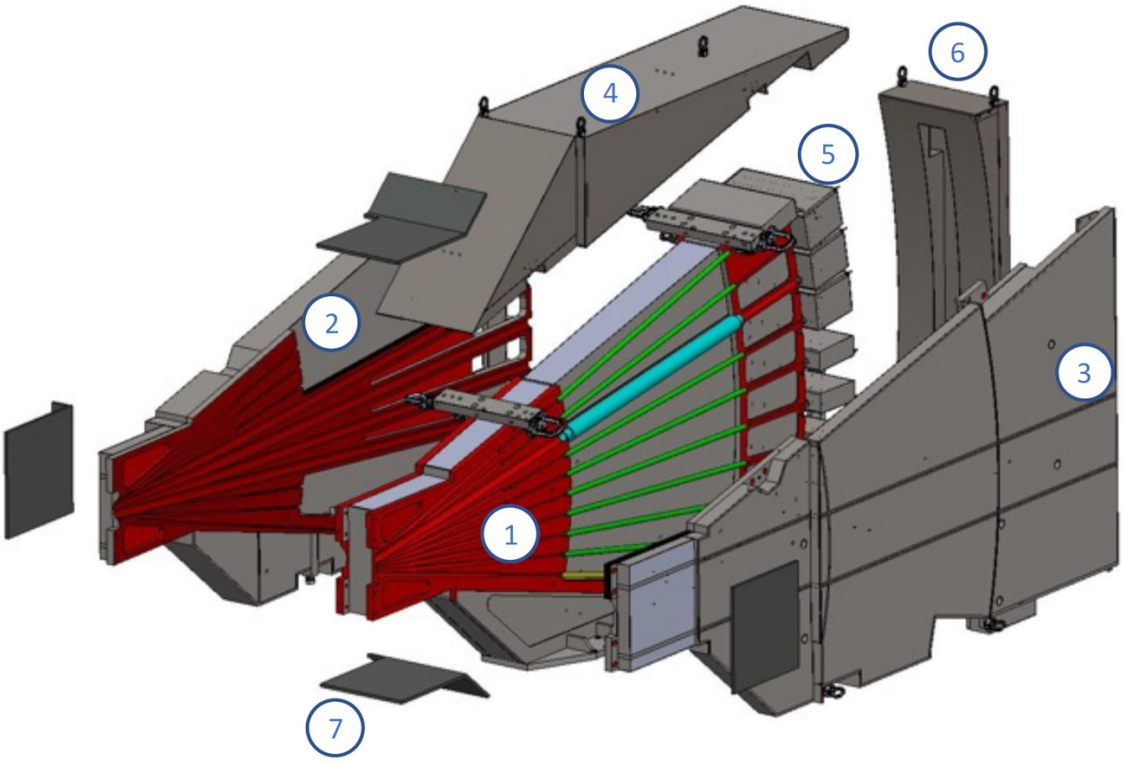

Figure 4.60: Ex-Port RNC Shielding block subsystems for manufacturing ([80]).

The manufacturing of the Ex-Port RNC Shielding subsystem involves a multi-phase procedure encompassing machining, welding, pouring of shielding material, and final assembly:

1. Machining: All component parts are precisely machined to achieve the necessary tolerances for subsequent assembly.

2. Welding: The machined parts are then welded together, forming the structural shell that will contain the shielding material. The external stainless steel sheath for the main parts of the shielding block is manufactured by metal plate welding. All onsite welding will undergo leak tests and non-destructive examination on site, as required by the applicable codes and standards [Req.#78].

3. Pouring: After welding, the shielding material is poured into the cavities within

the welded structure. A step involves re-filling the volumes to compensate for the reduction in material volume that occurs during the drying process, followed by curing.

4. Further Machining: Subsequent machining operations, such as milling, are performed to create the precise grooves for the collimators.

5. Final Assembly: Once all subcomponents are ready and processed, the final assembly of the shielding block is completed.

The supporting structure plates for the shielding blocks are notably made of SS 316L(N)-IG.

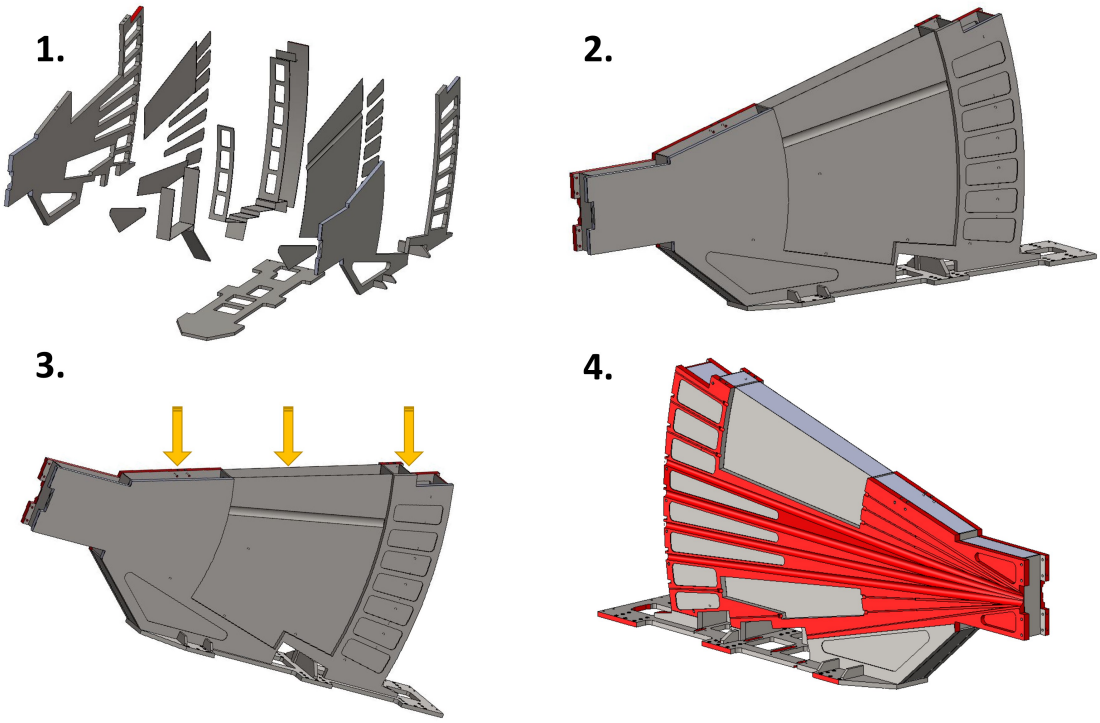

Figure 4.61: Ex-Port RNC manufacturing preparation (example of the Main center block): 1. Machining, 2. Welding, 3. Pouring, 4. Further machining ([80]).

Material Selection and Properties

The selection of neutron shielding materials is a critical aspect of the manufacturing assessment. Materials are evaluated based on several key properties[Req.#76]:

- Neutron shielding performance: The material's effectiveness in attenuating neutron flux.
- Fire and high-temperature resistance: Its ability to maintain integrity and function under extreme thermal conditions [Req.#65][Req.#66].
- Mechanical characteristics: Its strength, durability, and resilience under operational loads.
- Density: A critical factor for effective radiation attenuation, balanced against mass considerations.
- Workability and ease in setting up the block: Practicality aspects for manufacturing and assembly processes.

The materials considered in the analysis include concrete (similar to the ITER C-Lite model), borated polyethylene (with 5% Boron content), and a castable borated hydrogenated mix, which is described as being castable in situ with a specific mix ratio of 29.5 parts water on 100 parts dry mix. Diagnostic systems shall segregate activated systems or components wherever possible [Req.#80].

The final choice that respects all the requirements is the Shieldwerx SWX-277Z-5, a concrete-like castable material with a 5% Boron content.

4.3.4 Structural Assessment

The structural integrity of the Ex-Port RNC components is assessed to ensure their safe and reliable operation throughout all phases of ITER's life cycle. This assessment is comprehensively documented in the "Structural Integrity Report for the FDR of the ex-port RNC" [78]. The DA shall provide the RNC Structural Integrity Report as input for IO-CT to demonstrate that RNC does not jeopardize

the functioning of other components that provide a safety function during or after an earthquake [Req.#25]. The DA shall design the System according to Category 1, 2, 3 and 4 Load Cases, including combinations of these driving the structural integrity of all Safety Significant Components, as defined in the Load Specifications [Req.#26]. Safety functions of the Plant Instrumentation and Control SSCs shall be guaranteed against internal and external aggressions described in the System Load Specifications [Req.#29]. The analyses have been carried out with a Finite Element Method Approach, using ANSYS Mechanical v2021 R2 as software.

Design Code and FEM model

The structural integrity assessment is conducted using Finite-Element thermal-mechanical analyses. These analyses account for both single and combined loads experienced by the Ex-Port RNC during various operational conditions, including Plasma operation, Baking cycles, Installation procedures, and specified accidental events. The primary objective of this assessment is to verify the compliance of the current Ex-Port RNC design with the stringent requirements of the RCC-MRx design code, specifically the 2018 edition. Selected codes and standards will be in agreement with those defined in the Codes and Standards for ITER Mechanical Components [Req.#27].

The initial geometry of the Ex-Port RNC underwent defeaturing and simplifications to facilitate meshing. Specifically, position sensors were excluded from the model due to their negligible global structural impact. Detector boxes were represented as concentrated masses, while shielding materials were modeled as distributed masses, solely incorporating their inertial properties. The finite element mesh utilized standard ANSYS library elements, including BEAM189 for the detector support structure, top shield reinforcing beams, and collimator tubes; PIPE289 for the cooling circuit; SHELL281 for thin structural components; and SOLID187 for thicker sections. Figure 4.62 illustrates the final model employed for the analyses.

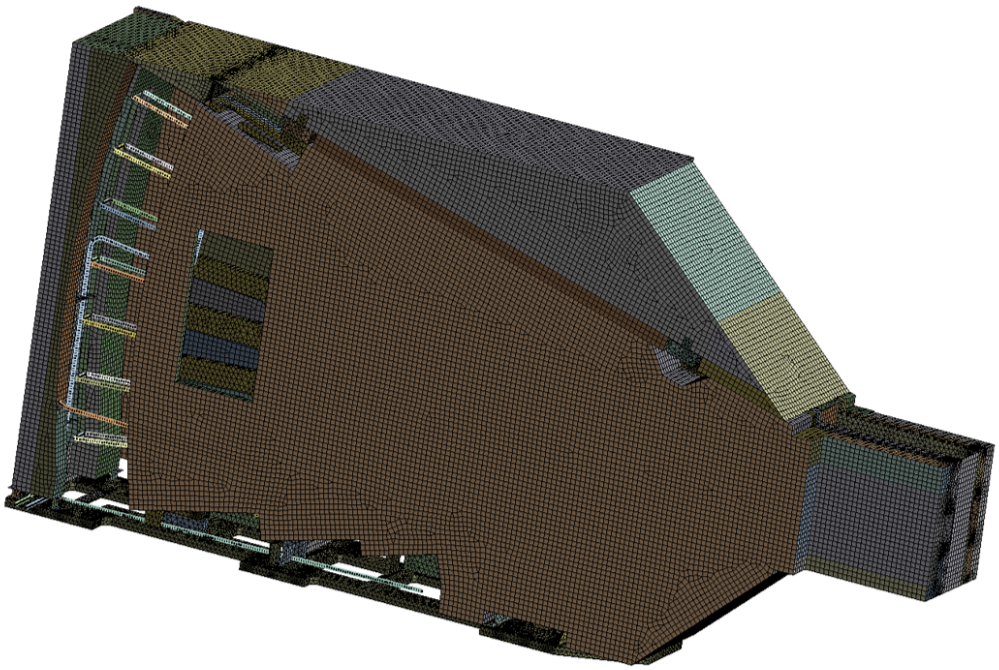

Figure 4.62: Overview of the ex-port RNC FE model mesh ([13]).

Loads and Analysis approach

For the RNC structural behavior study, the following loads were taken into account: gravitational self-weight, mechanical, thermal, and accidental loads, such as seismic events, fire, and Loss of Coolant Accident (LOCA). Conversely, electromagnetic loads were disregarded in this study because prior EM analyses had demonstrated their insignificance. Table 4.4 provides a summary of the loads and their combinations considered. In Table 4.4, the Operating Conditions include thermal and mechanical loads. The Category IV NOS are not considered for structural integrity verification. To accurately model these loads, linear analyses performed on the Ex-Port RNC model include:

- Steady-state thermal analyses to evaluate the temperature distribution under varying loading scenarios.

- Modal analysis was performed to determine the natural frequencies, mode shapes, and modal mass participation of the structure in each spatial direction.
- Response Spectrum Analysis was employed to simulate seismic events. Specifically, SL-2 spectra were utilized for this analysis, while SL-1 and SMHV results were derived by scaling the SL-2 results by factors of 0.33 and 0.73, respectively.
- Static structural analyses were conducted to determine the stress and displacement fields present in the Ex-Port RNC. These analyses encompassed equivalent static analyses performed to calculate the Inertial Amplification Factors (IAF) by applying the SL-2 spectra Zero Peak Accelerations. The IAFs are computed to account for the structure's dynamic behavior when loads are applied, and they were derived as the ratio between the Response Spectrum Analysis results and the equivalent static analysis results.

Table 4.4: Load Combinations.

ID	**Event Category**	**Service Level**	**Operating Conditions**	**Initiating Event**	**Concatenated Event**
BAK-I.1	I	A	Baking	-	-
BAK-II.1	II	A	Baking	SL-1	-
BAK-III.1	III	C	Baking	SMHV	-
BAK-IV.1	IV	D	Baking	SL-2	Fire
NOS-I.1	I	A	Normal Operation	-	-
NOS-II.2	II	A	Normal Operation	SL-1	-
NOS-III.2	III	C	Normal Operation	LOCA PC III	-

Table 4.4 continued from previous page

ID	Event Category	Service Level	Operating Conditions	Initiating Event	Concatenated Event
NOS-III.3	III	C	Normal Operation	SMHV	-
NOS-IV.2	IV	D	Normal Operation	SL-1	-
NOS-IV.3	IV	D	Normal Operation	SL-2	Fire

In addition, non-linear analyses were carried out to evaluate the bolted connections of the Ex-Port RNC. While linear analyses represented connections between bolted components using "Bonded Contacts," non-linear analyses integrated the bolts directly into the model and substituted "Bonded Contacts" with non-linear "Frictional Contacts." Moreover, given that the superposition principle is not applicable to non-linear analyses, each load combination was simulated by concurrently incorporating all corresponding loads.

Stress assessment strategy

The results obtained from the engineering analyses conducted on the Ex-Port RNC were synthesized for each load combination, assuming linear behavior. The resultant equivalent stresses from each load combination were evaluated against the criteria stipulated in the RCC-MRx rules.

Table 4.5 delineates the pertinent failure modes considered for the Ex-Port RNC, along with their corresponding RCC-MRx regulations. For load combinations comprising solely static loads, the total stress tensor was calculated as the algebraic sum of the individual stress components attributable to all loads. Subsequently, the Octahedral shear stress method, in accordance with RCC-MRx 2018, was employed to derive the equivalent stress from the total stress tensor. Conversely, in instances where dynamic loads were incorporated into a load combination, the "Upper-Limit

formulation" of the Von-Mises equivalent stress was adopted.

Table 4.5: Failure mode and RCC-MRx rule.

Damage Type	**Damage**	**Rule**
P type	Immediate excessive deformation	RB 3121.1
P type	Immediate plastic instability	RB 3121.2
S type	Progressive deformation	RB 3122.1
S type	Fatigue (progressive cracking)	RB 3122.2

Assessment results

The stress analyses for each load combination indicate that seismic loads are the primary design drivers for the Ex-Port RNC, while thermal loads do not substantially compromise the system's structural integrity.

Figure 4.63 illustrates the equivalent stress map for primary stresses under NOS-II.2, representing the most stringent load combination for Service Level A. The highlighted regions denote areas of the model where stresses exceed the 159 MPa threshold, which is the allowable stress value for SS 316L-IG at the pertinent temperatures. Although the main structure satisfies the structural integrity assessment as per RCC-MRx regulations, certain sections of the Ex-Port RNC exhibit stresses surpassing the allowable limit. Specifically, some steel sheets encasing the upper and central shielding prove insufficient to withstand the seismic accelerations.

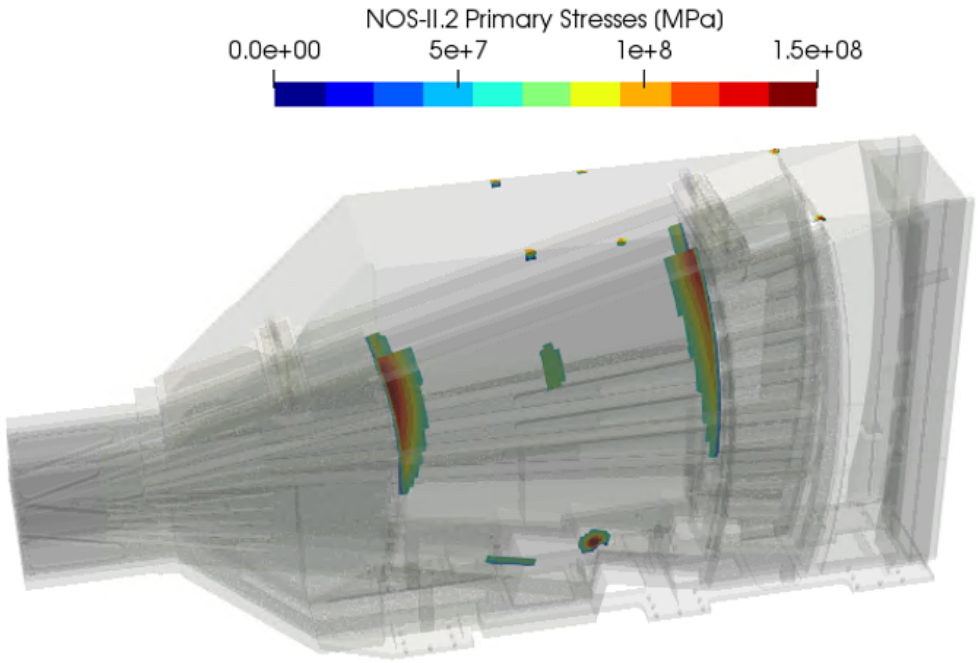

Figure 4.63: NOS-II.2 Primary stresses, threshold at Sm ([13]).

Table 4.6 presents for each load combination, the maximum Usage Fractions (UF) obtained as the ratio between the computed stresses and the allowable.

Table 4.6

ID	**Rule**	**Applied [MPa]**	**Allowable [MPa]**	**UF**
BAK-I.1	RB 3251.112	159	220	0.72
BAK-II.1	RB 3251.112	322	220	1.46
BAK-III.1	RB 3251.112	708	298	2.38
NOS-I.1	RB 3251.112	159	220	0.72
NOS-II.2	RB 3251.112	322	220	1.46
NOS-III.2	RB 3251.112	159	236	0.67
NOS-III.3	RB 3251.112	708	298	2.38

Based on the results of the structural assessment, several modifications must be implemented in the design:

- Extension of the main slabs to directly support the detector boxes, which allowed for the removal of the previous detector box supporting structure.
- An increase in the thickness of the thin steel sheets from 3 mm to 5 mm.
- Detachment of the upper triangle from the main upper shielding, with its subsequent connection to the supporting structure below.
- Reduction of the RNC Nose dimensions to increase clearances with the Port Plug Closure Plate, and the encapsulation of the Nose's lead covers into stainless steel sheets.

These design modifications and the verification process underscore a continuous refinement process driven by detailed structural analysis to enhance the robustness and reliability of the Ex-Port RNC, ensuring its compliance with RCC-MRx design code and functional requirements.

4.3.5 Validation Process of RNC Maintenance Operations using VR Simulation

This section outlines a robust validation process for maintenance operations of the ITER RNC using Virtual Reality simulation, augmented by ergonomic guidelines and a physical mock-up. This comprehensive approach aims to optimize procedures, minimize operator radiation exposure, and ensure safety in the challenging environment of a nuclear fusion plant. Further information can be found in the paper work [84] by the author of this thesis.

Context of ITER Component Maintenance Plan

The maintenance strategy for the RNC is intricately tailored to the location of its components, which dictates accessibility and potential radiation exposure [83]. The ITER Maintenance, Surveillance, and Inspection Program prescribes detailed rules for safe operations, adhering to stringent occupational and nuclear safety regulations [84].

Maintenance approaches are categorized by component location, shown in Figure 4.64:

- In-Port Plug Equipment: Due to extremely high radiation levels within the vacuum vessel, these components require unplanned maintenance performed exclusively via Remote Handling [83].

- Interspace Equipment: Located in the building area of the equatorial port, this category includes components such as piping, cables, fibers, and position monitoring sensors. Both remote and on-site inspections are possible. Corrective and preventive maintenance can be performed using Long-Term Maintenance or Short-Term Maintenance with hand-on tools. However, Short-Term Maintenance is discouraged to minimize operator radiation exposure [83]. A "run-to-failure" strategy is often adopted when specific supplier information on duty cycles or failure models is unavailable, or if the component's predicted lifetime exceeds the plant's operational period [83].

- Bio-Shield Plug Equipment: This involves the bio-shield itself and complex routing of pipes and cables designed to prevent direct neutron escape [83].

- Port Cell Equipment: Components in this area are accessible shortly after plant shutdown, often within a few hours [83].

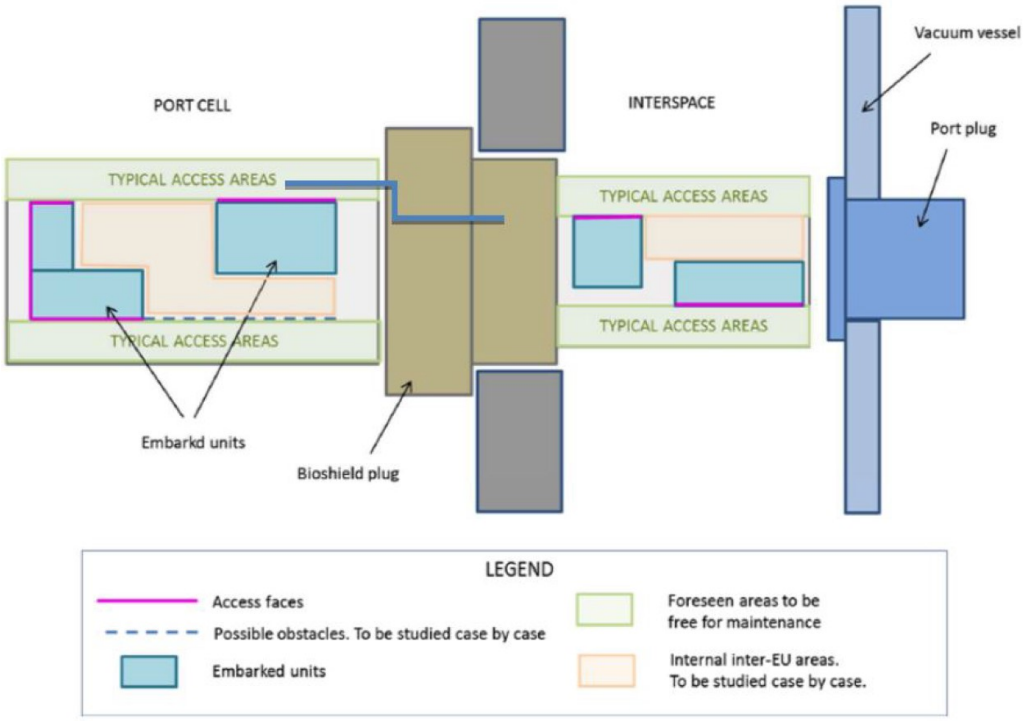

Figure 4.64: Schematic top view of the Equatorial Port #1 ([83]).

A detailed maintenance plan is only mandated for components with a probability of failure exceeding 10% over the plant's 20-year operational period, as determined by RAMI analysis. The detector boxes, which house the Helium-4 Scintillator, are identified as critical components requiring such plans [83, 84]. The RNC Maintenance Plan specifically foresees hands-on maintenance for replacing detector units upon failure [84]. For the 4He Scintillator, a Hands-On-Tool, corrective, run-to-failure activity is planned for execution directly in the Interspace zone [84]. The detailed sequence of operations is outlined in Table 4.7. The estimated time for this replacement, based on previous tokamak experience, was initially 66 minutes [84]. To minimize occupational radiation exposure, maintenance operations in the PC Interspace zone must adhere to the ALARA principle, which requires optimization of hands-on tasks [84]. Operators in the port interspace must wear specific radiation protection suits [83].

Table 4.7: Procedure for the replacement of the 4He Scintillator ([83]).

OPERATION	TASK DESCRIPTION	SUB-STEP	EXPECTED TIME [min]
1	Remove the external cassette front panel	1-2	3
2	Remove the internal cassette front lid	3-4	3
3	Unplug the connectors' plugs	5	15
4	Remove the failed detector	6-7-8	12
5	Install the new detector	9-10-11	12
6	Plug the connector's plugs	12	15
7	Mount the internal cassette front lid	13-14	3
8	Mount the external cassette front panel	15-16	4

Ergonomic Guidelines for ITER Maintenance

Ergonomics is a science that studies the interactions between worker, machines and environment in a work system, with the aim to improve performances and effectiveness of operations, ensuring worker's health and safety. Thus, ergonomics is paramount in the design and execution of maintenance activities within ITER to ensure worker health and safety, optimizing interactions between workers, machines, and the environment [83, 84]. The main objective is to design and develop the system, tools, and work environment to allow optimal interaction for personnel [84].

Environment ITER Requirements The work environment must allow for easy and safe movement of personnel, equipment, and materials, ensuring adequate space to prevent injuries or damage [83]. Furthermore, the design of complex mechanical systems must anticipate maintenance tasks by providing necessary accesses and spaces that comply with accessibility and maintenance standards [83]. ITER prioritizes inspectability, maintainability, and testability, ensuring sufficient space for personnel, tools, and remote handling where needed [83].

Defining minimal dimensions for openings and spaces for human access is crucial, taking into account protective equipment. ITER Ergonomic Guidelines provide detailed indications on the preferable dimensions for the access, dependent from the access type and the body portion involved. Figure 4.65 shows access ergonomic guidelines for the operations involved in the maintenance of the detector cassettes.

ACCESS TYPE	BODY PORTION INVOLVED	MINIMAL DIMENSIONS
Standard access	entire body	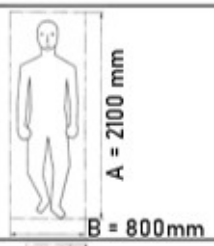
Sideway access	entire body	
Opening	one lower arm up to the elbow	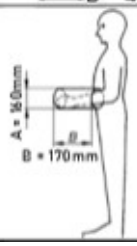

Figure 4.65: Access ergonomic guidelines ([83]).

These rules have been adapted to the Port Interspace zone where the Ex-Port RNC is located and where the maintenance is planned. This resulted in the ergonomic spatial division as visible in Figure 4.66. The maintenance procedure is focused on the Cassette #4, between acceptable and optimum zones.

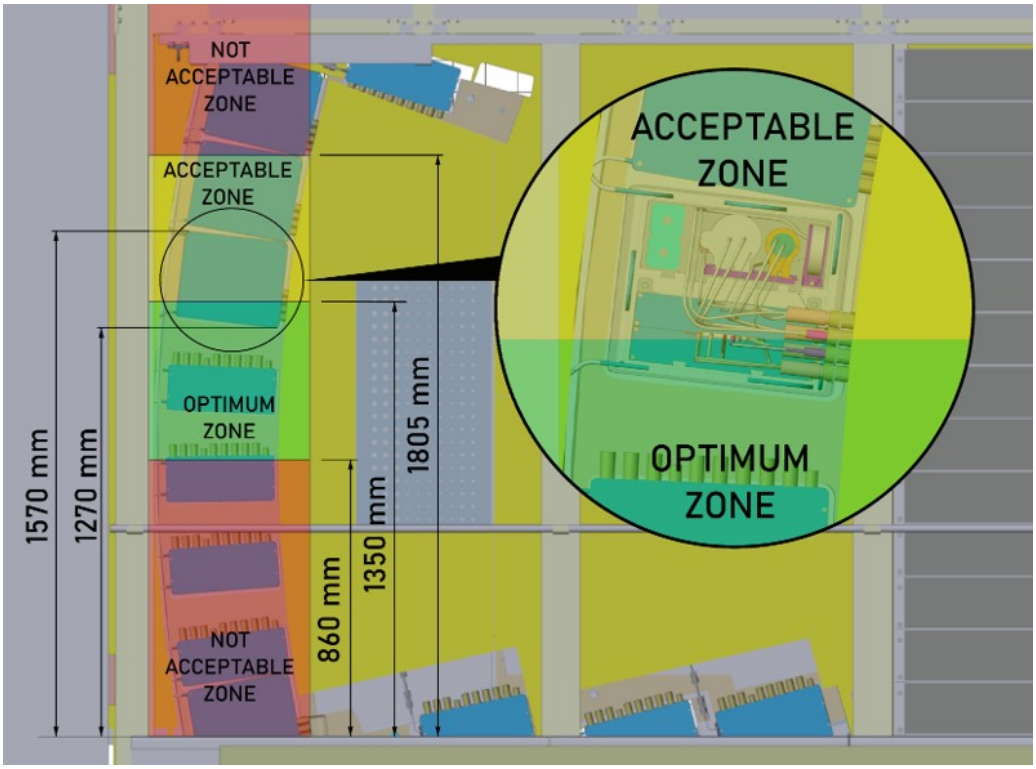

Figure 4.66: Ergonomic spatial division ([83]).

Physical Constraints for Safety Maintenance Operations Anthropometric constraints are strictly observed during all work and maintenance activities to prevent biomechanical overloads or musculoskeletal injuries from continuous and repetitive physical strain [83, 84]. The ITER Ergonomic Guidelines, based on the European standard EN 1005–4:2005 ("Human performance. Evaluation of working postures and movements in relation to machinery"), divide posture evaluation into three zones (Figure 4.67) [84]:

- Acceptable (green): Movements or static positions that do not pose a risk of pathologies over time.
- Acceptable under certain conditions (yellow): Hazardous activities requiring special preventive measures or limited duration.

- Unacceptable (red): Movements or static positions involving a high risk of injury or pathology if repeated [84].Proper posture, such as squatting or kneeling, is encouraged over twisting movements to achieve better trunk positions [83].

BODY PART	MOVEMENT DIRECTION	ZONE	ANGLE	EVALUATION	ZONES ILLUSTRATION
ARM	any	4	< 0°	NOT ACCEPTABLE	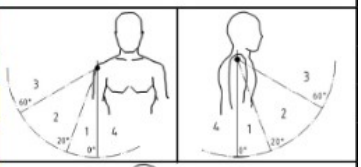
		1	0° - 20°	ACCEPTABLE	
		2	20° - 60°	CONDITIONALLY ACCEPTABLE	
		3	> 60°	NOT ACCEPTABLE	
TRUNK	forward/backward	4	< 0°	CONDITIONALLY ACCEPTABLE	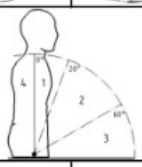
		1	0° - 20°	ACCEPTABLE	
		2	20° - 60°	CONDITIONALLY ACCEPTABLE	
		3	> 60°	NOT ACCEPTABLE	
	bending sideways or twisting	1	approximately 10° or less	ACCEPTABLE	
		2	approximately 10° ormore	NOT ACCEPTABLE	

Figure 4.67: Anthropometric ergonomic guidelines ([83]).

VR Setup and Model Creation for the Simulation

The development of a high-fidelity Virtual Reality simulation for the Ex-Port RNC maintenance process leverages Industry 4.0 and extended reality technologies [83, 84]. This simulation is designed to evaluate ergonomics and timing, and to train operators for complex and potentially hazardous operations in a radioactive environment, ultimately minimizing intervention times [83, 84].

Extended reality technologies provide significant advantages by allowing the evaluation of operational feasibility and procedures during the design phase, enabling direct modifications to the model without the need for physical prototypes. For complex procedures, extended reality offers realistic training, preparing operators for tasks and unforeseen issues, leading to quicker and more precise real-world operations [83].

Extended reality can be divided into three main types (Figure 4.68):

- Augmented Reality: it adds virtual information to the real world, and it is not possible to interact with it.
- Mixed Reality: it adds virtual elements or objects to the real world, allowing the user to interact with them.
- Virtual Reality: it immerses the user in a completely virtual world. Realism and immersivity are key aspects.

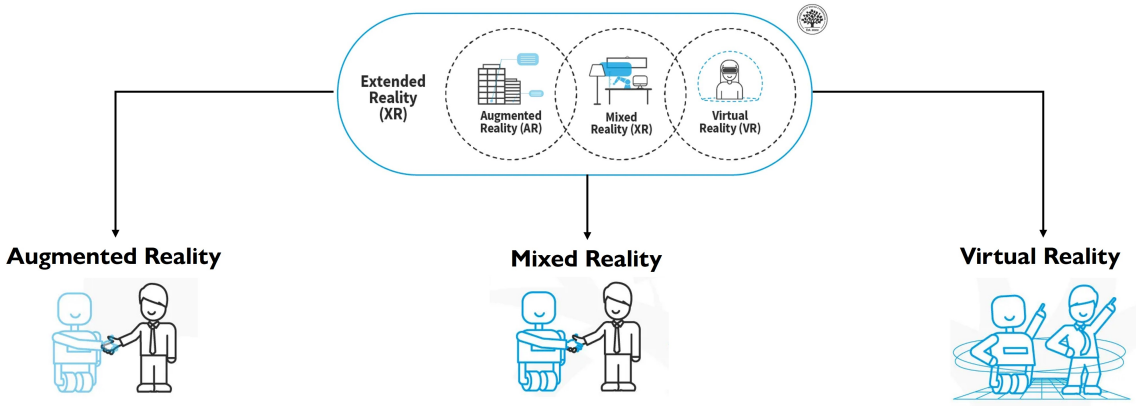

Figure 4.68: Extended reality: augmented, mixed and virtual reality ([83]).

Among the types of extended reality technologies available, the VR has been chosen.

VR Devices The immersive experience and the accuracy of ergonomic evaluations are heavily reliant on the chosen VR hardware. The HTC Vive Pro 2 system is employed, recognized for its effectiveness in research applications. The key components include:

- Provides a high-resolution 5K view (4896 x 2448 pixels) with a 120° field of view and a 120 Hz refresh rate. This ensures fluid, natural vision and offers 360-degree audio immersion, fundamental for a truly immersive experience.

- Equipped with sensors for precise tracking and multiple configurable buttons, allowing for intuitive interaction with virtual objects and the environment.
- Four Vive Trackers 3.0 are utilized in addition to the headset and controllers to enable comprehensive full-body tracking. These trackers are essential for capturing detailed operator movements, which is vital for accurate ergonomic assessments.
- These use an outside-in tracking system, where placed sensors (e.g., at opposite corners of a 3.5m square gaming area) triangulate the positions of the headset, controllers, and trackers. This setup ensures precise and consistent tracking of the user's movements within the defined VR space.

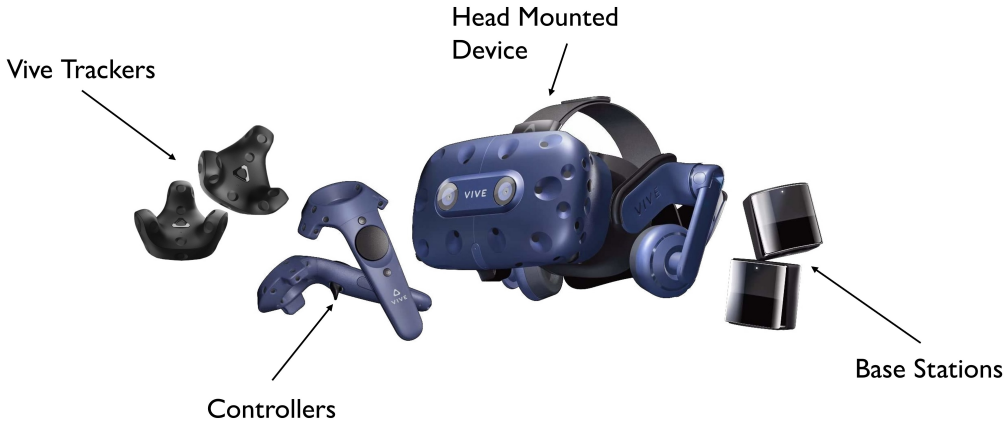

Figure 4.69: HTC Vive Pro 2 hardware set ([83]).

The entire hardware setup is connected to a powerful workstation (CPU: Intel i7, RAM: 32 GB, GPU: Nvidia GeForce RTX 3080) to maximize the graphic potential and ensure a fluid VR experience [84].

3D Model Optimization The Unity software is the chosen platform for developing the VR environment due to its versatility, robust features, and extensive community support, which offers a wealth of guidelines and tutorials. The development

process begins with optimizing existing CAD models of the ITER components, such as the Ex-Port RNC. This "lightening" process is crucial because original CAD models are often too heavy for real-time graphic rendering in VR. It involves:

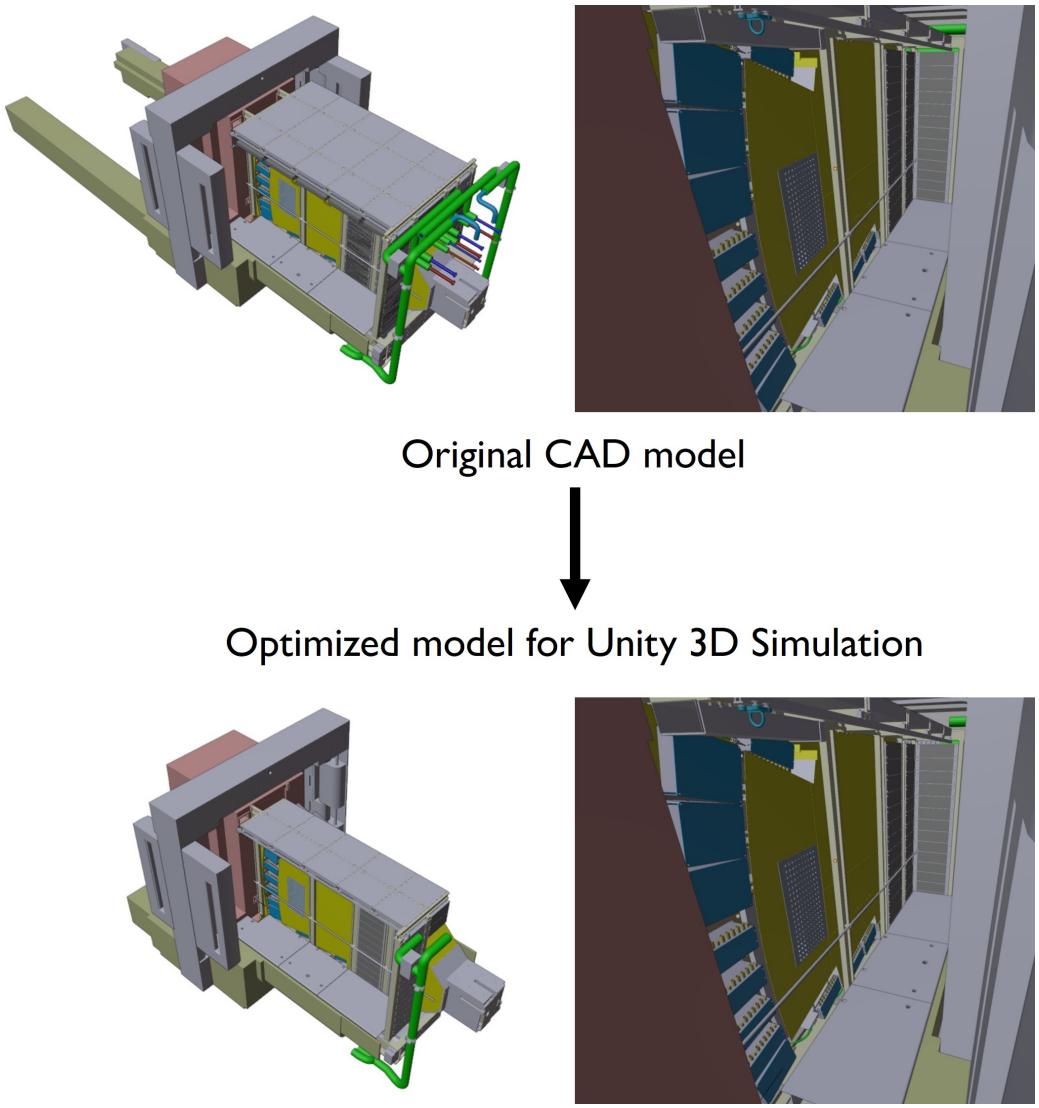

Figure 4.70: Ex-Port RNC lightening process ([83]).

- Simplification: Components that are not directly involved in or visible during the maintenance procedure are either removed or simplified. For instance,

complex solid bodies might be converted into simpler surfaces to reduce polygon count (Figure 4.70).

As one can see from the right hand side images of (Figure 4.70), despite the relevant lightening, the appearance to the operator is the same.

- Performance Enhancement: This optimization prevents lagging during the simulation and allows for precise collision detection, which is fundamental for realistic physical interaction within the virtual environment.

- Behavioral Coding: Each optimized component is then coded with its physical behavior. This includes assigning properties such as volume occupation and non-penetrability using Unity colliders. These colliders define the boundaries of objects and enable realistic interaction, allowing VR operators to "grab" and manipulate virtual objects (Figure 4.71).

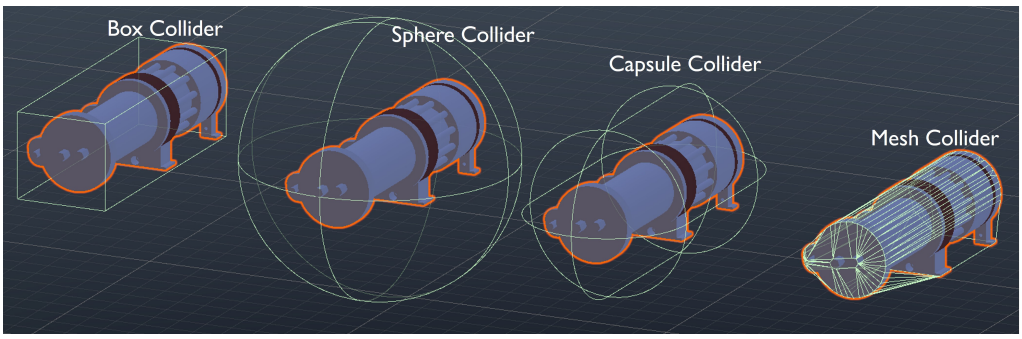

Figure 4.71: Types of collider modelling on the 4He Scintillator ([83]).

Among the different types, the mesh collider has been selected thanks to its finer accuracy on enveloping the body.

- Cable Modeling: The accurate modeling of cables, though time-consuming, is specifically highlighted as important for increasing the accuracy, reliability, and overall realism of the simulation (Figure 4.72).

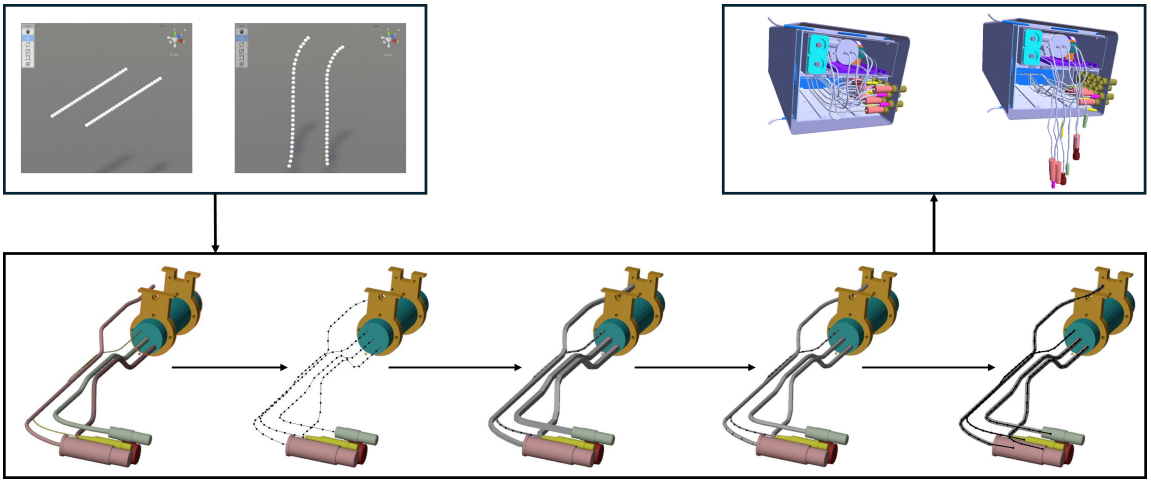

Figure 4.72: Cable modelling: creation of cable segments interconnected one to each other ([83]).

Script Development Specific scripts were developed within the Unity 3D software framework to manage realistic object behavior, for real-time monitoring of operator postures during maintenance, and to acquire the time necessary to complete each operation. These scripts were designed to be general and reusable for future VR simulations in various domains [83, 84].

To create a realistic and responsive virtual representation of the operator's body within the Virtual Reality environment, a virtual body preparation process is undertaken. This involves building a virtual skeleton and employing inverse kinematics to ensure the virtual body accurately mirrors the operator's real-world movements (Figure 4.73).

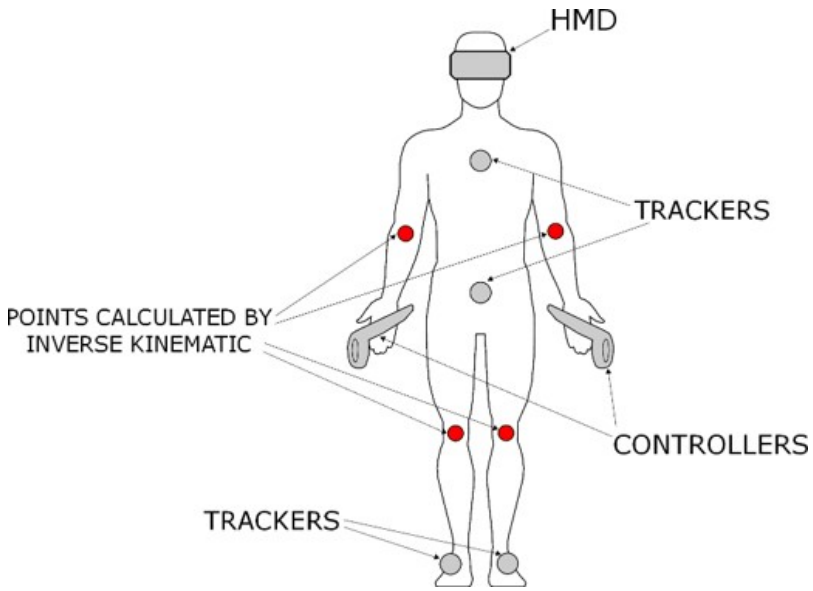

Figure 4.73: Position of the HTC Vive Pro 2 hardware set and points calculated by inverse kinematics ([83]).

The process begins with the construction of a virtual skeleton. This skeleton is built based on the positions reported by the body trackers and the headset of the VR system. These trackers capture the real-time movement and orientation of key body parts (Figure 4.73). Once the basic skeleton is established, inverse kinematics is applied. Inverse kinematics is a computational technique used to determine the joint parameters (angles and positions) of an articulated body in order to achieve a desired position and orientation of an end-effector (like a hand or foot). In this context, additional points on the virtual skeleton are calculated via inverse kinematics to make the operator's entire virtual body fully responsive to their real movements.

This sophisticated calculation ensures that every movement, gesture, and pose the operator makes in the real world is precisely replicated by their virtual counterpart, thereby enhancing the precision, reliability, and overall realism of the simulation. The result is a reliable and realistic adaptation of the virtual body - the avatar in the simulation - to the real-life movement of the operator (Figure 4.74).

Figure 4.74: Adaptation of the virtual body to the real-time movement ([83]).

To integrate the ITER Ergonomic Guidelines in the VR simulation context, the prescriptions of the anthropometric body constraints (Figure 4.67) are translated into a real-time User Interface stick figure, thanks to the body skeleton built (Figure 4.75).

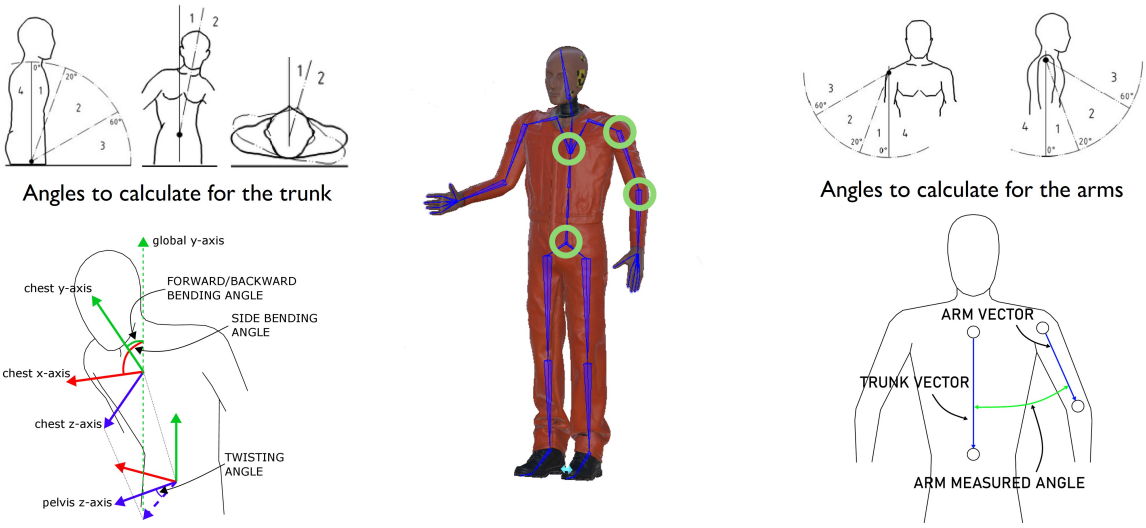

Figure 4.75: Angles and skeleton links used for the ergonomic reconstructions ([83]).

The UI figure is displayed in the headset, changing color (red, yellow, green) based on the posture acceptability as defined by the ergonomic guidelines, providing immediate feedback to the operator (Figure 4.75) [84].

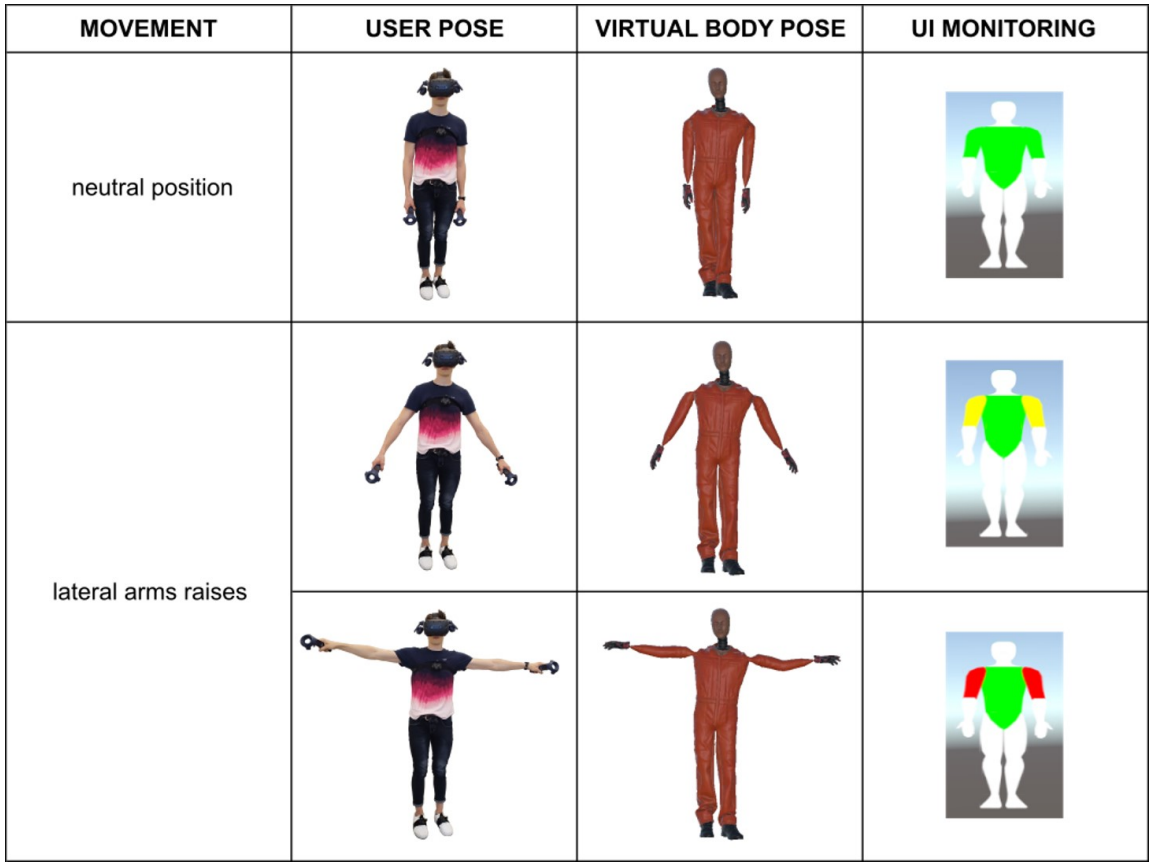

Figure 4.76: User Pose, corresponding Virtual body pose and UI figure for live ergonomics monitoring ([83]).

The simulation environment built is shown in Figure 4.77. Figure 4.77 shows a frame during the extraction of the Helium-4 scintillator: on the top-left corner the operator in the 3D-Lab is shown, on the bottom-left corner a third person view in the Port Interspace zone, in the main image a first person view - what the operator sees with the Headset, on the right side, the UI figure for the live check of the ergonomics.

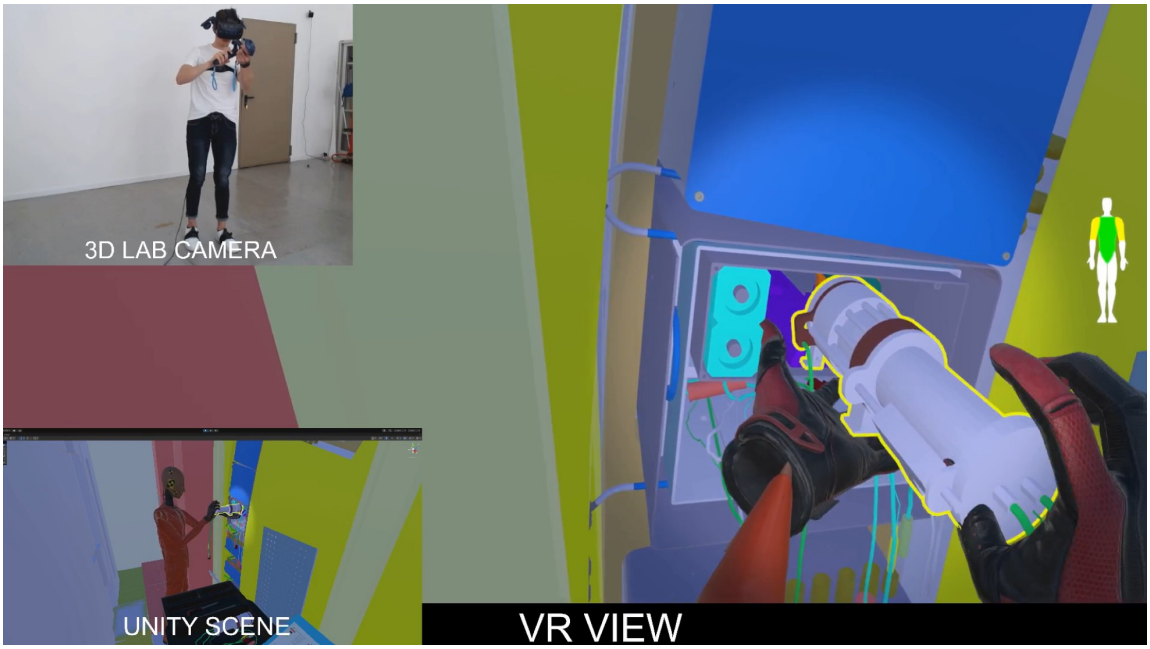

Figure 4.77: A scene from VR environment during the extraction of the Helium-4 scintillator.

Creation of the Physical Mock-up of the Cassette

To validate the VR simulation code and ensure its accuracy in replicating real-world scenarios, a simple physical mock-up of the detector box was manufactured [84]. A multi-objective study guided the selection of components for this mock-up, aiming to minimize costs, time, and physical dimensions, while still allowing for the execution of the key maintenance steps to be tested [84]. This mock-up consisted of a plywood Double cassette, which contained ABS 3D-printed detectors (Figure 4.78).

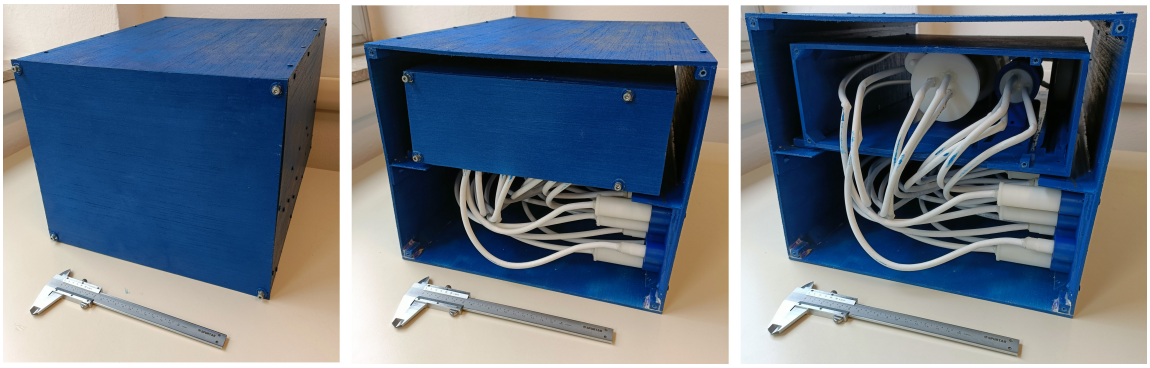

Figure 4.78: Physical mock-up of the Double Detector cassette ([84]).

These detectors were connected with aerial cables to corresponding ABS 3D-printed connectors (Figure 4.79). The primary purpose of creating this physical mock-up was to enable direct comparison of maintenance procedure times and execution with the VR simulation, thereby confirming the validity and fidelity of the VR code [84].

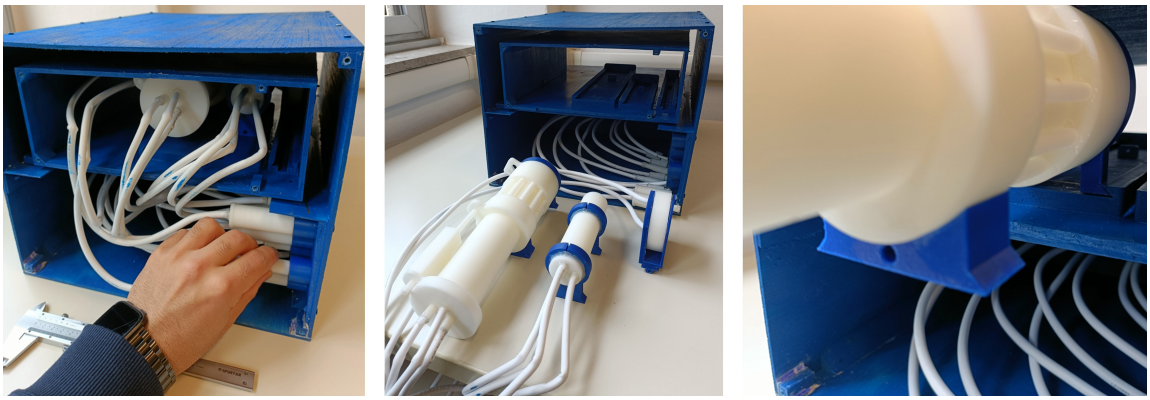

Figure 4.79: Details of the physical mock-up: ABS detectors and connectors and aerial cables ([84]).

Time and Ergonomic Results and Conclusions

The VR simulation provided a detailed and in-depth evaluation of the maintenance operations, particularly for the corrective replacement of Ex-Port RNC components [83].

Time Analysis The VR simulation of the maintenance task outlined in Table 4.7 was repeated 5 times. The results showed that the time required to complete the replacement procedure progressively decreased with repetition and then stabilized around 13 minutes after several trials [84]. This demonstrates the VR tool's effectiveness in operator training, as increased familiarity with the virtual environment and tasks leads to quicker execution [84]. This reduction in time is important for adhering to the ALARA principle by minimizing operator exposure to radiation [84].

Comparison Between VR and Physical Mock-up A direct comparison between the VR simulation and the physical mock-up revealed differences in task completion times [84].

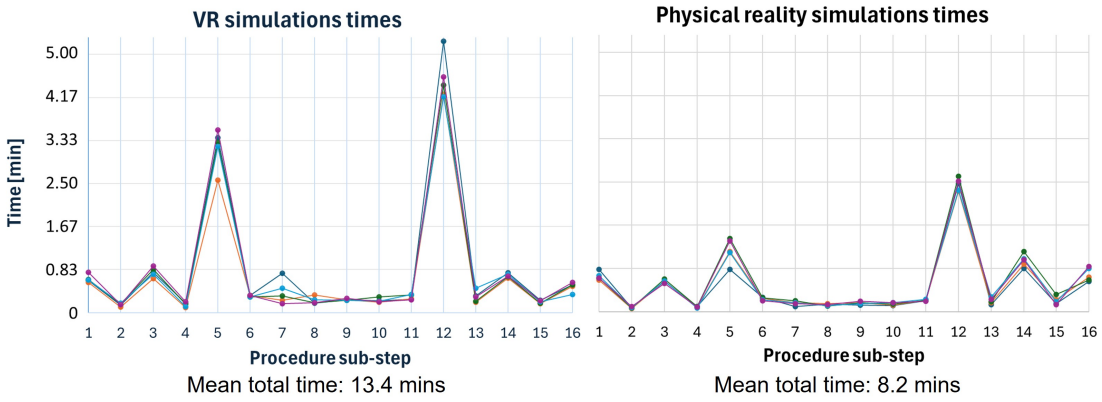

Figure 4.80: Time results of the VR (left) and physical (right) maintenance simulations ([84]).

The total time averaged over 5 runs for the VR simulation was 13.4 minutes, while for the physical mock-up it was 8.2 minutes (Figure 4.80) [84]. The discrepancies were primarily attributed to steps involving the unplugging and plugging of connectors. The physical 3D printed connectors proved to be more reliable and quicker to manipulate than their VR simulated counterparts. Despite this, the VR model was considered conservative, meaning it estimated longer times, which is generally safer for planning in hazardous environments [84]. Significantly, both the VR simulation (13.4 minutes) and the physical mock-up (8.2 minutes) completed the procedure well

within the initially estimated 66 minutes, which was based on previous tokamak experience, indicating a substantial improvement in the planned maintenance approach [84].

Ergonomic Statistics The simulation generated detailed ergonomic statistics for various body parts, including the trunk, left arm, and right arm, presented as percentages of time spent in each ergonomic zone (acceptable, acceptable under certain conditions, unacceptable) (Figure 4.80) [83, 84].

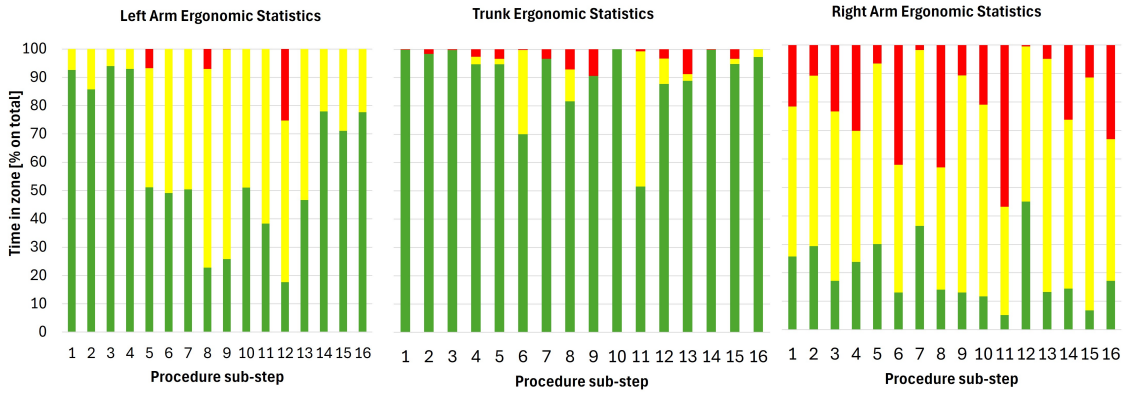

Figure 4.81: Ergonomics statistics of the VR simulation ([84]).

The trunk position (Figure 4.80) generally showed good ergonomic results, largely due to the emphasis on correct movements like squatting or kneeling to avoid twisting, which helps maintain a green zone posture [83, 84]. However, the right arm (Figure 4.80) exhibited more periods in "not acceptable" (red zone) positions. This was attributed to the fact that simulations were performed by right-handed individuals, leading to more intensive and sometimes awkward use of the right arm for manipulation tasks [83, 84]. Despite these suboptimal arm positions, the overall percentage of time spent in an unacceptable posture across the entire body was very low [83]. The analysis suggested potential design improvements, such as different detector fixing screw placements or enhanced connector feedthrough designs, to further improve ergonomics and reduce overall maintenance time [83, 84].

Conclusions The VR simulation successfully verified the maintenance procedure for the 4He Scintillator. It proved to be a powerful and faithful tool for both the verification and validation process and for operator training [84]. The integration of ergonomic guidelines significantly enhanced the utility of the VR tool by providing real-time feedback and quantifiable ergonomic data. This work establishes a robust methodological framework for assessing maintenance procedures for other components within nuclear fusion devices, contributing to enhanced operational efficiency and operator safety in challenging environments [84].

4.3.6 Tolerance Analysis of the RNC Ex-Vessel Collimators to the EP01 PP DSM 2 Optical Path

This section details the tolerance analysis for the alignment of the Ex-Port RNC with the Equatorial Port Plug (EP01 PP) Diagnostic Shielding Module 2 optical path [85]. The primary goal is to establish the conditions for correct alignment, addressing potential issues like vignetting and inaccuracies in Line Of Sight positioning [85].

Ex-Port RNC and Alignment Issue

Figure 4.82 shows the two main Embarked Units involved in the Tolerance Chain Analysis:

- EU01 DSM 2 Optical Path: Located in Port Plug in Drawer #2, this contains optical paths (penetrations in the DSM) that provide a clear view of the plasma to the RNC collimators.

- EU11 Ex-Port RNC: Located in the Port Interspace, this includes a massive Shielding Block made of stainless steel and shielding material, Flight Tubes, Collimation Units, and detector cassettes.

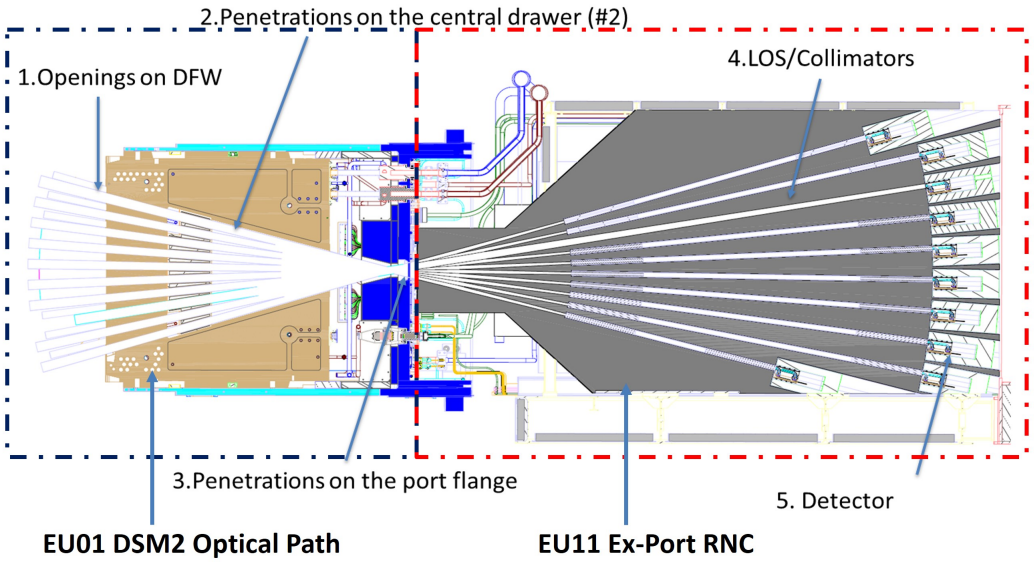

Figure 4.82: Section view of EU01 and EU11 ([85]).

Misalignment between the Ex-Port shielding block and the DSM2 can occur during installation or machine operation, leading to two critical effects [85]:

1. **Vignetting:** A partial or total loss of the direct view of the plasma along a given LOS due to misalignment between the Ex-Port collimators and the corresponding optical paths in DSM2.

2. **Mismatch:** A discrepancy between the reference LOS positions used by the inversion code and the actual LOS positions.

Scope of the Work

The main objective of this section is to establish the conditions required for the correct alignment of the Ex-Port RNC with respect to the Port Plug structure [85]. The work involves:

- Collection of installation tolerance values related to:

    1. Alignment of DSM with Equatorial Port Plug

2. Alignment of Equatorial Port Plug to Port Cell Assembly
3. Alignment of ISS with the Port Cell Assembly
4. Alignment of Ex-Port RNC on the ISS
5. Tolerances related to thermal expansion
6. Tolerances related to Dead Weight influence

- Collection of manufacturing tolerance values:

1. Manufacturing tolerances of DSM
7. Manufacturing tolerances of Ex-Port RNC

- Reconstruction of the tolerance chain

Despite the tolerance values taken from the different source documents can be below 0.1mm in absolute value, for the scope of the work we will consider 0.1mm as minimum value for the tolerances.

Collection of installation tolerances values

1. Alignment of DSM with Equatorial Port Plug (EPP) The installation and alignment of DSM are realized by targeting the EPP Datum System, named Equatorial Port Plug Datum system (PPD), with the DSM Datum system, named DSMD. The EPPD belongs to the EPP assembly and it is placed and oriented using datum A and B which are defined as per figures below:

- Radial direction: defined by the plane which interfaces with the shim (Figure 4.83)

- Vertical and Toroidal direction: defined by Datum B through the sum of the least squares of the positions of the hole's axes (Figure 4.84).

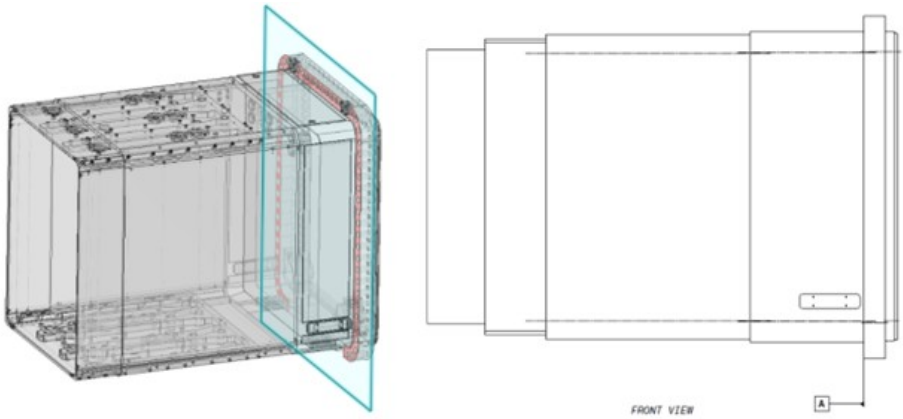

Figure 4.83: Radial reference of EPPD ([85]).

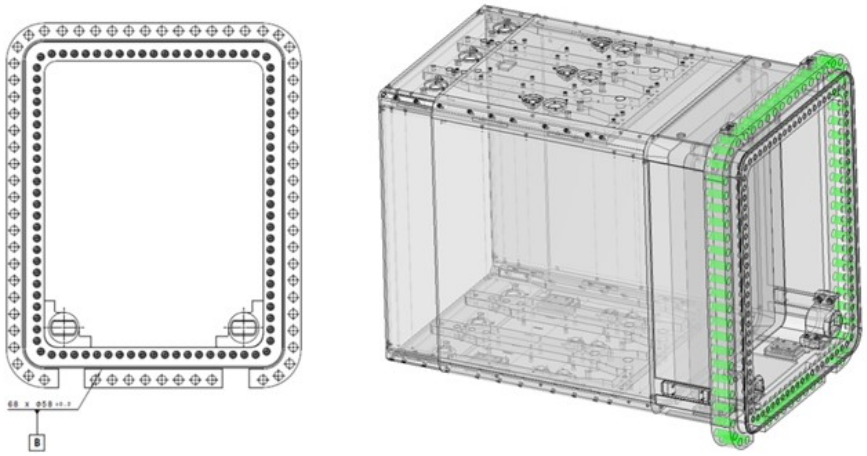

Figure 4.84: Vertical and Toroidal reference of EPPD ([85]).

DSMD belongs to DSM assembly and it is placed and oriented as follows:

- Radial direction: defined by the middle plane of upper and lower radial pins contact surfaces (Figure 4.85).
- Vertical direction: defined by the middle plane of upper and lower vertical keys contact surfaces (Figure 4.86).
- Toroidal direction: defined by the middle plane of toroidal pads contact surfaces in DSM (Figure 4.87).

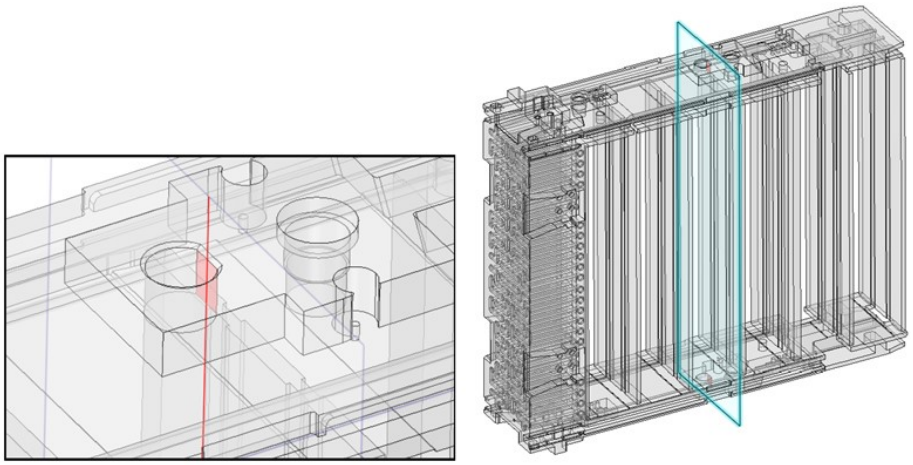

Figure 4.85: Radial reference of DSMD ([85]).

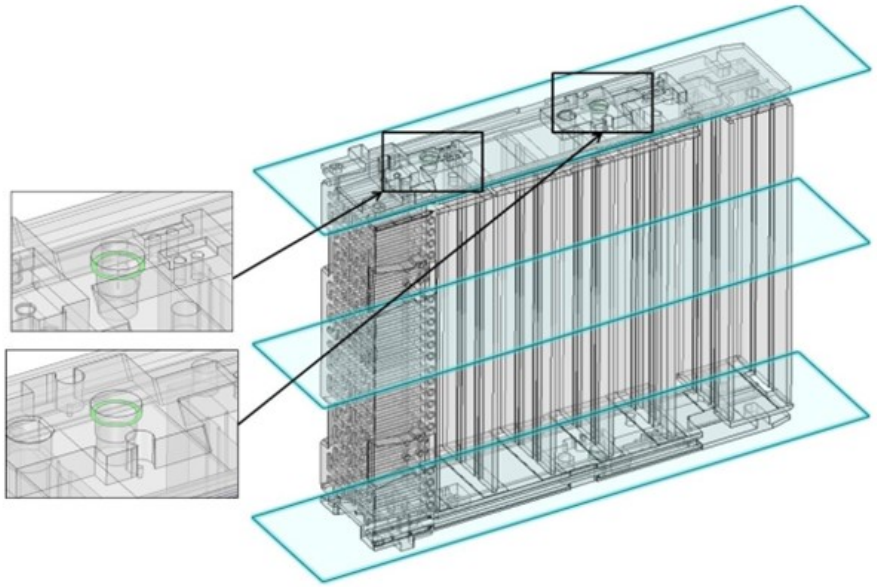

Figure 4.86: Vertical reference of DSMD ([85]).

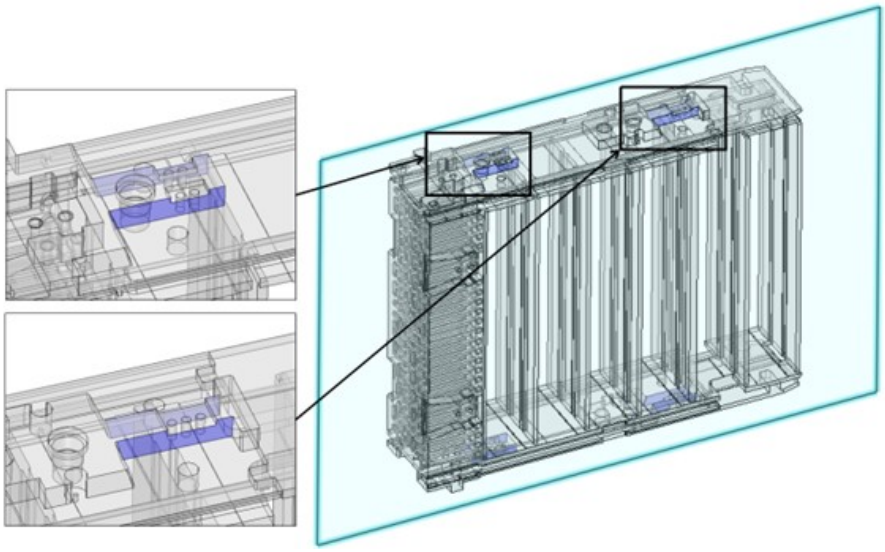

Figure 4.87: Toroidal reference of DSMD ([85]).

Radial, toroidal and vertical directions are referred to EP01 coordinate system. The maximum displacement and misalignment that can occur are shown in Table 4.8:

Table 4.8: DSM to EPP assembly tolerances ([85]).

	Radial [mm]	Toroidal [mm]	Vertical [mm]
Delta_DSM-EPP	**±0.1**	**±0.9**	**±0.2**

2. Alignment of EPP to Port Cell Assembly Once the DSM is positioned and aligned inside the EPP, it is now the EPP that needs to be installed inside the Port Plug Assembly (PPA), which is the Vacuum Vessel port extension that accommodates the Port Plug itself. The installation and alignment of EPP inside the PPA is realized by targeting the PPA Datum system, PPAD, with the EPP Datum System, PPD. The PPAD is composed by the following items, in reference to Figure 4.88:

- Origin: it is the centre of as-built Port Extension flange hole (intersection of the best fit

- central axis and extracted plane of interfacing flange).
- Radial direction: normal to outboard surfaces of as-built Plug to Port shims.
- Vertical direction: normal to as built top surfaces of in-VV rails.
- Toroidal direction: normal to guiding surfaces of as-built in-vessel rails.

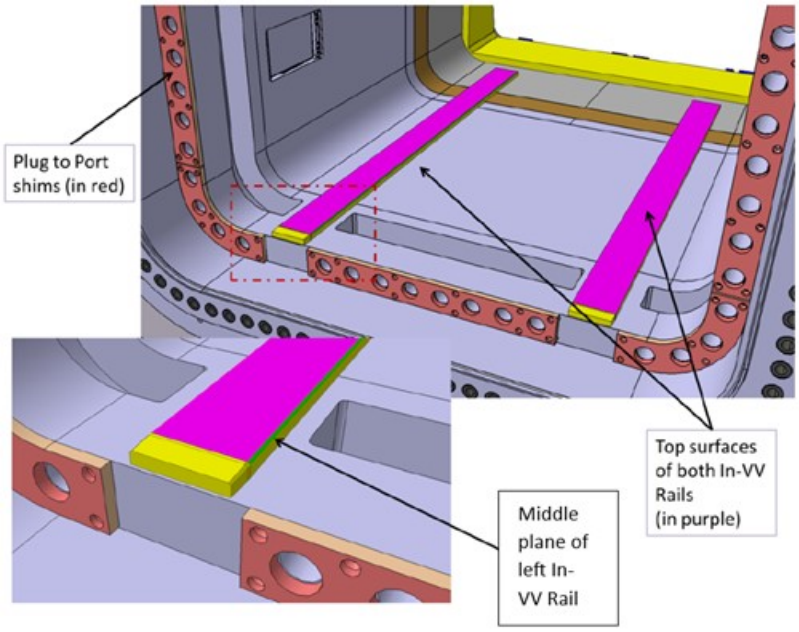

Figure 4.88: PPAD reference elements ([85]).

The maximum displacement and misalignment that can occur during installation of EPP inside PCA are shown in Table 4.9:

Table 4.9: EPP to PCA assembly tolerances ([85]).

	Radial [mm]	Toroidal [mm]	Vertical [mm]
Delta_DSM-EPP	±0.5	±1.5	±0.4

Now, the assembly EPP+PPA takes the name of Port Cell Assembly. The datum system that will be used to align the ISS with the Port Cell Assembly, however, is not

PPAD, but the Port Cell Assembly Datum System (PCAD). The PCAD is defined as follows:

- Reference axis of Port Cell Assembly datum system is coincident with PPAD axis realigned to as-built In-VV Rails and Plug to Port shims:
  - Top surfaces of as-built In-VV Rails are used to determine vertical direction;
  - Guiding surfaces of as-built In-VV Rails are used to determine toroidal direction;
  - Outboard surfaces of as-built Plug to Port shims are used to determine radial direction.
- Port Cell Assembly datum system for EQ Port is given by:
  - Origin is the intersection of previously defined Reference Axis and extracted plane of as-built Plug to Port shims surfaces;
  - X-axis is coincident with previously defined Reference Axis – also designates as Radial direction;
  - Z-axis is perpendicular to extracted plane of as-built In-VV Rails top surface also designates as Vertical direction;
  - Y-axis is perpendicular to X and Z such that XYZ forms an orthogonal system – also designates as Toroidal direction

Thus, the difference is the customization accuracy of the In-VV rails and shims (Figure 4.88). This can be summarized as follows (Table 4.10):

Table 4.10: PPAD to PCAD tolerances ([85]).

	Radial [mm]	Toroidal [mm]	Vertical [mm]
Delta_DSM-EPP	±0.5	±1.0	±0.5

The two contributions can be summed up as follows:

$$Delta\_EPP - PCA_i = Delta\_EPP - PPA_i + Delta\_PPA - PCA_i \tag{4.1}$$

where $i = rad, tor, ver$. We obtain (Table 4.11):

Table 4.11: EPP to PCA assembly tolerances ([85]).

	Radial [mm]	Toroidal [mm]	Vertical [mm]
Delta_EPP-PPA	±0.5	±1.5	±0.4
Delta_PPA-PCA	±0.5	±0.5	±0.5
Delta_EPP-PCA	**±1.0**	**±2.0**	**±0.9**

3. Alignment of ISS with the Port Cell Assembly The alignment is operated by targeting the Port Cell Assembly with the ISS. Figure 4.89 the isometric view of the ISS & PCSS (Port Cell Supporting Structure) Positioning, where both the Port Cell Assembly and the ISS, on which the Ex-Port RNC will be mounted, are visible. The ISS alignment is performed by targeting the Port Cell Assembly Datum (PCAD) with the ISS Datum system, ISSD.

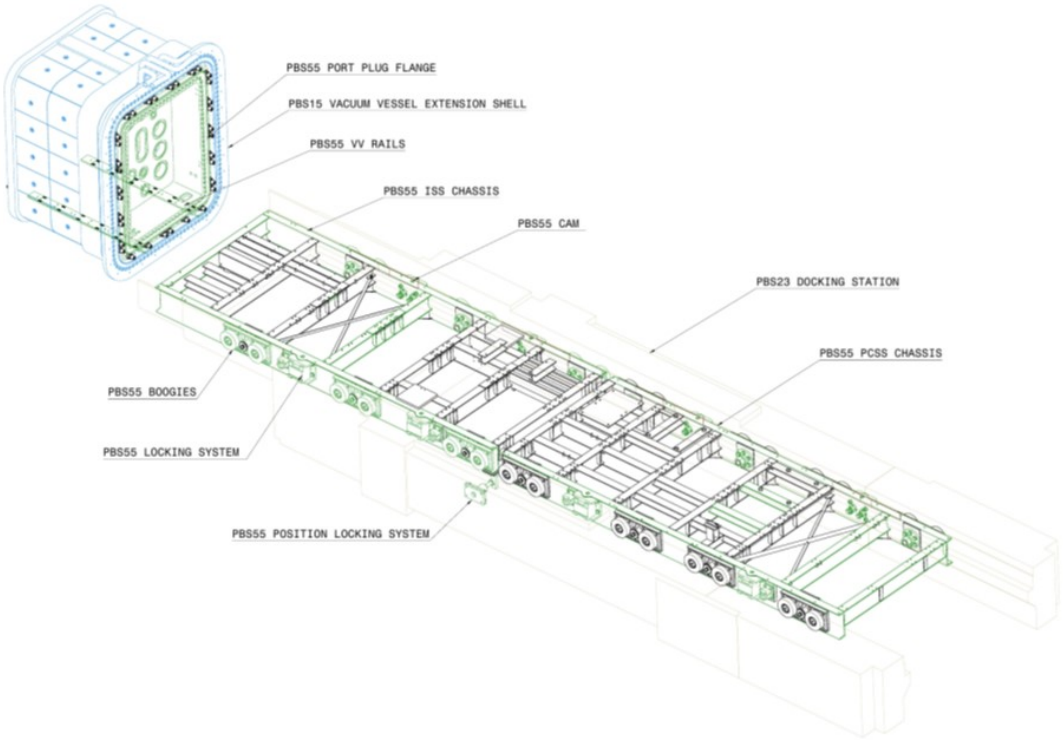

Figure 4.89: ISS& PCSS Positioning in Plasma Operating State Configuration ([85]).

The ISSD is given in Figure 4.90:

- D: horizontal plane that minimizes the least square distance from points 5, 6, 7, 8, 9, 10, 11 and 12;
- E: longitudinal vertical plane normal to D that minimizes the least square distance from Points 1, 2, 3 and 4;
- F: transversal vertical plane normal to D and E that minimizes the least square distance from Plane 1 (front Plane of ISS/PCSS structure, based on the end of the ISS and the anti-shock buffer of the PCSS structure

Points 1 to 12 are points on wheels, boogies and guiding rollers of ISS, referred to axis and planes. For example, Point 1 is center axis front left guiding roller, Point 5 is the intersection between the left side front bogie assembly center axis and its wheels vertical middle plane.

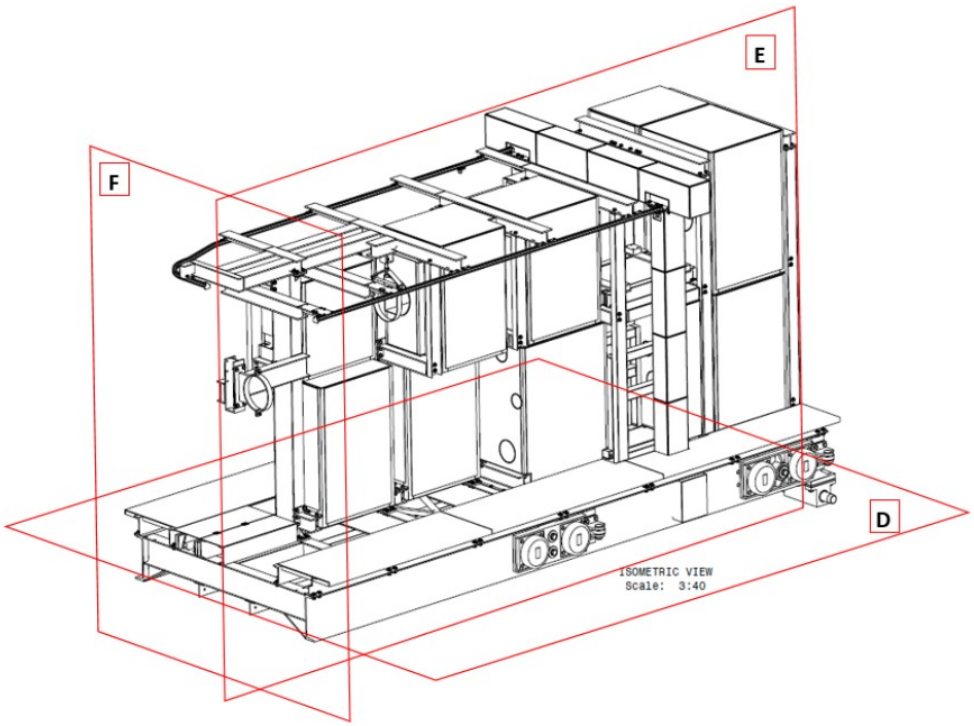

Figure 4.90: ISSD reference planes/points definition (Isometric view) ([85]).

By analyzing the boxes of ISS Datum System fully reported in the source document, Table 4.12 reports the alignment tolerances between ISS and Port Cell Assembly. A ±1.0 margin has been added to each term following a conservative approach:

Table 4.12: ISS to PCA assembly tolerances ([85]).

	Radial [mm]	Toroidal [mm]	Vertical [mm]
Delta_ISS-PCA	**±3.0**	**±3.0**	**±3.0**

4. Alignment of Ex-Port RNC on the ISS The installation of Ex-Port RNC on ISS is realized by bolting the Ex-Port structure on a threaded holes matrix belonging to the ISS, as shown in [8]. The bottom component of Ex-Port RNC is called Counterplate, a 30mm thick Stainless-Steel slab machined and drilled with a holes matrix that matches the one located on the ISS. Thus, the installation is realized by coupling two surfaces with holes, the top surface of the ISS and the bottom surface of Ex-Port RNC. Tolerance information must be given concerning the planarity of the surface and the positioning of the holes, for both components. To couple the Ex-Port RNC with the ISS, it is fundamental that the interaxle spacing between the holes is the same, as shown in Figure 4.91. If both ISS and Ex-Port RNC respects the dimensions of the interface, then the coupling can be realized under the tolerances specified in the next paragraphs.

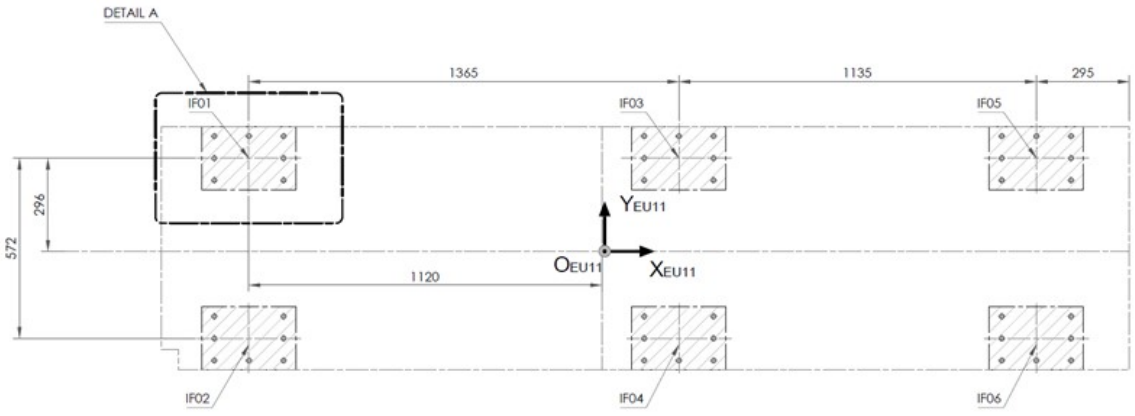

Figure 4.91: Geometrical Interfaces between ISS and Ex-Port RNC ([85]).

4.1 ISS Tolerancing For the positioning of holes on the ISS, the datum system is shown in Figure 10:

- datum A is shown in the drawing "SECTION VIEW B-B". Moreover, the surface from where datum A is defined is affected by a surface tolerance of 0.5mm,
- datum B is shown in "ISS BASE FRAME TOP VIEW",
- datum C is shown in "SECTION VIEW B-B".

From "DETAIL F" (Figure 11) and "DETAIL G", one can read that the axes of the holes are perpendicular to datum A and are contained inside a 0.5mm diameter circumference laying on datum A plane.

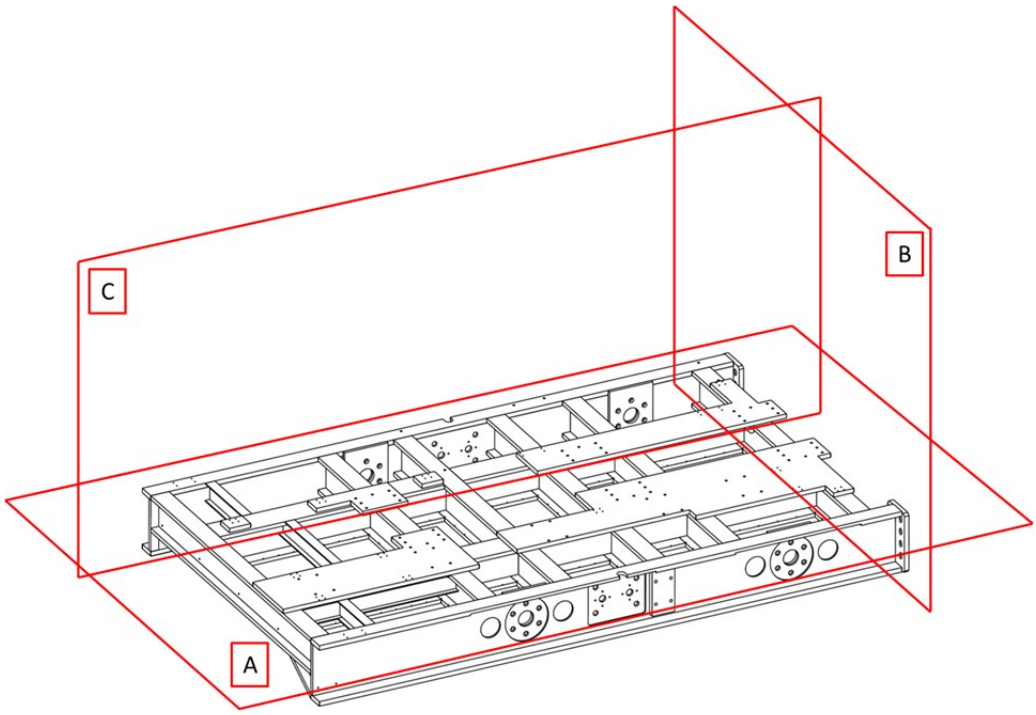

Figure 4.92: ISS interfaces datum system ([85]).

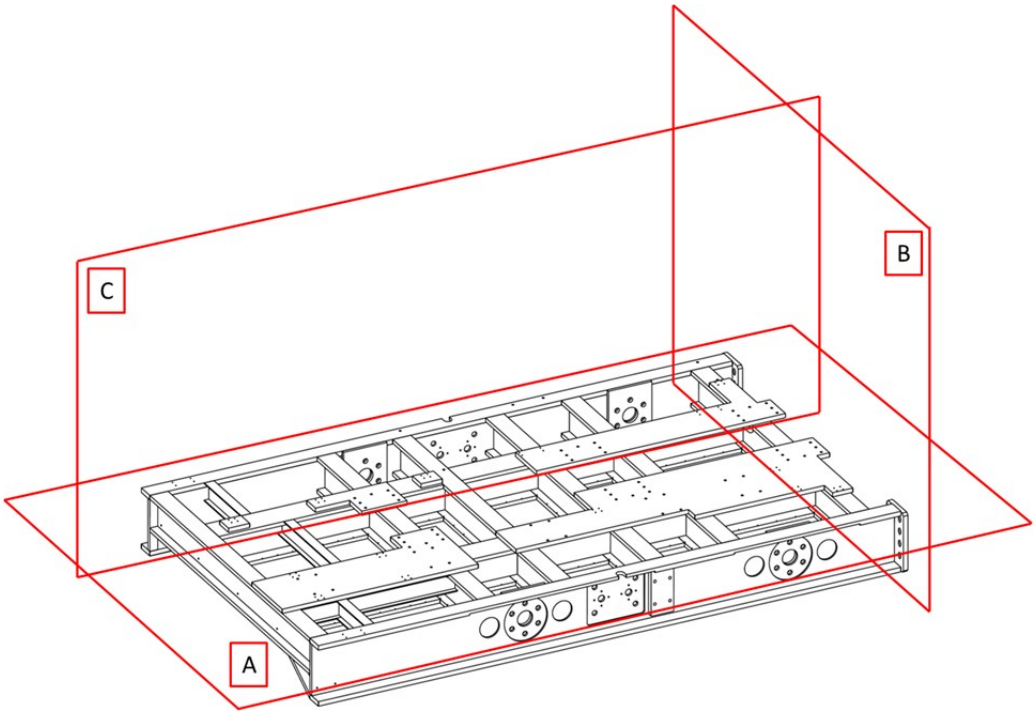

Figure 4.93: "DETAIL F": the holes matrix interface ([85]).

Even though the positioning is specified as of 0.5mm in diameter (Figure 11) this value has been increased to 2mm due to a conservative approach, since the current design maturity does not guarantee that the value will be the definitive one. The same approach has been used for the vertical deviation, now set as 2mm instead of 0.5mm. Now, referring to the EP01 coordinate system, these data can be written as in Figure 4.91:

Table 4.13: ISS to interface assembly tolerances ([85]).

	Radial [mm]	Toroidal [mm]	Vertical [mm]
Delta_ISS	±1.0	±1.0	±1.0

4.2 Ex-Port RNC Counterplate tolerancing The same holes positioning and holes and surface tolerancing can be applied to the Ex-Port RNC Base plate. The datum system has yet to be defined, but the tolerancing is set to be the same

as ISS. Thus, referring to the EP01 coordinate system, the tolerances are reported in 4.14:

Table 4.14: Ex-Port to interface assembly tolerances ([85]).

	Radial [mm]	Toroidal [mm]	Vertical [mm]
Delta_ISS	±1.0	±1.0	±1.0

4.3 Ex-Port RNC to ISS assembly tolerances Once the position tolerances of both Ex-Port and ISS with respect to the interface (Figure 4.91) are extracted from drawings, we can proceed to calculate the assembly tolerances between the Ex-Port RNC and the ISS. To do this, the following sum will be realized:

The two contributions can be summed up as follows:

$$Delta\_ExPort - ISS_i = Delta\_ExPort_i + Delta\_ISS_i \tag{4.2}$$

where i = *rad, tor, ver.* We obtain (Table 4.15):

Table 4.15: Ex-Port RNC to ISS assembly tolerances ([85]).

	Radial [mm]	Toroidal [mm]	Vertical [mm]
Delta_ExPort	±1.0	±1.0	±1.0
Delta_ISS	±1.0	±1.0	±1.0
Delta_EPP-PCA	**±2.0**	**±2.0**	**±2.0**

5. Tolerances related to the thermal expansion The next term of the tolerance chain is the one related to the thermal expansion. Being the machine at room temperature during installation, it reaches 100°C during normal plasma operations and 200°C during baking. Port Plug thermal displacements, relative to the basemat, related to the variation of temperature are reported in Table 4.16:

Table 4.16: Summary table of main maximal VV PHTS thermal expansion in TGCS ([85]).

Port structures		CSYS	@ 100°C			@ 200°C		
			Radial (mm)	Toroidal (mm)	Vertical (mm)	Radial (mm)	Toroidal (mm)	Vertical (mm)
#01to#03 #08to#18	Port Plug Flange	CS#I	14.603	-1.055	13.935	34.291	-2.477	32.393

However, there are no uncertainties associated to the above values. To correctly account those factors and correct NOS and BAK values, two terms are going to be considered: uncertainty on the thermal expansion FEM calculation and uncertainty on the Port Plug cooling water system temperature. The first term is set to be 20%, as a quantity commonly used for FEM simulations. Thus, the multiplication factor is 1.2. Concerning the second term, Table 4.17 specifies the coolant inlet temperature both for NOS and for BAK, and its rangeability. Because of the purpose of this study (the alignment of Ex-Port RNC with Port Plug during normal operation conditions), only the NOS case is considered.

Table 4.17: VV-Thermo-Hydraulic Requirements ([85]).

Thermo-Hydraulic Parameters	Plasma Operation	Baking
Coolant Inlet Temperature [°C] (rangeability, °C)	100 (-10/+12)	195 (-5/+0)

In particular, NOS coolant inlet temperature is 100°C with -10/+12°C as range. We consider the coolant inlet temperature as the reference temperature for the Port Plug. Thus, considering the worst tolerance value among plus and minus (i.e. +12), in NOS conditions the tolerance is of 12% (i.e. multiplication factor is 1.12). Thus, the total multiplication factor for NOS values is 1.34, as for the following formula:

$$Total\_factor = FEM\_factor \times Temperature\_factor = 1.2 \times 1.12 = 1.34 \quad (4.3)$$

Assuming a linear correlation between the temperature variation and the thermal expansion, the calculated factor of 1.34 is applied to the displacement values of Table 4.16 by multiplying each term by 1.34. We obtain the following tolerances (Table 4.18):

Table 4.18: Tolerances on thermal calculations ([85]).

	Radial [mm]	Toroidal [mm]	Vertical [mm]
Delta_th	5.0	0.4	4.8

6. Tolerance related to the Dead Weight influence The Ex-Port RNC part closer to the Port Plug closure plate lays on a cantilevered section of the ISS. Under the weight of the Ex-Port RNC (17 tons), the assembly ISS + Ex-Port may lower in this zone, especially for the so-called "nose" of the Ex-Port RNC (part of the Ex-Port RNC located at the minor machine radius). Such displacement has been evaluated by two FEM simulations: EP01 ISS FEM simulation and the Ex-Port RNC FEM simulation.

6.1 Displacement of the EP01 ISS due to DW This simulation considers the Ex-Port RNC as an input mass value and the ISS rails as fixed for evaluating the directional displacements of the EP01 ISS (Figure 4.94, example of vertical displacement).

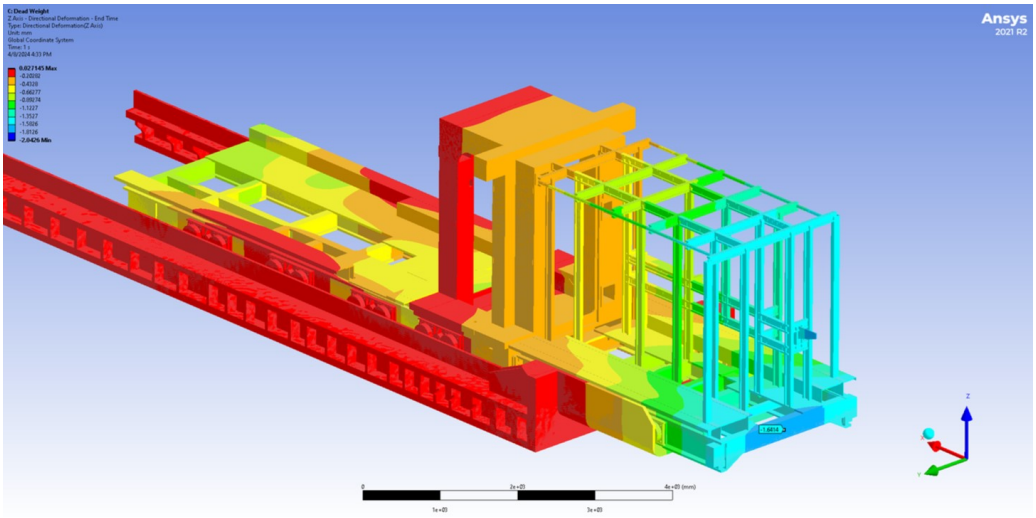

Figure 4.94: EP01 ISS z-direction displacement under DW ([85]).

We consider as reference the biggest value for a conservative approach; the point considered belongs to the beam located at the minimum machine radius (Figure 4.94). Table 4.19 sums up the maximum displacements occurred to the EP01 ISS due to the Dead Weight application, for each direction.

Table 4.19: Maximum displacement values of ISS due to DW ([85]).

	Radial [mm]	Toroidal [mm]	Vertical [mm]
Delta_DW_ISS	−0.07	0.00	−1.64

6.2 Displacement of the Ex-Port RNC due to DW This simulation considers the Ex-Port RNC sub-components as input mass values and the Ex-Port RNC base as fixed for evaluating the directional displacements of the Ex-Port RNC (Figure 4.95, example of vertical displacement).

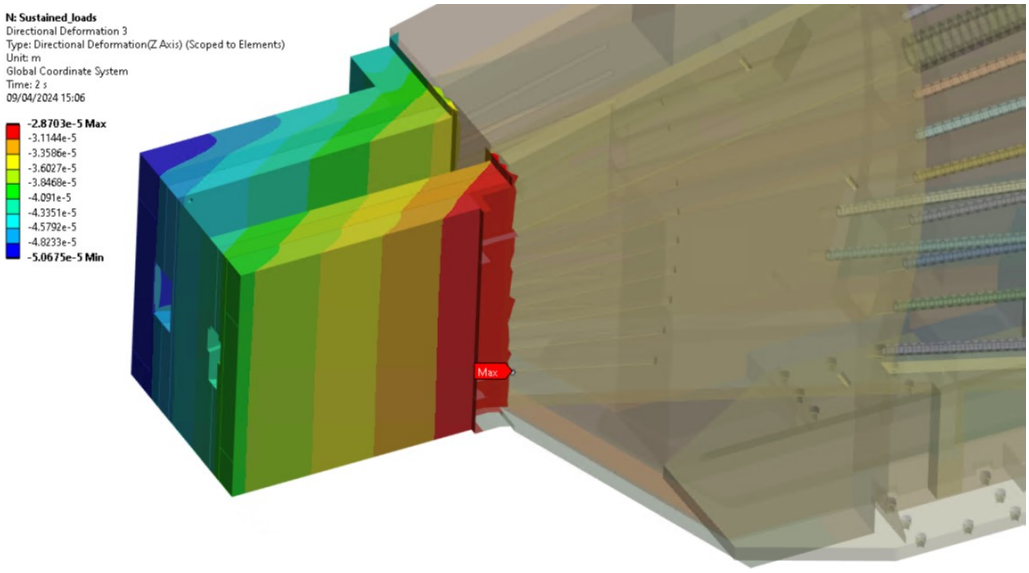

Figure 4.95: Ex-Port RNC z-direction displacement under DW ([85]).

Again, we consider the biggest value for a conservative approach; the point considered belongs to the Ex-Port RNC "nose". Table 4.20 sums up the maximum displacements occurred to the Ex-Port RNC due to the Dead Weight application, for each direction.

Table 4.20: Maximum displacement values of Ex-Port RNC due to DW ([85]).

	Radial [mm]	Toroidal [mm]	Vertical [mm]
Delta_DW_ExP	-0.02	0.02	-0.05

6.3 Influence of FEM simulation uncertainties The FEM simulation results can be affected by a simulation error. The uncertainty factor commonly used for this type of calculation is 20%. Thus, for example, the vertical displacement value of the ISS, $-1.64mm$ becomes $-1.64 \pm 0.33mm$ (where $0.33 = 1.64 \times 0.2$). In conclusion, by applying the 20% factor to all terms and considering as acceptable values only the ones bigger than $0.1mm$, we obtain (Table 4.21):

Table 4.21: Tolerance values due to DW influence ([85]).

	Radial [mm]	Toroidal [mm]	Vertical [mm]
Delta_DW_ISS	±0.01	±0.00	±0.33
Delta_DW_ExP	±0.00	±0.00	±0.01
Delta_DW	**±0.0**	**±0.0**	**±0.3**

Collection of manufacturing tolerances values

7. Manufacturing tolerances of DSM There is no available information on the manufacturing tolerances of the DSM. By considering the manufacturing procedures, the nominal dimensions of the components directly involved in the tolerance chain and the applicable standard for manufacturing tolerances ISO 2768 (m) (Table 4.22), the manufacturing tolerances of the DSM can be estimated as reported in Table 4.23.

Table 4.22: Standard ISO 2768.

Permissible deviations in mm for ranges in nominal lengths	Tolerance Class Designation (Description)			
	f (fine)	m (medium)	c (coarse)	v (very coarse)
0.5 up to 3	±0.05	±0.1	±0.2	--
over 3 up to 6	±0.05	±0.1	±0.3	±0.5
over 6 up to 30	±0.1	±0.2	±0.5	±1.0
over 30 up to 120	±0.15	±0.3	±0.8	±1.5
over 120 up to 400	±0.2	±0.5	±1.2	±2.5
over 400 up to 1000	±0.3	±0.8	±2.0	±4.0
over 1000 up to 2000	±0.5	±1.2	±3.0	±6.0
over 2000 up to 4000	--	±2.0	±4.0	±8.0

Table 4.23: Manufacturing tolerances of the DSM ([85]).

	Radial [mm]	Toroidal [mm]	Vertical [mm]
Delta_DW_ExP	±0.8	±0.8	±0.8

8. Manufacturing tolerances of the Ex-Port RNC Similarly to the manufacturing tolerances of the DSM, considering applicable standard ISO 2768 (m)

(Table 4.22) and Ex-Port RNC nominal dimensions of the components directly involved in the tolerance chain, the manufacturing tolerances of the Ex-Port RNC can be estimated as follows (Table 4.24):

Table 4.24: Manufacturing tolerances of the Ex-Port RNC ([85]).

	Radial [mm]	Toroidal [mm]	Vertical [mm]
Delta_DW_ExP	±0.8	±0.8	±0.8

Reconstruction of the tolerance chain

Once the tolerances chain is completed, the interest is focused on its worst-case scenario. The question to be answered is what is the maximum misalignment that occurs between Ex-Port RNC and Port Plug due to installation procedures. To calculate this, Table 4.25 collects all data from previous paragraphs and provides the final sum. The sum is realized with the following formula:

$$\begin{aligned} &Delta\_total_i = \\ &Delta\_DSM\_EPP_i + Delta\_EPP\_PCA_i + Delta\_ISS\_PCA_i + \\ &+ Delta\_ExPort\_ISS_i + Delta\_th_i + Delta\_DW + \\ &+ Delta\_man\_DSM_i + Delta\_man\_ExP_i \end{aligned}$$

where $i = rad,\ tor,\ ver.$

Table 4.25: Ex-Port RNC to ISS assembly tolerances ([85]).

	Radial [mm]	Toroidal [mm]	Vertical [mm]
Delta_DSM-EPP	±0.1	±0.9	±0.2
Delta_EPP-PCA	±1.0	±2.0	±0.9
Delta_ISS-PCA	±3.0	±3.0	±3.0
Delta_ExPort-ISS	±2.0	±2.0	±2.0
Delta_th	±5.0	±0.4	±4.8
Delta_DW	±0.0	±0.0	±0.3
Delta_man_DSM	±0.8	±0.8	±0.8
Delta_man_ExP	±0.8	±0.8	±0.8
Delta_total	**±12.7**	**±9.9**	**±12.8**

Conclusions

The obtained values show how the maximum misalignment, due to installation only, is not negligible. In fact, Ex-Port RNC's LOS are sixteen in total: one of them have an $8mm$ collimating diameter, the other fifteen of $11mm$.

By comparing this geometrical values with the values obtained in Table 4.25, we can conclude that, already in this configuration, if the vertical misalignment is at its worse value of $+12.8mm$, the $8mm$ collimating diameter LOS completely lose their field of view; and for the other fifteen 11mm collimating diameter LOS the value correction would be excessive. This value correction is realized thanks to a software that takes as inputs the measurements of the Position Monitoring System.

But if the misalignment is too significant (as for values of Table 4.25), the correction on the detected value can lead to an unreliable final value. Again, this consideration is valid for the fourteen $11mm$ collimating diameter LOS. For the two $8mm$ collimating diameter LOS, the data is not even detected.

As confirmed by Port Integrator team, no alignment system is foreseen for the ISS, on which the Ex-Port RNC is mounted.

Thus, the necessity of an alignment system for the Ex-Port RNC is emerging.

The tolerance analysis presented is limited to three Degrees Of Freedom (DOF), i.e. the three translations along the three main axes, due to the limits of the available

source data. The LAISE tool presented will be applied considering 3 DOF only (3 translations), while keeping locked the three rotations. Thus, for instance, the alignment system will be capable of realigning the Ex-Port RNC along the three directions - and not *around*. However, the alignment system will be designed to foresee the capability of adjusting of the three rotations as well.

4.4 Application of the LAISE tool with the Ex-Port RNC AS

This section present the methodical application of the novel LAISE tool to the Ex-Port RNC project, for integrating a brand-new Alignment System. The section demonstrate the success of the LAISE tool with a complex case-study, from the necessity of an alignment system to its realization and validation, while keeping guaranteed the other design requirements.

The RNC Ex-Port subsystem faced a significant design challenge related to the alignment of its Lines Of Sight with the Diagnostic Shielding Module optical path. Despite initial design and analysis, a detailed tolerance chain analysis revealed a requirement gap: the potential for excessive misalignment that could severely compromise the RNC's functionality. This issue necessitates a late-stage design intervention, which was systematically managed using the LAISE method.

4.4.1 Phase 0 — Trigger & Baseline Lock: Need for an Alignment System

Trigger

The LAISE workflow was unequivocally triggered by the concerning results of the tolerance chain analysis for the RNC Ex-Vessel Collimators to the EP01 PP DSM 2 Optical Path [85]. This analysis identified that, in a worst-case scenario, the total misalignment could reach $\pm 12.7mm$ in the radial direction, $\pm 9.9mm$ in the toroidal

direction and $\pm 12.8mm$ in the vertical direction (Table 4.25). Such a misalignment poses a critical threat to the RNC's primary function:

- Vignetting and Loss of Field of View: A vertical misalignment of +12.8 mm would lead to the complete loss of the field of view for the 8 mm collimating diameter LOS, and an excessive correction would be required for the 11 mm LOS. The passive alignment capabilities of the DSM2 Optical Paths are insufficient to compensate for worst-case misalignment scenarios.

- Mismatch in LOS Positions: This misalignment also creates a discrepancy between the reference LOS positions used for data inversion and the actual LOS positions, leading to inaccurate diagnostic measurements [85].

The realization that the existing design could not guarantee the required LOS alignment under all conditions constituted a clear "requirement deviation" or "performance gap", necessitating a corrective subsystem.

Baseline Lock & ECR Raised

Upon identification of this critical issue, the current system baseline for the Ex-Port RNC, including its structural integrity, RAMI analysis, and existing design description, has been formally frozen within the Product Lifecycle Management environment.

In the ENOVIA environment, this corresponds to freeze the CAD model at the version "–J", as shown in Figure 4.96. The version –J, then, is set to be the last EU11 CAD version without any Alignment System.

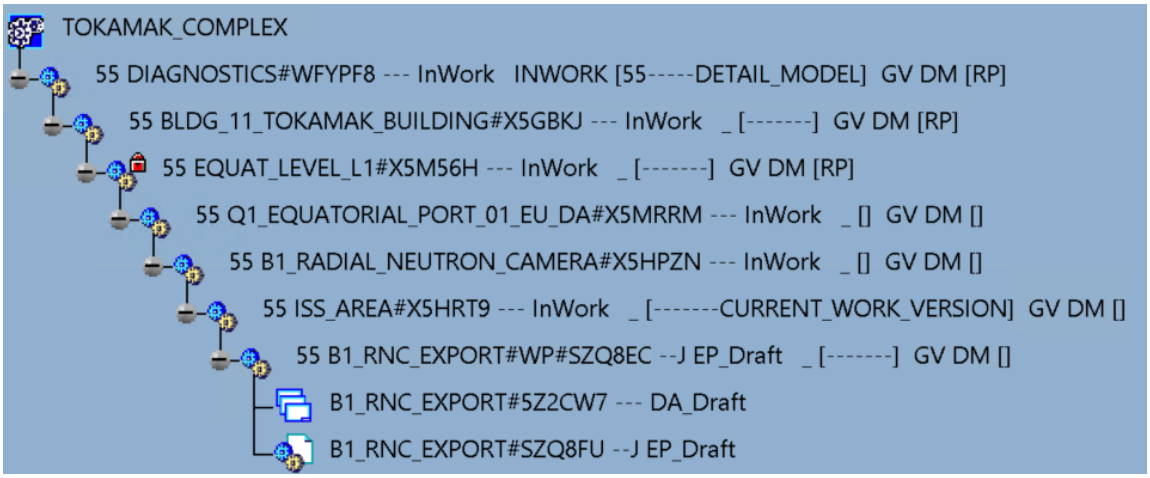

Figure 4.96: ENOVIA branch of the –J version of the Ex-Port RNC.

This action establishes a stable reference point against which all subsequent changes for the Alignment System would be managed. An Engineering Change Request must be raised to formally initiate the change process, articulating the need for an active alignment solution to rectify the identified tolerance violations and ensure the RNC's operational integrity.

4.4.2 Phase 1 — Re-Requirements: Defining the Alignment System (AS)

Requirement Update

The identified requirement gap — the inability to maintain precise LOS alignment under worst-case tolerance stack-up — necessitated the formal definition of new, derived, or modified requirements for the Ex-Port RNC. The core RNC requirements state its need for precise measurement of un-collided 14 MeV and 2.5 MeV neutrons and accurate assessment of fusion power generation. To achieve this, the precise alignment of the LOS is fundamental. Therefore, a new derived requirement is established: *"The Ex-Port RNC system shall incorporate an Alignment System (AS) capable of compensating for manufacturing and installation misalignments up*

to $\pm 12.7mm$ *in the radial direction,* $\pm 9.9mm$ *in the toroidal direction and* $\pm 12.8mm$ *in the vertical direction to ensure precise LOS alignment and prevent vignetting."* This derived requirement directly supports the existing functional requirements of the RNC.

AS requirements definition

Once defined the core functional requirement of the AS, specific requirements for the AS correct functioning can be outlined:

1. The AS shall have a minimum range of 25.4mm in the radial direction, 19.8mm in the toroidal direction and 25.6mm in the vertical direction

2. The AS shall be capable of aligning the 17 tons structure of the Ex-Port RNC

3. The AS shall not affect negatively the Tolerance Chain Analysis during its functioning, i.e. the AS shall have an accuracy below the reconstruction error of the Position Monitoring System, the manufacturing tolerances and the installation tolerances

4. The AS shall respect the external interfaces of EU11 with the Interspace Supporting Structure, the Temperature Stabilization System and the Electrical interface

5. The AS shall not exceed the boundaries of the EU11 Configuration Model

6. The AS shall be accessible in the Port Interspace Area by the workers

7. The AS shall be withstands the thermal loads that characterize the Port Interspace Area

8. The AS shall be withstands the electromagnetic loads that characterize the Port Interspace Area

4.4.3 Phase 2 — Trade-off & Decision: Selecting the Alignment System

Alternative Comparison

During this phase, different alternative solutions for the corrective Alignment System would have been compared.

Based on the AS requirements defined in the Phase 1, the trade-off analysis has to evaluate potential AS designs based on:

- Technical Performance: Ability to achieve the listed requirements.
- Cost Implications: Manufacturing, installation, and operational costs.
- Risk: Technical risks, integration risks, and operational risks.
- Schedule: Impact on project timelines.
- Safety: Compliance with ITER safety standards and minimizing human intervention in hazardous areas.
- Maintainability: Ease of repair or replacement.

Selection of the AS

The selection of the AS has followed the considerations:

- The selection of the AS has been primarily driven by the Ex-Port RNC mass, that is 16.2 tons. In fact, the alignment should be executed by relocating the entire Ex-Port RNC block, in order to realign the two sets of cutouts: the Optical Paths inside EU01 and the collimators inside the Ex-Port RNC.
- Along with the loads, the ranges and the accuracy must be respected: the combination of these requirements restrict the choice field.

- It is fundamental to state that the AS is set to be actioned only during the first installation of the Ex-Port RNC inside the EP01 and during the planned Long Term Maintenance. An active, remotely-controlled AS is not necessary for the scope.
- A critical issue is the tridimensionality of the problem: the AS must be capable of realign along 3 axes (3 translations) and around the same 3 axes (3 rotations).
- The AS subsystems must be as small as possible, in order to fit between the base of the Ex-Port RNC and the ISS
- The material of the AS subsystems must be fire resistant.

These considerations, combined with the requirements, lead the proposal of the following alternatives:

- hydraulic lifters
- mechanical jacks
- double-wedged mechanical lifters

The hydraulic lifters have excellent behavior for heavy loads, but the presence of a working liquid can bring different issues that cannot be opportunely solved. Moreover, they are multi-elements systems, with a complex scheme of tubes and operating livers. This extends their volume occupation, making impossible their integration inside the available volume. The mechanical jacks have good lifting capabilities. The main problem is related to the central screw, that occupies a considerable volume. Similar to the mechanical jacks in terms of actioning, the double-wedged mechanical lifters have a considerable small volume occupation. The commercially available double-wedged systems have an excellent use in heavy loads solutions. Among the three solutions evaluated, the double-wedged system has been chosen.

After having carried out a trade-off research in the specific market sector, the *Fixators* have been selected (Figure 4.97).

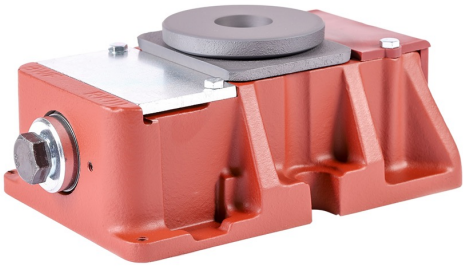

Figure 4.97: Example of Fixator.

The Fixators are double-wedged mechanical lifters actioned by rotating the adjusting screw. Inside the Fixator, the screw pushes or pulls the bottom wedge, that in turn lifts or lowers the upper wedge.

To properly use the Fixators in the AS for the Ex-Port RNC, a number of them must be used to distribute the load, i.e. the Ex-Port RNC mass, for instance. The horizontal use, with the adjusting screw axis as horizontal and the lifting direction axis as vertical, is directly associable to the z-direction translation. To cover the two other translations, the Fixators must be also arranged in a vertical configuration (with the adjusting screw axis as vertical and the lifting direction axis as horizontal). The Fixators can satisfy this requirement.

The dimensions of a Fixator are shown in Figure 4.98 reported in Table 4.26. The overall dimensions, especially for the smaller Sizes, result very suitable for the scope of the AS.

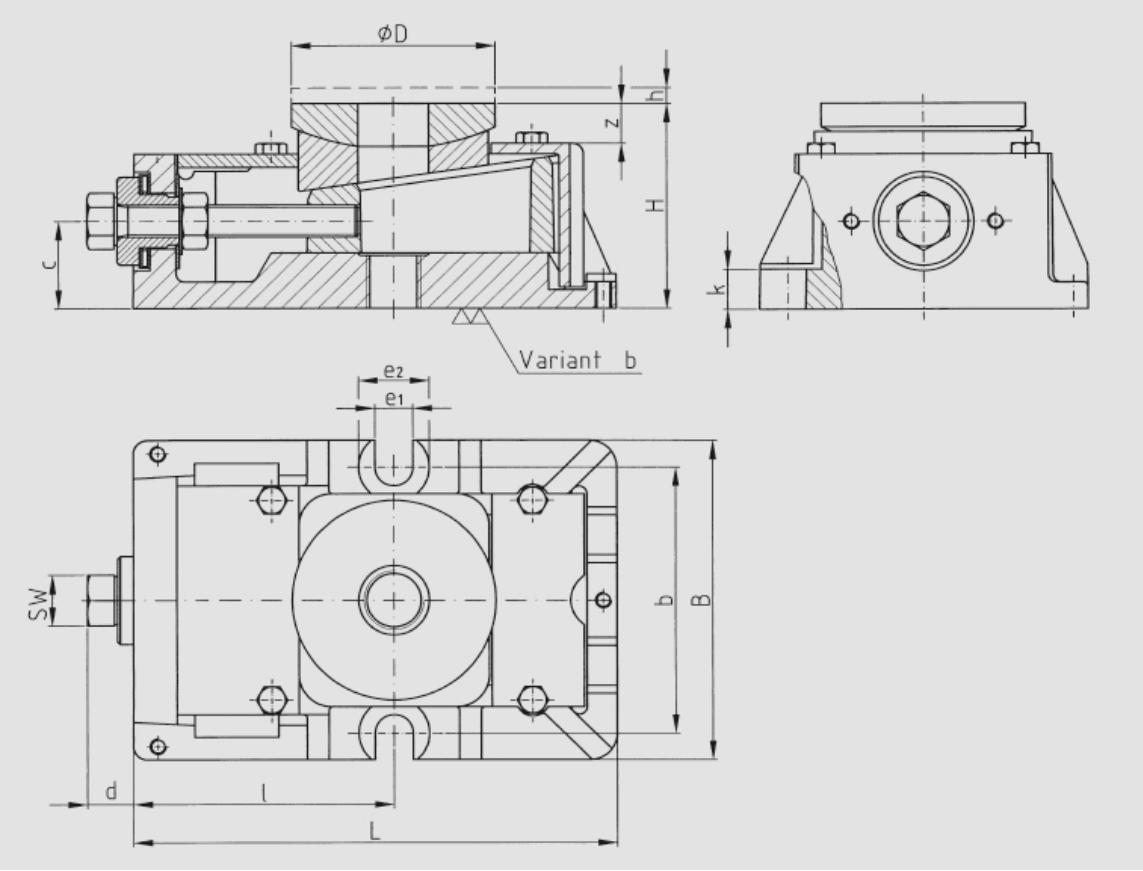

Figure 4.98: Section drawing of a Fixator - the dimensions are reported in Table 4.26.

Table 4.26: Characteristic dimensions of a Fixators. All dimensions in [mm].

Size	**L**	**B**	**H**	**ØD**	**SW**	**d**	**c**	**z**	**h**	**l**	**b**	**e1**	**e2**	**k**
I	175	105	55	60	19	16	21	13	5	92	90	14	26	12
II	178	120	75	75	19	15	31	15	5	96	100	14	26	13
III	220	150	95	90	24	22	40	17	6	118	130	18	32	22
IV	275	180	115	110	30	24	49	17	8	142	160	24	38	24

In terms of load capability and accuracy, the Fixator manufacturer reports the technical data of Table 4.27.

Table 4.27: Technical Data of the Fixators.

Description	**Dim.**	**RKII**	**RKIII**
Recommended machine dead weight	kg	1996	4037
Maximum allowable lifting load per FIXATOR	kg	12020	24267
Vertical adjustment per revolution of height adjusting screw	mm	0.25	0.3
Maximum vertical adjustment	mm	5	6.1
Approximate torque required to turn adjusting screw	N m /1000kg	3	3.9
Maximum allowable torque on adjusting screw	N m	36.6	96.3

Table 4.27 indicates that the maximum vertical adjustment, for the RKII Size, is 5mm. This is not sufficient to cover the maximum alignment range foreseen of 25.6mm (in the vertical direction). To solve this problem, the use of dedicated Stainless Steel Disks is proposed (Figure 4.99). The Disks, in an assortment of 2.5mm interval, can be added, substituted or removed from the top of the Fixator dependently on the quantity to be adjusted.

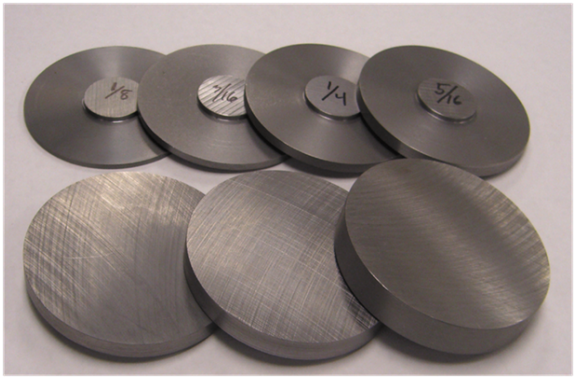

Figure 4.99: Assortment of Disks for increasing the range.

As shown in Table 4.27, the attention has been focused on the RKII and RKIII Fixators for their smaller dimensions and high loading performances.

Now that the basic element of the AS, the Fixator, has been chosen, the AS must

be designed by positioning the Fixators inside the available volume to make them respecting the functional requirements.

4.4.4 Phase 3 — Digital Thread Activation: Integrating into PLM

PLM Linkage & Configuration Management Update

Once selected the AS base components, the design must be studied and implemented in the CAD model of EU11. To do this, the ENOVIA model should be updated. To be able to modify the CAD model, a new version must be created. Thus, from the version –J the new version *–K* is created (Figure 4.100).

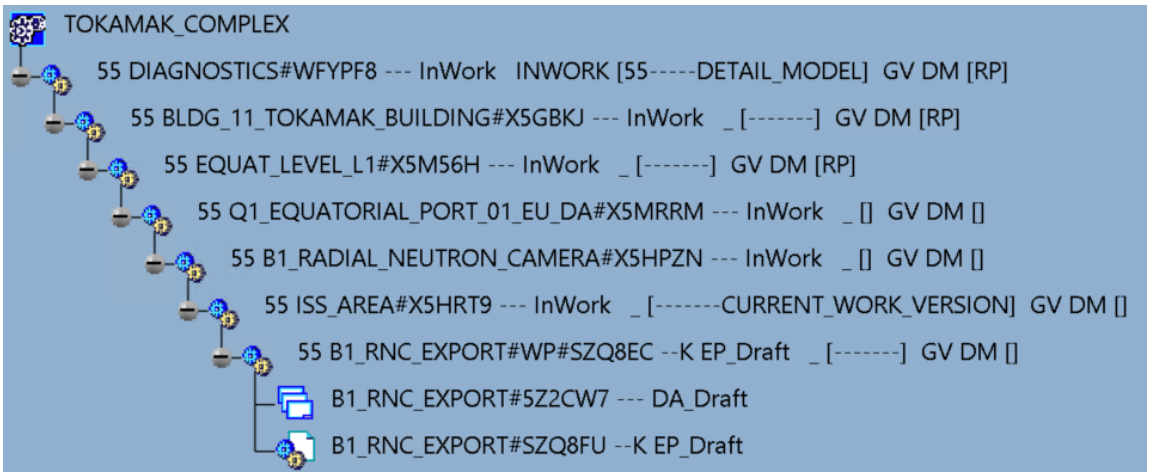

Figure 4.100: ENOVIA branch of the –K version of the Ex-Port RNC.

Within the version –K, the implementation of the AS can be deeply studied. Only in the ENOVIA/CATIA environment it is possible to load the Ex-Port RNC CAD model (to be modified) and the EU11 CM CAD model, containing the external interfaces, in the same modification CATIA window. In this way, the modifications can be implemented by constantly controlling the available volume and the external interfaces, thus satisfying the related requirements.

4.4.5 Phase 4 — MBSE Impact Analysis: Assessing Consequences

The integration study can be carried out in the Ex-Port RNC CAD model. The study is iterative: in this phase, the interfaces are constantly checked and the model modified consequently. The impact on the internal Ex-Port RNC components is also considered, and the total mass increasing monitored.

After the implementation of the AS, a draft of the Alignment Procedure will be discussed, in order to evaluate the respect of the functional requirements.

Finally, the impact on the Position Monitoring System is outlined, and the PMS model modified accordingly.

Model Update

The basic idea for the AS implementation is to position the Fixators between the Ex-Port RNC Base plate and the ISS, as shown in Figure 4.101.

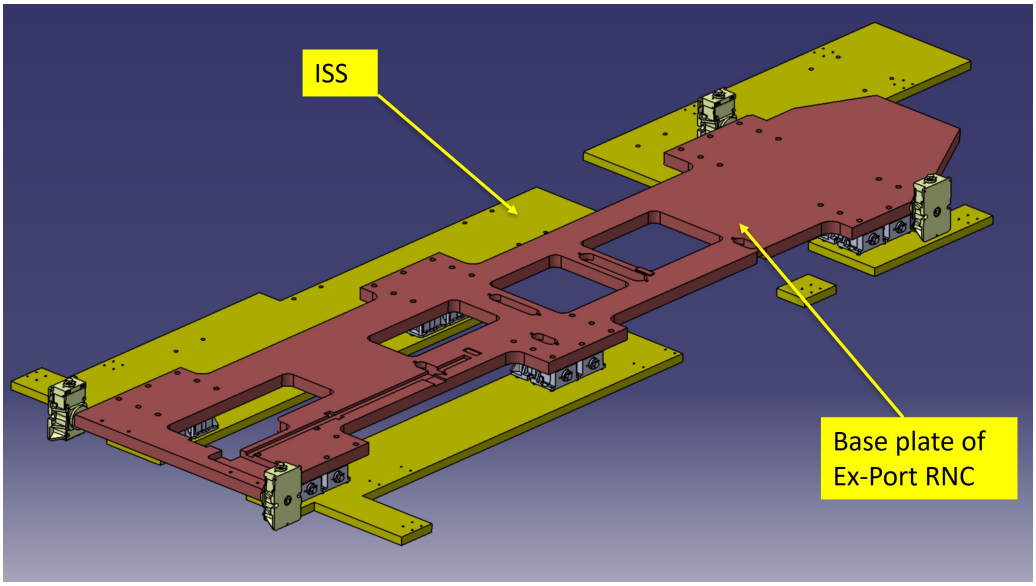

Figure 4.101: First sketch of the AS integration.

This solution is focusing on the AS but does not properly consider the internal

and external interfaces. For instance, Figure 4.101 is showing a $+z$ translation of the Ex-Port Base from the ISS where, as the current design, is directly bolted. But, considering the requirement of the alignment of the LOS, the position of the Ex-Port Base cannot be modified. This would mean that, if a $+z$ translation of the Ex-Port is not possible, a $-z$ translation of ISS is required. However, also this option cannot be selected, because the ISS design is out of the scope of the RNC design team and cannot be easily modified. The ISS is in the scope of IO design team, who is stating that the ISS is in a relevant frozen version and cannot be further modified.

To cope with this problem, a solution like the one shown in Figure 4.102 is proposed and implemented.

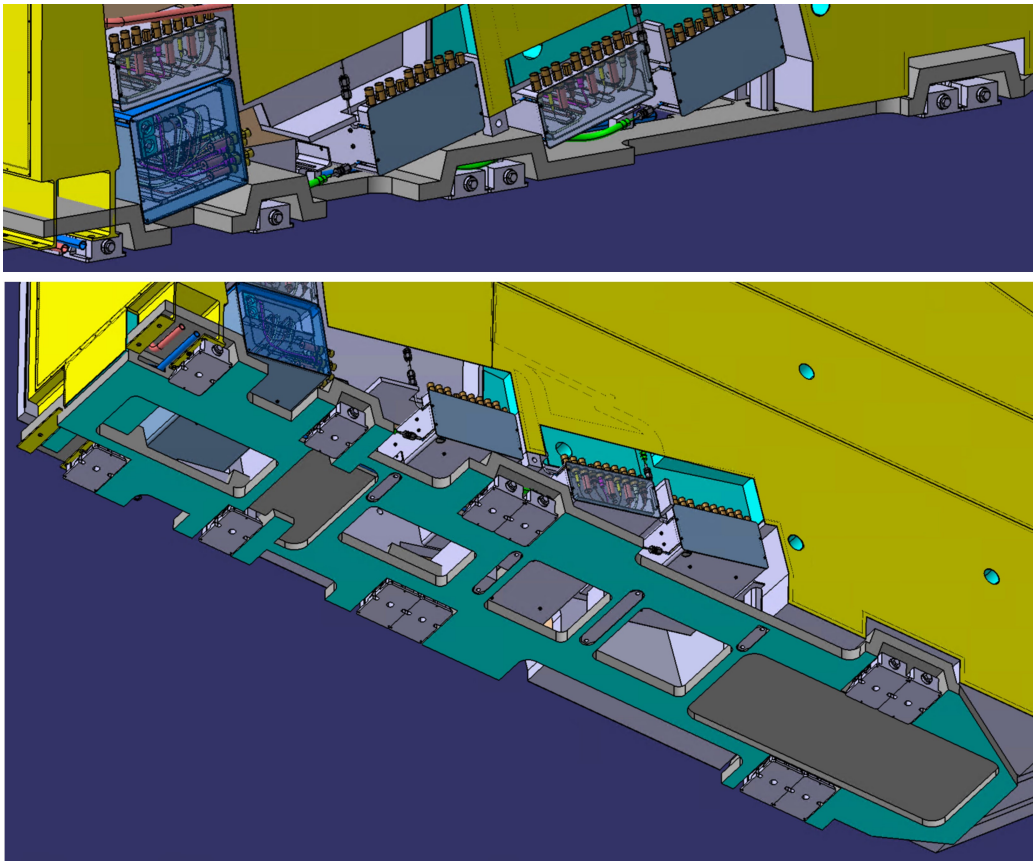

Figure 4.102: Second sketch of the AS integration.

With this solution, the needed volume for the integration of the Fixators is found inside the EU11 CM. This required a relevant design modification of the Base Plate. The placement of the Fixators is driven by the presence of the ISS plate *under them* (Figure 4.101) and the presence of the Ex-Port RNC internal components *above them* (Figure 4.102).

The AS sketch of Figure 4.102 presents a number of Fixators for the z-direction translation, but not for x-direction (radial) nor y-direction (toroidal). Their integration is outlined in (Figure 4.103).

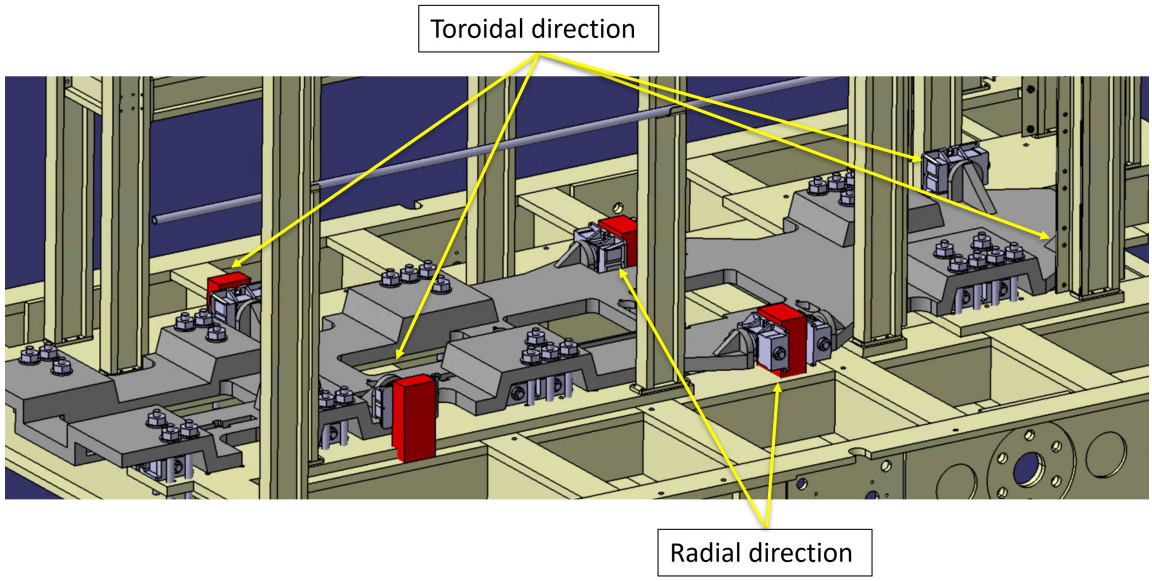

Figure 4.103: Third sketch of the AS integration.

Figure 4.103 also shows the modifications needed for accommodating them and for realizing the fixed supports where to push (in red).

This brings to the same issue on the ISS modification: for the AS integration, the RNC design team cannot rely on any ISS design change.

To definitively solve the problem, a *Counterplate* is thought to be introduced (Figure 4.104). The Counterplate is a 30mm thick S-S plate that is used for uncoupling the interface between Fixators and Base plate from the interface between Base

plate and ISS.

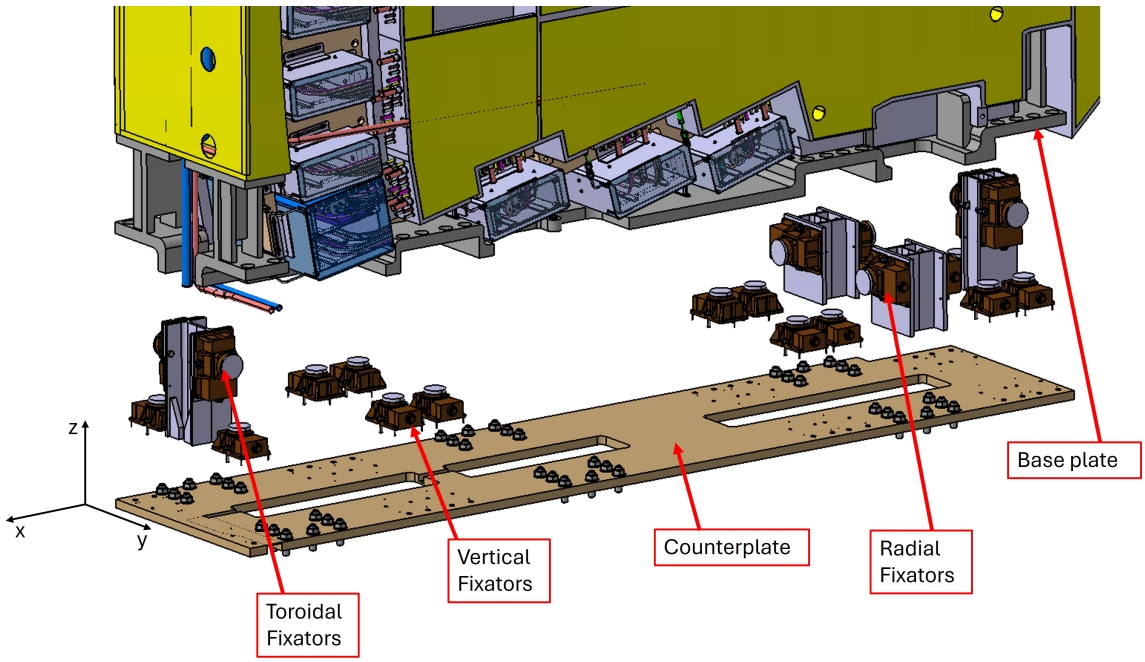

Figure 4.104: Integration of the Counterplate in the AS ([86]).

With the Counterplate use, the Fixators can be opportunely placed while the interface with the ISS is ensured. Figure 4.104 also shows the vertical posts, welded on the Counterplate, that are needed for the assembly of the radial and toroidal Fixators.

Ultimately, the AS is composed of 22 Fixators, divided in:

- 4 RKIII radial Fixators
- 4 RKIII toroidal Fixators
- 14 RKII vertical Fixators

The AS is completed with the Counterplate, the vertical posts and the 28 M22 bolts that connect the Ex-Port RNC to the Counterplate once the Alignment Procedure is completed.

The AS integration is completed. The interfaces with the ISS are respected thanks to the introduction of the Counterplate, with all the elements fit within the EU11 CM.

Updated description of the Alignment Procedure

With the first version of the AS outlined and fully integrated, to correctly assess the AS requirements respect, the Alignment Procedure must be updated by following the brand new AS architecture.

The Alignment Procedure (AP) starts from the definition of misalignment measurements, the type of AP foreseen, the definition of the Ex-Port RNC "zero position" for concluding with the procedure itself.

First measurement: cold measurement (CMT) With the Position Monitoring System working, a first measurement is taken at Room Temperature (RT) conditions – during the Ex-Port RNC commissioning or during a Long Term Maintenance (LTM) period, called "cold" because it refers to the tolerance chain deviations (and not to the thermal expansion ones). The Cold Measurements (CMT) are raw data taken with the PMS sensors. Thanks to the PMS-associated software, the CMT are transformed into CMT'. The CMT' correspond to the location, in the three coordinates of EU11 CS, of the Ex-Port RNC.

First realignment: cold realignment (CRA) Now, a first realignment can be executed at RT conditions, named *cold* because it refers to the tolerance chain deviations. The Cold ReAlignment (CRA) deviations to be corrected with the Fixators are calculated as follows:

$$CRA_{i,j} = NP_{i,j} – CMT'_{i,j} \tag{4.4}$$

where:

- i = ID of the Fixator

- j = x, y, z (the three directions of EU11 CS)
- NP are the Nominal Position (calculated for each direction and each Fixator)
- $CMT'_{i,j}$ are the Cold deviated position (calculated for each direction and each Fixator)

The biggest among $CRA_{i,j}$ values should be found within the range identified by the maximum deviations expected, thus the *Delta_total* row of Table 4.25. The CRA is not sufficient for a complete realignment of the Ex-Port RNC, because it does not consider the effects of the thermal expansion deviations.

Second measurement: the "hot" measurement (HMT) During the time interval between ITER first plasma and the Ex-Port RNC installation, there shall be the possibility of measuring the Vacuum Vessel displacements (with respect to the Port Cell) due to the thermal expansion. While the machine is in NOS conditions, a second measurement is taken thanks to the PMS, called "hot" because it involves the thermal expansion deviations. The Hot Measurement (HMT) states the relative position, along the three coordinates, between the Port Cell and the Port Plug Closure Plate during NOS. Since it is expected that the FEM simulation values are not equal to the real ones measured, a difference (i.e. HMT) is measured. Now, the HMT raw data is elaborated so that one can obtain HMT'. HMT' corresponds to the location, in the EU11 CS, of the Port Cell. The hypothesis is that the Port Cell and, when installed, the Ex-Port RNC do not experience any differential thermal expansion. Under this hypothesis, the HMT' can be used to realign the Ex-Port RNC. The HMT can be taken only when the machine is in NOS conditions. This means that the first time the machine is set in NOS conditions after the installation of the Ex-Port RNC, the Ex-Port RNC will be probably misaligned. However, if there were the possibility of taking the HMT before the Ex-Port RNC installation, such values would be used during the CRA, and the following HRA would be suppressed.

Second realignment: the "hot" realignment (HRA) In the case of absence of HMT values before the Ex-Port RNC commissioning, a second realignment must

be executed. The Hot ReAlignment (HRA) takes place at RT conditions, namely during a Long Term Maintenance period. It is named "hot" because it refers to the thermal expansion deviations. The HRA deviations to be corrected with the alignment tool are calculated as follows:

$$HRA_{i,j} = NP_{i,j} – HMT'_{i,j} \tag{4.5}$$

where:

- i = ID of the Fixator
- j = x, y, z (the three directions of EU11 CS)
- NP are the Nominal Position (calculated for each direction and each Fixator)
- $HMT'_{i,j}$ are the Hot deviated position (calculated for each direction and each Fixator)

Definition of Ex-Port RNC "zero position" For assessing the Alignment procedure, a *zero position* shall be defined. In the Ex-Port RNC case, considering the z-direction as example, to fulfill the 25.6mm travel range, i.e. ±12.8mm, a "zero position" for the alignment shall be identified. To do this, first the Fixator's travel is set to 0mm (Figure 4.105).

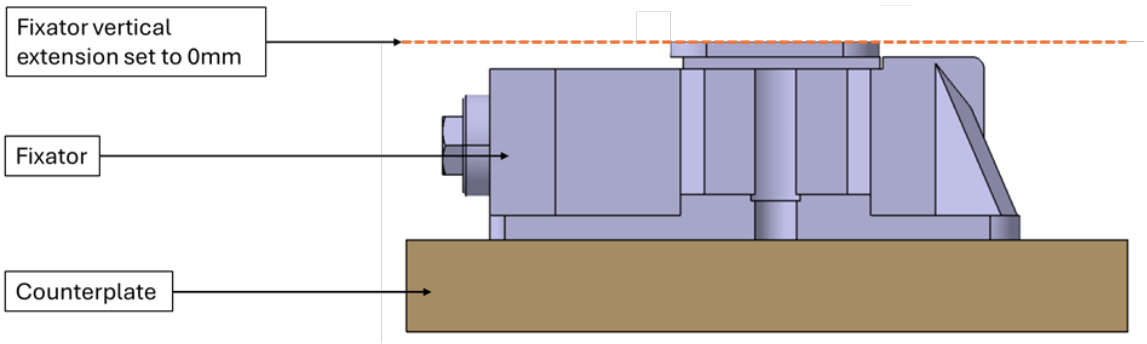

Figure 4.105: Fixator set to 0mm vertical extension ([86]).

Then, a 12.5mm Disk is positioned on the Fixator, and the remaining 0.3mm (12.8-12.5) is covered by the actioning of the Fixator thanks to its adjusting screw. The accuracy of this adjustment can be read in Table 4.27. For the RKII it is 0.25mm per complete rotation of the adjusting screw. For the RKIII, it is 0.3mm. Now, the Ex-Port RNC can be mounted on the Fixator+Disk assembly. Figure 4.106 show the *alignment zero position* (blue line).

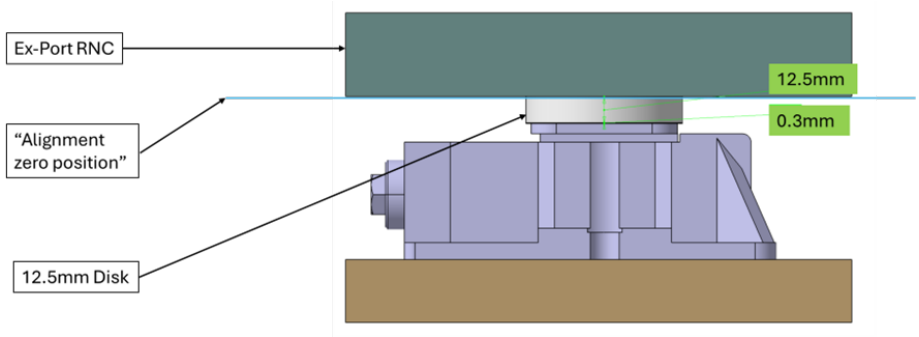

Figure 4.106: Ex-Port RNC mounted on the Fixator+Disk assembly in its *alignment zero position* ([86]).

Figure 4.107 shows the Fixator+Disk assembly in details: the 12.5mm is visible, the yellow strip is the 0.3mm elevation of the Fixator (by the using of the adjusting screw), the dashed red line is at the Fixator's elevation equal to 0mm, and the blue line represents the *alignment zero position*.

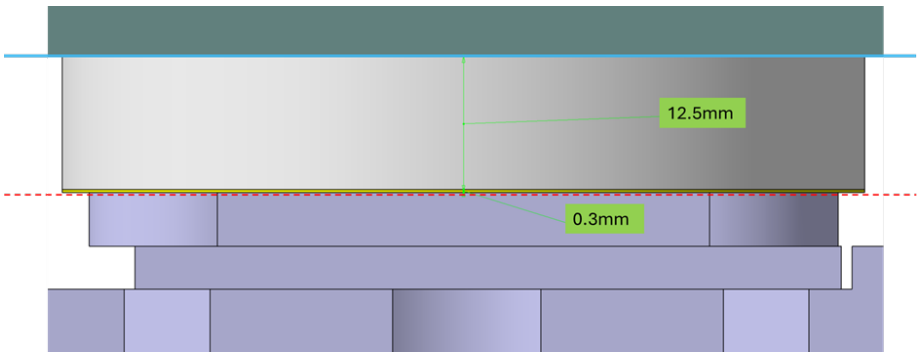

Figure 4.107: Detail of the Fixator+Disk assembly ([86]).

Now, for reaching the two limit configurations, i.e. +12.8mm and -12.8mm with respect to the *alignment zero position*, the Disks must be added or subtracted, respectively. Figure 4.108 shows the +12.8mm configuration, obtained first by substituting the 12.5mm Disk with the 25mm Disk (the height thus reached is +12.5mm with respect to the *alignment zero position*), and then by adjusting the Fixator by elevating it of 0.3mm (the final height of +12.8mm with respect to the *alignment zero position* is obtained). Thus, it is clear that the height of the Ex-Port RNC with respect to the dashed red line (Figure 4.108) is 25.6mm, i.e. 25mm of the Disk plus 0.6mm of the Fixator's adjustment.

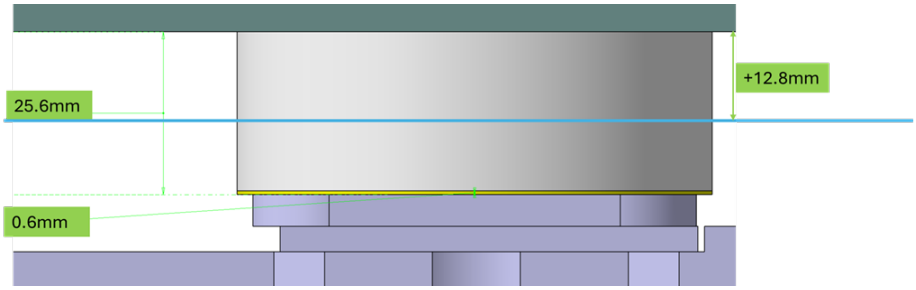

Figure 4.108: Fixator+Disk assembly's +12.8mm configuration ([86]).

Concerning the -12.8mm configuration, the operation is simpler. Starting from the *alignment zero position* (Figure 4.106), one must remove the 12.5mm Disk and adjust the Fixator to lower it by 0.3mm. What is obtained is shown in the initial Figure 4.105. For every intermediate position, the procedure is similar, with the difference that other Disks within the assortment shall be used. One must choose a Disk so that the difference between the Disk's height and the objective height is less than 5mm; which is the travel range of the Fixator so that the final difference can be covered by adjusting the Fixator. To be noted that the choice of the Disk is not unique. For example, to reach the initial *alignment zero position*, a 12.5mm Disk has been chosen, followed by adjusting the screw by 0.3mm. Another solution could have been a 10mm Disk followed by a 2.8mm adjusting.

Execution of the Alignment procedure with Fixators To proceed with the Alignment operation, the following steps need to be followed:

1. Unbolt the M22 connection bolts between Ex-Port RNC and Counterplate, to release the preload (Figure 4.109). Figure 16 shows a detail of 4 bolts, but the total number of bolts is 28 (14 in the RHS and 14 on the LHS). Figure 4.109 shows only the RHS and indicates with the blue arrows the other groups of bolts on the RHS. With the preload released, the Ex-Port RNC dead weight stands on the 14 vertical direction Fixators only.

2. Operate the adjustments one Fixator at a time by adding/subtracting disks and/or screwing/unscrewing the Fixator's adjustment screw.

3. Bolt the connection bolts between Ex-Port RNC and Counterplate.

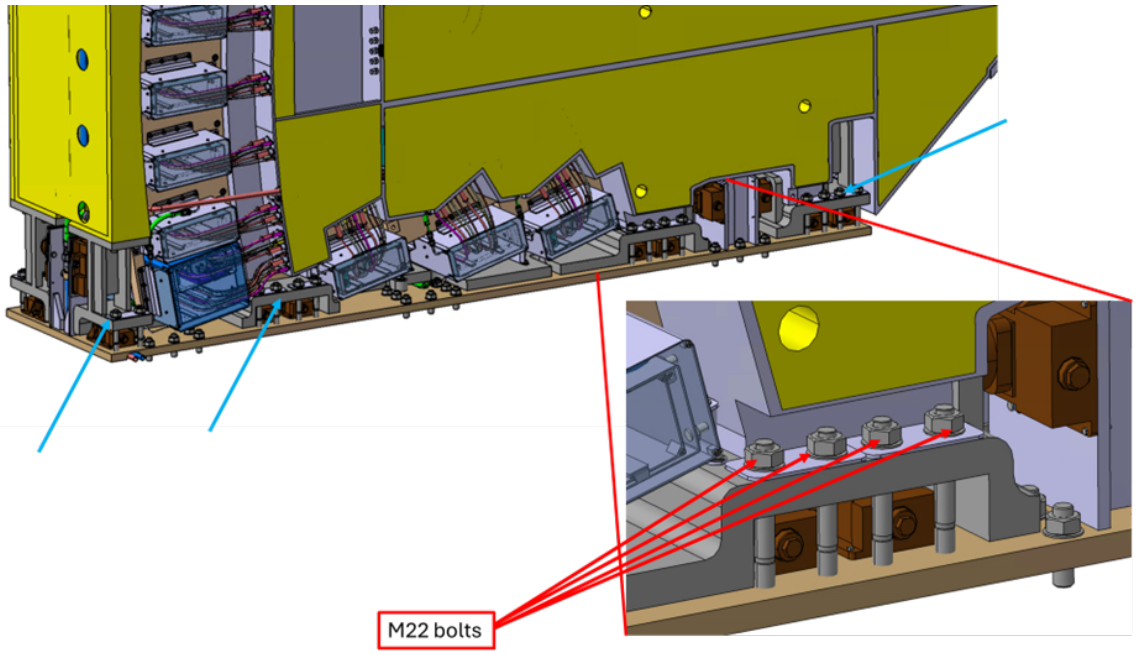

Figure 4.109: Detail of 4 (out of 28) M22 connection bolts between Ex-Port RNC and Counterplate ([86]).

The step no.2 of the procedure is now fully illustrated. The procedure of adding and subtracting Disks is shown in Figure 17. To elevate the Ex-Port RNC from the initial configuration (Figure 4.110 (a)):

- the Fix.2 is adjusted to elevate the Ex-Port RNC by at least 2.5mm (the increment of thickness between two successive Disks in the assortment); now the load is only on the Fix.2 (Figure 4.110 (b)).

- the new Disk 2 (which thickness is bigger than the thickness of Disk 1) is positioned on the Fix.1 (Figure 4.110 (c)).

- Fix.1 is adjusted until it overcomes the height of the Fix.2; now the load is on the Fix.1 (Figure 4.110 (d)).

- Fix.2 is adjusted by decreasing its height (to facilitate the insertion of the new Disk 2) (Figure 4.110 (e)).

- Disk 2 is positioned on the top of Fix.2 (Figure 4.110 (f)).

- Both Fixators are adjusted until they reach the final position (Figure 4.110 (g)).

The procedure shown illustrates how to increase the total height. To decrease the height, a Disk with smaller thickness must be substituted. The procedure is the same. The precision of this operation depends on the fraction of rotation we can apply to the Fixator's adjusting bolt. From Table 3, a complete revolution of the adjusting bolt equals to 0.254mm in height. With a 90° rotation, the elevation becomes one quarter, thus 0.0635mm.

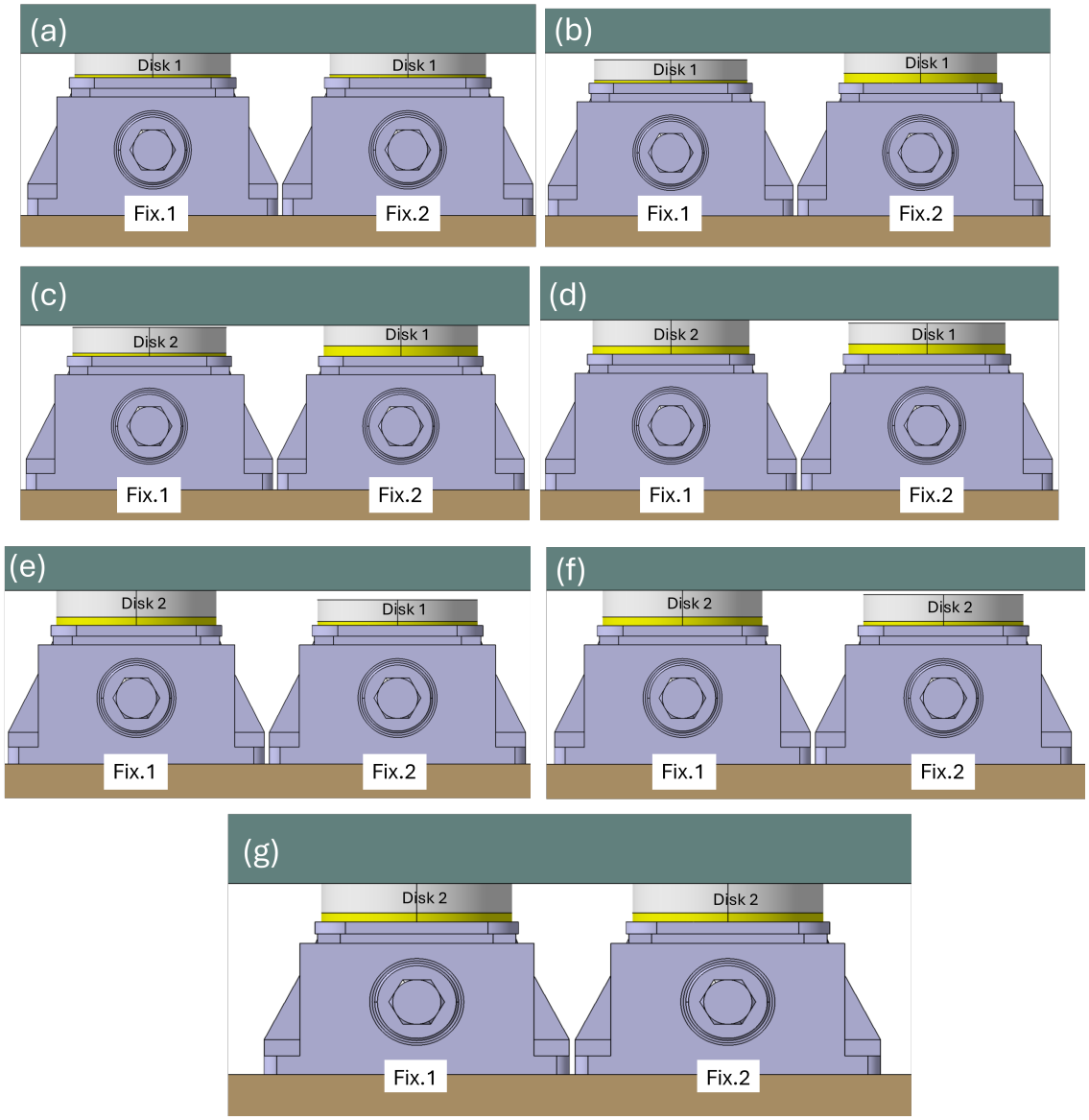

Figure 4.110: Adjusting procedure with Disks: (a) Initial configuration with Disk 1. (b) Fix.2 is adjusted to be elevated of at least 2.5mm. (c) Disk 1 of Fix.1 is substituted with Disk 2. (d) Fix.1 is adjusted until it overcomes the height of Fix.2. (e) Fix.2 is lowered. (f) Disk 2 is positioned on the Fix.2. (g) Both Fixators are adjusted to the final position ([86]).

This procedure is specific for the Fixators with a z-direction translation. For the

Fixators with a x or y directions, the procedure is simpler, since they do not carry any loads. The procedure can be executed without the necessity of the coupling of two Fixators, thus one Fixator at a time can be modified. The procedure is shown in Figure 4.111:

- To adjust the Fix by decreasing the extension of the yellow part.
- To substitute the Disk 1 with Disk 2.
- To adjust the Fix until it reaches the final position.

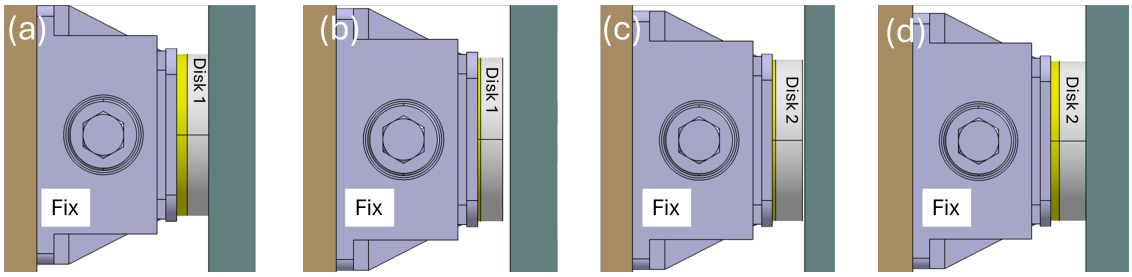

Figure 4.111: x-y direction adjustment procedure: (a) Initial position. (b) Decreasing the extension of Fix. (c) Disk 2 substituted by Disk 2. (d) Fix adjusted to final position ([86]).

The adjustment sequence of the 22 Fixators will be iterative: first you measure the displacement with the PMS, then you adjust, then you measure again. If the displacement is not zero, the adjustment starts again. The sequence will stop when the displacement measured is within the measurement errors. For the adjustment order of the Fixators, there are two possibilities: total quantity adjustment and successive quantity adjustment. The total quantity adjustment foresees that you adjust one Fixator at a time of the total adjustment quantity calculated for that Fixator, from the 1st to the 22nd. The successive quantity adjustment foresees that you adjust one Fixator at a time of a fraction of the total quantity calculated for that Fixator, from the 1st to the 22nd. In this case, you need to operate more *rounds*, depending on the dividing number of the total quantity. The successive quantity adjustment is slower than the total quantity adjustment, but it causes less stresses

to the Ex-Port RNC structure than the total quantity adjustment and it allows you to constantly check the residual displacement measured from the PMS, after every round.

Adjustment tools To screw the adjusting bolt, a torque wrench is needed. The torque to be applied is 3.9Nm/1000kg (Table 4.27, considering the maximum between RKII and RKIII). For calculating the torque needed while adjusting one Fixator, an assumption is made. Considering the Ex-Port RNC's mass of 17000kg, it is safe to assume that, while adjusting less than 13mm of a structure that is 4.5m long, 2.3m high and 1.5m wide, the total mass will not be concentrated on the Fixator being adjusted only. We consider, still in a conservative approach, half of the Ex-Port RNC will be concentrated on the Fixator, at maximum. Thus, for 8500kg, the torque needed to adjust the Fixator is approximately 33.1Nm. This torque can be easily covered by a commercial torque wrench with control of torque and angles, like the one in Figure 4.112.

Figure 4.112: Commercial torque wrench.

The Disks may need to be handled with some tools while positioned on the Fixator. A pincer can be useful, since the mass of the Disks is little. For the thinner Disks, a flat pincer can be used (Figure 4.113, left). For thicker Disks, a circular pincer can be more useful (Figure 4.113, right).

Figure 4.113: Examples of pincers for Disks handling.

Impact Analysis on the Position Monitoring System

The integration of the AS and the modification on the Ex-Port RNC *nose*, that foresaw a shortening in the radial direction, made impossible to only use 7 sensors of the Position Monitoring System (PMS) and to use a push-mode sensor.

Moreover, the introduction of the AS requires a finer reconstruction of the Port Plug Closure plate displacements, for which only 7 sensors are not sufficient. To correctly reconstruct the 6DOF transformation - combination of 3 rotations and 3 translations - a reference plane must be built and then measured. To build a plane, 3 points are necessary, which can be tracked thanks to the use of 3 sensors each (one for each direction).

Thus, a new PMS layout is needed to be integrated.

The new PMS layout is composed of 9 sensors mounted on the Ex-Port RNC nose, grouped in three triplets of 3 sensors (Figure 4.114).

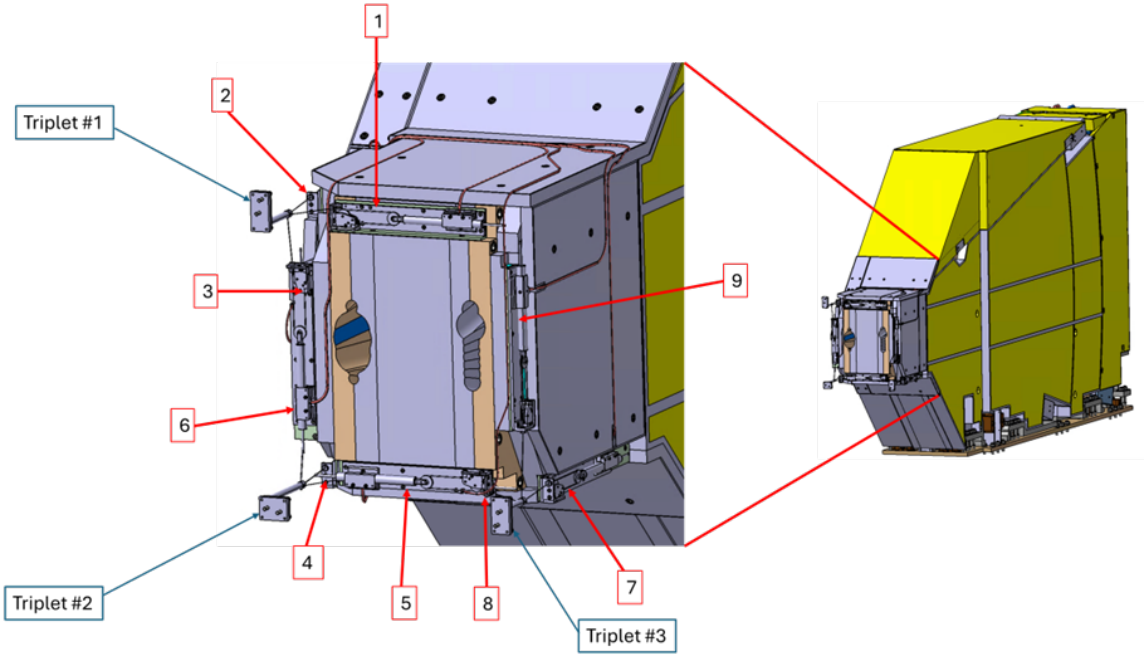

Figure 4.114: New layout of the PMS sensors on the Ex-Port RNC nose ([86]).

The current PMS sensor considered for the Ex-Port RNC is the Fabry Perot displacement sensors produced by Smartec company. To mitigate the problem of the nose reduction, the sensor type chosen for the new layout is the pull-mode, shown in Figure 4.115.

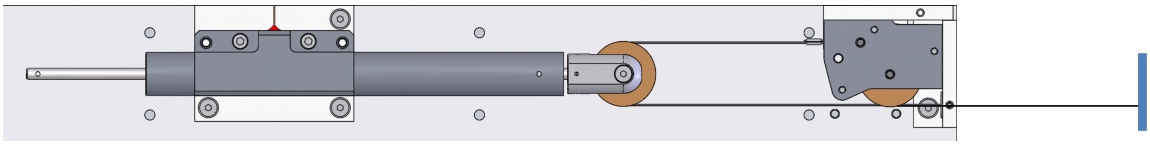

Figure 4.115: Pull-mode Smartec sensor ([86]).

Each sensors triplet is composed by three sensors, one for each direction (Figure 4.116). From each sensor, a wire is connected to a fiducial rod. The fiducial rod is welded to an Intermediate plate, bolted with four M6 bolts to the Interface plate (Figure 4.117). The Interface plate is bolted to the PP closure plate with two M8 bolts, respecting the interfaces.

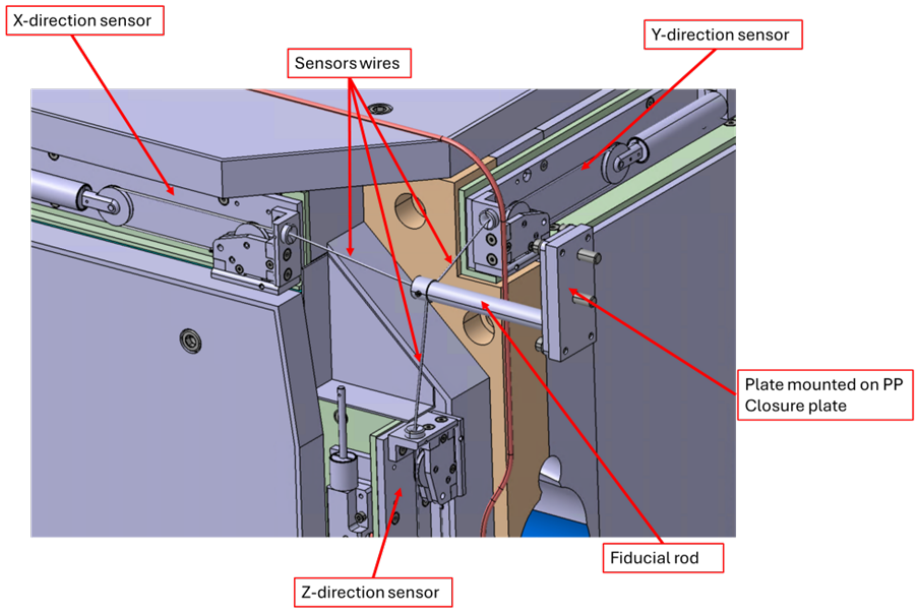

Figure 4.116: Detail of the Triplet#1 - overview ([86]).

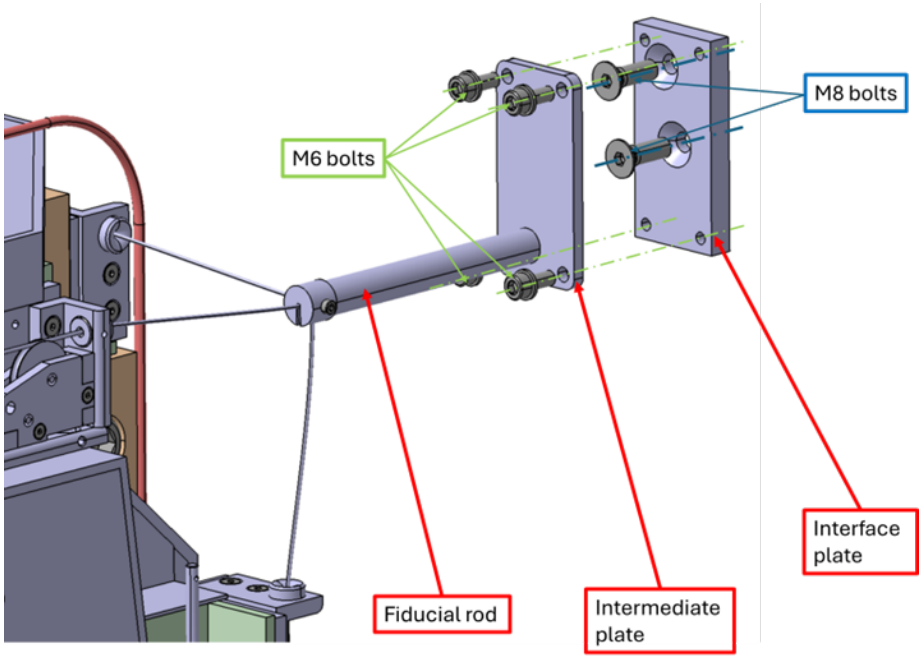

Figure 4.117: Detail of Triplet#1 - attachment system ([86]).

Thus, the PMS is composed by three main parts:

- Moving Part: this part is located on the PP Closure Plate and moves rigidly with the PP Closure plate. This part is made up of the Fiducial rod, the Intermediate plate and the Interface plate.
- Fixed Part: this component is integrated on the Ex-Port RNC. This part is made up of the sensor bodies assembled on the Ex-Port RNC nose.
- Connection element: this part connects the Fixed part to the Moving part. This corresponds to the sensors' wires.

Figure 4.118 shows the assembly Ex-Port RNC + PP, once the PMS is connected.

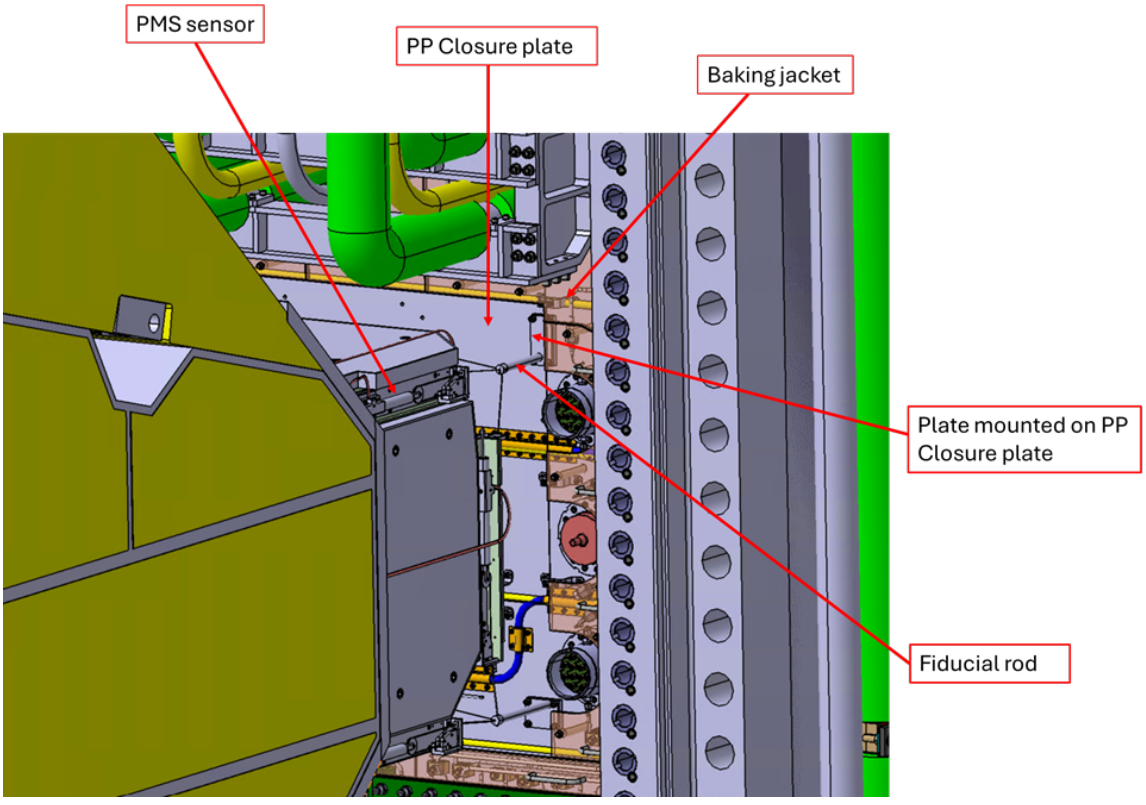

Figure 4.118: Ex-Port RNC PMS assembled to the PP Closure plate ([86]).

Associated with the hardware side, a reconstruction software is needed to elaborate the raw data coming from the PMS. The software shall reconstruct both the translations and the rotations of the Ex-Port RNC relatively to the Port Plug Closure Plate, along the three axes of EU11 CS. Such reconstructed values will be the input data for the alignment tool.

The reconstruction of the displacements is based on the calculation of the coordinates of the three Reference points, one for each sensor Triplet (Figure 4.114). The three Reference points identify a plane and a centroid. The initial position of the PP Closure plate determines an initial plane and an initial centroid. After the movement of the PP Closure plate, a final plane and a final centroid can be determined. The differences between the initial and final centroids and initial and final planes determines the translations and the rotations.

The coordinates of the reference points are determined by building a tetrahedron for each triplet of sensors. In Figure 4.119, the Triplet#1 is taken as example.

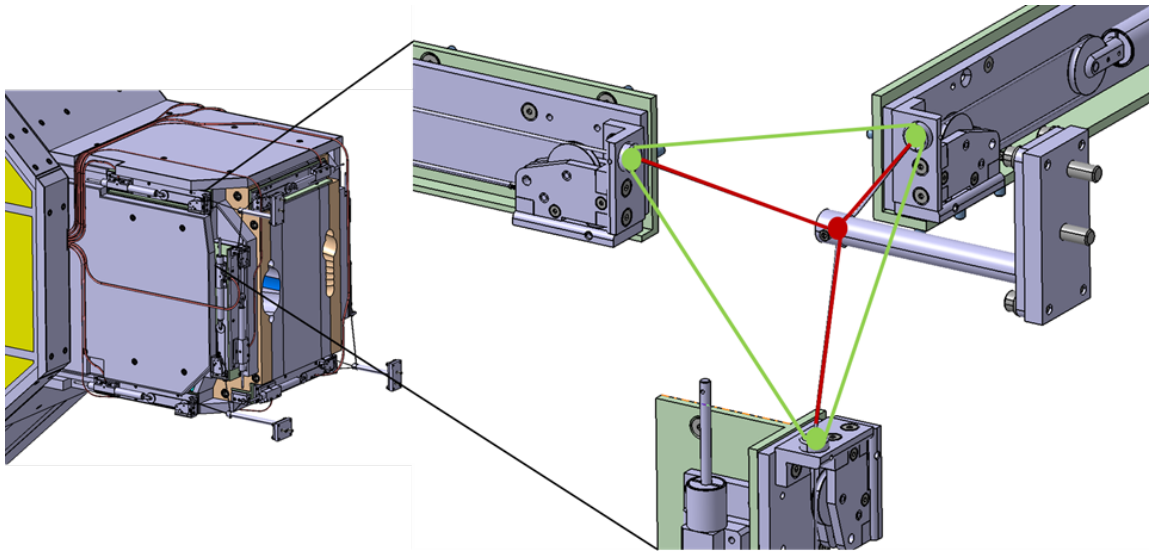

Figure 4.119: Tetrahedron for the reconstruction of the Reference point position in its initial position ([86]).

The vertices of each tetrahedron are the *inlet* points on the three sensors (green

spots in Figure 4.119) and the reference point. The inlet points identify where the wire enters the sensor's body. They belong to the sensors and are fixed in space since the sensors are fixed to the shielding block. The reference point identifies the tip of the Fiducial rod where the three wires meet (red spot in Figure 4.119) and is free to move since the rod is fixed to the closure plate. To determine the coordinates of the Reference point, the algorithm uses the information of the tetrahedron edges. The three green edges (Figure 4.119), connecting one fixed point to another, have fixed lengths. The red edges, however, changes their length as the Reference moves. In Figure 4.119, the Triplet#1 is in its initial position. This means that we know the coordinates of the Reference point, thus the lengths of the red edges. When the Reference point get farther from the Ex-Port RNC, for example, it pulls the sensor's wire, and the sensor reads a displacement (Figure 4.120).

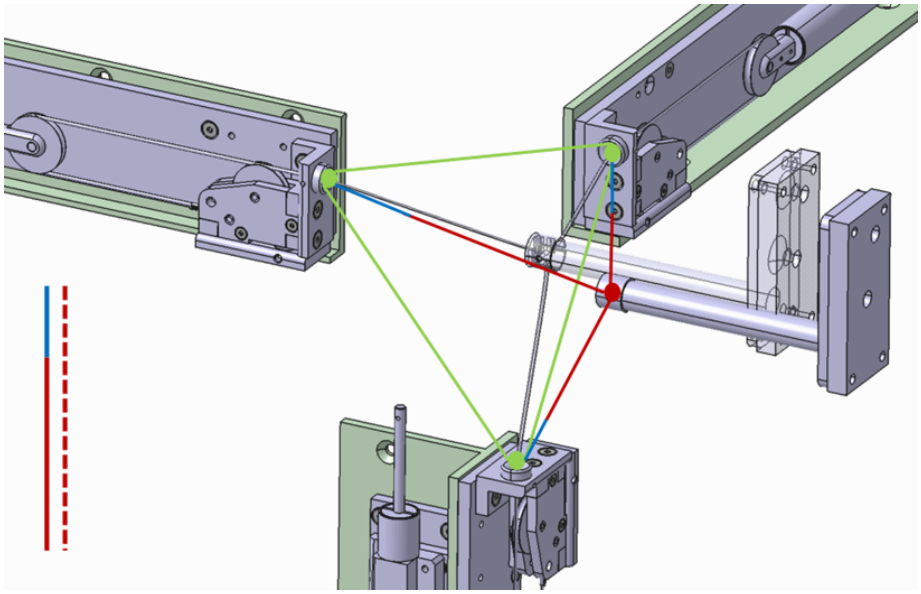

Figure 4.120: Final position of the Reference point after PP Closure plate movement ([86]).

Thus, the new length of the red edges (now dotted in Figure 4.120) can be calculated as the sum of the initial length (continue red lines in Figure 4.120) and the displacement read by the sensor (blue line in Figure 4.120).

4.4.6 Phase 5 — Tolerance & Interface Budgeting: Precision Allocation

Tolerance and Error Budget Allocation

This phase built directly upon the initial tolerance chain analysis that triggered the LAISE process. With the Alignment System now conceptualized, a detailed dimensional analysis is performed. This analysis aims to ensure the physical compatibility, manufacturability, and performance of the AS within specified tolerances.

Specifically, this analysis aims to verify if the integrated AS affects negatively the Tolerance Chain Analysis results, i.e. if the uncertainties related to the AS are found inside or outside the Tolerance Chain results.

The comparison term is set equal to the worst accuracy of the Position Monitoring System sensor. The accuracy of a single PMS sensor is 0.5 mm at variable temperature; 0.1 mm accuracy is achievable if a measurement of temperature is available. Thus, let us consider 0.5mm as limit.

Accuracy of the Fixators The accuracy of the Fixator is 0.25mm per revolution of the screw for the RKII type and 0.3mm for the RKIII type (Table 4.27), thus minor than the 0.5mm limit. Moreover, with the adjusting tools, it is possible to manipulate the adjusting screw less than one revolution, namely half revolution or one quarter. In this way, the accuracy increases to 0.125mm or 0.0625mm for RKII and 0.15mm or 0.075mm for RKIII.

Uncertainty associated to the PMS reconstruction algorithm The first element to be considered is the Position Monitoring System. The PMS is the system that provides the inputs to the Alignment System by measuring the displacements between the Ex-Port RNC and the Port Plug Closure Plate. The maximum of these displacements should be found within the range indicated by the Delta_total row of Table 4.25.

As stated, the accuracy of a single PMS sensor is 0.5 mm at variable temperature; 0.1 mm accuracy is achievable if a measurement of temperature is available. A thermocouple is associated to each sensor to improve the displacement measurements, but a conservative accuracy of 0.5 mm has been considered in the following.

As mentioned, during the alignment procedure the 22 fixators are adjusted acting on the screws until all PMS sensors are in their reference *zero position*. This is possible since the 0.25 mm (RKII) or 0.3mm (RKIII) adjustments per revolution of the fixators screw are smaller than the 0.5 mm accuracy of the PMS sensors and the movement of the screws is continuous. Therefore, the final uncertainty in the position of the RNC shielding block depends only on the overall measurement error of the PMS determined by the ± 0.5 mm accuracy of the single sensors.

An integrated algorithm has been developed to calculate the overall measurement error of the PMS. The algorithm evaluates the RNC shielding block displacements (translations and rotations) that are not detectable by the PMS since they are within the accuracy of the single PMS sensor (± 0.5 mm).

The algorithm is based on the following steps:

1. The RNC shielding block and the closure plate are perfectly aligned, and the reference position of the centroid is determined.

2. A displacement equal to ± 0.5 mm is added to the measurement of each sensor considering all possible combinations ($2^9 = 512$).

3. For each combination the translation of the centroid with respect to its reference position and the rotation with respect to the mid-point between the two focuses of the Ex-port RNC collimators are determined.

4. Average and standard deviation values of the 512 displacements/rotations are evaluated.

The trilateration-based reconstruction algorithm has been presented in the previous sections. The algorithm is python-based, and considers the lengths of the 9 sensor wires that are difficult to replicate with a python code. Thus, a digital twin has been realized with CATIA V5 in order to support the evaluation.

The PMS digital twin (PMS DT) is a schematic representation of the connection between the Ex-Port RNC and the Port Plug Closure plate (Figure 4.121).

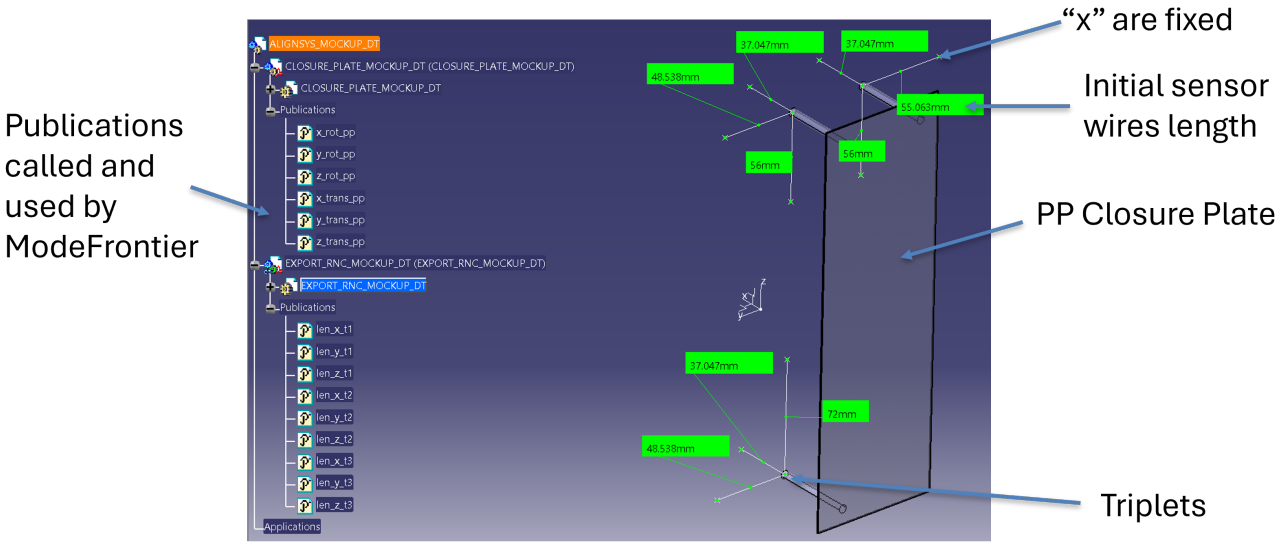

Figure 4.121: PMS digital twin realized in CATIA V5.

From Figure 4.121, the x-points are fixed in the space, and represent the exiting points of the wires from the PMS sensors. The fiducial rods are then visible, and the 9 wires (3 for each triplet) are drawn as segments with their relative lengths. The PMS DT has the possibility of choosing the translations and rotations quantities of the Port Plug - i.e. to impose a displacement. These quantities, along with the lengths of the sensor wires, are published in order to be used externally from CATIA, namely called by a ModeFrontier workflow. ModeFrontier is an integration platform for multidisciplinary and multiobjective optimization. For this work, we use the capability of integrate different software in a logic workflow (Figure 4.122).

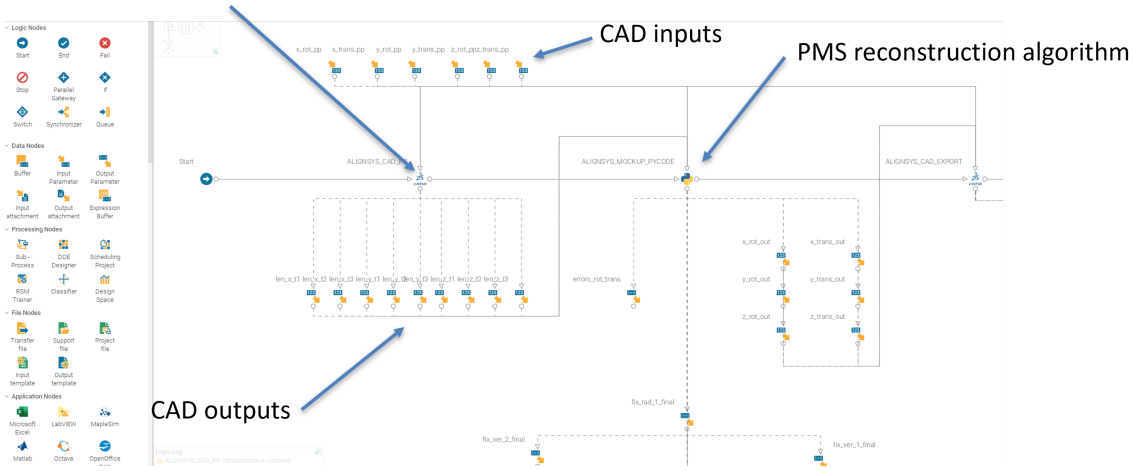

Figure 4.122: PMS DT workflow in ModeFrontier.

Figure 4.122 shows the ModeFrontier workflow for the PMS DT and the different nodes. The most important nodes are CATIA V5 node, where there is the CAD model of the PMS DT, and the python node, where there is the reconstruction code.

Now, to compute the 512 combinations, a simple Design Of Experiments is imposed. Thanks to this, ModeFrontier automatically computes all the combinations and calculates the errors associated.

The average values of the rotations/translations evaluated with the procedure described above are equal to zero within numerical errors. The PMS measurement error is associated to the standard deviations of the distributions which are summarized in Table 4.28.

Table 4.28: PMS measurement uncertainty.

	Radial	**Toroidal**	**Vertical**
Translation standard deviation (mm)	0.3	0.3	0.3
Rotation standard deviation (°)	0.04	0.04	0.04

These errors can be found within the accuracy of the single PMS sensor, ± 0.5 mm. Thus, the PMS reconstruction code can be accepted.

Uncertainties on the internal alignment The introduction of the AS, Fixators and Counterplate, raised an internal alignment issue, during first assembly. Since the *zero position* is fundamental for the correct functioning of the AS, a procedure must be foreseen for the correct assembly of the Ex-Port RNC on the Counterplate (with the Fixators already mounted).

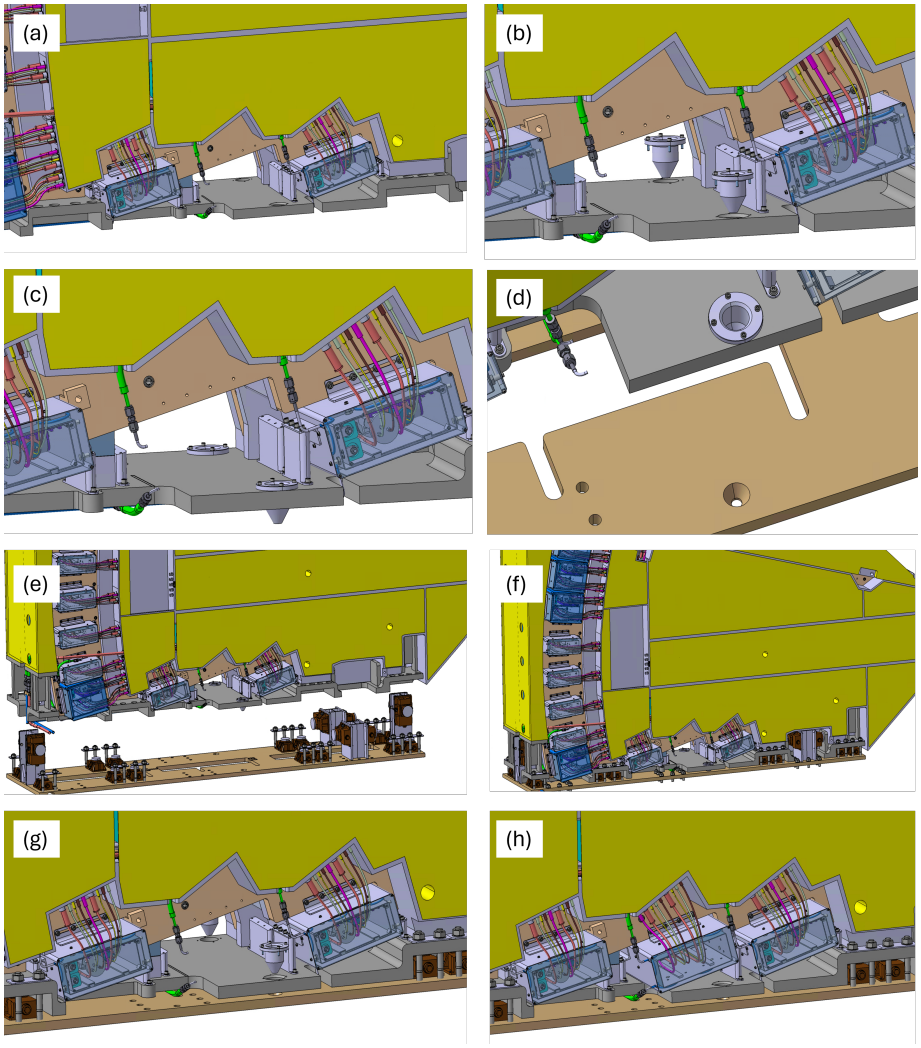

Figure 4.123: Centering procedure of the Ex-Port RNC block on the AS ([80]).

The Ex-Port RNC presents two holes on the Baseplate in the zone of the De-

tector Cassette #11, not yet assembled (Figure 4.123 - a). In these two holes, two customized centering cones are inserted from the top (Figure 4.123 - b) and bolted to the Baseplate thanks to four M6 bolts each (Figure 4.123 - c). The Ex-Port Shielding block can be lifted and positioned on the top of the Counterplate where two conical holes are located for the matching (Figure 4.123 – d and Figure 4.123 - e). The Ex-Port Shielding block can be lowered until the centering cones match the Counterplate conical holes and, at the same time, the Ex-Port Shielding block leans on the AS vertical Fixators (Figure 4.123 - f). Finally, the centering cones can be unbolted and removed (Figure 4.123 – g) and the Detector Cassette #11 assembled (Figure 4.123 - h).

Interface Control Established

The Ex-Port RNC CAD model modification due to the integration of the AS has been carried out by considering the external and internal interfaces. It is fundamental, however, to check all the interfaces and to consider also surrounding ITER systems.

EU11 Configuration Model The integration of the AS has been executed considering the volumes available constantly checked with the EU11 CM CAD model (Figure 4.28) and its dimensions (Figure 4.29). Moreover, at the end of the integration process, a *Clash Analysis* has been conducted by using a CATIA V5 dedicated tool. The analysis reported that no clash is occurring between the AS CAD model and the EU11 CM, meaning that the AS is not intersecting the EU11 CM.

PMS update The PMS update has been realized by strictly following the matrix holes on the Port Plug Closure plate (Figure 4.37) and the shape and volumes of the Ex-Port RNC in the nose zone (Figure 4.29) while creating the interface plate for the fiducial rods (Figure 4.117 and Figure 4.118).

ISS interface The respect of the ISS interface (Figure 4.31 and Figure 4.32) is inherently verified with the introduction of the Counterplate.

TSS interface The Temperature Stabilization System is rigidly connected to the external piping scheme through two areas (Figure 4.36 and **??**). The top area is used for the connection of the inlet and outlet manifolds for the normal operation. The bottom area is used for connecting the drainage pipes. The pipes outside the Ex-Port RNC are fixed to the concrete structure of the Port Interspace.

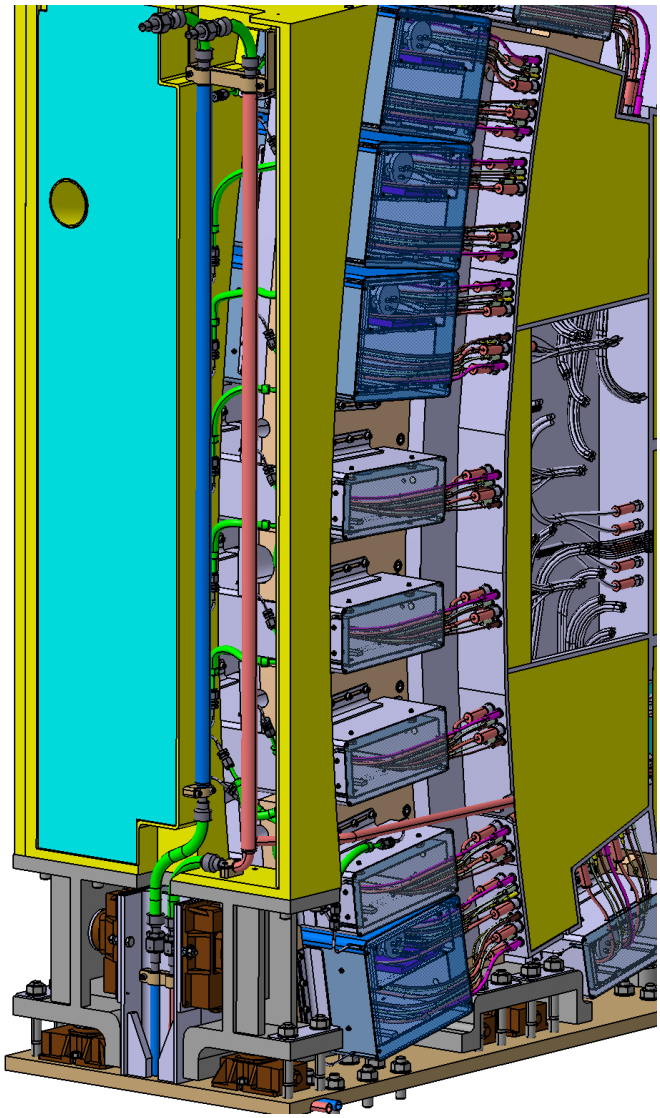

Figure 4.124: Overview on the new Temperature Stabilization System manifolds layout ([80]).

Having introduced the AS, a relative movement is foreseen during the Alignment Procedure. This cannot be accepted, in terms of structural behavior, by the pipes connections. In fact, if the connection is rigid, the AS movement would induce a relatively high stress concentration on the connection points.

To mitigate this problem, the use of sections of flexible pipes is proposed. The manifolds are divided into two sections, one attached to the Ex-Port RNC movable block (thus movable as well) and one attached to the Counterplate (thus fixed). The connection between the two sections is obtained by the use of flexible pipes (green in Figure 4.124), as the connections of the top part of the manifolds to the external piping scheme.

Details on the connections of the top connection area and bottom connection area are visible in Figure 4.125 and Figure 4.126 respectively.

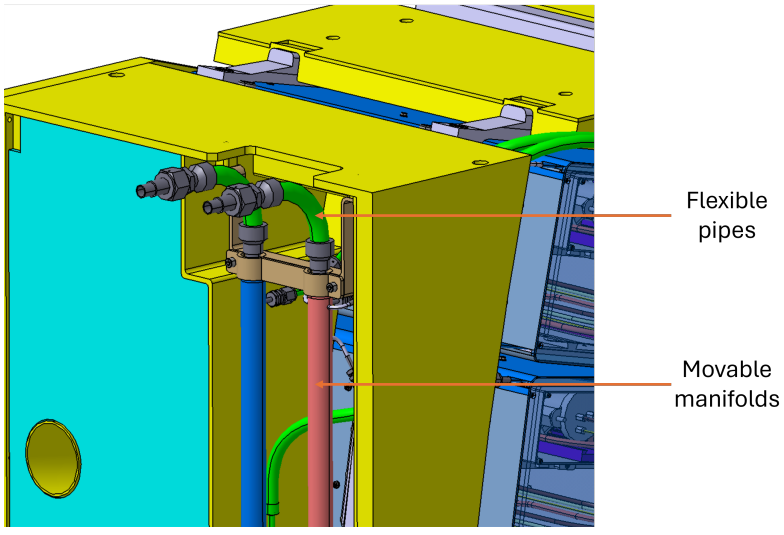

Figure 4.125: Details on the new manifolds layout on the top connection area ([80]).

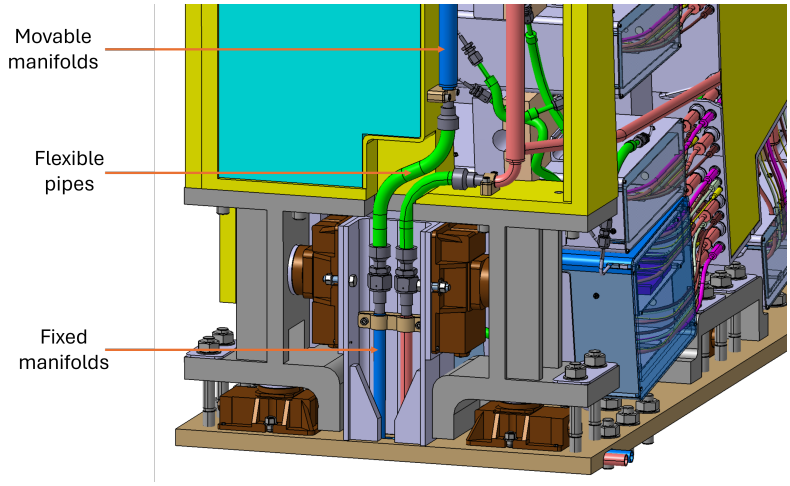

Figure 4.126: Details on the new manifolds layout on the bottom connection area ([80]).

The connections between manifolds and flexible pipes are realized with threaded Swagelock components, easily connectable.

Access to the AS The last aspect to be considered is crucial for the correct use of the AS: its accessibility.

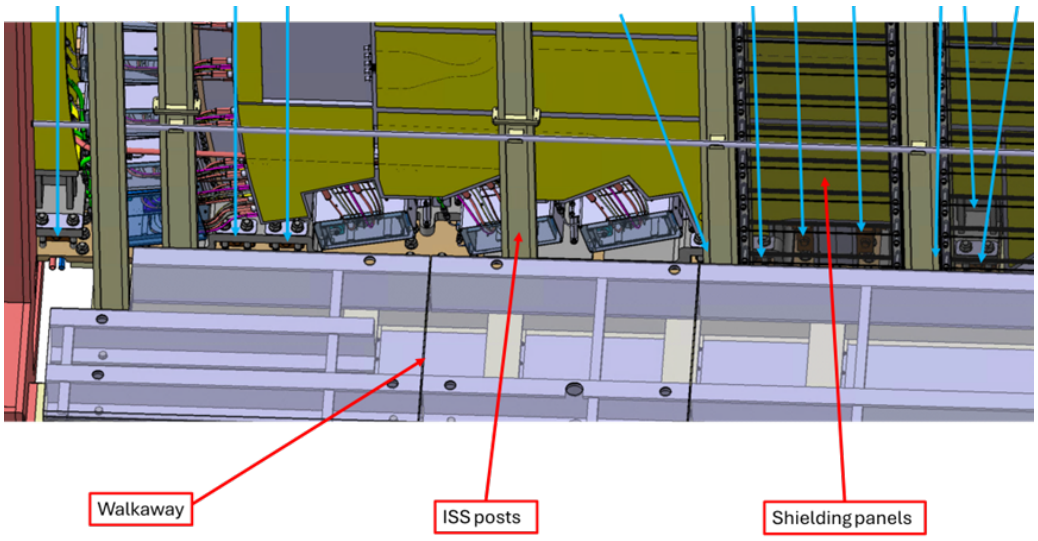

Figure 4.127: Access to Fixators on the RHS ([80]).

The access to the Fixators from the walkaway to execute the adjustment operations has to face two main obstacles: the ISS (on the RHS and the LHS) and the Motion Stark Effect (MSE) diagnostic (only on the LHS). The Fixators layout has been designed taking into account these constraints. Concerning the RHS, the access to the Fixators (indicated by blue arrows in Figure 4.127) is impeded by the ISS posts, the shielding panels and the walkaway.

For each obstacle, a solution or a combination of solutions shall be found. The shielding panels can be removed for the duration of the procedure and then put back in place once completed. For the posts, the same actions can be adopted: removing the posts, completing the alignment procedure, repositioning the posts. To complete the operation, the walkaway must be removed. To do this, the walkaway panels will be either removed completely or thanks to a trapdoor system.

Concerning the LHS, the access to the Fixators (indicated by blue arrows in Figure 4.128) is also impeded by the ISS posts, the shielding panels and the walkaway. Similar solutions as for the RHS can be adopted to bypass these obstacles.

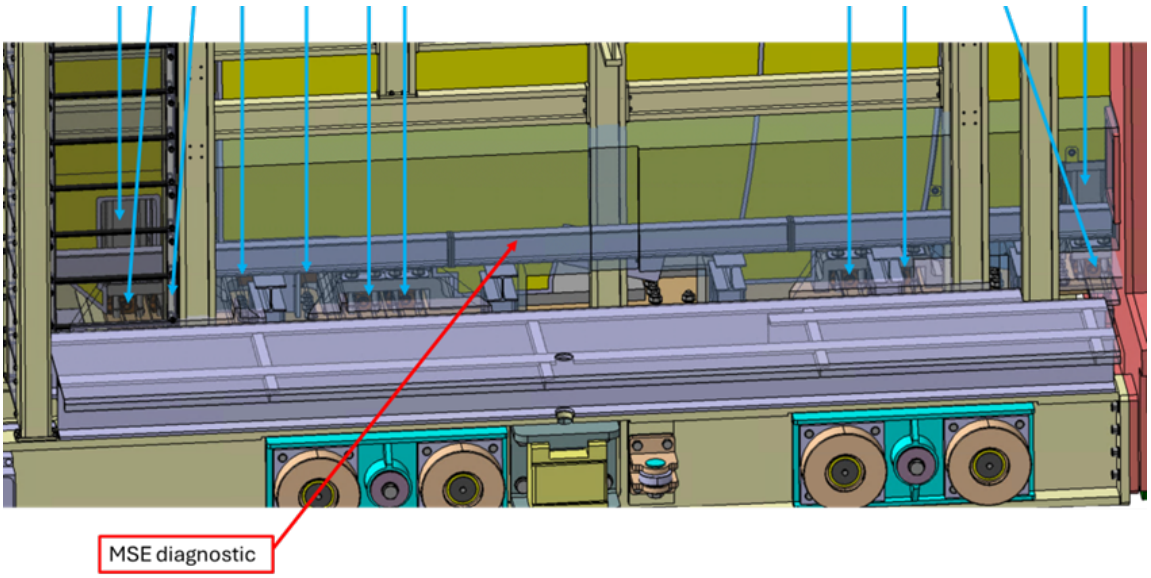

Figure 4.128: Access to Fixators on the LHS ([80]).

The presence of the MSE diagnostic must taken into account while implementing the CAD model of the AS. As the current design, the access to the adjusting screw of the toroidal Fixators is blocked by the presence of the MSE diagnostic. The solution has been found with the toroidal Fixators mounted vertically with the adjusting screw *on the bottom* (Figure 4.129), in accordance with the MSE team as this solution does not interfere with the MSE diagnostic.

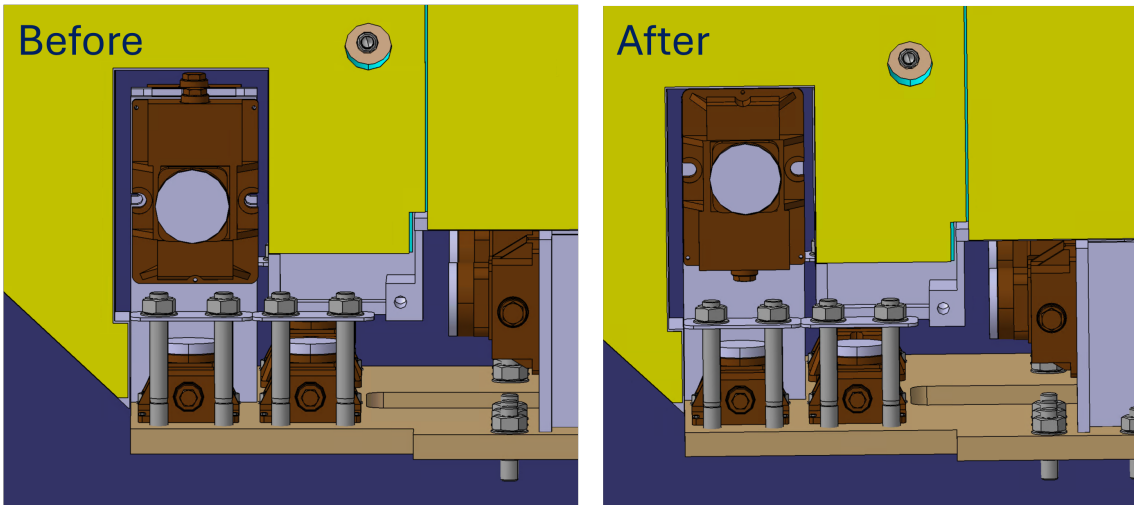

Figure 4.129: Modification on the toroidal Fixators: rotation due to the MSE diagnostic presence.

The rotation of the toroidal Fixators caused a further Ex-Port RNC CAD modification that does not affect any of the previous modifications and checks.

4.4.7 Phase 6 — Targeted V&V: Ensuring Functionality

The Verification and Validation phase is a crucial phase in several Systems Engineering based design approaches and tools. The LAISE foresees a V&V as well, that testifies that the subsystem newly introduced does not affect any of the existent requirements and satisfies the new.

Ex-Port RNC mass increase

After having modified the Ex-Port RNC with the integration of the AS, a mass increase is expected mainly due to the presence of the Counterplate, a 30mm thick Stainless Steel plate.

With the measuring tool of CATIA V5, the new mass is evaluated as 16940kg, close to the limit of 17000 but still below.

Thus, the modifications can be accepted.

Ex-Port RNC loads on AS and bolt assessment

To verify the choice of the M22 bolts that connect the Ex-Port RNC to the Counterplate, an assessment is conducted.

Bolts preload and Fixators resistance during NOS The bolts preloads have been calculated based on the worst conditions that the RNC shall face i.e., SL-2. This is due to the fact that, although the RNC shall not be assessed against Cat. IV events such as SL-2, it cannot become a missile for neighboring SIC systems, and therefore the supporting system shall not fail under these conditions. The SL-2 accelerations applied are the ZPA ones, i.e.:

- X direction: $9.125 m/s^2$
- Y direction: $10.875 m/s^2$
- Z direction: $16.625 m/s^2$

The acceleration in the vertical direction shall be combined with gravity in the worst case. This means that the calculations shall be performed with a net upward acceleration result of the SL-2 one minus 1g, i.e., $6.815 m/s^2$. This is because the upward acceleration reduces the adhesion between the baseplate and the fixators and consequently reduces the friction forces counterbalancing the seismic horizontal accelerations. Since the mass of the RNC is 17 tons, the forces due to SL-2 are:

- $F_{horizontal}(SL-2) = 17 \cdot (9.1252 + 10.8752) \cdot 0.5 = 241 kN$

- $F_{vertical}(SL-2) = 17 \cdot 6.815 = 116kN$

Therefore, the friction force to counterbalance the SL-2 horizontal force shall be at least 241 kN. In order to achieve this force, and considering a friction coefficient of 0.3, the global vertical force shall be at least:
$F_{vertical(global)} = -241/0.3 = -803kN$
(the negative signs highlights that the force is directed in the -Z direction)

The total preload force shall, at the same time, provide the needed vertical force and counterbalance the SL-2 vertical upward force:
$F_{preload} = -803kN$–$116kN = -919kN$

Now, the Fixators datasheet (Table 4.27) shows that the maximum allowable lifting weight per Fixator is 12020kg, or 118kN in forces terms. The total vertical force transmitted to the fixators in NOS conditions can be calculated as the total preload force + the weight of the Ex-Port RNC:
$F_{vertical}(NOS) = -919kN$–$17 \cdot 9.81 = -1086kN$

Dividing this force by the number fixators used in the z-direction (14) we can calculate the actual deadweight + preload force received by each fixator:
$F_{vertical} = 1086kN/14 = 78kN$

Only the 14 z-direction Fixators have been considered because it is supposed that the 8 remaining Fixators are only used during the alignment procedure, and are unloaded during NOS. Fvertical (78 kN) is smaller than 118 kN, the maximum allowable lifting weight per Fixator RKII. Thus, the RKII Fixator is suitable for this task.

Fixators resistance during the Alignment Procedure Along with NOS conditions, the Fixators resistance need to be verified also during the alignment procedure. In this case, all the bolts connecting the Ex-Port RNC to the Counterplate will be unloaded, thus only the Ex-Port RNC dead weight is acting on the 14 Fixators. We can calculate:

$FDW = -17000 \cdot 9.81N = -167kN$

It is safe stating that, during the adjustment procedure with the Fixators, even though one Fixator at a time is lifted, it is not lifting the total Ex-Port RNC DW. This is due to the small adjustment range foreseen with respect to the total radial dimension of the diagnostics (13mm against 4500mm). In this sense, a deformation is expected so that the Ex-Port RNC base preserves its contacts with the other 13 Fixators. In a conservative approach, we can consider that each Fixator will lift half of the DW, i.e. -83.5kN, which is smaller than 118kN, the maximum allowable lifting weight per Fixator. To guarantee the contact, we suggest operating the adjustment procedure (fully explained in the next paragraph) in an iterative way. For example, if the adjustment to be covered is of 5mm, instead of adjusting each Fixator of 5mm once, it is preferable to adjust each Fixator of 1mm five times (i.e. five adjustment *rounds* of 1mm). Concerning the other two groups of 4 Fixators each (toroidal and radial direction), each Fixator must overcome the friction force between the Ex-Port RNC baseplate and the Counterplate, due to the DW only (again, during alignment procedure, bolts are unloaded). This force can be calculated as follows:
$F_{friction} = 0.74 \cdot 17000 \cdot 9.81N = 123kN$
Since the maximum allowable lifting weight per Fixator RKII is 118kN, this type is not usable, even if compact in volumes. Thus, for these 8 Fixators, the correct choice is RKIII (Table 4.27), with a maximum allowable lifting weight per Fixator RKIII equal to 24267kg, or 238kN in forces terms.

These calculations validated the choice of the Fixators types for the radial, toroidal and vertical direction uses.

AS effects on the static ferromagnetic forces

The introduction of the Fixators establishes the introduction of different kinds of elements with different materials. The issue has been raised for the presence of cast iron in the Fixator's body. It is important to estimate the ferromagnetic forces acting

on the magnetic components on the Fixators as the consequence of the interaction between the static magnetic field at equilibrium and the objects under analysis with magnetic properties.

For the scope of this analysis, only three Fixators are considered, the ones closest to the plasma. Since they are subjected to the highest file, the force acting on them are estimated to be the highest of all the Fixators.

The magnetic flux density field considered in this analysis is estimated by considering the reference 17 MA plasma scenario.

The Fixators are then simplified as boxes and meshed to be used for calculations in the CARIDDI software, where the exact location of the Fixators with the magnetic flux density field are used for calculating the resulting ferromagnetic forces.

The results of the three force components (radial, toroidal, and vertical) related to the ferromagnetic loads acting on the three Fixators considered are (only the maximum for each direction is reported):

- $F_{x,max} = -576.82N$
- $F_{y,max} = 168.04N$
- $F_{z,max} = 228.89N$

The results demonstrates that the presence of the Fixators is negligible in terms of static ferromagnetic forces, if these results are compared with the calculation results on the bolts preload ($-1086kN$ in the vertical direction).

AS and AP V&V: AS mock-up realization and test

The introduction of the AS, based on the use of 22 Fixators, has caused different integration issues. The insertion of the AS elements has been conducted, and the CAD integration process has resulted successful.

The Alignment Procedure has been outlined carefully, and the functioning of a single Fixator is well-known. At the same time, the reconstruction code has been validated thanks to the PMS Digital Twin.

However, a validation of the AS as a whole is still missing and needed for the completion of the LAISE application. To fulfill this scope, a physical mock-up is needed and has been established to be designed and used for the AS V&V. Thus, the scopes of the V&V phase of the AS are to assess if:

- the reconstruction code, considering real wire-based sensors, is capable to reconstruct the displacements with the designed accuracy of $\varepsilon = 0.1mm$
- it is possible to operate the Fixators in a combined use to obtain the realignment in a coordinated way
- it is possible to adjust the Fixators with the designed tools and in a sufficient ergonomic ease
- the realignment is possible to be reached by respecting the accuracy and in a limited operational time

Once the AS mock-up scopes are assessed, the AS mock-up design and test plan can be outlined:

1. Assessment of the test plan
2. Design of the AS mock-up, with the support of CATIA V5
3. Procurement of plates, Fixators, 6DOF stage, sensors and DAQ
4. Assembly of the supplied components
5. Realization of the AP software
6. Execution of the tests
7. Results and conclusions

Assessment of the test plan The AS mock-up shall be designed in order to evaluate both the PMS reconstruction code and the feasibility of the Alignment Procedure. Thus, the AS mock-up shall be divided into two functional subsystems:

- PMS dummy: to evaluate the PMS reconstruction code, a Ex-Port RNC nose dummy and a Port Plug Closure plate dummy are foreseen. The PMS should be composed of 9 wire-based sensors; not necessarily the Fabry Perot optical fiber sensor of the Ex-Port RNC, but with the same accuracy. These sensors are attached opportunely to the Ex-Port RNC nose dummy.

- Fixators: the Ex-Port RNC nose dummy should be assembled on a Ex-Port RNC base plate dummy, located on the Fixators that are fixed on a Counter-plate dummy. The Fixators shall be the same of the Ex-Port RNC.

The Alignment Procedure starts from the imposition of a known translations and rotations set to the Port Plug Closure plate dummy, with a system to be evaluated. As the imposed transformation is known, the reconstruction code can be easily validated. The displacement of the Port Plug Closure plate dummy causes the modifications of the PMS wires. This activates the data acquisition and the reconstruction code. The outcomes of the codes indicate the operator the adjustment quantity for each Fixator. After the adjustment, a new PMS acquisition is launched. The process is iterated until the Alignment is reached, i.e. the realignment error is under the PMS accuracy.

The test plan is schematized in Figure 4.130.

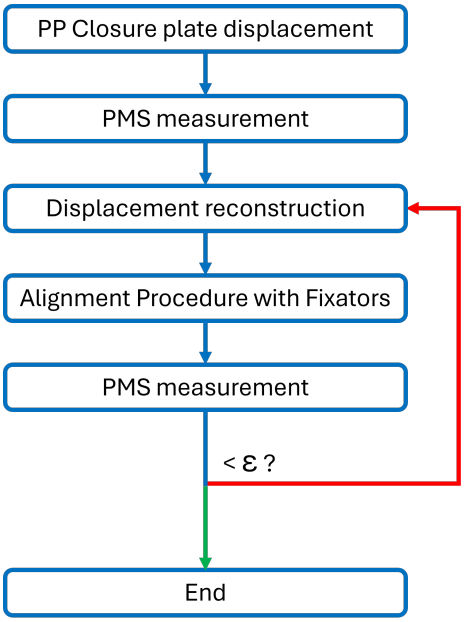

Figure 4.130: Schematic workflow of the AS & AP test plan.

Design of the AS mock-up Considering the requirements outlined, a CATIA V5 model has been realized, shown in Figure 4.131.

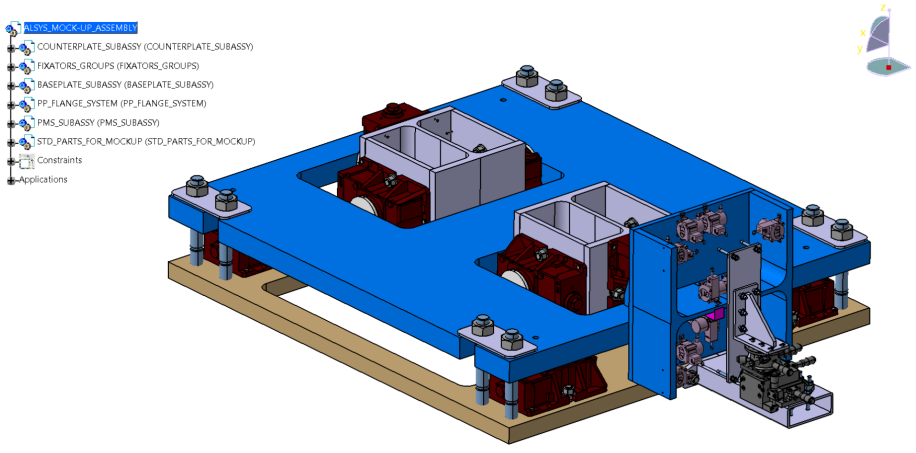

Figure 4.131: Overview of the CATIA V5 model of the AS mock-up.

The main dimensions are reported in Figure 4.132.

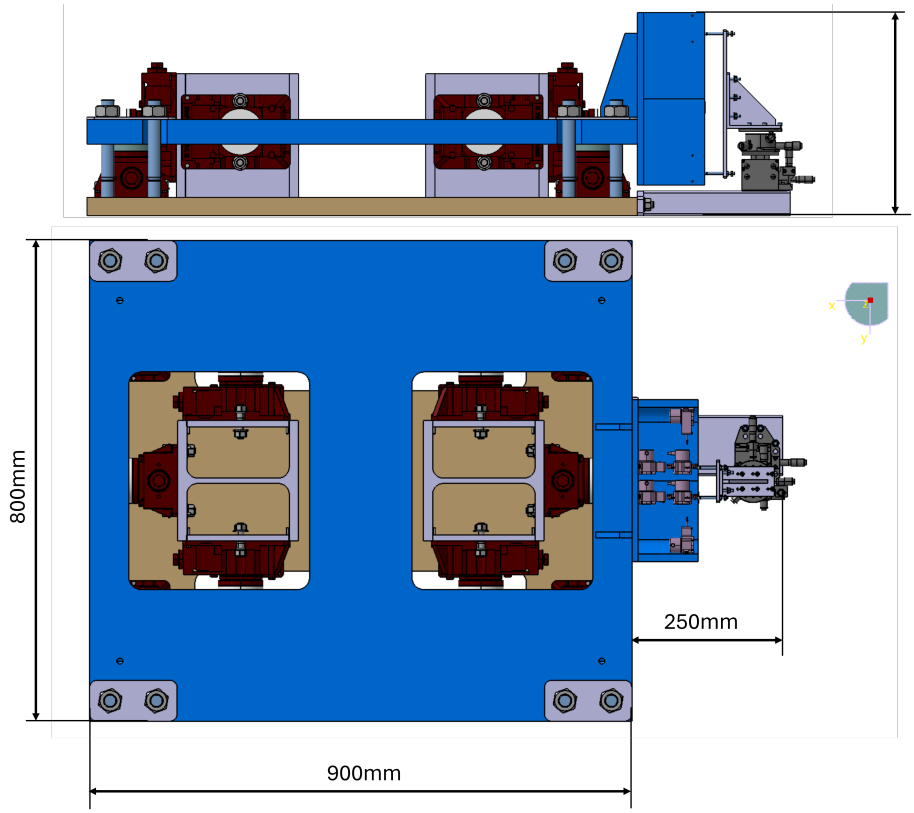

Figure 4.132: AS mock-up main dimensions.

The AS mock-up features (Figure 4.133 and Figure 4.134):

- 40mm thick SS Base plate, same thickness as Ex-Port RNC
- 30mm thick SS Counterplate, same thickness as Ex-Port RNC
- 2 radial Fixators RKII, same as Ex-Port RNC
- 4 toroidal Fixators RKII, same as Ex-Port RNC
- 4 vertical Fixators RKII, same as Ex-Port RNC
- Set of Disks for the Fixators, same as Ex-Port RNC
- 8 M22 bolts, same as Ex-Port RNC

- 9 microEpsilon wire-based sensors
- 6DOF multiaxes stage
- 3 fiducial rods

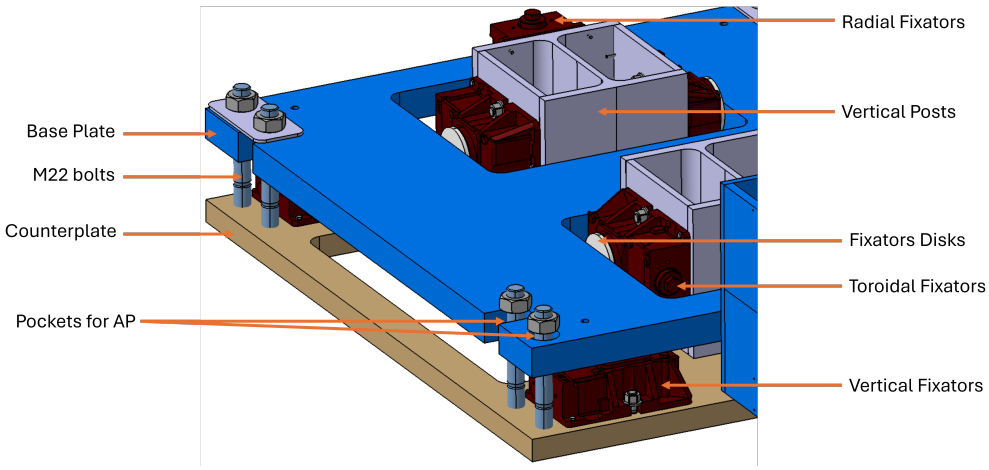

Figure 4.133: AS mock-up details of the Ex-Port RNC dummy.

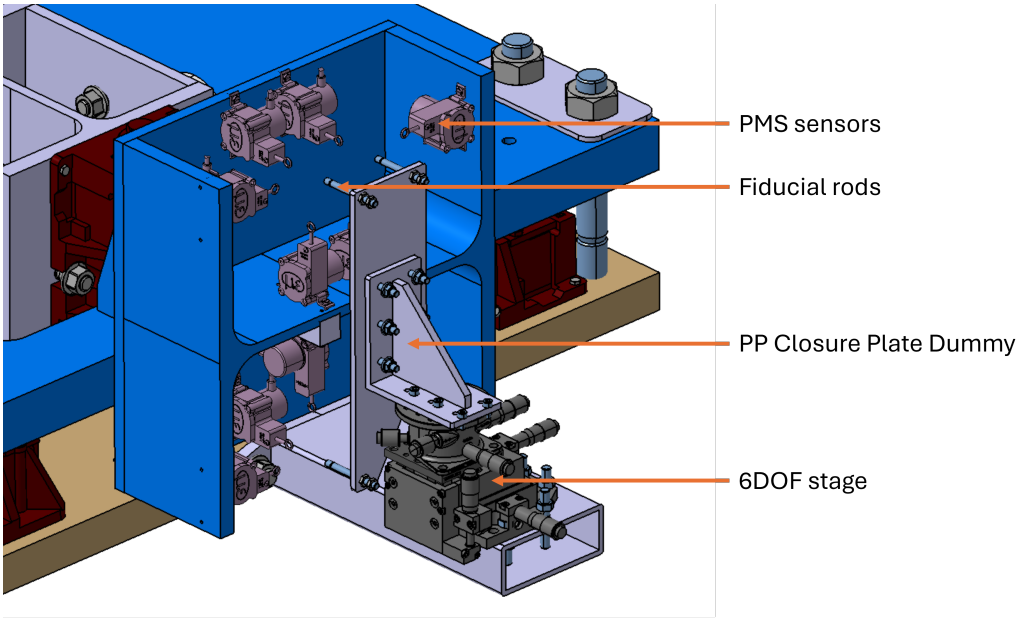

Figure 4.134: AS mock-up details of the PMS and Port Plug Closure plate dummy.

The overall dimensions (Figure 4.132) are smaller than the Ex-Port RNC real ones. However, the distance between the Base plate and the Counterplate, regulated by the Fixator and the Disk, is the same.

As for the Ex-Port RNC, the design of the AS mock-up is based on the *zero position*, obtained by using the Disks.

Procurement of plates, Fixators, 6DOF stage, sensors and DAQ Having completed the design, the procurement of the components has started. The correct choice of the commercial components such as the sensors, the 6DOF stage and the Fixators, however, had already been established during the CAD design, in order to integrate them opportunely and model the SS plates consequently.

The components procurement involved:

- **Plates** Concluded the 3D modelling of the two plates, Base plate and Counterplate, the detailed drawings have been realized. The technical documentation was sent to the manufacturer. The chosen material is S355 for its supply ease and the relaxed requirements on the structural behavior of the plates.

  The supplied plates are shown in Figure 4.135.

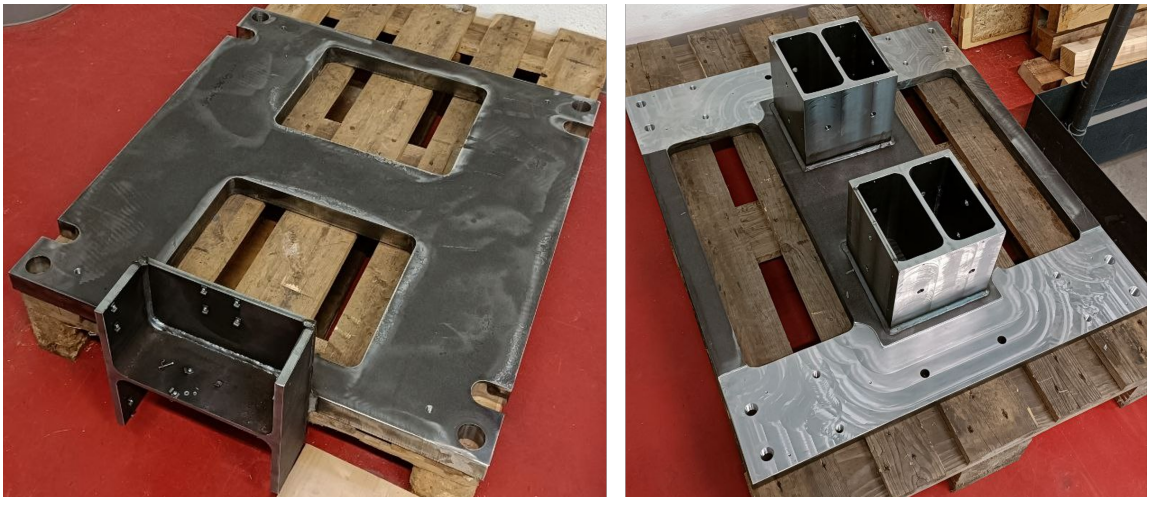

Figure 4.135: Base plate (left) and Counterplate (right) as supplied by manufacturer.

As visible from Figure 4.135, some areas of the Counterplate are more shining: this is due to a surface refinement in the zones where the imposed tolerance was stricter. These zones, in fact, are the location assembly of the Fixators, where the planarity tolerance is fundamental for carrying the Base plate horizontal.

The handling of the plates has been a tough task, as the Base plate weights 168kg and the Counterplate 155kg.

- **Fixators** The Fixators selection has been lead by the already chosen Fixators for the Ex-Port RNC. A total of 12 RKII Fixators have been supplied, along with 8 sets of 2mm, 4mm and 6mm Disks. In Figure 4.136, a RKII Fixator with its Disks is shown.

Figure 4.136: RKII Fixator with its set of Disks.

- **6DOF stage** The selection of the 6DOF stage was lead by the requirements of having the possibility of imposing 3 translations and 3 rotations with an accuracy not minor than the PMS accuracy of $\varepsilon = 0.1$. The final choice is a combination of two Thorlabs 3DOF stage (Figure 4.137), one for the three

translations (R13M) and one for the three rotations (TTR001M), actioned by micrometer screws.

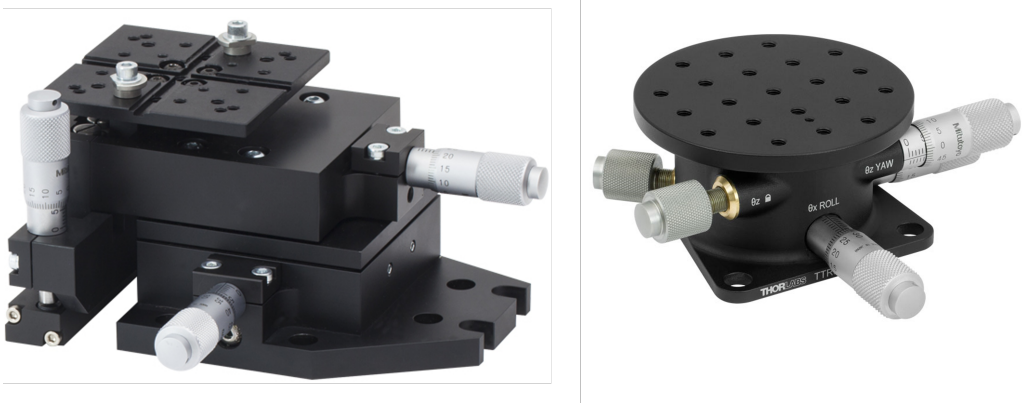

Figure 4.137: R13M translation 3DOF stage (left) and TTR001M rotation 3DOF stage (right).

The assembly of the 6DOF stage is realized by mounting the TTR001M on the top of R13M, as indicated by the manufacturer.

The technical data of the stages are reported in Table 4.29. As shown in Table 4.29, the 6DOF stage choice respects the requirements.

Table 4.29: Technical data of RB13M and TTR001M stages.

	RB13M
Travel Mechanism	Crossed-Roller Bearings
Deck Height (Nominal)	62.5 mm (2.46”)
Optical Axis Height (Nominal)	75 mm (2.95”)
Load Capacity (Max)	4.4 kg (9.7 lbs)
Straightness	$\pm 10\ \mu m$
Travel Range	13 mm (1/2”)
Resolution	5.0 μm

Table 4.29 continued from previous page

	RB13M
Coarse Adjustment	500 μm/rev

	TTR001M
Tip/Tilt (Pitch and Roll) Adjustment Range	±5°
Tip/Tilt (Pitch and Roll) Micrometer Resolution	0.036°
Rotation (Yaw) Adjustment Range	±10°
Rotation (Yaw) Micrometer Resolution	0.03°
Deck Height	1.48” (37.5 mm)
Deck Height with TTR001SP1(/M) Mounting Plate	2.46” (62.5 mm)
Load Capacitya,b (Max)	11.0 lbs (5.0 kg)
Construction	Aluminum

- **Sensors** The choice of the sensors for the PMS dummy is driven by the accuracy of the Fabry Perot optical fiber sensor ($\varepsilon = 0.1$) and the *wire-based* characteristic. The selected sensor is the MicroEpsilo WPS-150-MK30 (Figure 4.138). The main technical data are reported in Table 4.30.

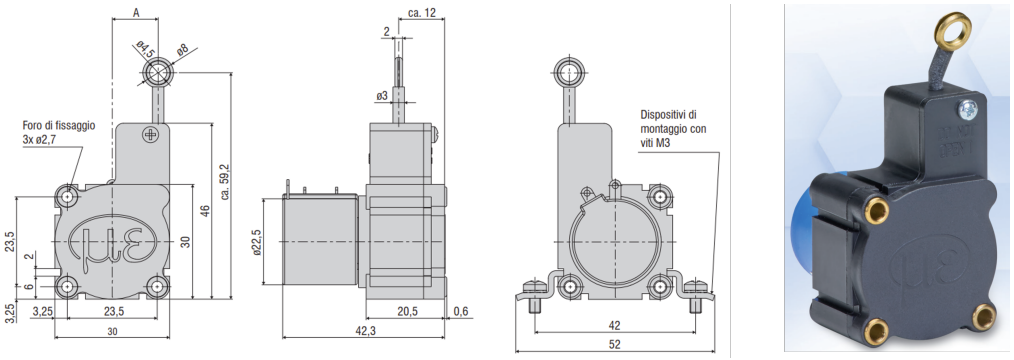

Figure 4.138: Wire-based sensor WPS-150-MK30.

Table 4.30: Technical data of WPS-150-MK30.

	WPS-150-MK30
Measuring range	50mm
Resolution	towards infinity
Potentiometer	$\leq \pm 0.25$ % FSO
Linearity	$\leq \pm 0.375mm$
Sensor element	Hybrid potentiometer
Wire extension force (max.)	2.5N
Wire retraction force (min.)	1N
Wire acceleration (max.)	5g
Material	Plastic and Polyamide-coated stainless steel ($\phi 0.36mm$)
Temperature range	-20°C/+80°C
Weight	45g

- **DAQ** Having 9 sensors, the DAQ should have at least 9 channels. The chosen sensor is potentiometer-based, so it needs to be powered and has an analog output. The choice of the Data Acquisition System should be driven by this two requirements. The final choice is the DEWESoft IOLITE-16xLV, a 16-channel CH-GND isolated IOLITE distributable module for Low Voltage (Figure 4.139).

Figure 4.139: DEWESoft IOLITE-16xLV.

Associated with the hardware, the DEWESoft software is also provided.

With all the components correctly supplied, the assembly of the AS mock-up can start.

Assembly of the supplied components The assembly of the AS mock-up has been realized at the Laboratory of Mechanics of University of Trieste. The AS mock-up is assembled as to respect the *zero alignment* configuration. The result is shown in Figure 4.140.

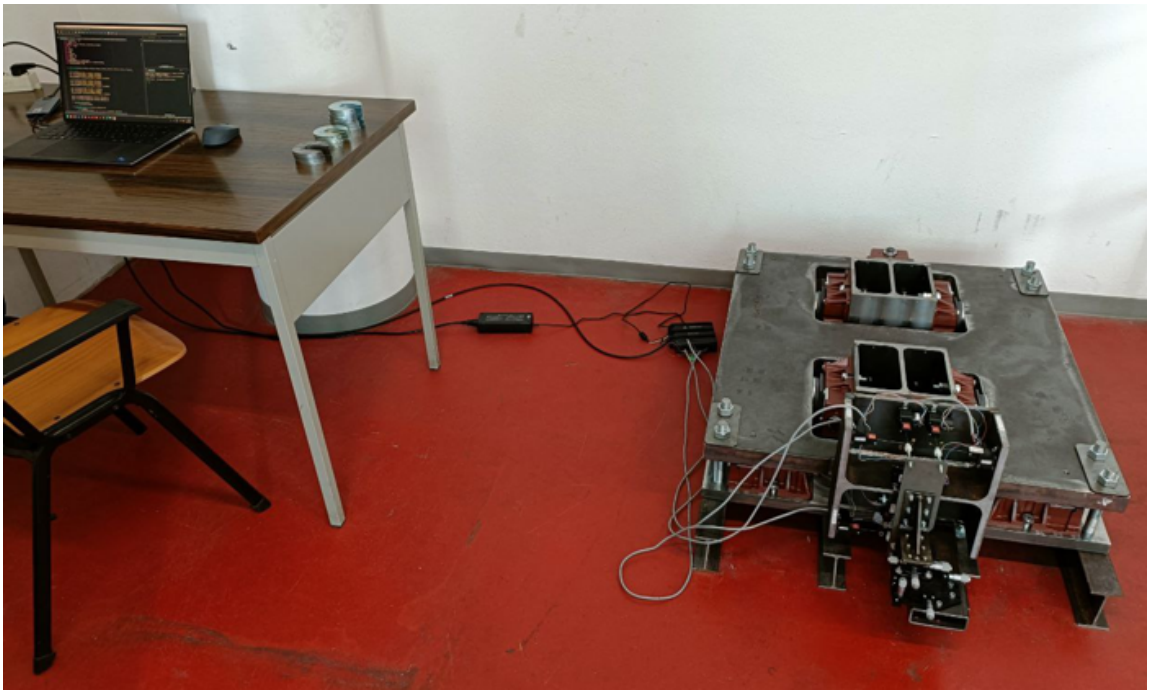

Figure 4.140: AS mock-up assembled.

Figure 4.141 shows the details of the vertical Fixators. The Base plate and the Counterplate are interleaved by the vertical Fixators on the top of which the Disk is placed. The M22 bolts complete the assembly between the two plates. From the left figure, the particular of the Pockets for AP is shown. Their function is to allow enough clearance between the M22 bolt and the Base plate during the AP. Their

dimensioning followed the maximum alignment foreseen due to the results of the Tolerance Chain Analysis (Table 4.25), in particular along the x and y directions. The worst is the 12.7mm of the x-direction. Thus, a clearance dimensioned as a circular crown of 13mm thickness is set. The *U-shaped* clearance of the left bolt is due to the possibility of extracting the bolt during the AP for facilitating the accessibility to the Disk replacement.

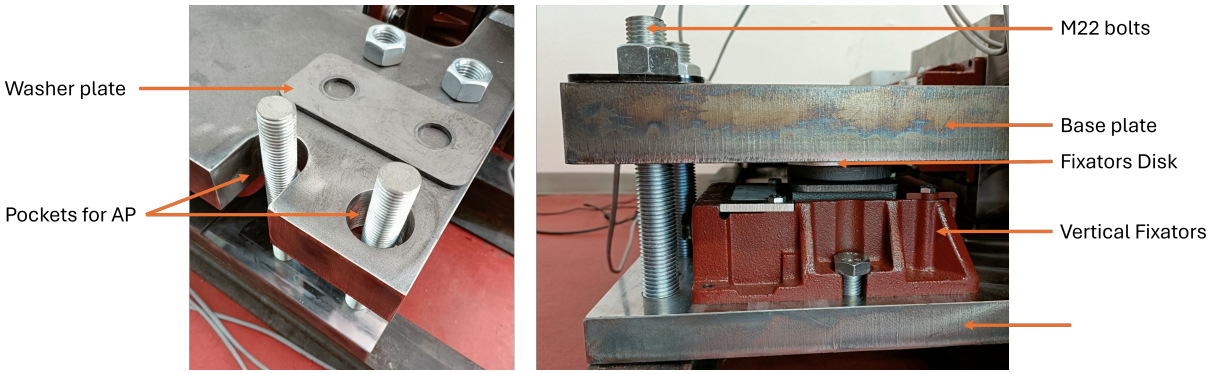

Figure 4.141: AS mock-up details on vertical Fixators.

Figure 4.142 shows the details of the radial and toroidal Fixators.

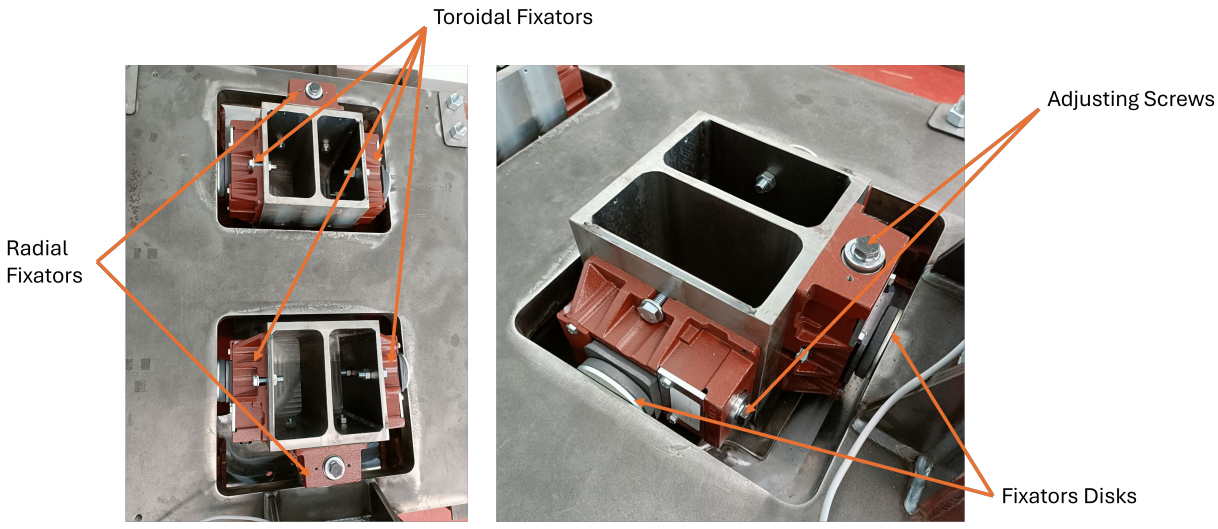

Figure 4.142: AS mock-up details on radial and toroidal Fixators.

The Port Plug Closure plate dummy is realized as a simple L-shaped clamp bolted on the 6DOF stage (Figure 4.143). Figure 4.143 shows the 9 sensors grouped into three triplets.

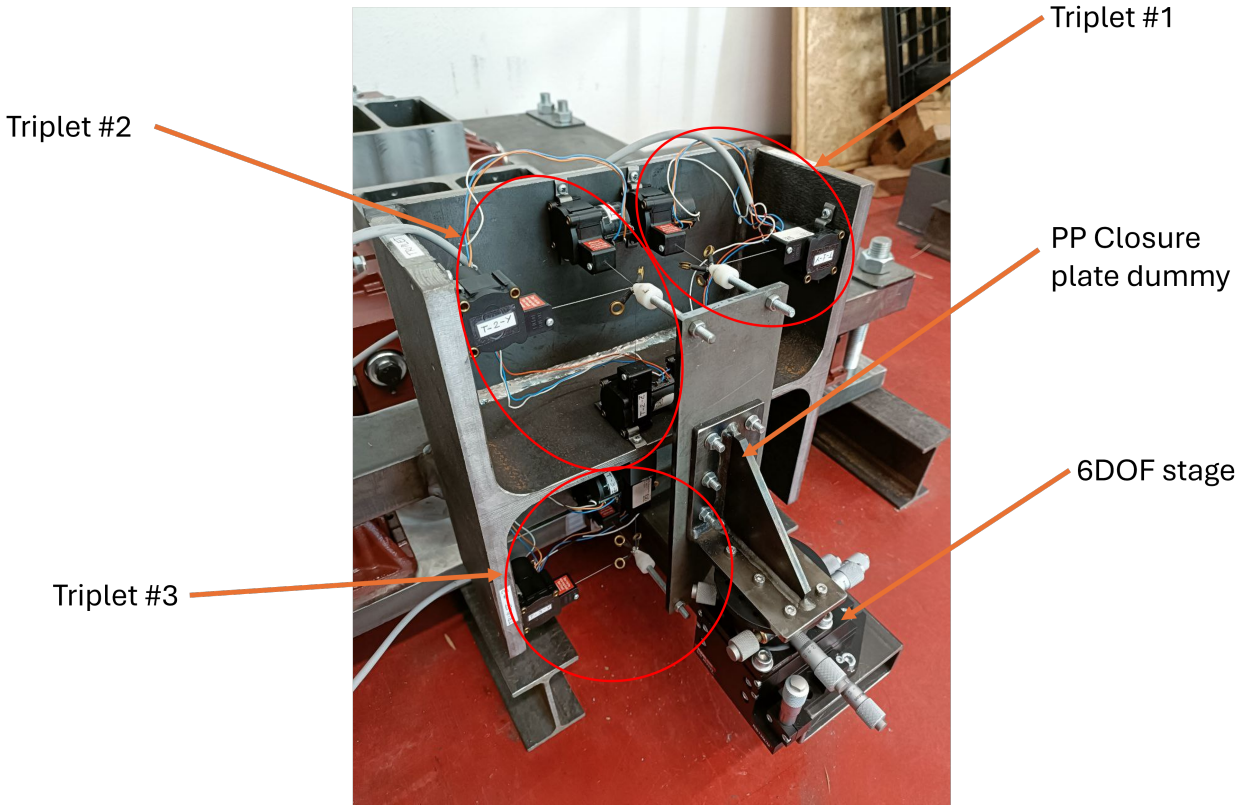

Figure 4.143: AS mock-up details on PMS and PP Closure plate dummies.

The attachment of the WPS-150-MK30 wires to the corresponding Fiducial rod is realized thanks to a plastic tip, modelled and 3D printed (Figure 4.144).

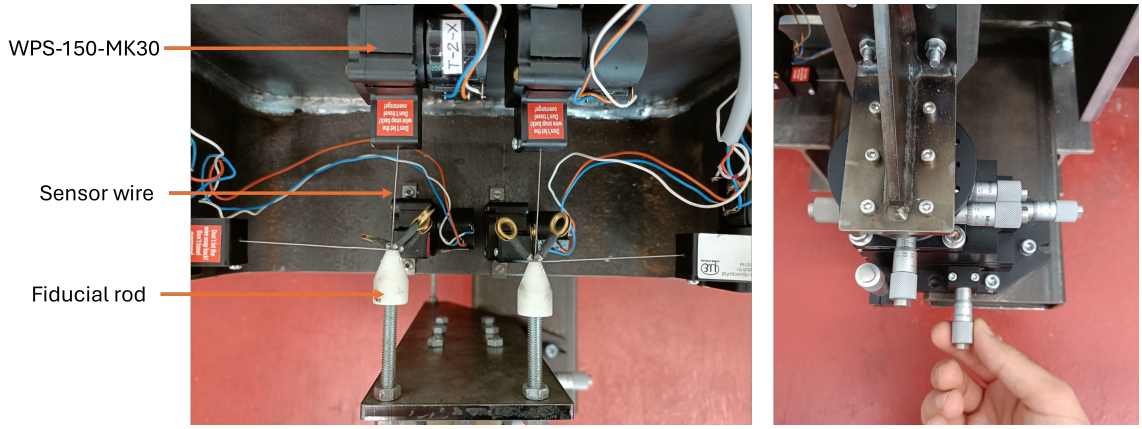

Figure 4.144: AS mock-up details on sensors attachment.

The signal and power cables from the WPS-150-MK30 sensors are connected to the DAQ, where the analog signal is converted into digital signal which is delivered to the computer thanks to the Ethernet cable (Figure 4.145).

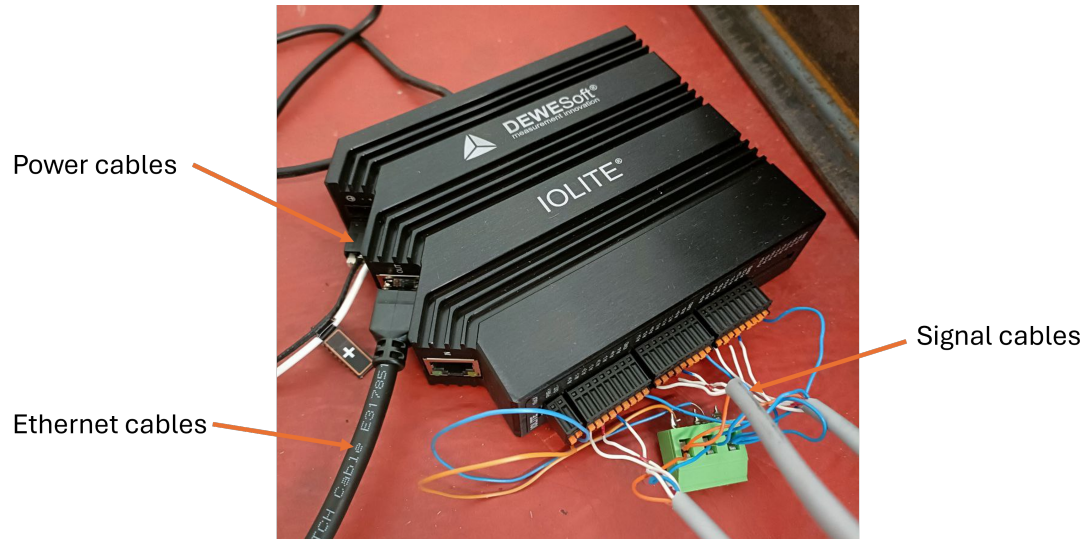

Figure 4.145: AS mock-up details on DAQ.

Realization of the AP software To integrate the reconstruction code and the AP, a software suite named *planeRunner* is realized with python language (Fig-

ure 4.146). The planeRunner is the user interface that allows the operator to easily and correctly use the AS.

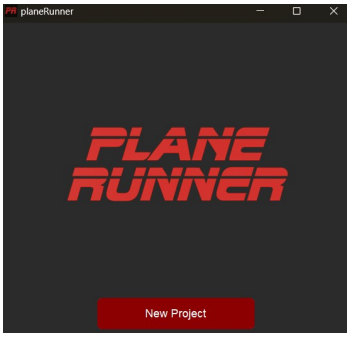

Figure 4.146: Initial page of planeRunner.

The planeRunner features are built by following the AP workflow. Such features are translated into modes and buttons activated only when allowed by the AP. The features are (Figure 4.147):

- *Start Alignment Zero*: it starts the project. First of all, you need to be sure that AS mock-up is in the *zero position*. This features allows to operate the zero realignment: a PMS acquisition is launched thanks to *Launch Dewesoft* button, the misalignment is measured and planeRunner shows the alignment quantity for each Fixator.

- *Stop Alignment Zero*: it stops the Alignment Zero. The user can choose when to stop, normally when the error is below the accuracy threshold of $\varepsilon = 0.1mm$. After clicking on this button, the *zero* is automatically set in Dewesoft for each channel, in order to "clean" it.

- *Start Alignment Test*: it starts the Alignment test. The user can start several tests in the project, when the previous test is stopped. When this button is clicked, the *Insert Port Plug movement* is triggered. After having inserted the movements, the *Launch Dewesoft* button is triggered and the realignment procedure can start.

- *Stop Alignment Test*: it stops the Alignment test.
- *Insert Port Plug movement*: it is triggered by the *Start Alignment Test*. It allows the user to tell the planeRunner what is the misalignment quantity that is physically imposed to the 6DOF. This is useful for validating the reconstruction code.
- *Launch Dewesoft*: it launches the Dewesoft acquisition of the sensors signals. After the acquisition, it creates a csv file that is read by the planeRunner. Here, the reconstruction code is finally used: the planeRunner elaborates the misalignment occurred and displays the alignment quantity for each Fixator (Figure 4.148).

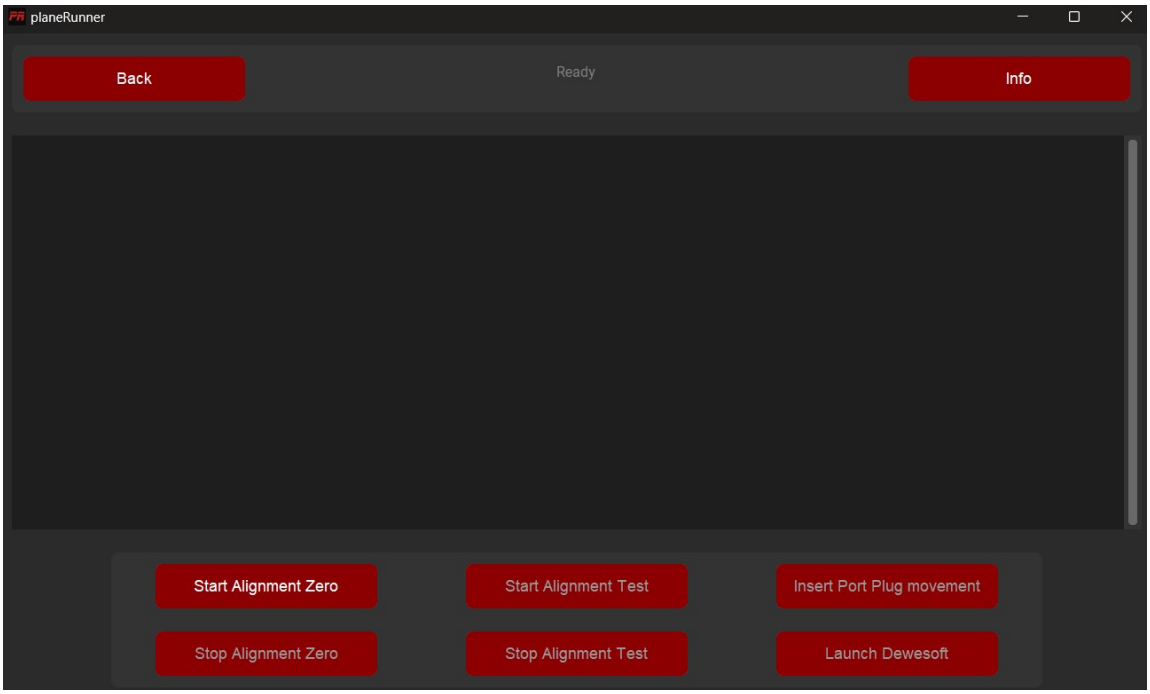

Figure 4.147: Project home page of planeRunner.

Figure 4.148 shows the planeRunner once the AP simulation is started. On the left, the planeRunner displays the alignment quantity for each fixator and the reconstructed misalignment. The alignment quantity is calculated as follows:

1. From the reconstruction phase, the transformation matrix - related to the occurred rototranslation - is extracted

2. The transformation matrix is applied to the initial coordinates vector of the central point of the lifting wedge of the Fixator, finding the final coordinates vector

3. The difference between the two vectors is calculated

4. The vector component that is related to the working direction of the Fixator is saved

5. Such extracted vector component is displayed

For example, for the FR1 (Fixator Radial 1), the transformation matrix is applied to the wedge central point and the x-component of the difference vector is displayed. This is motivated by the limitation of the working direction of one Fixator - obliged to push along only one direction. By combining the work of all the Fixators, each one working along its own direction, the realignment can be achieved.

Figure 4.148: Alignment Process project initialized and other features.

To monitor the realignment process, a Convergence graphic is displayed and updated at every iteration (Figure 4.148). The convergence criteria is based on the sensors wires lengths: at *zero position*, we know such lengths - as designed; but when a misalignment occurs, such lengths change. From the point of view of the sensors wires, the realignment is achieved when their lengths return equal to the design values within the uncertainties (i.e. under $\varepsilon = 0.1mm$). Thus, when the biggest value among the 9 differences between the measured wires length and the design length is finally below $0.1mm$, the realignment can be considered achieved. In the graphic, the planeRunner shows precisely this value. The operator, then, can have a visual monitoring of the realignment trend.

Execution of the test As mentioned before, the AS is going to be tested considering 3 DOF only - three translations. Rotational DOF are locked and not considered. Following the AP with the planeRunner, the first step is to start the Alignment Zero (Figure 4.149). The Alignment Zero has stopped, the data saved in Dewesoft and the planeRunner ready for the Alignment Test.

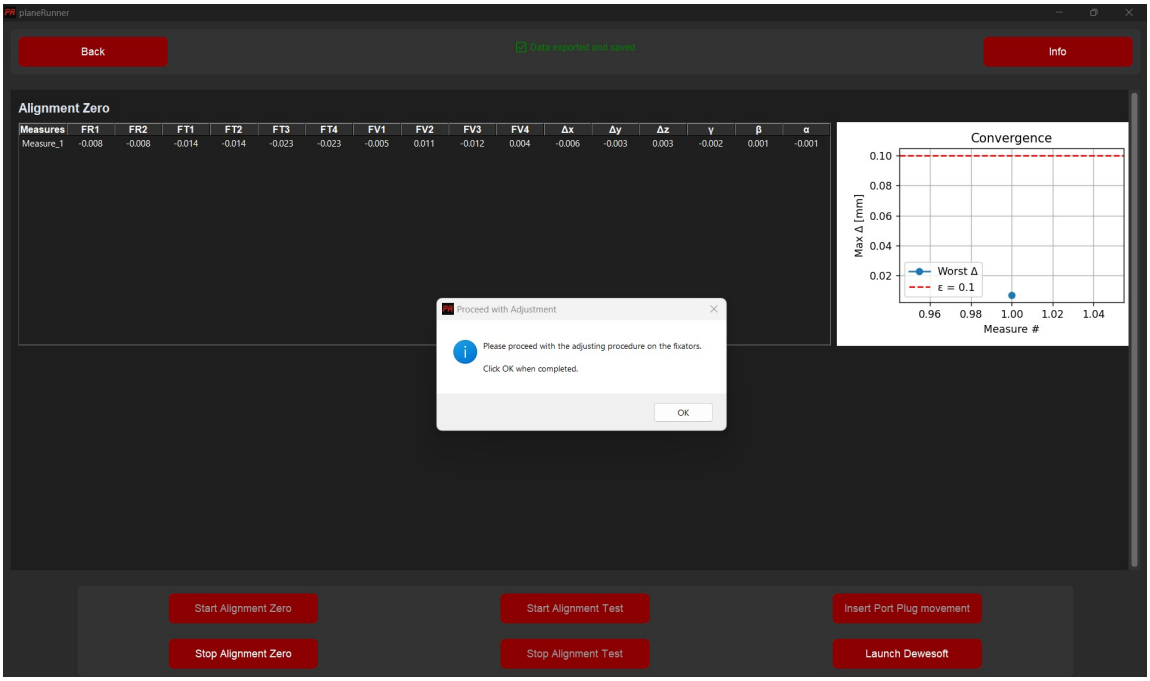

Figure 4.149: Alignment Zero set correctly. The residual error is below $0.02mm$.

The Alignment Test can start. After clicking on the *Start Alignment Test* button, the *Insert Port Plug movement* button is triggered and clicked (Figure 4.150).

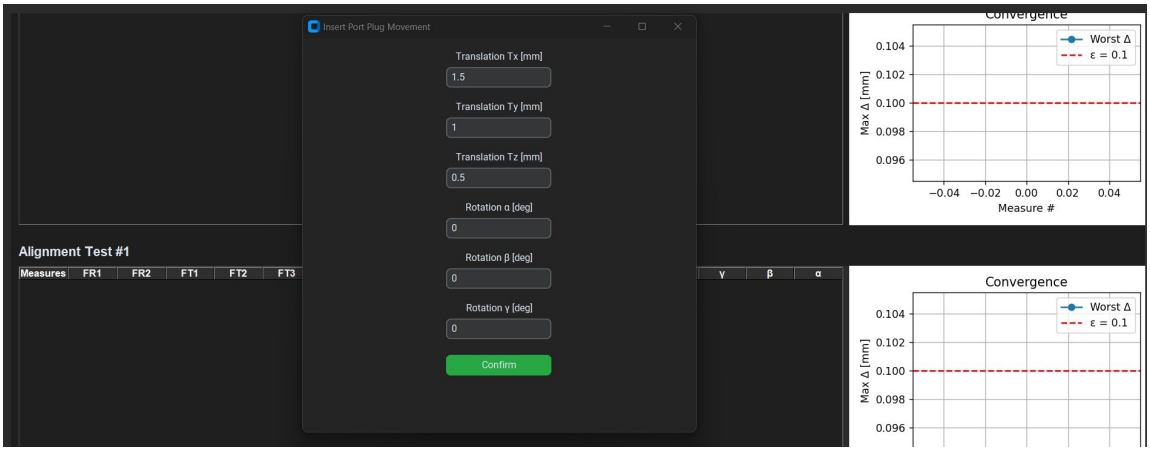

Figure 4.150: Port Plug movement inserted.

Now, the *Launch Dewesoft* button can be clicked, and after the acquisition, the

planeRunner displays the reconstructed misalignment (yellow box) and the alignment quantity for each Fixator (green box) (Figure 4.151).

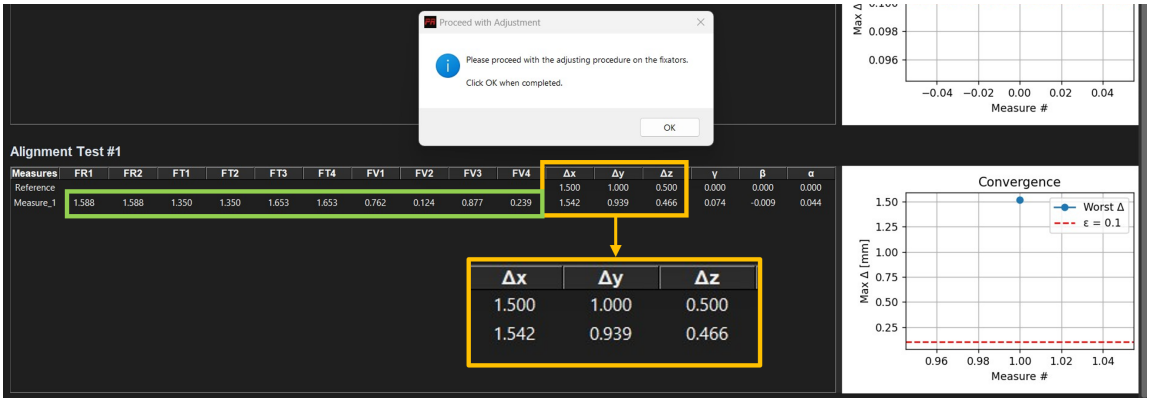

Figure 4.151: Reconstruction of the Port Plug displacement.

Now, as the warning message indicates, the adjustment operations on the Fixators can start. The approach on the realignment with the Fixators can be different. For the purpose of this work, a *direction-by-direction* adjustment approach has been followed. It consists in adjusting the Fixators along one direction, reaching the alignment in that direction, then proceeding with adjusting the second, then the third (Figure 4.152).

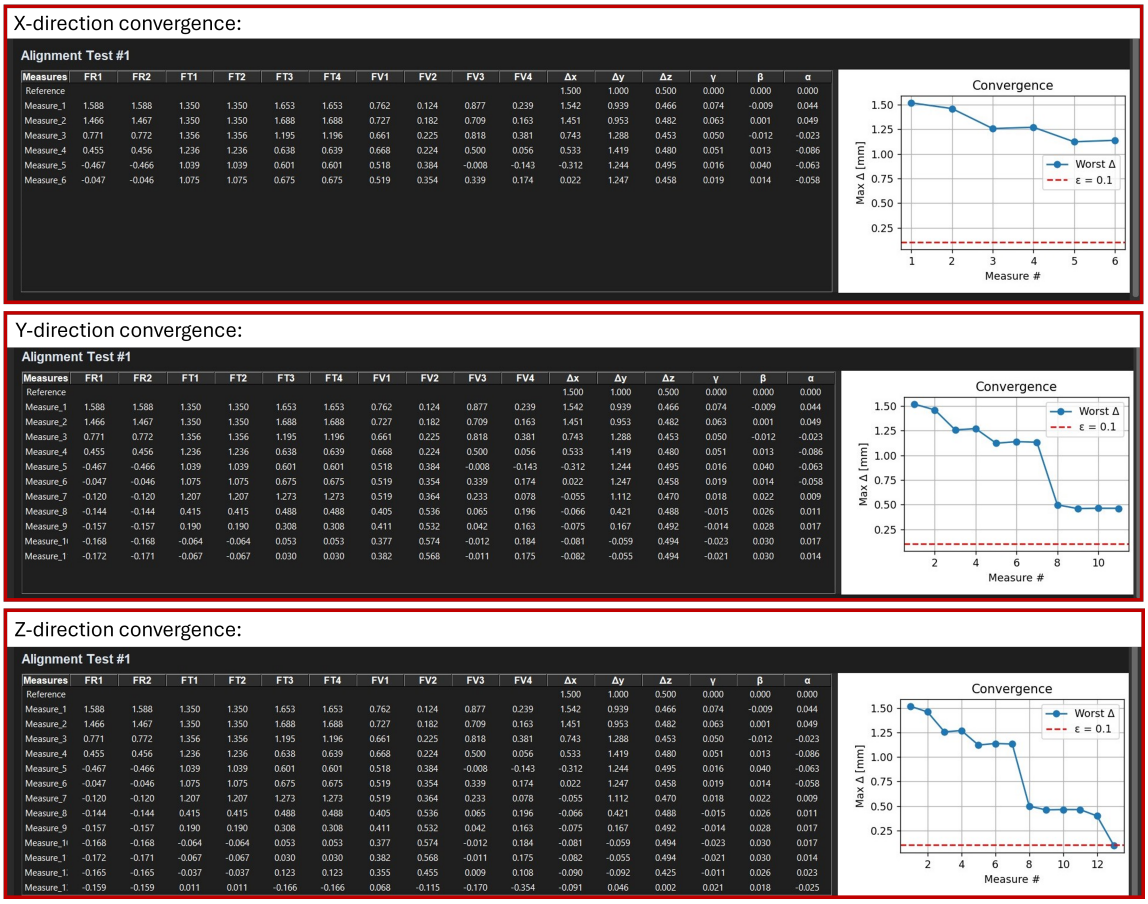

Figure 4.152: Realignment process as direction-by-direction.

Results Two APs have been executed. In both cases, the chosen Port Plug movement have been opportunely set on the 6DOF stage and are reported in Table 4.31.

Table 4.31: Imposed displacements of the PP Closure plate.

Imposed displacements [mm]		
x	**y**	**z**
1.5	1.0	0.5

The reconstruction gave the results indicated in Table 4.32.

Table 4.32: Results of misalignment reconstruction.

	Reconstructed [mm]			**Errors [mm]**		
	x	y	z	x	y	z
Test #1	1.488	1.029	0.517	0.012	0.029	0.017
Test #2	1.542	0.939	0.466	0.042	0.061	0.034

The results demonstrate that the reconstruction code, on which the PMS is based, is able to reconstruct the misalignment within the allowed accuracy of $\varepsilon = 0.1mm$.

After validating the reconstruction code, the AP can be executed for the two tests. Figure 4.153 shows the error-iterations graph for Test #1, Figure 4.154 for Test#2, along with the report of the total time spent for the AP.

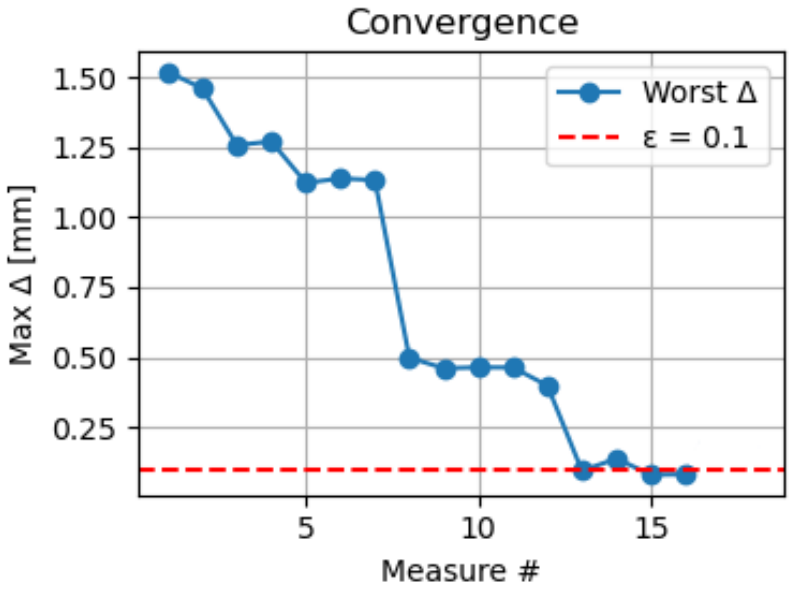

Figure 4.153: Error-iterations graphic for Test #1 - time spent for the AP: 1 hour 30 minutes.

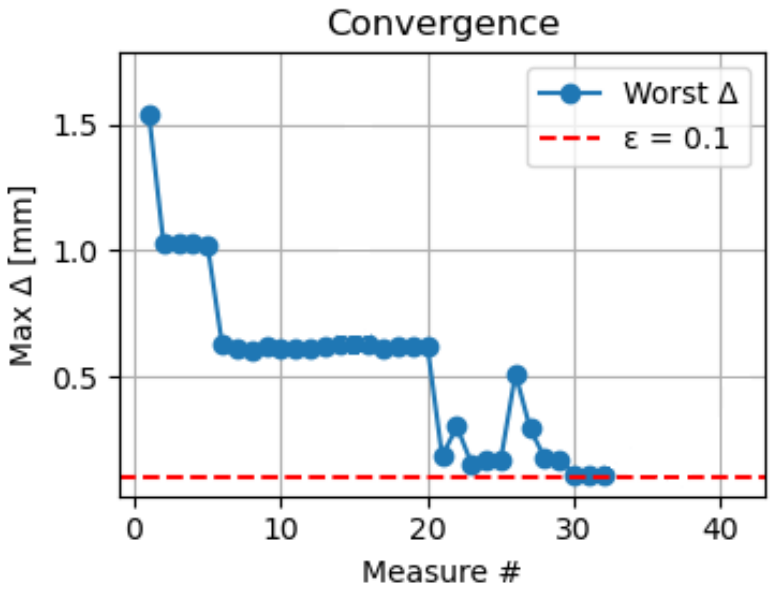

Figure 4.154: Error-iterations graphic for Test #2 - time spent for the AP: 50 minutes.

The AP can be executed as planned, with an easy access to the Fixators and the possibility of substituting the Disks. The only issue experienced regards the Disks for radial and toroidal Fixators. They stay in place - between Base plate and Fixator - only with friction. So, when a Fixator is retreated, they tend to fall (as the contact vanishes). A solution can be find in inserting an expansive element (as a spring) that supports the Disk in every Fixator configuration.

The number of iterations, and so the time spent, for reaching the alignment are considerably high (Figure 4.153 and Figure 4.154). The x-direction is sufficiently immediate, as the number of Fixators is 2. The difficult is to retract one Fixator for allowing the other to extend. This difficulty is enhanced along the y-direction, where the number of Fixators is 4. The z-direction, where the Base plate is standing on the Fixators, is relatively easy to manage because there is always contact between the Base plate and the Fixators.

Considering the reduced number of Fixators in the AS mock-up with respect to

the Ex-Port RNC, it is expected that the number of iterations and the time for the real alignment will be higher.

4.4.8 Phase 7 — Implementation & Closure: Full Integration and Lessons Learned

Subsystem Integration & ECN Issuance

The physical integration of the corrective Alignment System, based on the approved fixator mechanisms, was then carried out within the Ex-Port RNC EU11 assembly. This involved the precise installation and connection of the AS components to the existing structure.

Following successful physical integration and V&V activities, an Engineering Change Notice was issued. This document formally confirmed the completed change, and the system baseline in the PLM environment was updated to reflect the final as-built configuration of the Ex-Port RNC, now including the integrated Alignment System.

Lessons Learned

Key lessons learned throughout the LAISE process, from the initial trigger by the tolerance analysis to the successful implementation of the AS, are recorded. These insights are invaluable for informing and improving future similar interventions within ITER or other complex engineering projects, enhancing overall project resilience and adapting to unforeseen design modifications. The success of the AS demonstrates the LAISE method's efficacy in managing critical late-stage engineering changes.

4.5 Ex-Port RNC at Final Design stage

This section presents the outcomes of the successful application of the LAISE tool to the Ex-Port RNC by showing the final CAD model of the Ex-Port RNC after the

modifications due to the introduction of the AS, along with other modifications that follow the structural assessment and the VR V&V of the detector maintenance.

From the Preliminary Design Stage of the Ex-Port RNC considered at the beginning of this thesis, a number of assessments and integrations have been realized. The design modification must be tracked in order to evaluate its consequences in terms of engineering aspects (such as total mass, percentage of materials, structural behavior) and managerial aspects (cost increase, manufacturing ease, material supply).

It is also critical to understand *how* the assessments are reflected on the overall change design.

In this section, the Final Design Stage of the Ex-Port RNC is described, including:

- Results of the Structural Assessment
- Considerations on the Ex-Port RNC nose encapsulation
- Change of Detector Cassette Supporting structure
- VR validation of the Cables accessibility (change of connectors panel)
- Introduction of the Alignment System
- Update of the Position Monitoring System
- Modifications on the Temperature Stabilization System

4.5.1 Results of the Structural Assessment

The structural assessment of the Ex-Port RNC (Section 4.3.4) brought to the urge of modifying different internal components that did not pass the structural verification. Most of them are minor aspects (such as thickening of internal sheets), but some modifications are more relevant, and need to be outlined.

Detachment of the Upper Shielding Block

In the PDR Ex-Port RNC CAD model, the Upper Shielding Block is a standalone component. Its shape is formed by two triangles joint in a single line (Figure 4.155).

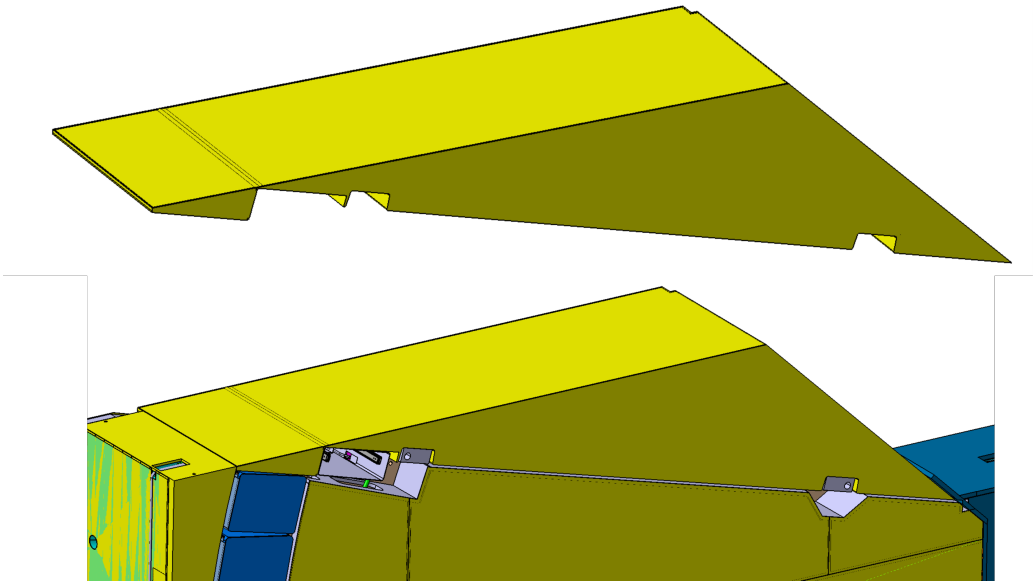

Figure 4.155: PDR version of the Upper Shielding Block.

The assembly of the Upper Shielding Block is realized by bolting the bigger triangle on the Collimators Slabs through an intermediate supporting beam; thus, the smaller triangle is a cantilever element. The structural assessment highlighted that the joining line is too thin and weak to sustain the loads of the cantilever smaller triangle. The task is to divide the two triangles, and bolting the smaller triangle separately on the Collimators Slabs by using intermediate supporting beam (Figure 4.156).

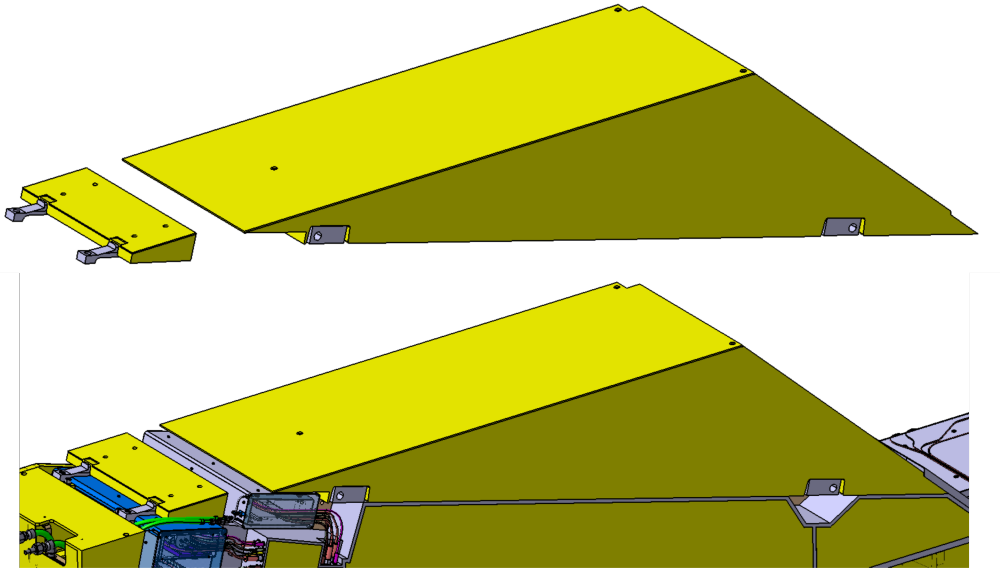

Figure 4.156: FDR version of the Upper Shielding Block.

Considerations on the Ex-Port RNC nose encapsulation

The Ex-Port RNC nose is the closest area of the Ex-Port RNC to the Port Plug Closure plate. At the PDR stage, the nose consists in 7 lead plates with a thickness of 20mm, modelled in order to accommodate the PMS sensors. The structural verification highlighted that, in cases of Fire accidents, the temperature of this area can increase over the melting temperature of the lead. To overcome possible melting phenomena during such scenarios, the lead plates are thought to be encapsulated in a sandwich-like assembly of 4mm thick Stainless-Steel sheets (Figure 4.157). The plates are then bolted with M12 screws on the Collimators slabs.

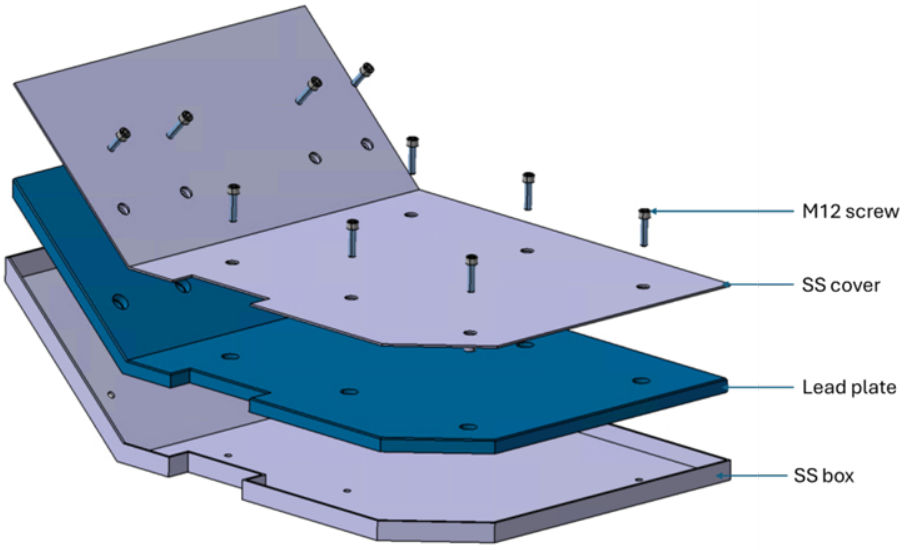

Figure 4.157: Upper lead plates encapsulated in the sandwich-like structure.

The result of the Ex-Port RNC nose encapsulation is shown in Figure 4.165.

Detector Cassettes alignment

The PDR version of the Detector Cassette supporting structure is visible in Figure 4.56. This shelf-like structure is thought to provide the alignment od the Detector Cassettes with the LOS.

Due to internal changes on the cooling circuits of the Detector Cassettes, these needed to be enlarged in external dimensions. This change lead to thin the shelves, resulting in 1-2mm thickness. The structural assessment states that the shelves are too thin to sustain the dead weight of the Detector Cassette (weighting the Double Cassette 90kg).

To cope with this problem and ensuring the correct alignment of the Detector Cassettes with the LOS, a substantial modification on the Collimators Slabs is proposed and implemented. The Collimators Slabs are elongated to create embodied shelves that accommodate the Detector Cassettes (Figure 4.158).

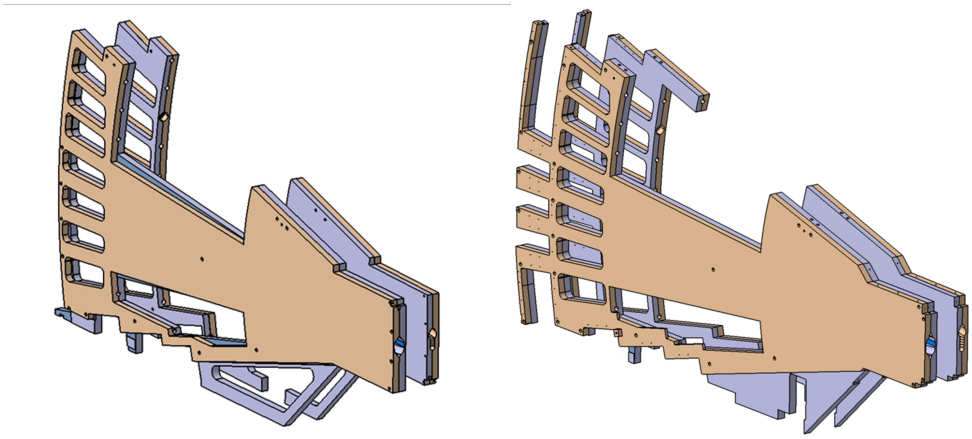

Figure 4.158: PDR version of the Collimators Slabs (left) and FDR version with elongations (right).

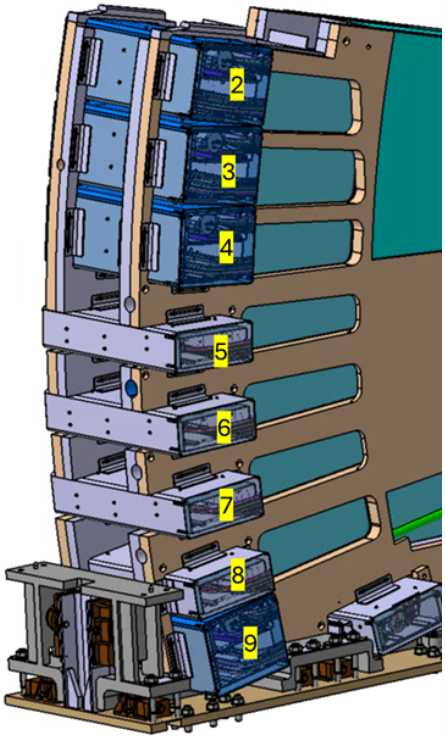

Figure 4.159: Detector Cassettes from n.2 to n. 9 mounted on the Collimators Slabs.

Now, the Detector cassettes no. 2, 3, 4, 5, 6, 7, 8 and 9 (Figure 4.159) are mounted on the elongations of the Collimators slabs thanks to support brackets welded on the Detector cassettes and bolted on the Collimators slabs.

Detector Cassettes no. 2, 3, 4 are inserted from above (first no. 4, then 3, then 2), as indicated by the red arrow in Figure 4.160. To close the top part, an upper slabs joining bridges are bolted between the Collimators slabs and the elongations

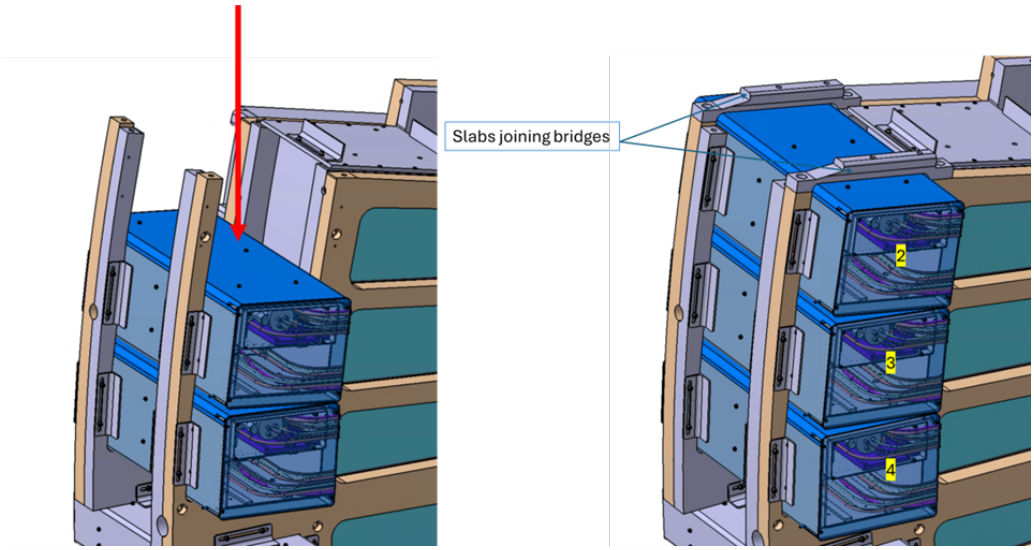

Figure 4.160: Detector cassette 2 to 4, inserted and bolted.

Detector cassettes no. 5, 6, 7 are inserted from the back to the front direction (Figure 4.161), and then bolted.

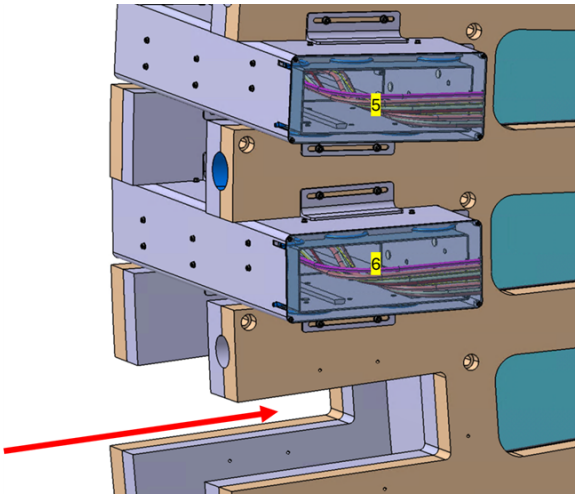

Figure 4.161: Detector cassette 2 to 4, inserted and bolted.

The alignment with the LOS is ensured with alignment pins in the interface between the supporting brackets (welded on the Detector Cassette) and the Collimators Slab.

4.5.2 VR validation of the Cables accessibility

The VR simulation of the Maintenance procedure of the Ex-Port RNC (Section 4.3.5) verified the feasibility of the detector replacement. However, a difficult access to the connectors inside the Detector Cassette was experienced from the operator, both in the VR simulation and in the physical mock-up. The difficulty is remarked by the trends of the result times (Figure 4.80), where two peaks are clearly visible (in both time trends, VR and physical), corresponding to the operation of disconnection and connection of the cables connectors.

Since the time spent in the Port Interspace zone is a tricky factor for the calculation of the radiation dose absorbed by the operator during the maintenance procedure, an alternative is proposed.

Instead of having the connector panels on the Detector cassette body, the cables are routed outside and plugged on connectors that are now located on a dedicated *connectors panel* (Figure 4.162).

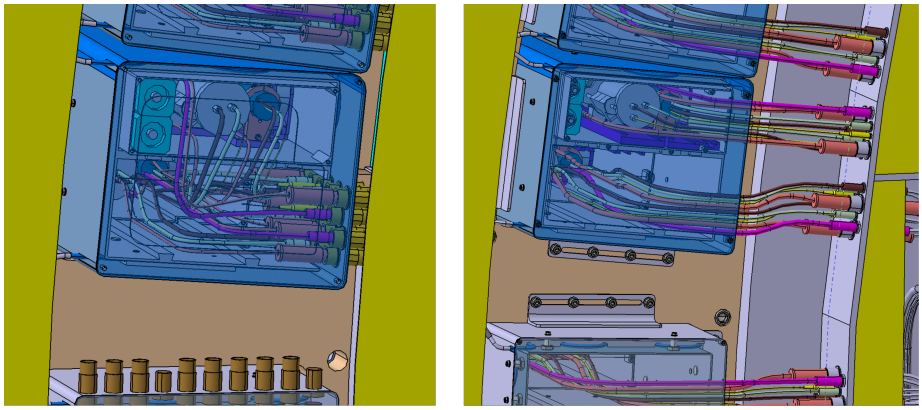

Figure 4.162: PDR connectors on the Detector Cassette body (left) and the FDR version on the connectors panel (right).

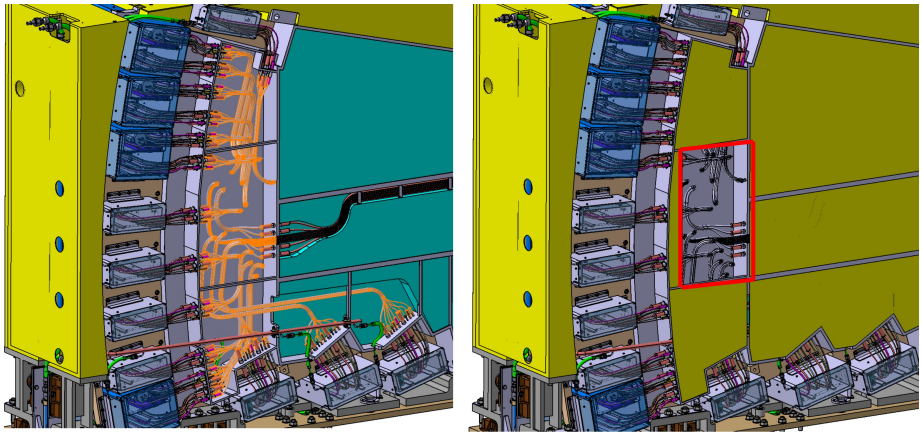

Figure 4.163: Cables connected to the connectors panel both sides (left) and the EU11 electrical interface (right).

Now, the cables from all the Detector cassettes are routed up to the connectors panel. Here an internal interface is set, from where the cables coming from outside EU11 are connected on the other side of the connectors panel (Figure 4.163). These cables, to respect the EU11 Electrical interfaces (Figure 4.33), must pass through the rectangular aperture defined in (marked in red in Figure 4.163).

4.5.3 Introduction of the Alignment System

The Ex-Port CAD modifications due to the integration of the Alignment System (Section 4.4.7) has been already presented during the application of the LAISE tool. For having a complete overview of the FDR CAD changes, the AS integration-related modifications are here summed up.

Integration of the AS

The first modification is the integration of the AS itself. The main changes involve the introduction of the Counterplate, the vertical posts and the 22 fixators (Figure 4.164).

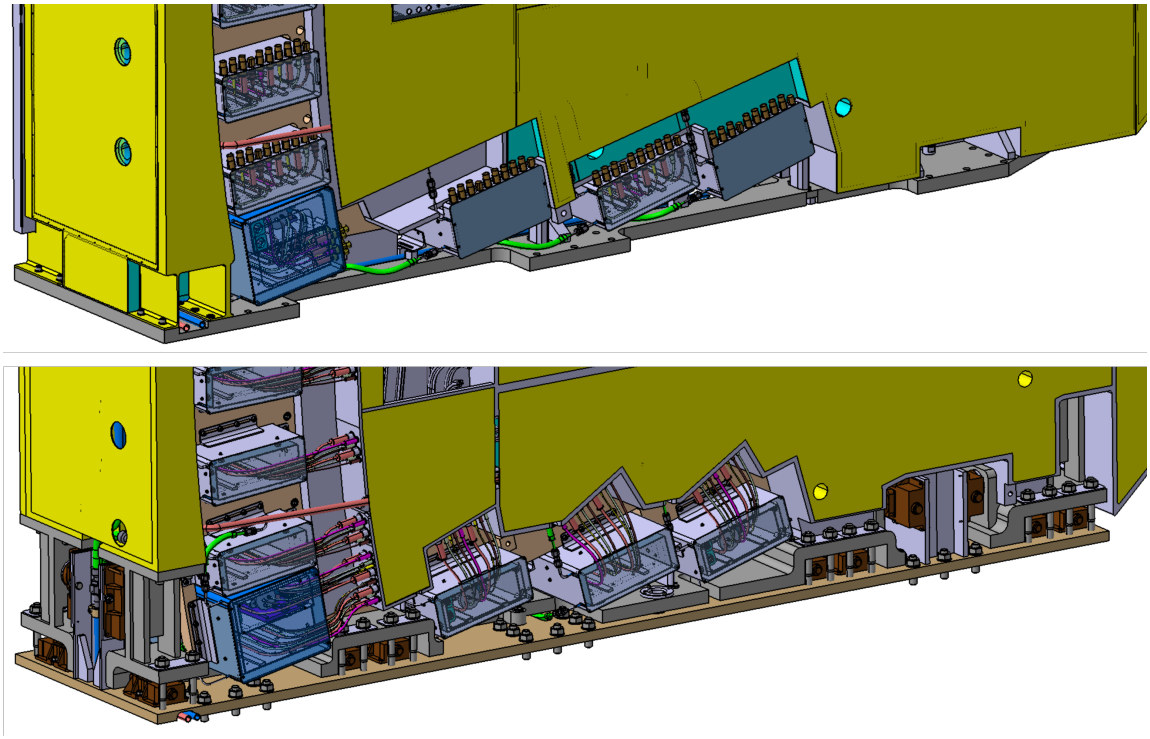

Figure 4.164: PDR version of the bottom zone of the Ex-Port RNC (top) and FDR version with the AS (bottom).

Update of the Position Monitoring System

The PMS sensors layout has changed from 7 sensors (5 pull mode, 2 push mode) to 9 sensors (all pull mode), organized in three groups of three sensors and a fiducial rod for each Triplet (Figure 4.165).

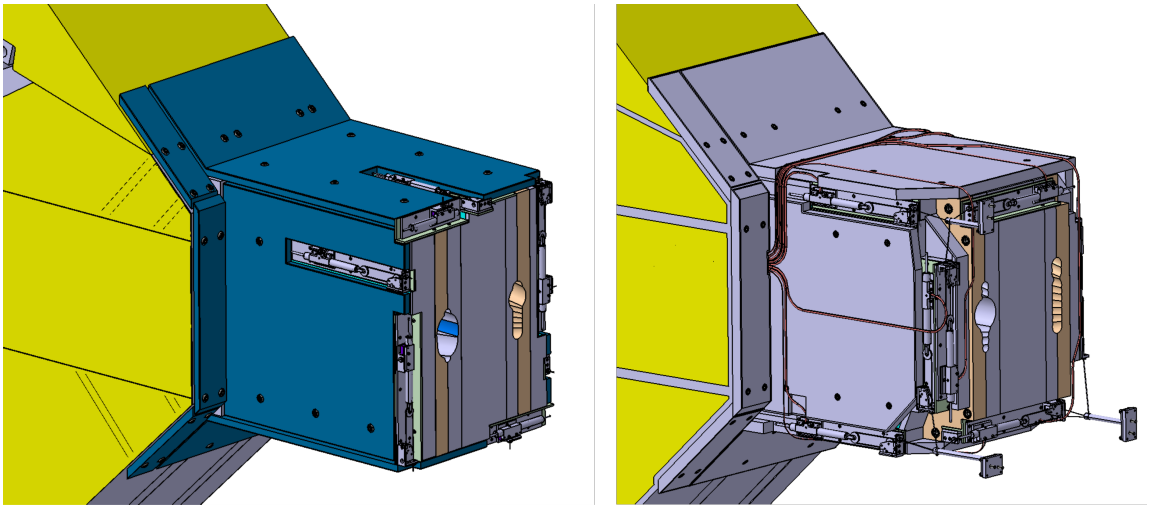

Figure 4.165: PDR version of the PMS with 7 sensors (left) and FDR version with the 9 sensors (right).

Modifications on the Temperature Stabilization System

The last modification caused by the integration of the AS concerned the Temperature Stabilization System. The main design changes are the division of the manifolds in a movable part and a fixed part and the subsequent introduction of flexible pipes between the two, in order to ensure the correct functioning of the AS without stress increase (Figure 4.166).

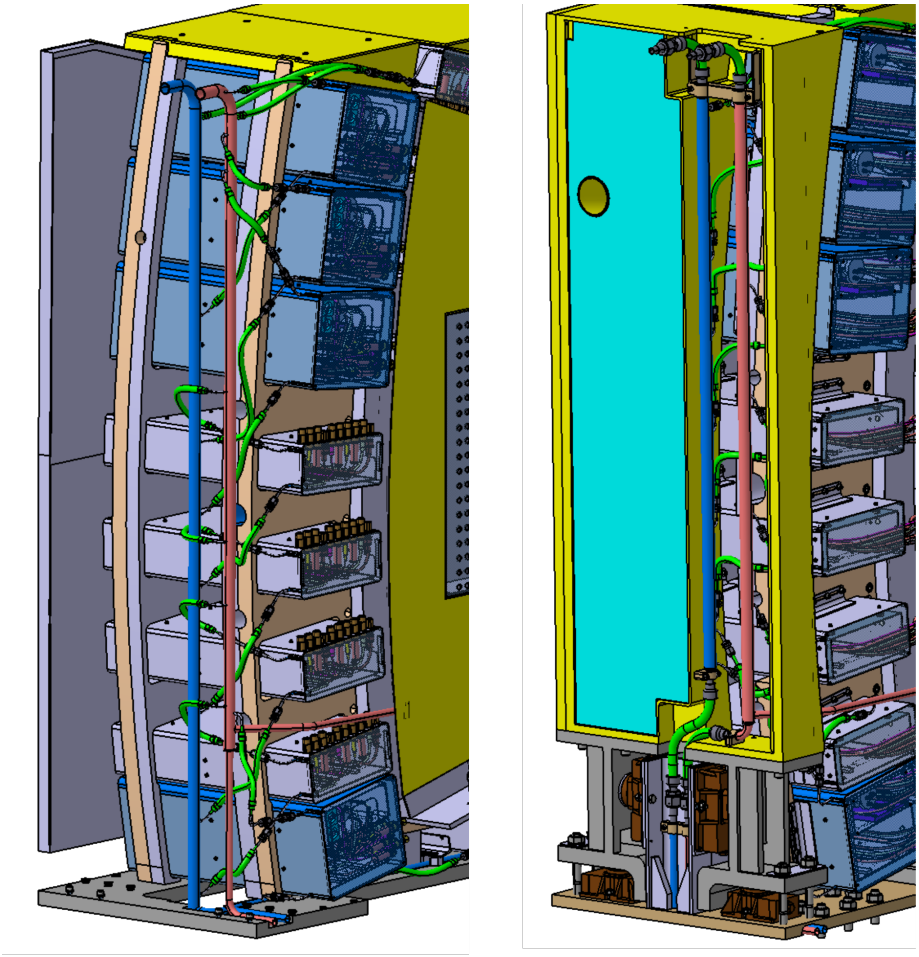

Figure 4.166: PDR version of the TSS (left) and FDR version with the flexible pipes (right).

4.5.4 Overall design change

The overall design changes of the Ex-Port RNC can be appreciated with a prospective view of the diagnostic (Figure 4.167).

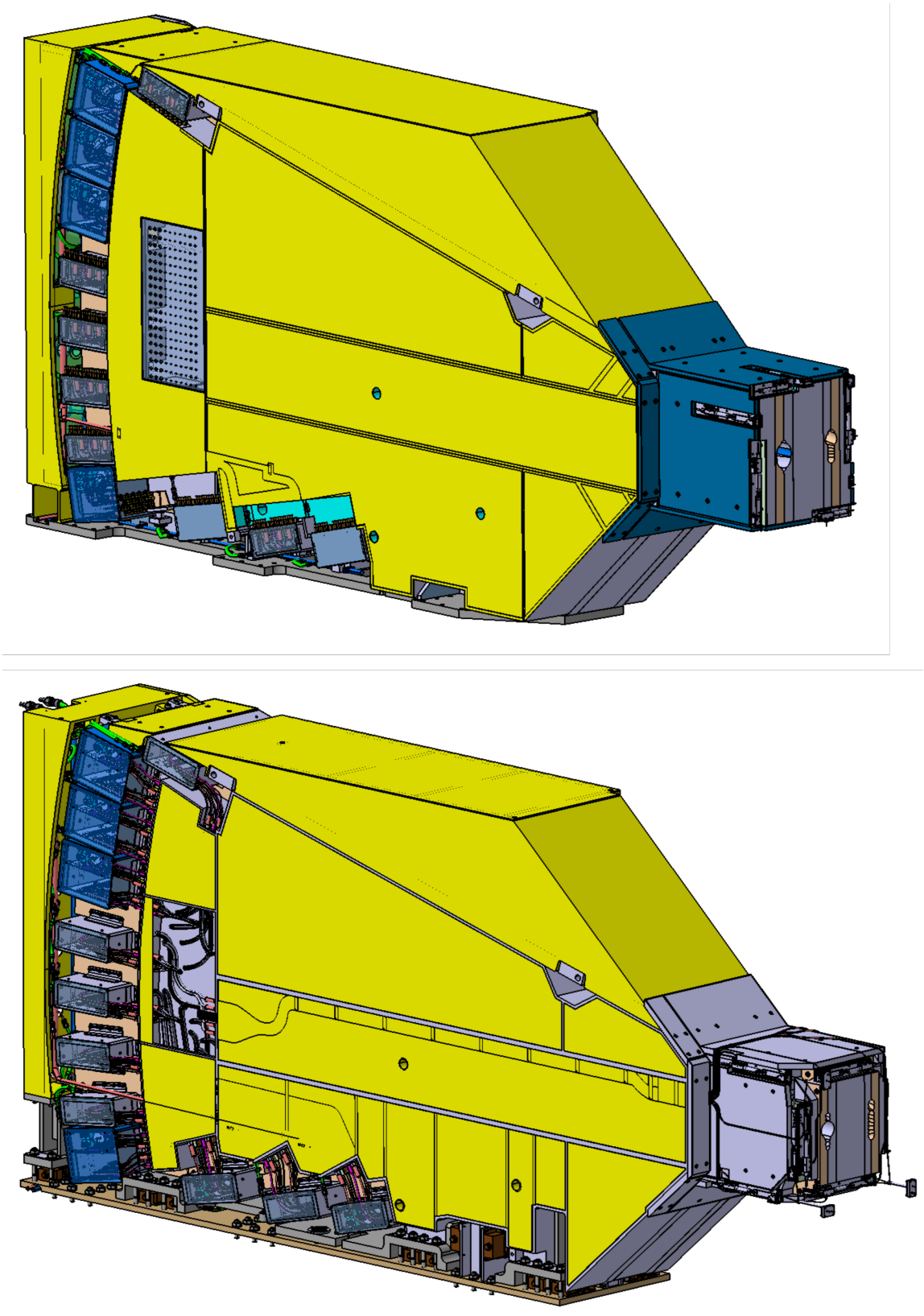

Figure 4.167: PDR version of the Ex-Port RNC (top) and FDR version (bottom).

Chapter 5

Conclusions

This research has addressed a critical challenge inherent to complex, long-cycle engineering projects: the systematic integration of corrective subsystems during advanced design stages, when the cost of change is high and the risk of disruption is significant. The work presented constitutes a dual contribution, encompassing both the development of a novel methodological framework and its comprehensive application to a critical diagnostic system within the ITER project. The resulting Late-Stage Add-In via Systems Engineering (LAISE) method was conceived, formalized, and validated through a successful case study, the integration of an Alignment System (AS) for the ITER Radial Neutron Camera (RNC).

5.1 Principal Contributions and Validation

The research was validated through a series of interconnected technical activities that defined its core contributions. It commenced with a detailed tolerance chain analysis, which quantified a latent risk of mechanical misalignment between the Ex-Port RNC collimators and the Diagnostic Shielding Module optical paths. This analytical finding provided the quantitative justification for a corrective intervention, leading to the subsequent design and integration of a bespoke Alignment System. This activity encompassed the selection of commercial double-wedged fixators, the design of

a custom disk assortment and counterplate, and the complete CAD modelling within the ITER ENOVIA PLM environment, which was managed as part of this work to ensure configuration control and traceability.

The proposed solution underwent a dual validation strategy. A full-scale, functional AS mock-up was designed, procured, and tested to validate the mechanical adjustment procedure and its required precision under representative conditions. In parallel, a Virtual Reality simulation was developed to validate and optimize the maintainability procedures for the newly designed detector cassettes, incorporating formal ergonomic analysis derived from ITER standards. This combination of physical and virtual validation provided robust evidence for the technical feasibility and operational safety of the integrated design.

5.2 From PDR to FDR

A primary outcome of this work is the documentation and facilitation of a complete design maturation cycle for the Ex-Port RNC subsystem. The LAISE framework provided the structured workflow that guided the subsystem from its Preliminary Design Review (PDR) baseline to a Final Design Review (FDR) ready state. This progression was managed through systematic execution of structural assessments, interface management, and detailed procedure definition (encompassing both cold and hot alignment processes), all of which were directly incorporated into the final design package. The In-Port RNC, presented as a stable design at FDR, serves as a comparative benchmark, illustrating the distinct yet structured path required to resolve late-emerging integration challenges.

5.3 The LAISE Framework

The development of the LAISE methodology represents a contribution to Systems Engineering practice, providing a formalized response to late-stage integration challenges. The framework demonstrated efficacy through three core mechanisms:

1. Requirement Gap Formalization and Traceability: By mandating that performance deviations be formally treated as derived requirements, LAISE prevented ad-hoc fixes and maintained an auditable requirements baseline throughout the change process.

2. Interface-Centric Management: The enforcement of explicit Interface Control Contracts ensured precise definition of boundaries between the existing system and the new subsystem, mitigating a common source of integration error and delay.

3. Targeted Verification & Validation: The principle of focused V&V, exemplified by the specific tests on the AS mock-up and the targeted VR maintenance simulation, efficiently confirmed functionality while avoiding unnecessary full-system retesting.

5.4 Efficacy and Broader Applicability

The completion of the RNC Alignment System design at FDR level, substantiated by physical and virtual validation, confirms the practical utility of the LAISE framework. It demonstrates that a disciplined, model-driven, and PLM-anchored process can effectively govern high-impact changes late in a project lifecycle, thereby enhancing project resilience. The underlying principles of LAISE—formalized gap analysis, digital thread integration, and targeted V&V—are transferable to other complex, long-lifecycle engineering domains such as aerospace, naval architecture, and large-scale infrastructure, where late-stage modifications are both costly and inevitable.

5.5 Future Developments

While this research validates the LAISE framework within the context of the ITER RNC, it establishes a foundation for several avenues of future investigation:

- Cross-Domain Validation: The generalizability of LAISE should be tested in other high-complexity sectors. Adapting its phases to domains like aerospace or civil mega-projects would further establish its theoretical robustness and practical utility.

- Integration with Advanced Digital Engineering: Future iterations could be integrated with Digital Twin platforms and enhanced by Machine Learning algorithms. This would enable predictive, real-time impact analysis for proposed changes, shifting from a reactive to a proactive change management paradigm.

- Quantification of Methodological Efficacy: Developing a quantitative model to benchmark the efficiency gains of the LAISE approach is a critical next step. Metrics for "Cost of Late Change Avoidance" could be established by comparing schedule adherence and rework levels between LAISE-guided and traditional change processes in comparable project environments.

- Extension to Full 6-DOF Alignment: The current AS design, validated for 3 translational degrees of freedom (DOF), was conceived with future expansion in mind. The logical progression is the detailed design, prototyping, and testing of the capability to also adjust the three rotational DOFs, achieving full 6-DOF alignment.

5.6 Concluding Remarks

This thesis has demonstrated that the integration of corrective subsystems at advanced project stages can be managed with rigor and control. The contributions—spanning initial tolerance analysis, AS design, CAD and PLM management, physical mock-up testing, and VR simulation—have resolved a critical problem for the ITER RNC while simultaneously developing and validating the LAISE methodological framework. By ensuring disciplined traceability, explicit interface control, and a structured progression from PDR to FDR, the LAISE method enhances a project's capacity to adapt to unforeseen technical challenges without compromising overall system in-

tegrity. The successful maturation of the Ex-Port RNC, guided by this framework, confirms its practical effectiveness and its potential to inform best practices in the management of complexity across engineering disciplines.

Bibliography

[1] R. Sliger, H. H. Altfeld, S. Chiocchio, T. Luce, R. Rotella, A. Alekseev, S. Calpena, J. J. Cordier, K. Okayama, S. Orlandi, H. Pialot, E. Tada, Z. Zhao, and G. S. Lee. *ITER Systems Engineering Management Plan (SEMP) (Private communication)*. July 2019.

[2] A. Sharon, V. Perelman, and D. Dori. "8.2.2 A Project-Product Lifecycle Management approach for improved systems engineering practices". In: *INCOSE International Symposium* 18 (1 June 2008), pp. 942–957. ISSN: 2334-5837. DOI: 10.1002/j.2334-5837.2008.tb00854.x.

[3] T. J. Higgins. "Systems engineering handbook". In: *Journal of the Franklin Institute* 281 (6 June 1966), pp. 522–523. ISSN: 0016-0032, 1879-2693. DOI: 10.1016/0016-0032(66)90450-9.

[4] K. Samset. "Systems Engineering in Front-End Governance of Major Public Investment Projects". In: *Systems* 5 (1 Feb. 2017), pp. 13–13. ISSN: 2079-8954. DOI: 10.3390/systems5010013.

[5] R. A. de Carvalho. "Modern Design Methodologies and the Development of Mechatronic Products". In: *arXiv (Cornell University)* (Jan. 2020). DOI: 10.48550/arXiv.2007.10962.

[6] J. Ni, X. Yin, X. Lu, X. Li, J. Wei, R. Tong, M. Tang, and P. Du. "CADDesigner: Conceptual Design of CAD Models Based on General-Purpose Agent". In: (Jan. 2025). DOI: 10.48550/ARXIV.2508.01031.

[7] R. Sibois, T. Määttä, M. Siuko, and J. Mattila. "Simulation-based design process for the verification of ITER remote handling systems". In: *Fusion Engineering and Design* 89 (Mar. 2014), pp. 2341–2346. ISSN: 0920-3796, 1873-7196. DOI: 10.1016/j.fusengdes.2014.02.049.

[8] R. A. de Carvalho, H. R. M. da Hora, and R. Fernandes. "A process for designing innovative mechatronic products". In: *International Journal of Production Economics* 231 (July 2020), pp. 107887–107887. ISSN: 0925-5273, 1873-7579. DOI: 10.1016/j.ijpe.2020.107887.

[9] D. Escudero-Mancebo, N. F. Villalobos, Ó. Martín, and A. Martínez-Monés. "Research methods in engineering design: a synthesis of recent studies using a systematic literature review". In: *Research in Engineering Design* 34 (2 Jan. 2023), pp. 221–256. ISSN: 0934-9839, 1435-6066. DOI: 10.1007/s00163-022-00406-y.

[10] M. Abdulla and Y. R. Shayan. "On the Peculiarities of Design: An Engineering Perspective". In: Surveillance Studies Network, June 2013. DOI: 10.24908/pceea.v0i0.4823.

[11] M. Abdulla and Y. R. Shayan. "On the Peculiarities of Design: An Engineering Perspective". In: *arXiv (Cornell University)* (Jan. 2013). DOI: 10.48550/arXiv.1305.4148.

[12] J. Halbe, J. Adamowski, and C. Pahl-Wostl. "The role of paradigms in engineering practice and education for sustainable development". In: *Journal of Cleaner Production* 106 (Mar. 2015), pp. 272–282. ISSN: 0959-6526, 1879-1786. DOI: 10.1016/j.jclepro.2015.01.093.

[13] D. Marzullo, E. Occhiuto, G. Brolatti, D. Falco, D. Laghi, D. Marocco, and B. Esposito. "Mechanical design of ITER radial neutron camera Ex-Port system". In: *Fusion Engineering and Design* 203 (2024). Cited by: 2; All Open Access, Green Open Access, Hybrid Gold Open Access. DOI: 10.1016/j.fusengdes.2024.114477.

[14] F. Z. Fang, Z.-Y. Li, A. Arokiam, and T. Gorman. "Closed Loop PMI Driven Dimensional Quality Lifecycle Management Approach for Smart Manufacturing System". In: *Procedia CIRP* 56 (Jan. 2016), pp. 614–619. ISSN: 2212-8271. DOI: 10.1016/j.procir.2016.10.121.

[15] T. Schumacher, C. Müller, and D. Inkermann. "SysML Process Chains in MBSE: Systematic Literature Review and Future Research Directions". In: *Digital engineering.* (Feb. 2025), pp. 100037–100037. ISSN: 2950-550X. DOI: 10.1016/j.dte.2025.100037.

[16] D. Pandey, U. Suman, and A. Ramani. "An Effective Requirement Engineering Process Model for Software Development and Requirements Management". In: (Oct. 2010), pp. 287–291. DOI: 10.1109/artcom.2010.24.

[17] P. Müller. "Configuration Management – A Core Competence for Successful through-life Systems Engineering and Engineering Services". In: *Procedia CIRP* 11 (Jan. 2013), pp. 187–192. ISSN: 2212-8271. DOI: 10.1016/j.procir.2013.07.032.

[18] S. Watts and M. Kossmann. "11.3.3 The Significance of Configuration Management in the Context of Systems Engineering". In: *INCOSE International Symposium* 20 (1 July 2010), pp. 1396–1404. ISSN: 2334-5837. DOI: 10.1002/j.2334-5837.2010.tb01148.x.

[19] H. Habib, R. Menhas, and O. McDermott. "Managing Engineering Change within the Paradigm of Product Lifecycle Management". In: *Processes* 10 (9 Sept. 2022), pp. 1770–1770. ISSN: 2227-9717. DOI: 10.3390/pr10091770.

[20] A. Przybyło. "PLM forensics: understanding the design evolution and intent by following the trail of change". In: *International Journal of Product Lifecycle Management* 10 (4 Jan. 2017), pp. 375–375. ISSN: 1743-5110, 1743-5129. DOI: 10.1504/ijplm.2017.090331.

[21] J. Hassine, J. Rilling, and R. Dssouli. "An evaluation of timed scenario notations". In: *Journal of Systems and Software* 83 (2 Sept. 2009), pp. 326–350. ISSN: 0164-1212, 1873-1228. DOI: 10.1016/j.jss.2009.09.014.

[22] C. Stechert and H.-J. Franke. "Managing requirements as the core of multi-disciplinary product development". In: *CIRP journal of manufacturing science and technology* 1 (3 Nov. 2008), pp. 153–158. ISSN: 1878-0016, 1755-5817. DOI: 10.1016/j.cirpj.2008.09.008.

[23] F. Tian, T. Wang, P. Liang, C. Wang, A. A. Khan, and M. A. Babar. "The impact of traceability on software maintenance and evolution: A mapping study". In: *Journal of Software Evolution and Process* 33 (10 Aug. 2021). ISSN: 2047-7473, 2047-7481. DOI: 10.1002/smr.2374.

[24] N. Mogk. "A Requirements Management System based on an Optimization Model of the Design Process". In: *Procedia Computer Science* 28 (Jan. 2014), pp. 221–227. ISSN: 1877-0509. DOI: 10.1016/j.procs.2014.03.028.

[25] C. A. Aldridge and M. E. Colvin. "Writing SMART objectives for natural resource and environmental management". In: *Ecological Solutions and Evidence* 5 (1 Jan. 2024). ISSN: 2688-8319. DOI: 10.1002/2688-8319.12313.

[26] M. R. Asadabadi, M. Saberi, O. Zwikael, and E. Chang. "Ambiguous requirements: A semi-automated approach to identify and clarify ambiguity in large-scale projects". In: *Computers & Industrial Engineering* 149 (Sept. 2020), pp. 106828–106828. ISSN: 0360-8352, 1879-0550. DOI: 10.1016/j.cie.2020.106828.

[27] V. Stewart, S. S. McMillan, J. Hu, J. C. Collins, S. El-Den, C. L. O'Reilly, and A. Wheeler. "Are SMART goals fit-for-purpose? Goal planning with mental health service-users in Australian community pharmacies". In: *International Journal for Quality in Health Care* 36 (1 Jan. 2024). ISSN: 1353-4505, 1464-3677. DOI: 10.1093/intqhc/mzae009.

[28] M. A. Adeoye and C. Adong. "The Power of Precision: Why Your Research Focus Should be SMART?" In: *Journal of Education Action Research* 7 (4 Dec. 2023), pp. 569–577. ISSN: 2549-3272, 2580-4790. DOI: 10.23887/jear.v7i4.69757.

[29] L. E. Voth-Gaeddert. "Improving Use of SMART Goals in Science Diplomacy: An Overview of Concepts and Approaches". In: (July 2024). DOI: 10.31235/osf.io/m682d.

[30] V. Kirova, N. Kirby, D. Kothari, and G. Childress. "Effective requirements traceability: Models, tools, and practices". In: *Bell Labs Technical Journal* 12 (4 Feb. 2008), pp. 143–157. ISSN: 1089-7089, 1538-7035, 1538-7305. DOI: 10.1002/bltj.20272.

[31] M. R. I. Nekvi and N. H. Madhavji. "Impediments to Regulatory Compliance of Requirements in Contractual Systems Engineering Projects". In: *ACM Transactions on Management Information Systems* 5 (3 Dec. 2014), pp. 1–35. ISSN: 2158-656X, 2158-6578. DOI: 10.1145/2629432.

[32] M. Meißner, G. Jacobs, P. Jagla, and J. Sprehe. "Model based systems engineering as enabler for rapid engineering change management". In: *Procedia CIRP* 100 (Jan. 2021), pp. 61–66. ISSN: 2212-8271. DOI: 10.1016/j.procir.2021.05.010.

[33] P. Rempel and P. Mader. "Preventing Defects: The Impact of Requirements Traceability Completeness on Software Quality". In: *IEEE Transactions on Software Engineering* 43 (8 Oct. 2016), pp. 777–797. ISSN: 0098-5589, 1939-3520, 2326-3881. DOI: 10.1109/tse.2016.2622264.

[34] T. Gülke, B. Rumpe⋆, M. Jansen, and J. Axmann. "High-Level Requirements Management and Complexity Costs in Automotive Development Projects: A Problem Statement". In: Springer Science+Business Media, Jan. 2012, pp. 94–100. DOI: 10.1007/978-3-642-28714-5_8.

[35] N. Wang. "ERMM: An Engineering Requirements Management Method". In: *Journal of Computing and Information Science in Engineering* 6 (2 Apr. 2006), pp. 196–199. ISSN: 1530-9827, 1944-7078. DOI: 10.1115/1.2202869.

[36] M. Masmoudi, P. Leclaire, M. Zolghadri, and M. Haddar. "Engineering Change Management: A novel approach for dependency identification and change prop-

agation for product redesign". In: *IFAC-PapersOnLine* 50 (1 July 2017), pp. 12410–12415. ISSN: 2405-8963, 2405-8971. DOI: 10.1016/j.ifacol.2017.08.2427.

[37] J. Tryczak, A. M. Lis, P. Ziemiański, and J. Czyżewicz. "Towards a Universal Model of Engineering Change Management". In: *Journal of the Knowledge Economy* 15 (3 Nov. 2023), pp. 12422–12438. ISSN: 1868-7865, 1868-7873. DOI: 10.1007/s13132-023-01576-3.

[38] N. Iakymenko, A. Romsdal, M. Semini, and J. O. Strandhagen. "Engineering Change Management in the Engineer-to-Order Production Environment: Insights from Two Case Studies". In: Springer Science+Business Media, Jan. 2018, pp. 131–138. DOI: 10.1007/978-3-319-99704-9_17.

[39] A. Stekolschik. "Engineering Change Management Method Framework in Mechanical Engineering". In: vol. 157. IOP Publishing, Nov. 2016, pp. 12008–12008. DOI: 10.1088/1757-899x/157/1/012008.

[40] J. Wilberg, F. Elezi, I. D. Tommelein, and U. Lindemann. "Using a Systemic Perspective to Support Engineering Change Management". In: *Procedia Computer Science* 61 (Jan. 2015), pp. 287–292. ISSN: 1877-0509. DOI: 10.1016/j.procs.2015.09.217.

[41] E. Rebentisch, G. Schuh, M. Riesener, S. Breunig, A. Pott, and K. P. Sinha. "Assessment of Changes in Technical Systems and their Effects on Cost and Duration based on Structural Complexity". In: *Procedia CIRP* 55 (Jan. 2016), pp. 35–40. ISSN: 2212-8271. DOI: 10.1016/j.procir.2016.07.033.

[42] S.-P. Leino, L. Jokinen, J.-P. Anttila, and A. Pulkkinen. "Case Study on Engineering Change Management and Digital Manufacturing". In: Springer Science+Business Media, Jan. 2016, pp. 591–600. DOI: 10.1007/978-3-319-33111-9_53.

[43] J. Han, S.-H. Lee, and P. Nyamsuren. "An integrated engineering change management process model for a project-based manufacturing". In: *International Journal of Computer Integrated Manufacturing* 28 (7 July 2014), pp. 745–752. ISSN: 0951-192X, 1362-3052. DOI: 10.1080/0951192x.2014.924342.

[44] P. Potdar and V. Jonnalagedda. "Design and development of a framework for effective engineering change management in manufacturing industries". In: *International Journal of Product Lifecycle Management* 11 (4 Jan. 2018), pp. 368–368. ISSN: 1743-5110, 1743-5129. DOI: 10.1504/ijplm.2018.097880.

[45] S. S. Kolapkar, R. Bharsakade, and A. Rajurkar. "Lead Time Reduction for managing Engineering Changes". In: vol. 998. IOP Publishing, Dec. 2020, pp. 12027–12027. DOI: 10.1088/1757-899x/998/1/012027.

[46] L. Jokinen, V. Vainio, and A. Pulkkinen. "Engineering Change Management Data Analysis from the Perspective of Information Quality". In: *Procedia Manufacturing* 11 (Jan. 2017), pp. 1626–1633. ISSN: 2351-9789. DOI: 10.1016/j.promfg.2017.07.312.

[47] M. Rajabalinejad, L. van Dongen, and M. Ramtahalsing. "Systems integration theory and fundamentals". In: *Safety and Reliability* 39 (1 Jan. 2020), pp. 83–113. ISSN: 0961-7353, 2469-4126. DOI: 10.1080/09617353.2020.1712918.

[48] J. Whyte and A. Davies. "Reframing Systems Integration: A Process Perspective on Projects". In: *Project Management Journal* 52 (3 Mar. 2021), pp. 237–249. ISSN: 1938-9507, 8756-9728. DOI: 10.1177/8756972821992246.

[49] J. L. Grumbach and L. D. Thomas. "Integration principles for complex systems". In: *Systems Engineering* 23 (6 Sept. 2020), pp. 684–706. ISSN: 1098-1241, 1520-6858. DOI: 10.1002/sys.21554.

[50] G. Xiong, Y. Wu, and Y. Li. "Research on Information Integration of Construction Project Management Based on BIM". In: *IOP Conference Series Earth and Environmental Science* 267 (3 May 2019), pp. 32069–32069. ISSN: 1755-1315, 1755-1307. DOI: 10.1088/1755-1315/267/3/032069.

[51] M. Chami, A. Aleksandraviciene, A. Morkevičius, and J.-M. Bruel. "Towards Solving MBSE Adoption Challenges: The D3 MBSE Adoption Toolbox". In: *INCOSE International Symposium* 28 (1 July 2018), pp. 1463–1477. ISSN: 2334-5837. DOI: 10.1002/j.2334-5837.2018.00561.x.

[52] S. Chiocchio, E. Martin, P. Barabaschi, H. W. Bartels, J. How, and W. R. Spears. "System engineering and configuration management in ITER". In: *Fusion Engineering and Design* 82 (Aug. 2007), pp. 548–554. ISSN: 0920-3796, 1873-7196. DOI: 10.1016/j.fusengdes.2007.06.019.

[53] B. Mészáros, M. Shannon, D. Marzullo, C. Woodley, S. Rowe, and G. D. Gironimo. "Configuration management of the EU DEMO conceptual design data". In: *Fusion Engineering and Design* (Dec. 2015), pp. 1619–1623. ISSN: 0920-3796, 1873-7196. DOI: 10.1016/j.fusengdes.2015.11.008.

[54] F. J. Fuentes, J.-J. Cordier, P. Leonard, L. Scherrer, D. J. Wilson, H. Gagueche, and T. Popa. "Methodology for reverse engineering analysis of ITER as-built integrated systems". In: *Fusion Engineering and Design* 146 (Apr. 2019), pp. 2268–2272. ISSN: 0920-3796, 1873-7196. DOI: 10.1016/j.fusengdes.2019.03.169.

[55] D. Campbell. "The first fusion reactor: ITER". In: *Europhysics news* 47 (Sept. 2016), pp. 28–31. ISSN: 0531-7479, 1432-1092. DOI: 10.1051/epn/2016504.

[56] D. van Houtte, F. Sagot, K. Okayama, and K. Blackler. "A functional approach for managing ITER operations". In: *Fusion Engineering and Design* 87 (Feb. 2012), pp. 652–656. ISSN: 0920-3796, 1873-7196. DOI: 10.1016/j.fusengdes.2012.01.033.

[57] R. Aymar, P. Barabaschi, and Y. Shimomura. "The ITER design". In: *Plasma Physics and Controlled Fusion* 44 (5 Apr. 2002), pp. 519–565. ISSN: 0741-3335, 1361-6587. DOI: 10.1088/0741-3335/44/5/304.

[58] J. G. Enríquez, J. M. Sánchez-Begínes, F. J. D. Mayo, J. A. García-García, and M. J. Escalona. "An approach to characterize and evaluate the quality of Product Lifecycle Management Software Systems". In: *Computer Standards & Interfaces* 61 (May 2018), pp. 77–88. ISSN: 0920-5489, 1872-7018. DOI: 10.1016/j.csi.2018.05.003.

[59] G. Liu, R. Man, and Y. Wang. "A Data Management Approach Based on Product Morphology in Product Lifecycle Management". In: *Processes* 9 (7 July 2021), pp. 1235–1235. ISSN: 2227-9717. DOI: 10.3390/pr9071235.

[60] R. M. Rangan, S. M. Rohde, R. S. Peak, B. Chadha, and P. I. Bliznakov. "Streamlining Product Lifecycle Processes: A Survey of Product Lifecycle Management Implementations, Directions, and Challenges". In: *Journal of Computing and Information Science in Engineering* 5 (3 Aug. 2005), pp. 227–237. ISSN: 1530-9827, 1944-7078. DOI: 10.1115/1.2031270.

[61] P. Clermont and B. Kamsu-Foguem. "Experience feedback in product lifecycle management". In: *Computers in Industry* 95 (Nov. 2017), pp. 1–14. ISSN: 0166-3615, 1872-6194. DOI: 10.1016/j.compind.2017.11.002.

[62] F. M. Mulla, V. N. Kulkarni, V. Gaitonde, and B. B. Kottürshettar. *PLM as a tool for collaboration in aerospace industries - A review*. Jan. 2021. DOI: 10.1063/5.0036546.

[63] S. Zina, M. Lombard, and L. Lossent. "INTEGRATION OF CONTEXTUAL VIEWS IN CONFIGURATION MANAGEMENT FOR PLM APPLICATIONS". In: *IFAC Proceedings Volumes* 39 (4 Jan. 2006), pp. 225–231. ISSN: 1474-6670, 2589-3653. DOI: 10.3182/20060522-3-fr-2904.00036.

[64] D. Adamenko, S. Kunnen, and A. Nagarajah. "Digital Twin and Product Lifecycle Management: What Is the Difference?" In: Springer Science+Business Media, Jan. 2020, pp. 150–162. DOI: 10.1007/978-3-030-62807-9_13.

[65] D. Krob. "CESAM: CESAMES Systems Architecting Method - A Pocket Guide". In: *HAL (Le Centre pour la Communication Scientifique Directe)* (Jan. 2017).

[66] E. R. Helmeid. "Development of a Hybrid Product Breakdown Structure and Variability Model". In: *Insight* 24 (1 Apr. 2021), pp. 22–29. ISSN: 2156-485X, 2156-4868. DOI: 10.1002/inst.12324.

[67] F. Blampain, M. Bricogne, B. Eynard, C. Bricogne, and S. Pinon. "Digital solution for planning and management of construction site operations: a proposal of BIM-based software architecture and methodology". In: *HAL (Le Centre pour la Communication Scientifique Directe)* (Sept. 2022).

[68] B. Brichard and A. E. Carbo. *RT-F4E FPA327 07-13 - Ex-Port RNC on-site assembly plan (Private communication)*. Sept. 2025.

[69] B. L., A. de kerdrel, A. A., B. B., P. S., B. R., C. Q., Y. C., L. F., L. T. Y., L. H., T. K., T. pinedo A., U. V., W. M., and B. B. *5.5.P1.EU.15 Appendix 2 Technical Requirements Annex (Private communication)*. Dec. 2019.

[70] D. Marocco and B. Esposito. *RNC Design Description Document (DDD) (Private communication)*. Feb. 2025.

[71] D. Marocco, B. Esposito, and D. Marocco. *RT-F4E FPA327 06- 40 - In-port RNC Design Description Document (DDD) (Private communication)*. Nov. 2021.

[72] D. Marocco, F. Cau, C. Colomer, D. Combescure, P. Gopalkrishna, V. Krasilnikov, and B. Brichard. *Structural integrity report for In-port RNC port plug components (Private communication)*. Nov. 2021.

[73] D. Marocco, B. Brichard, F. Cau, C. Colomer, D. Combescure, J. Guirao, V. Krasilnikov, M. Loughlin, R. Roccella, P. Ruiz, P. Testoni, X. Zhang, and B. Brichard. *System load specifications for Port-Plug RNC Components (Private communication)*. Dec. 2021.

[74] B. Esposito, B. Brichard, G. Gandolfo, D. Marocco, and F. Belli. *In-Port RNC Design Description Document: Sub-System Detector Module (Private communication)*. Nov. 2021.

[75] D. Marocco, V. Krasilnikov, J. S. Martinez, T. Pinna, B. Esposito, and D. Dongiovanni. *RAMI analysis for the In-Port Radial Neutron Camera (Private communication)*. Nov. 2021.

[76] D. Jiménez, R. Diego, S. Terrón, L. de Bilbao, C. Sanchez, J. Puig, L. S. Garcia, B. Brichard, and M. C. S. Macua. *Manufacturing and Assembly Assessment of the in-port RNC (Private communication)*. Nov. 2021.

[77] D. Marzullo, E. Occhiuto, G. Brolatti, D. Falco, D. Laghi, D. Marocco, and B. Esposito. "Mechanical design of ITER radial neutron camera Ex-Port system". In: *Fusion Engineering and Design* 203 (Apr. 2024), pp. 114477–114477. ISSN: 0920-3796, 1873-7196. DOI: 10.1016/j.fusengdes.2024.114477.

[78] D. Laghi, D. Marzullo, D. Marocco, D. Falco, V. L. Salandra, D. Marzullo, D. Marocco, B. Brichard, and A. C. Esteve. *Structural Integrity Report (SIR) for the FDR of the ex-port RNC (Private communication)*. Feb. 2025.

[79] D. Dongiovanni, B. Esposito, D. Marocco, B. Brichard, and A. E. Carbo. *RT-F4E FPA327 07-20 - RAMI analysis for the Ex-port Radial Neutron Camera (Private communication)*. May 2025.

[80] E. O. e. a. D. Marzullo. *RT-F4E FPA327 07-71 D3.2-02 FDR Ex-port RNC Design Description Document: shielding subsystem (Private communication)*. Jan. 2025.

[81] T. Giacomin. *EP01 coordinates systems (Private communication)*. Apr. 2022.

[82] E. Boter. *ITR-55.Q1-EQ port 01 55.B1 RNC (Drawing) (Private communication)*. Dec. 2023.

[83] F. Malaroda, D. Marzullo, E. Occhiuto, and U. Bonavolontà. *Simulation and ergonomic evaluation by virtual reality of ITER Radial Neutron Camera maintenance operations (Private communication)*. Aug. 2024.

[84] E. Occhiuto, D. Marzullo, D. N. Dongiovanni, U. Bonavolontà, F. Malaroda, D. Marocco, and B. Esposito. "Maintenance plan of the ITER Radial Neutron Camera: Verification and validation by virtual reality simulation". In: *Fusion Engineering and Design* 215 (Mar. 2025), pp. 114980–114980. ISSN: 0920-3796, 1873-7196. DOI: 10.1016/j.fusengdes.2025.114980.

[85] V. Krasilnikov, E. Occhiuto, B. Brichard, B. Coriton, B. Esposito, T. Giacomin, J. Guirao, F. Josseaume, L. Meneses, and C. Ye. *Tolerance Analysis of the RNC Ex-Vessel Collimators to the EP01 PP DSM 2 Optical Path (Private communication)*. June 2024.

[86] E. Occhiuto. *NT-F4E FPA327 07-10 - EX-PORT RNC ALIGNMENT PROCEDURE (Private communication)*. May 2025.